

Development of Novel HIV-1 Latency Reversing Agents

Jonathan Colin Jacobson
BSc (Hons)

Submitted in total fulfillment of the requirements of the degree of
Doctor of Philosophy

(June 2018)

This thesis is printed on archival paper

Department of Microbiology and Immunology
The Peter Doherty Institute for Infection and Immunology
The University of Melbourne



Dedicated to the immortal spirit of Freddie Mercury.



Abstract

The development of effective antiretroviral therapy has seen HIV-1 infection turn from a near certain death sentence to a manageable chronic disease. However, current therapy is not capable of clearing the reservoir of latently infected cells that is established early in infection and persists indefinitely for the life of the patient. The risk of viral rebound reseeded from the latent reservoir necessitates lifelong treatment, contributing the significant global financial HIV-1 burden worldwide. Additionally, long term suppressive therapy is commonly associated with secondary toxicities which shorten the life expectancy of HIV+ patients. The search for a cure for HIV-1 is therefore a global effort of high priority.

A latent infection occurs when a complex combination of restrictions prevent the expression of viral genes. Understanding the nature of these restrictions is still a developing field of research. To date, several “druggable” molecular targets/pathways have been identified and become the subject of intense study, with the hopes that therapeutic intervention with Latency Reversing Agents (LRAs) may result in the clearance of all latently infected cells harboring an inducible provirus, ie, a functional HIV-1 cure.

The work presented in this thesis details the generation and validation of a set of novel *in vitro* models, engineered for the detection of small drug like compounds that reactivate HIV-1 from latency in a highly specific manner, as well as their use in the discovery of 7 novel families of specific latency reversing agents. This work also includes a detailed study of the synergistic relationship these novel compounds have in combination with widely studied latency reversing agents already at the forefront of HIV-1 cure research. It is the sincere hope of the author that this work may contribute in a meaningful way to the worldwide efforts at a future HIV-1 cure.

Declaration

I declare that this thesis contains only original work towards the PhD, carried out from the 14th February 2012, the official commencement date of this research program.

Due acknowledgement has been made in the text to all other materials and services used.

This thesis is less than 100,000 words in length, exclusive of tables, maps, footnotes, appendices and bibliographies.

Jonathan C Jacobson

Acknowledgements

I would like to begin by thanking our amazing collaborators from the Walter and Eliza Hall Institute for all of their help in the early days of my PhD, giving me access to their facilities, time and knowledge. A very big thank you to the Dr Kurt Lackovic for all this guidance from day one, helping conceive the ideas that would translate to the FlipIn dual reporter cell lines. It has been a privilege collaborating with such a professional, and thank you for all the marathon motivations. Thanks to Dr Kate Jarmen for her tireless work during the primary High Throughput Chemical Screen, churning through over 100,000 compounds across hundreds of plates and making the entire PhD possible.

To Dr Brad Sleebs, our font of all knowledge drug-related, thank you for all your amazing help and continued help on this project. Finally to our analogue-producing machine Dr William Nguyen for producing compounds faster than we knew what to do with them.

From the Doherty Institute, I'd like to begin at the start and thanks the Jane Howard for teaching me all the molecular techniques I know since honours in 2011, I couldn't have asked for a better teacher. Thank you also for your hard work, and that of Charlene Mackenzie, at keeping the lab & PC3 running smoothly. To Dr Georges Khoury and Dr Con Sonza for all their technical and theoretical input, which has always been greatly appreciated.

To my fellow PhD students: To Michelle Lee, it has been amazing to begin our friendship by teaching you and then watch you utterly surpass me in every way the lab is concerned. I have no doubt you will be an amazing researcher in the future and look forward to watching your meteoric rise. To Leigh Harty my personal encyclopedia and guru of everything "HIV latency", life has thrown everything at you in the last few years and you've overcome it all spectacularly, I look forward to sharing a dram of Lagavulin and Montecrito #2 with Dr Harty in the near future. To Talia Mota, the most passionate HIV-1 cure researcher I know, your friendship has meant the most to me over the course of our PhDs, from the early days running around Princes park during crazy thunderstorms to today and into the far future. You are such an amazing person. Don't ever change.

And to Professor Damian Purcell, who has been the single most influential person in my life. Thank you so much for taking a chance and giving an overeager 2nd year student the opportunity to come into your lab and be exposed to the world of science. Thank you for helping me cut my teeth in the research world in my 3rd year research project, for giving me such an amazing project to tackle in honours and continue on in my PhD, which has been incredibly challenging and equally rewarding. Thank you for always making time for me. Finally thank you for giving me something to aspire to and someone to look up to. I hope we stay colleagues and friends for many years to come.

Table Of Contents

Chapter 1 Introduction.

	Page
1.1 Introduction.	
1.1.1 Introduction.	21
1.2 An overview of HIV-1 and AIDS.	
1.2.1 An overview of HIV-1 and AIDS.	22
1.2.2 Genome structure.	26
1.2.3 HIV-1 viral proteins.	29
1.2.4 Alternative RNA splicing.	35
1.2.5 The Long Terminal Repeats.	38
1.3 The HIV-1 lifecycle.	
1.3.1 Attachment, entry and uncoating.	41
1.3.2 Reverse transcription and integration.	41
1.3.3 Gene expression in the early phase.	42
1.3.4 Gene expression in the late phase.	42
1.3.5 Budding and maturation.	43
1.4 An overview of HIV-1 latency and cure.	
1.4.1 HIV-1 latency.	45
1.4.2 HIV-1 suppression, viral rebound and a functional cure.	46
1.4.3 The shock and kill method.	48

1.5 The molecular mechanisms of HIV-1 latency.	
1.5.1 Integration sites and HIV-1 latency.	51
1.5.2 Activation of cellular transcription factors.	52
1.5.3 Chromatin structure.	57
1.5.4 Acetylation and deacetylation.	59
1.5.5 Methylation.	62
1.5.6 DNA methylation.	65
1.5.7 The Positive Transcription Elongation Factor b (P-TEFb).	67
1.5.8 Posttranslational modifications of Tat.	70
1.5.9 Tat mediated transactivation of HIV-1 transcription.	73
1.5.10 Overview.	75
1.5.10 Compound synergy.	79
1.6 Project Aims.	81

Chapter 2 Materials and Methods.

	Page
2.1 Reagents.	
2.1.1 Chemicals.	82
2.1.2 Oligonucleotides.	82
2.1.3 Plasmids.	83
2.1.4 Drugs, compounds and molecular probes.	85
2.2 Cloning.	
2.2.1 Splice Overlap Extension PCR.	86
2.2.2 DNA gel electrophoresis.	88
2.2.3 Gel purification of DNA.	88
2.2.4 Restriction digestion of DNA.	88
2.2.5 DNA ligation.	88
2.2.6 Transformation of chemically competent <i>E. coli</i> .	89
2.2.7 Plasmid DNA preparation.	89
2.2.8 DNA quantification.	89
2.2.9 Sequencing.	90
2.2.10 Whole RNA extraction using TRIzol® reagent.	90
2.2.11 Phenol Chloroform extraction.	90
2.2.12 Alcohol precipitation of DNA and RNA.	90
2.2.13 Reverse Transcription PCR from whole RNA.	91
2.3 Culturing Mammalian Cell Lines.	
2.3.1 Cell Lines.	92
2.3.2 Transient DNA plasmid transfection of adherent stable cell line.	92
2.3.3 Drug treatment of adherent stable cell lines.	93
2.3.4 Drug treatment of suspension cell lines.	93
2.3.5 Firefly luciferase assay of adherent stable cell lines.	93
2.3.6 Click Beetle luciferase assay of adherent stable cell line.	94

2.4 Creating stable cell lines.	
2.4.1 Transfection for Flpase mediated (FlipIn) recombination.	95
2.4.2 Pseudovirus production.	95
2.4.3 Transduction of cells.	96
2.5 Flow cytometry.	
2.5.1 Preparation of J.Lats for flow cytometry.	97
2.5.2 Flow cytometry of J.Lats using FACSCalibur.	97
2.5.3 Preparation of leukapheresis cells for flow cytometry.	97
2.5.3 Flow cytometry of leukapheresis cells using LSRIL.	98
2.6 Primary cell experiments.	
2.6.1 Isolation of PBMCs from buffy coats.	99
2.6.2 Isolation of CD4+ T cells form PBMCs.	99
2.6.3 MTS cell viability/proliferation assay.	101
2.7 Reactivation of HIV from HIV+ patients following suppressive cART.	
2.7.1 Isolation of CD4+ T cells form leukapheresis samples.	102
2.7.2 Reactivation of leukapheresis samples.	102
2.7.3 Harvesting reactivated leukapheresis cells.	102
2.7.4 DNase treatment of whole RNA.	102
2.7.5 cDNA synthesis.	103
2.7.6 First round PCR.	103
2.7.7 qPCR of HIV DNA.	103
2.8 Data presentation and statistical analysis.	
2.8.1 Data presentation and statistical analysis.	104

Chapter 3 Platforms to assess specific reactivation of HIV-1 from latency

	Page
3.1 Aim.	105
3.2 Introduction.	105
3.3 Results.	109
3.3.1 Construction of FlipIn.FM dual reporter cell line.	
3.3.1.1 CBG luciferase expression from bicistronic constructs.	109
3.3.1.2 HIV-1 Tat expression from bicistronic construct.	112
3.3.1.3 Hygromycin B selection of FlipIn.CBG.T4+CChGH ⁺ cells.	114
3.3.1.4 Dose dependent expression from LTR-driven CBR reporter.	115
3.3.1.5 Augmenting Tat expression within reporter cell lines.	117
3.3.1.6 Selection of completed FlipIn.FM (clone C2).	119
3.3.2 Construction of FlipIn.RV dual reporter cell line.	
3.3.2.1 CBR luciferase expression from bicistronic construct.	121
3.3.2.2 Hygromycin B selection of FlipIn.CBR T4+CChGH ⁺ cells.	123
3.3.2.3 Dose dependent expression from LTR-driven CBR reporter.	124
3.3.2.4 Selection of completed FlipIn.RV (clone B6).	126
3.3.3 Validating FlipIn.FM and FlipIn.RV dual reporter cell lines.	
3.3.3.1 Dose dependent responses to Tat plasmid in cell lines.	128
3.3.3.2 Dose dependent responses to Tat protein in cell lines.	130
3.3.4 Modifying J.Lat latently infected Jurkat T cell line.	
3.3.4.1 Generating T-cell derived J.Lat.FM dual reporter populations.	132
3.3.3.2 Validating J.Lat.FM populations.	136
3.4 Discussion.	138

Chapter 4 Validating dual reporter cell lines using a panel of mechanistically diverse known Latency Reversing Agents

	Page
4.1 Aim.	142
4.2 Introduction.	142
4.3 Results.	147
4.3.1 Assessing known Transcription Factor Activators.	
4.3.1.1 (A) TNF α .	148
4.3.1.2 (B) PMA.	148
4.3.1.3 (C) Briostatin-1	149
4.3.2 Assessing known Histone Deacetylase Inhibitors.	
4.3.2.1 (D) Vorinostat.	152
4.3.2.2 (E) Panobinostat.	153
4.3.2.3 (F) Romidepsin.	153
4.3.3 Assessing known Histone Methyltransferase Inhibitors	
4.3.3.1 (G) DZNep.	155
4.3.3.2 (H) UNC-0638.	155
4.3.4 Assessing known Bromodomain Inhibitors	
4.3.4.1 (I) JQ1 (+).	157
4.3.4.2 (J) PFI-1.	158
4.3.4.3 (K) LY-303511.	158
4.3.5 Assessing a known Heat Shock Protein 90 Inhibitor	
4.3.5.1 (L) CCT-018159.	160
4.3.6 Assessing known modulators of Tat Posttranslational modifications	
4.3.6.1 (M) BML-278.	162
4.3.6.2 (N) EX-527.	162
4.3.6.3 (O) Rocilinostat.	162
4.4 Discussion.	165

Chapter 5 Discovery of 7 novel families of highly specific HIV-1 Latency Reversing Agents.

	Page
5.1 Aim.	170
5.2 Introduction.	170
5.3 Results.	177
5.3.1 Characterizing the 7 series of novel Latency Reversing Agents.	
5.3.1.1 Characterizing the 7 series of novel Latency Reversing Agents.	177
5.3.1.2 Bromodomain inhibition alpha screen.	179
5.3.2 Assessing novel Latency Reversing Agents in the FlipIn cell lines.	
5.3.2.1 FlipIn.FM response to novel LRAs.	181
5.3.2.2 FlipIn.RV response to novel LRAs.	184
5.3.3 Assessing novel Latency Reversing Agents in the J.Lat cell lines.	
5.3.3.1 J.Lat10.6FM response to novel LRAs.	186
5.3.3.2 J.Lat6.3FM response to novel LRAs.	188
5.3.4 Drug associated toxicity of novel Latency Reversing Agents.	
5.3.4.1 FlipIn.FM (HEK293) toxicity response to novel LRAs.	190
5.3.4.2 Primary CD4+ T cell toxicity response to novel LRAs.	192
5.4 Discussion.	194

Chapter 6 Synergistic reactivation of HIV-1 gene expression using known and novel Latency Reversing Agents.

	Page
6.1 Aim.	199
6.2 Introduction.	199
6.3 Results.	204
6.3.1 Synergy in FlipIn cell.	
6.3.1.1 Synergy in FlipIn.FM cells.	204
6.3.1.2 Bliss Independence in FlipIn.FM cells.	207
6.3.1.3 Synergy in FlipIn.RV cells.	210
6.3.1.4 Bliss Independence in FlipIn.RV cells.	213
6.3.2 Synergy in J.Lat cells.	
6.3.2.1 Synergy in J.Lat10.6FM cells.	216
6.3.2.2 Bliss Independence in J.Lat10.6FM cells.	219
6.3.2.3 Synergy in J.Lat6.3FM cells.	221
6.3.2.4 Bliss Independence in J.Lat6.3FM cells.	223
6.3.3 Reactivation of leukapheresis derived primary CD4+ cells.	
6.3.3.1 Viability of Leukapheresis primary cells 72hr post treatment.	225
6.3.3.2 Single LRA reactivation of HIV-1 from leukapheresis samples	227
6.3.3.3 Synergistic reactivation of HIV-1 from leukapheresis samples	229
6.4 Discussion.	231

Chapter 7 General Discussion.

Page

234

Appendix 1: Expression of Tat protein from the *tat* exon 2 IRES

Page

240

Appendix 2: Models of HIV-1 latency

Page

244

Appendix 3: Latency Reversing Agents

Page

246

Chapter 8 References.

Page

251

List of abbreviations.

AIDS	Acquired immune deficiency syndrome
APOBEC3G	Apolipoprotein B mRNA editing enzyme, catalytic polypeptide-like 3G
AP-1	activator protein 1
BET	bromodomain and extraterminal
bp	base pair(s)
BDi	bromodomain inhibitor
BIS	Bliss independence (synergy) score
BRD	bromodomain containing protein
BSA	bovine serum albumin
CA	capsid protein
cART	combinational antiretroviral therapy
CBG	click beetle green
CBP	CREB binding protein
CBR	click beetle red
CCR5	CC chemokine receptor 5
CD4	Cluster of differentiation 4
cDNA	complimentary DNA
C/EBP	CCAAT enhanced binding protein
CMV-IE	cytomegalovirus immediate early promoter
CoREST	REST corepressor 1
CTD	carboxy terminal domain
CTL	cytotoxic T lymphocyte
CXCR4	CXC chemokine receptor 4
DDPK	DNA dependent protein kinase
DNDP	DNA demethylase
DIS	Dimerisation signal
DMEM	Dulbecco's Modified Eagle Medium
DNA	Deoxyribonucleic acid
dNTP	Nucleoside triphosphate
DP	Damian Purcell
DSIF	DRB sensitivity factor
DS.Red^{Exp}	Double stranded red (express)

dsDNA	double stranded deoxyribonucleic acid
DTT	dithiotheritol
DZNep	3-Dezaneplanocin A
EDTA	ethylenediamine tetra-acetic acid
EGFP	enhanced green fluorescent protein
Env	envelope glycoprotein
EZH2	Enhancer of zeste homolog 2
FCS	fetal calf serum
FRT	flippase recombination target
Gag	group specific antigen
GALT	gut-associated lymphoid tissue
GNAT	Gcn5-related N-acetyltransferase
gp160	glycoprotein (envelope)
HAART	highly active antiretroviral therapy
HAT	histone acetyltransferase
hGH	human growth hormone
HEK	human embryonic kidney
HDAC	histone deacetylase
HDACi	histone deacetylase inhibitor
HIV-1	human immunodeficiency virus type 1
hr	hour
HMT	histone methyltransferase
HMTi	histone methyltransferase inhibitor
HP1	heterochromatin protein 1
HSP90	heat shock protein 90
IFN	interferon
I$\kappa$$\kappa$	I κ B kinase
IN	Integrase enzyme
IRES	internal ribosome entry site
JAK	Janus kinase
J.Lat	Jurkat <u>l</u> atently infected with HIV-1
JNK	Jun N-terminal kinase
KAT	lysine acetyltransferases
Kbp	kilo base pair(s)

LARP7	La-related protein 7
LB	Luria Bertani (broth)
LEDGF	Lens epithelium-derived factor
LRA	latency reversing agent
LSD1	lysine-specific histone demethylase 1
LTR	long terminal repeat
MA	matrix protein
MAPK	MAP kinase
MAPKK	MAP kinase kinase
MAPKKK	MAP kinase kinase kinase
MBD2	Methylated CpG binding protein
MHC	major histocompatibility complex
MOA	mechanism of action
miRNA	micro RNA
mM	milli molar
mRNA	messenger RNA
MYST	MOZ, YBF2, SAS2 and TIP60 containing family of HATs
μL	micro litre
μM	micro molar
NELF	negative elongation factor
NFAT	Nuclear factor of activated T cells
NC	Nucleocapsid protein
N-CoR	nuclear receptor corepressor
Nef	negative factor for viral replication
NES	nuclear export signal
NF-κB	nuclear factor kappa-light-chain of activated B cells
NLS	nuclear localization signal
NMD	nonsense mediated RNA decay
NuRD	Nuclear remodeling and deacetylation complex
Odp	oligonucleotide Damian Purcell
ORF	open reading frame
PBMC	peripheral blood mononuclear cell
PBS	phosphate buffer saline
PBS	primer binding site

PCAF	p300/CBP-associated factor
PCR	polymerase chain reaction
PEV	position effect variegation
PFI	Pfizer
PIC	pre-integration complex
PKC	protein kinase C
Pol	polymerase
PMA	Phorbol 12-myristate 13-acetate
PR	protease enzyme
PRMT6	Protein arginine N-methyltransferase 6
P-TEFb	positive elongation factor b
RE	restriction enzyme
Rev	regulator of expression of virion protein
RNA	ribonucleic acid
RNA pol II	RNA polymerase II
RNP	ribonuclearprotein
RPMI	Roswell Park Memorial Institute medium
RRE	rev responsive element
RSV	Rous sarcoma virus
RT	reverse transcriptase enzyme
shRNA	short hairpin RNA
siRNA	short interfereing RNA
SA	splice acceptor sequence
SD	splice donor sequence
SEC	superelongation complex
SIN	self-inactivating (LTR)
SIRT	sirtuin
SL28	Sharon Lewin oligonucleotide #28
snRNP	small nuclear ribonuclear protein
SOE	splice overlap extension
SP-1	specificity protein 1
ssRNA	single stranded RNA
STAT	signal transducer and activator of transcription
SU	surface (gp120 component of env)

TAR	trans-activation response element
Tat	trans-activator of transcription
TCID₅₀	tissue culture infectious dose 50%
TE	Tris-EDTA
TM	trans-membrane (gp41 component of env)
TM1	Talia Mota oligonucleotide #1
TNFα	tumor necrosis factor alpha
tRNA	transfer RNA
TSS	transcription start site
USF	upstream stimulatory factor
UTR	untranslated region
vif	viral infectivity factor
vpr	viral protein R
vpu	viral protein U
WECC	<u>W</u> alter and <u>E</u> liza Hall Institute / <u>C</u> hildren's <u>C</u> ancer Institute Australia
WEHI	Walter and Eliza Hall institute
WT	Wild type

Chapter 1 Introduction

1.1 Introduction.

1.1.1 Introduction.

Approximately 35 years since the discovery of the human immunodeficiency virus type 1 (HIV-1) and the acquired immune deficiency syndrome (AIDS), the HIV/AIDS pandemic has seen approximately 76.1 million people infected worldwide with 35 million-43 million deaths caused by AIDS related illness. As of 2016, 30.8 million-42.9 million people were estimated to be living with HIV globally, with a yearly death toll of approximately 1 million as estimated by UNAIDS. Currently, each year sees 1.8 million new infections. The introduction of combinational antiretroviral therapy (cART) also termed highly active antiretroviral therapy (HAART), has seen a transition of HIV-1 infection from a death sentence to a manageable chronic disease (Gulick et al., 1997; Hammer et al., 1997). 13.6 million people worldwide have access to cART, although prolonged use has been shown to bring with it side effects that can reduce the life expectancy for patients over non-infected individuals. Currently, an effective vaccine to prevent new infections remains elusive and no cure for HIV-1 exists. The difficulty in creating an effective HIV-1 cure is a result of the persistence of a small population of latently infected CD4+ T cells, which are not susceptible to cART or eradicated by immune effectors.

The work presented in this thesis details the generation and characterization of a set of *in vitro* HIV-1 latency models and their subsequent use in the process of drug screening to detect novel compounds that may be useful in future HIV-1 cure regimes. Such regimes would involve eliminating all activity of the virus, allowing patients to live without ongoing antiretroviral therapy. In the proceeding chapter, a general overview of HIV/AIDS is given, including a brief overview on the progression to AIDS related complications for HIV+ people, the arrangement and organization of the viral genome, structure and HIV-1 lifecycle, as well as an in depth introduction into the molecular biology surrounding HIV-1 latency and the current attempts at a cure strategy using the method of “shock and kill”.

1.2 An overview of HIV-1 and AIDS.

1.2.1 An overview of HIV-1 and AIDS.

The Human Immunodeficiency Virus type 1 is a complex retrovirus belonging to the genus *Lentivirus* of the family *Retroviridae*. HIV-1, as with other members of the *Retroviridae* family, produces spherical virions approximately 80-120nm in diameter, which contain a conical shaped viral core displaying icosahedral symmetry enveloped derived by a host cell membrane phospholipid bi-layer. The virion contains a genetic payload of 2 copies of the (+) ssRNA genome, of approximately 9kbp, as well as several viral proteins necessary for enzymatic functions and modulating the host cell immune response. The acquired immune deficiency syndrome (AIDS) was first observed in San Francisco, USA in 1981, with the appearance of *Pneumocystis* pneumonia and Kaposi's sarcoma, opportunistic infections synonymous with immuno-suppression, in previously healthy patients (Gottlieb et al., 1981; Masur et al., 1981). HIV-1 was later discovered as the etiological agent of AIDS both in France, whereupon the virus was named lymphadenopathy associated virus (LAV) (Barre-Sinoussi et al., 1983), and concurrently in the United States of America where it was named human T-lymphotropic virus type III (HTLV-III) (Gallo et al., 1984). Upon realization that both groups had discovered the same virus, it was renamed human immunodeficiency virus in 1986 (Coffin et al., 1986). Two types of HIV have been identified, HIV-1 and the closely related HIV-2, with the former being the cause of the ongoing worldwide pandemic, and the focus of this thesis.

A brief overview of HIV-1 transmission and the progression to AIDS is described below and is summarized in Figure 1.1. HIV-1 transmission occurs following transfer of infectious virions across mucosal surfaces. The acute stage of infection takes place generally within the first 8 weeks and is typically associated with presentation of with flu-like symptoms (Little et al., 1999). Initially, CD4+ T cells in the mucosa localized around the site of transmission become infected and rapidly produce progeny virus, with the infection quickly spreading to the gut associated lymphoid tissues (GALT) as infected cells expressing the integrin $\alpha 4\beta 7$ cell adhesion receptor traffic to the gut (Cicala et al., 2009). What follows is a sharp decrease in the number of memory CD4+ T cells from the lamina propria (Li et al., 2005) and from the GALT (Brenchley et al., 2004; Guadalupe et al., 2003). The virus is subsequently spread to the associated lymphoid tissue, and a persistent reservoir of latently infected cells is established (Alexaki et al., 2008). The peak in viral load

and related decrease in CD4+ T cells occurs 4-8 weeks post infection. Following seroconversion and the production of an adaptive immune response, a decrease in the viral load occurs and typically achieves a “viral set point”. The viral set point represents a steady state where the virus is kept in check, sometimes enduring for over 10 years post infection. The viral load detectable at the viral set point changes from case to case, however a high set point without the implementation of cART is likely to see a more rapid disease progression (Mellors et al., 1996). During this chronic phase a continuous low-level of immune activation helps drive viral replication and CD4+ T cell depletion. Without cART, most patients develop late stage symptoms around 10 years after infection (Anderson and Medley, 1988; Yates et al., 2007), with AIDS being defined as a CD4+ T cell count below 200cells/mL of plasma. AIDS is characterized by profound immunosuppression and an increase in the occurrence of opportunistic infections including: *Pneumocystis jirovecii* (Morris, 2008), Cytomegalovirus (Steininger et al., 2006) and Kaposi’s sarcoma (Carbone et al., 2009). Inevitably, this immunodeficiency prevents generation of any effective adaptive immune responses, resulting in AIDS related complications and death.

Patients with access to cART are typically able to achieve significant suppression of HIV-1 replication, reducing viremia to levels below the detectable limits of some clinical assays, effectively holding off the progression to AIDS. This amazing feat of medicine is achieved by targeting several key stages (enzymatic processes) in the viral lifecycle, including attachment and entry, reverse transcription, integration and protease mediated maturation. While cART has and continues to save the lives of many millions of people around the world, cART functions by inhibiting the viral replication cycle, preventing new infections within the body, but is not capable of eliminating the reservoir of latently infected cells that is established early in infection (Chun et al., 2000; Palmer et al., 2008). The latent reservoir comprises of several cell subsets including: CD4+ T cells, (Chun et al., 1998; Chun et al., 1997), monocytes and macrophages, (McElrath et al., 1991; Mikovits et al., 1992) as well as astrocytes (Lawrence et al., 2004), however due to the very long lifespan of resting memory CD4+ T cells and their slow turnover rate, elimination of the latent reservoir by prolonged cART is estimated to require over 60yrs (Siliciano et al., 2003). Moreover, cessation of cART invariably sees a rapid viral rebound as the latent reservoir reseeds the infection (Chun et al., 2000). Efforts are therefore being taken to develop a functional HIV-1 cure, where the reservoir of infected cells containing replication

competent provirus is eradicated. A sterilizing cure would involve the elimination of all cells containing a HIV-1 provirus, inducible or not, and is discussed below.

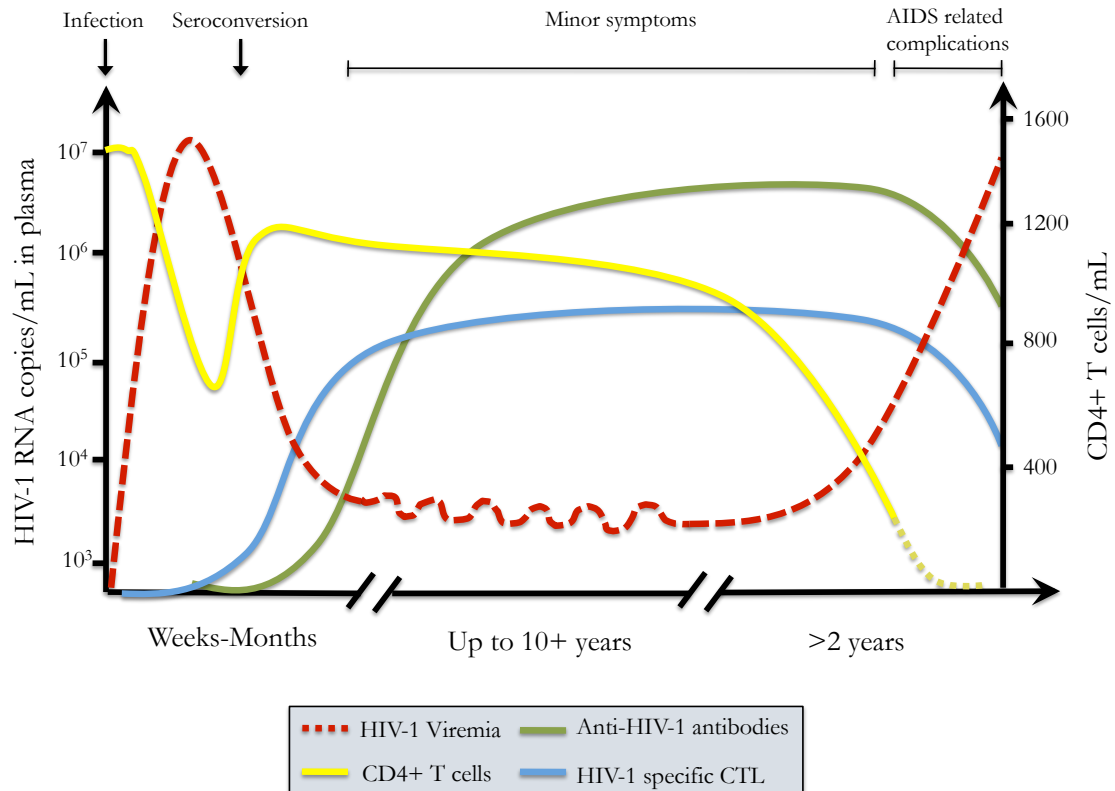


Figure 1.1: HIV-1 infection and the progression to AIDS. Following infection, an early peak of viremia can be detected in the first few weeks, followed by a sharp reduction in the number of CD4+ T cells. Following seroconversion and the generation of anti-HIV-1 antibodies targeting envelope glycoprotein, and the generation of HIV-1 specific CTLs, the virus can be controlled up to 10+ years. At some point, generally >2 years post infection, the virus is able to escape the immune system and proliferate uncontrolled, leading to the steady decrease in CD4+ T cells to below 200 CD4+ T cells/mL and the progression to AIDS. Typically death by AIDS related complications shortly follows.

1.2.2 Genome structure.

HIV-1 is a complex retrovirus and contains the three common retrovirus polyprotein coding genes *gag*, encoding for the structural proteins Matrix (MA), Capsid (CA) and Nucleocapsid (NC), *pol*, encoding for the viral enzymes Protease (PR), Reverse Transcriptase (RT) and Integrase (IN) and *env* encoding for the surface glycoprotein Envelope (Env or gp160). As a complex lentivirus, HIV-1 contains a number of other protein coding genes (Cullen, 1991) seen in Figure 1.2. These include:

- *vif*, encoding for Virion infectivity factor (Vif),
- *vpr*, encoding for Viral protein R (Vpr),
- *tat*, encoding for the Transactivator of transcription (Tat),
- *rev*, encoding for the Regulator of virion expression (Rev),
- *vpu*, encoding for Viral protein U (Vpu) and
- *nef*, encoding for the Negative regulatory factor (Nef)

The protein coding sequence of the viral genome is flanked by the long terminal repeats (LTRs), repeated sequences that contain highly conserved sequences (and structures once transcribed to RNA) that play a number of roles in the viral lifecycle (Das et al., 1998). As an integrated dsDNA provirus, both of the 5' and 3' LTRs contain a U3 and a U5 component. As a (+) ssRNA molecule found in the virion particle, the 5' untranslated region (UTR) encoded by the LTR consists of the R (repeated) sequence and the U5 (unique to 5' end) sequence, whereas the 3' LTR contains a U3 (unique to the 3' end) and an identical R sequence. The presence of the R sequence, that copies and duplicates all sequences at the termini for the RNA to make the LTR structure in the cDNA, is necessary for template strand switching during the process of reverse transcription, following entry into a cell. HIV-1 demonstrated remarkable economy in its protein coding, making an impressive 15 proteins from a single, relatively small, ~9.7kb RNA genome. The genomic economy of HIV-1 can be attributed to two properties. The first property involves the use of several overlapping reading frames, where different open reading frames (ORFs) share common RNA sequence. In fact, there are only two short stretches, between *tat/rev* ORF1 and *vpu* and between *env* and *nef*, where there are no protein coding sequences. The other property that allows HIV-1 to express such a complex array of proteins from a single precursor RNA involves the use of a complex set of splice donor and acceptor sites, which work in tandem to produce over 45 distinct mRNAs (Purcell and Martin, 1993), from which HIV-1 can control its protein expression profile. Many of these distinct mRNAs incorporate one or more non-coding exons, which are interspersed throughout the HIV-

1 genome. In various combinations, achieved through alternative splicing patterns, these exons form 5'UTRs of differing length upstream of the native mRNA start codons but have no effect on the protein produced from said mRNAs. For the genes encoding the major structural proteins and viral enzymes *gag* and *pol*, an overlapping sequence is seen which allows for a ribosome shunt event in the translation of the Gag/Pol polyprotein. In the case of the regulatory proteins Tat, Rev and Nef, the protein coding sequences, named open reading frames (ORFs) are separated by an intronic sequences, and thus must be spliced together to form the full length ORFs from which their respective proteins can be translated. As Tat is of major importance in this thesis, it is important to mention that the first ORF of Tat (from *tat* exon 2) is sufficient to express the 1-exon or 72 amino acid isoform of the Tat protein (Tat72aa), which is alone capable of performing its transactivation role at the LTR, however less efficiently than the 2-exon form (Tong-Starksen et al., 1993).

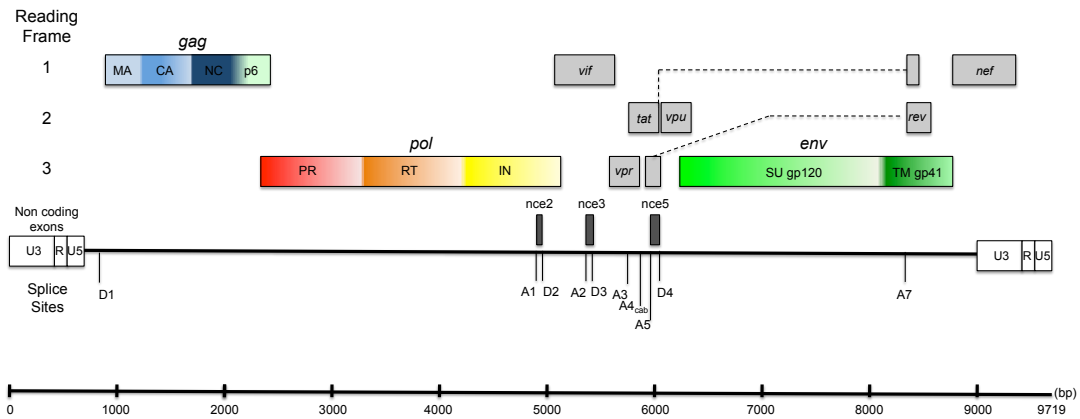


Figure 1.2: HIV-1 genome arrangement. As an integrated provirus, the dsDNA genome of HIV-1 measure around 9.7kbp and is flanked by the Long Terminal Repeats, which serve many functions described later in Figure 1.5. Remarkably, HIV-1 is able to encode for 15 proteins from a single progenitor 9kb RNA, demonstrating remarkable genetic economy. The virus achieves this by utilizing a complex set of splice donor and acceptor sites, resulting in a large number of spliced variants from the single 9kb progenitor RNA (Figure 1.4). Additionally, the virus encodes three genes (*gag*, *pol* and *env*), which each produce a number of distinct proteins following post-translational processing. The first of these is the group-associated antigen (*gag*), which encodes for the structural proteins, which make up the viral matrix, capsid and nucleoprotein complexes. The second, *pol*, encodes for the HIV-1 enzymes Reverse Transcriptase, Integrase and Protease, responsible for key steps in the viral lifecycle, but which also represent targets for cART. The third gene, *env*, encodes for the glycoproteins that protrude from the viral envelope and facilitate attachment to a cell. Two of the important regulatory proteins, Tat and Rev, are encoded by the *tat* and *rev* genes that require complete splicing to join two open reading frames together (denoted by a dotted line). HIV-1 also encodes several other accessory protein coding genes: *vif*, *vpr*, *vpu* and *nef*.

1.2.3 HIV-1 viral proteins.

Structural proteins

Gag

The group associated antigen (*gag*) gene encodes for the major structural proteins that make up the HIV-1 virion (Briggs 2011). The Gag polyprotein is translated from the 9kb unspliced (genome length) RNA as either a Gag p55 precursor or occasionally the Gag/Pol p160 polyprotein. The Gag polyprotein contains, in order of N-terminus to C-terminus, the Matrix (MA), Capsid (CA), Nucleocapsid (NC) and p6 proteins that require proteolytic cleavage from the precursor (Bell and Lever, 2013). Gag plays a role in the assembly of progeny virion by recruiting other virion components to the cell surface including the viral enzymes (Lener et al., 1998), the surface glycoprotein envelope (Murakami and Freed, 2000), as well as the 9kb RNA genome (Berkowitz and Goff, 1994). Occurring either concurrently, or shortly after release of the immature virion particle, protease mediated maturation occurs. The Gag polyprotein precursors undergo HIV-1 protease mediated proteolytic cleavage into MA, CA, NC and p6. The spherical Gag shell then undergoes rearrangement to form infectious virus particles. MA remains associated with the viral envelope, whereas CA condenses to form the conical core structure that houses NC bound to the RNA genome.

Pol

The 5' *pol* gene overlaps the upstream 3' *gag* gene (Figure 1.2) and encodes for the viral enzymes Protease (PR), Reverse Transcriptase (RT) and Integrase (IN). Translation of the Pol polyprotein is dependent on a ribosome frameshift, whereby a ribosome initiates translation of the Gag polyprotein then encounters an RNA sequence that re-aligns the ribosome in a -1 position, into a different reading frame containing the Pol ORF, where the Pol polyprotein can then be translated. This process accounts for roughly 5% of the translation events initiating at the Gag start codon. The result is the Gag/Pol polyprotein. Protease is responsible for the proteolytic cleavage of the Gag p55 and Gag/Pol p160 precursors, an essential part of virion maturation after budding (Kohl et al., 1988). Reverse transcriptase serves as an RNA and DNA dependent DNA polymerase (Temin and Baltimore, 1972), catalyzing the synthesis of the HIV-1 dsDNA genome from its RNA precursor preceding integration. HIV-1 RT contains an RNase activity that is to degrade the RNA component of the transient DNA-RNA hybrid.

The high mutation rate of HIV-1 can be attributed to the lack of a 3'-5' exonuclease proof reading function for RT (Bebenek et al., 1989), resulting in rapid evolution of the virus. Integrase (Chiu and Davies, 2004), along with the newly synthesized dsDNA viral genome assembles with host factors including LEDGF/p75 to form the pre integration complex (PIC) (Bukrinsky et al., 1993; Ciuffi et al., 2005). Within the nucleus, Integrase catalyses the incorporation of the dsDNA HIV-1 genome into the host cell genome in a recombination event called integration (Bushman and Craigie, 1991). The site of integration is of great interest in the field of HIV-1 latency, as the site of integration can determine the accessibility of a provirus to cellular transcription factors, and thus whether or not the provirus can undergo viral gene expression. Selection of a HIV-1 integration site, once thought to be a mostly random process, occurs preferentially within actively transcribed areas of the host cell genome (Albanese et al., 2008; Felice et al., 2009; Han et al., 2004). These points will be discussed in detail below.

Env

The *env* gene encodes for the immature precursor of gp120 and gp41 that matures to form the Envelope gp160 glycoprotein. Following translation, gp160 undergoes extensive post-translational modifications and cleavage by cellular furin-like protease into the gp120 and gp41 subunits (Otteken et al., 1996). At the virion surface, Env consists of a trimer of gp120 surface glycoprotein linked to a trimer of gp41 transmembrane anchor. Upon contacting a susceptible cell, Env enacts attachment to CD4 molecules, undergoing a conformational change allowing for subsequent binding of co-receptors CCR5 or CXCR4 (Clapham and McKnight, 2001) which facilitate fusion of the viral envelope with the host cell membrane (Murakami and Freed, 2000).

Regulatory proteins

Tat

The Transactivator of transcription protein (Tat) is the single protein of greatest interest for this thesis, and as such, a detailed description of Tat is provided in the introduction to HIV-1 latency below, with this section providing a brief overview. Tat plays many essential roles in the viral replication cycle, but in particular, as discovered in the early 90's, at the stage of transcription elongation (Berkhout et al., 1990; Feinberg et al., 1991; Frankel, 1992). Following transcription initiation at the proviral LTR promoter, the 59nt trans-activation response (TAR) stem loop is formed and cellular RNA polymerase II (RNA

polII) enzymes typically pause elongation and dissociate from the DNA template (Berkhout et al., 1989). At a very low rate, transcription proceeds through the 9kb viral genome and the resulting preRNA is co-transcriptionally processed and spliced into the fully spliced 2kb mRNA. Tat protein can be translated from this mRNA, where upon the protein re-enters the nucleus to bind a bulged U-rich portion of a stem loop structure at the nascent HIV-1 RNA called the trans-activation response element (TAR) (Roy et al., 1990)(Berkhout et al., 1989; Gatignol and Buckler-White, 1991). Tat, when complexed to the TAR RNA stem loop recruits cellular Positive Elongation Factor b (P-TEFb) to the TAR stemloop, and into proximity of the stalled RNA polII complex (Mancebo et al., 1997; Zhu et al., 1997). P-TEFb comprises of the cyclin dependent kinase 9 (CDK9) along with its cyclin T1 binding partner. P-TEFb is also usually sequestered in an inactive form, complexed with 7SK snRNP. Tat recruits P-TEFb to the paused RNA polII in order to phosphorylate serine residues within the C-terminal domain of RNA polII and greatly enhances its transcription elongation capabilities (Fujinaga et al., 1998; Zhou et al., 2004; Zhou et al., 1998). Hyperphosphorylated RNA polII then elongates transcription from the viral LTR promoter at high efficiency. When Tat enhances viral RNA synthesis (viral gene expression), it directly augments the transcription of its own mRNA, forming a positive feedback loop. Outside of its role as the transactivator of transcription, Tat plays many other important roles including: a role in reverse transcription (Harrich et al., 1997; Ulich et al., 1999), recruitment of cellular histone Acetyltransferase (HAT) enzymes, allowing for promoter access by cellular transcription factors. (Marzio et al., 1998), modulating HIV-1 RNA splicing (Jablonski et al., 2009), downregulating MHC-I expression (Howcraft et al., 1993), interfering with the innate immune regulator PKR (Cai et al., 2000; McMillian et al., 1995) as well as with the biogenesis of micro-RNAs (Qian et al., 2009).

Rev

The regulator of virion expression (Rev), like Tat, is a trans-acting protein on HIV-1 RNA, and like Tat, is also expressed from the fully spliced 2kb group of mRNAs early in the course of the HIV-1 lifecycle. Rev functions by facilitating the export of the larger 9kb and 4kb mRNAs, which encode for the structural proteins, out of the nucleus and into the cytoplasm. To traffic into the nuclear compartment and exert its function, Rev utilizes its N-terminal nuclear localization signal (NLS) to bind importin β , which interacts with the nuclear pore complex (Henderson, 1997). Once inside the nucleus, the arginine rich domain of Rev serves as a RNA binding motif, allowing for binding to a G-rich region of

a highly conserved *cis*-acting RNA structural element names the Rev Response Element (RRE) (Itoh et al., 1989; Malim et al., 1989). It is thought that initially a single Rev monomer binds, then up to 12 more Rev monomers. The Rev-RRE complex then uses the nuclear export signal (NES) of Rev to bind exportin 1 (CRM1) and possibly hRIP, Sam68 and eIF5a, and is then shuttled out of the nucleus into the cytoplasm for protein translation (Fritz and Green, 1996). Once these larger mRNAs are exported to the cytoplasm, the structural gene products Gag/Pol and Env can be expressed, bringing about the late stage of HIV-1 replication (Malim, 1991).

Accessory proteins

Nef

The Negative Regulatory Factor (Nef) protein is encoded by the *nef* gene, which is exclusive to the primate lentiviruses. Like Tat and Rev, Nef is expressed early in the HIV-1 lifecycle from 2kb mRNAs and, like Tat and Rev, Nef also is a multifunctional protein. Nef interacts with the cytoplasmic tail of CD4 molecules on the surface of infected cells and recruits the clathrin adaptor protein complex 2 (AP2) which acts by internalizing CD4 through clathrin coated pits, leading to lysosomal degradation (Chaudhuri et al., 2007). Down-regulation of CD4 also prevents inappropriate association of CD4 with Env within infected cells, enhancing virion budding (Janvier et al., 2001). Nef also down-regulates the major histocompatibility complex class I (MHC-I) molecules (Roeth and Collins, 2006), either by interaction with the cytoplasmic tail of MHC-I and recruitment of AP1 to mis-route MHC-1 to endosomes rather than the cell surface (Roeth et al., 2004), or assembly of a multi-component Src-family kinase containing cascade to induce endocytosis from the cell surface (Atkins et al., 2008). Nef also interferes with the endocytosis of TCR-CD3 complexes formed at the immunological synapse, resulting in reduced clustering of TCR-CD3 and inefficient synapse formation (Atkins et al., 2008). Modulation of CD4, MHC-I and TCR-CD3 function by Nef results in impaired immune signaling protection of infected cells from CTL responses (Le Gall et al., 1997; Mangasarian et al., 1999; Schwartz et al., 1996a).

Vif

The Viral Infectivity Factor (Vif) is packaged into progeny virions and serves to disrupt co-packaging of the cellular cytidine deaminase enzymes named apolipoprotein B mRNA-editing enzyme catalytic polypeptide-like 3G (APOBEC3G or A3G) proteins, which

possess antiviral activity through deamination of cytidine (C) to uracil (U) within the first strand cDNA reverse transcripts (Mangeat et al., 2003; Sheehy et al., 2002). The resulting dsDNA is therefore G-A hypermutated (a form of error catastrophe). In the absence of Vif, APOBEC3G is packaged into budding viral particles complexed with the viral RNA genome and Gag (Bogerd, 2008), however in the presence of Vif, APOBEC3G is polyubiquitinated by the recruitment of cullin-RING ubiquitin ligase, and subsequently degraded in the proteasome.

Vpr

The Viral Protein R (Vpr) plays a role in the HIV-1 lifecycle following fusion and entry by mediating the transport of the pre-integration complex (PIC) to the host cell nucleus (Heinzinger et al., 1994; Popov et al., 1998), reverse transcription (Mansky et al., 2000; Stark and Hay, 1998) as well as integration into the host cell genome. This role of Vpr is particularly important for infection of non-dividing cells such as macrophages. Vpr can also arrest the cell cycle at the G2 phase (Andersen et al., 2006; Andersen et al., 2008) and potentially induce apoptosis through cellular caspase activity (Stewart et al., 2000) and loss of mitochondrial membrane integrity by ion channel formation (Piller et al., 1996).

Vpu

Viral Protein U (Vpu), like Nef, is implicated in the down-regulation of CD4 from the cell surface. Vpu is a dimeric integral membrane protein that induced CD4 turnover by recruiting cullin1-Spk1 ubiquitin ligase complex to the cytoplasmic tail of CD4 bound to HIV-1 Env retained in the endoplasmic reticulum. Vpu binds to the Spk1-binding receptor protein β -TrCP triggering, polyubiquitination and proteasomal degradation of CD4 (Binette et al., 2007; Meusser, 2004). The interferon-induced restriction factor, B-cell stromal factor 2 (BST-2) or tetherin prevents Vpu mutant particle budding at the cell surface, resulting in the viral particles being subsequently transported to endosomes. Vpu inhibits the function of tetherin, allowing for budding of progeny virion, however the interaction between Vpu and tetherin is not fully resolved. ((Neil et al., 2006; Neil et al., 2008).

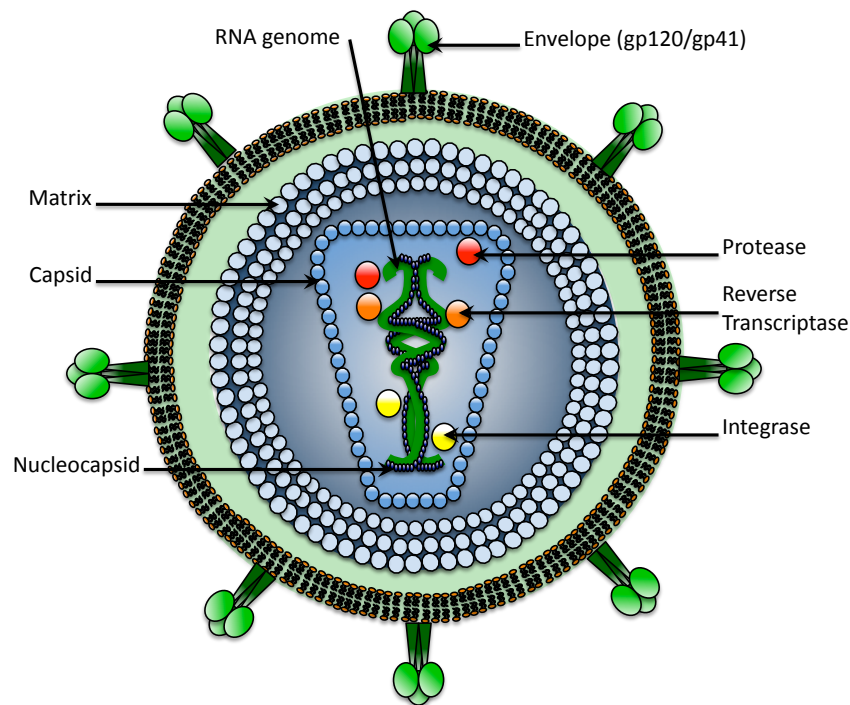


Figure 1.3: HIV-1 virion structure. Belonging to the family *Retroviridae*, the HIV-1 virion is cloaked in a cell membrane-derived lipid bilayer, which it acquires when budding from an infected cell and from which its Envelope glycoprotein trimers (gp120/gp41) extend to facilitate attachment to CD4 and envelope fusion with a susceptible cell. The viral envelope has a rough diameter of 80-120nm and is associated with the underlying virion matrix protein shell. Condensed within the matrix shell is the conical shaped capsid protein structure, which houses two copies of the HIV-1 (+) ssRNA 9kb genome, complexed with nucleocapsid protein. HIV-1 virion particles contain the essential viral enzymes: Reverse Transcriptase, Integrase and Protease. HIV-1 virions also contain a number of accessory proteins, unique to complex retroviruses, including: Nef, Vif and Vpr (not shown).

1.2.4 Alternative RNA splicing.

Splicing is the process of removing intervening intronic sequences from preRNA following transcription and the ligation of two exonic (coding) sequences together. Alternative splicing allows for the formation of many mature mRNAs (potentially encoding for different protein isoforms) from a single precursor preRNA. In eukaryotes, and for viruses that infect eukaryotic cells such as HIV-1, splicing is carried out in a series of reactions catalyzed by a ribonuclear protein complex known as the spliceosome. The spliceosome is made up of 6 small nuclear RNAs (snRNAs), each with an associated small nuclear ribonuclear proteins (snRNPs). Cleavage of the target preRNA requires extensive RNA-RNA interactions with the snRNAs and is directed to the appropriate 5' splice donor (SD) and 3' splice acceptor (SA) site and branch point A nucleotide by *cis*-acting signals named splicing regulatory elements (SREs). Assembly of the spliceosome begins with the binding of U1 snRNP to the SD and U2 to the branch point on the preRNA. U4/6 and U5 also bind, bridging the U1 and U2 snRNPs together and forming a bulge (lariat) in the preRNA. The branch point A nucleotide and SD are brought into proximity where the SD is cleaved by the catalytic activity of U5/U6 and the 5' end of the intron is covalently bound to the branch point. U4 dissociates at this stage. The 3' end of the upstream exon is then tethered to the 5' end of the downstream exon, effectively removing the intron lariat, which is degraded. The product is two exons joined together by an exon-exon junction. The HIV-1 genome contains an extensive suite of SD and SA sites that allow the virus to produce over 40 distinct mRNAs from a single 9kb preRNA. The large number of mRNAs possible through the alternative splicing process also allows the virus to tightly control its protein expression profile, allowing a distinction between the early and late phases of its replication cycle. If exported from the nucleus to the cytoplasm before splicing can occur, the 9kb mRNA can be used to express the Gag and Gag/Pol polyproteins. Following the first splice event, which removes the *gag/pol* sequence, the 9kb precursor mRNA is reduced to one of the 4kb mRNAs, from which the Vif, Vpr, Vpu and Env proteins are translated. Further splicing produces one of the 2kb mRNAs from which Tat, Rev and Nef are expressed. Early in the HIV-1 lifecycle, the larger 9kb and 4kb mRNAs are retained in the nucleus by cellular factors, as they contain RNA sequences recognized by the cell as introns. The 2kb mRNAs however, are freely exported to the cytoplasm, where Tat and Rev are translated. The presence of Rev ushers in the late phase of the replication cycle, as discussed in more detail below, however, the expression of Rev

is dependent on the splicing events that produce the 2kb mRNA, demonstrating HIV-1s need for splicing.

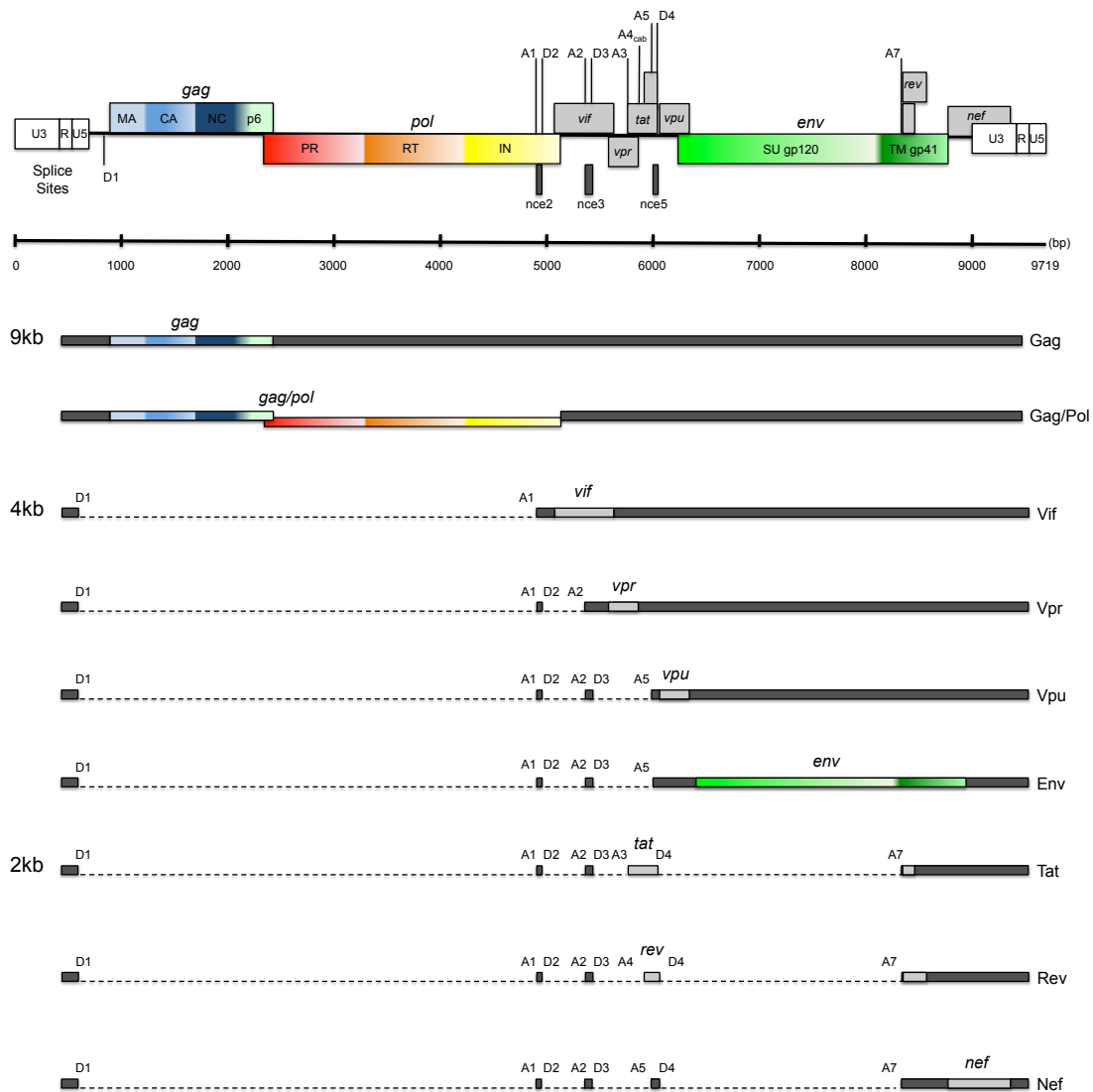


Figure 1.4: Alternative splicing of HIV-1 RNA. The HIV-1 9kb progenitor RNA contains a number of splice donor (D) and acceptor (A) sites embedded throughout its sequence that allow for a wide range of possible spliced variants, summarized above. The RNAs produced by alternative splicing can be broadly grouped into three categories, the ~9kb full-length RNA, the ~4kb partially spliced RNAs and the ~2kb fully spliced RNAs. Not only does the 9kb RNA act as the viral genome when packaged into progeny virions, it also allows for the translation of the Gag/Pol polyprotein which is cleaved to form the Gag structural proteins as well as the Pol viral enzymes. Undergoing a splice event to remove the *gag/pol* sequence, the 4kb partially spliced species of RNA are used to express Env, Vif, Vpr and Vpu. If the RNA undergoes a second splice event to remove the *env* sequence, it forms the 2kb fully spliced RNAs, from which Tat, Rev and Nef are translated. Dark grey = non-coding exon sequence, light grey = protein coding sequence, dashed line = intron removed by splicing.

1.2.5 The Long Terminal Repeats.

The sequences flanking the genome of a retrovirus such as HIV-1 are direct repeated sequences called the long terminal repeats (LTRs) and are highly conserved across many subtypes. The complete 5' and 3' LTRs co-exist only in viral DNA when the virus exists as an integrated provirus. The HIV-1 LTR is divided into 3 sections, including the U3 (unique to the 3' end of the RNA), R (repeated at both 5' and 3' ends of the RNA) and U5 (unique to the 5' end of the RNA) sequences. The U3 region can be broken up further into the modulatory sequence, the Enhancer (E) sequence and the basal sequence adjacent to the transcriptional start site (TSS) Figure 1.5.

The U3 region contains several important transcription factor-binding sites, which serve in assembling the transcription complex and initiating transcription. The cellular transcription factor NF- κ B, a heterodimer of p65/p50, represents one of the main modulators of HIV-1 transcription. NF- κ B binding sites exist in the core promoter of the U3 region and are indispensable for the viral replication (Mingyan et al., 2009). During cell quiescence, NF- κ B is retained in the cytoplasm bound with the inhibitory complex I κ B (Baeuerle and Baltimore, 1988). Phosphorylation and ubiquitination of I κ B allows for the release of NF- κ B from I κ B and its translocation into the nucleus to serve as a master transcription factor. Recruitment of NF- κ B is facilitated by SP-1 binding in the basal promoter of the LTR adjacent to the TATA box (Jones et al., 1988). CCAAT enhanced binding protein (C/EBP) binds to three sequences upstream of the transcription start site (Mondal et al., 1994). C/EBP plays a role in chromatin remodelling by recruiting the SWI/SNF and p300/CREB complexes to enhance access to the viral promoter (Kowenz-Leutz and Leutz, 1999; Mink et al., 1997). AP-1 complex is composed of members of the *c-jun* and *c-fos* families and can act both as a positive and negative regulator of HIV-1 transcription. Following transcription, the HIV-1 RNA adopts extensive secondary structure, which play many important roles in the viral lifecycle.

The R region begins at the transcription start site (TSS (+1)) and encodes for the Trans-activation response element (TAR stem-loop) (Das et al., 1998). This stem-loop plays a critical role when nascent HIV-1 RNA is produced by cellular RNA polIII, allowing for Tat binding and recruitment of P-TEFb (see subsection for Tat). At the 3' LTR, the poly(A) signal stem-loops within the R sequence function by signaling the termination of the polIII and the addition of the poly(A) tail by cellular RNA processing enzymes (Das et al., 1998).

The U5 region combined, together with an adjacent downstream sequence (outside of the LTR), encode the primer binding site (PBS), which serves as the site for cellular tRNAs to hybridize with the viral RNA and primer the initiation of reverse transcription, shortly after entry into a newly infected cell.

Outside of the LTR (further downstream), several other important RNA elements are encoded as a part of the 5' untranslated region (5' UTR). The dimerisation signal (DIS) and packaging signal (Ψ) allow for the duplexing of two copies of the RNA genome and complexing with Gag for packaging (respectively) in the steps preceding virion budding. The major splice donor (D1) is also located within this region (Berkhout and van Wamel, 2000).

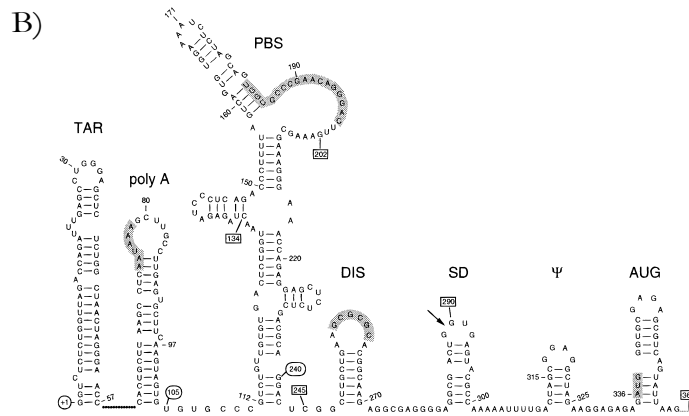
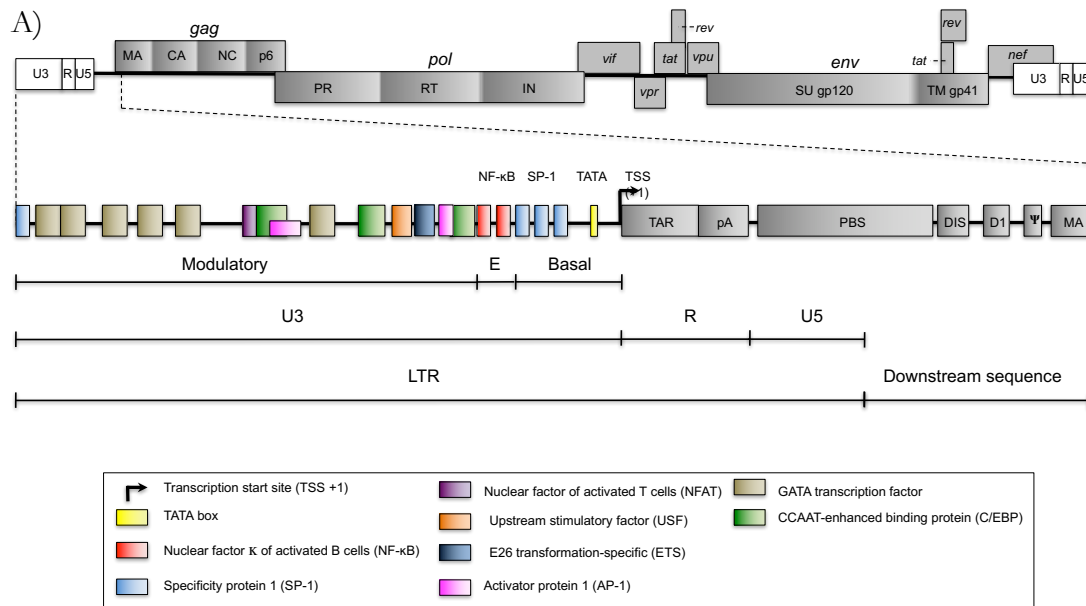


Figure 1.5: The HIV-1 Long Terminal Repeat (LTR) and 5' UTR. A) This diagram shows the viral LTR following reverse transcription in the context of an integrated dsDNA provirus. The U3 region can be broken up further into the modulatory sequence, where transcription factors such as NFAT, AP-1 and C/EBP bind to control transcription, the Enhancer (E) sequence where NF-κB binds, and the basal sequence where SP-1 binds. The R region begins as the transcription start site (TSS (+1)) and encodes for the TAR and poly-A signal (shaded AAUAAA) stem-loops. The U5 region and adjacent downstream sequence encodes for several structural RNA elements including the Primer Binding Site (PBS), which serves as a site for tRNA hybridization and the initiation of the reverse transcription, the dimerisation signal (DIS) and phi (Ψ) packaging signal which serve by allowing the 9kb RNA to be packaged into progeny virions at the budding stage. The major splice donor (D1) is also located within this region. B) The *in silico* predicted nascent RNA, with secondary structure, is also included.

1.3 The HIV-1 lifecycle.

The steps of the HIV-1 replication cycle are shown in Figure 1.6 and the individual steps are described in detail in the text below.

1.3.1 Attachment, entry and uncoating.

Figure 1.6, part 1&2) Retroviruses such as HIV-1 utilize a host cell membrane-derived viral envelope from which its Envelope (Env) glycoproteins extend to mediate attachment and entry into susceptible cells (Zhu et al., 2006). Upon coming into contact with CD4 molecules on the surface of such susceptible cells (Dalglish et al., 1984), the gp120 component of the Envelope trimer attach and undergo a conformational change allowing further binding to co-receptors primarily CCR5 or CXCR4 (Berger et al., 1999). The hydrophobic fusion domain of the gp41 subunits are then exposed and inserted into the cell's plasma membrane, facilitating the fusion of the viral envelope with the host cell plasma membrane. The viral genetic payload, encapsulated within the viral core, then enters the cell. Fusion presents one of the stages in the HIV-1 lifecycle that is currently targeted in some cART regimes by fusion inhibitors (Dorr et al., 2005).

1.3.2 Reverse transcription and integration.

Figure 1.6, part 3) In the cytoplasm of the infected cell, the (+) ssRNA genome (green) is used as a template and converted to complimentary dsDNA (Red) by the viral RNA and DNA dependent DNA polymerase enzyme RT. The RT enzyme also contains an RNase H domain that serves to cleave the RNA component of the RNA-DNA transition state (Furfine and Reardon, 1991). This process is made possible with the LTR sequences that flank the viral genome, and utilizes cellular tRNA_{3^{Lys}} as a primer to initiate the synthesis of DNA (Zhang et al., 1998). This process is also highly error prone, due to the RT enzyme lacking a 3' to 5' proofreading capacity (Boyer et al., 1992), leading to high genetic variation and immune escape. Reverse transcription presents another target for cART therapy (Jonckheere et al., 2000). Figure 1.6, part 4) Once the dsDNA genome has been synthesized, the pre-integration complex (PIC), comprising of the viral genome, IN enzyme, RT enzyme as well as cellular factors including Lens epithelium-derived growth factor (LEDGF)/p75 is formed and utilizes the host cell microtubule network to migrate into the nucleus of the infected cell (Ciuffi et al., 2005). Vpr aids in the reverse transcription and nuclear migration of the PIC (Mansky et al., 2000). Figure 1.6, part 5) Once inside the

nucleus, viral IN enzymes mediates incorporation of the viral DNA into the host cell genome, creating the highly stable state called the provirus.

1.3.3 Gene expression in the early phase.

Figure 1.6, part 6) The integrated provirus utilizes conserved sequences within its LTR to serve as a promoter for RNA transcription initiation, mediated by cellular RNApolIII. The early “pioneer” rounds of transcription (without HIV-1 Tat protein) initiating from the viral promoter are mostly abortive, yielding short functionless transcripts that are quickly degraded. This is due largely to the lack of phosphorylation of polIII and the suppressive cellular factors such as the negative elongation factor (NELF) and DRB sensitivity factor (DSIF) (Pagano et al., 2014). At a low frequency, however, a full length ~9kb transcript will be produced. Figure 1.6, part 7a & b) Cellular spliceosomes assemble on the newly synthesized RNA, splicing out two large intronic sequences, firstly the *gag/pol* sequence in splice event (a), yielding the 4kb mRNAs, then subsequently removing the *env* sequence in splice event (b), yielding the fully spliced 2kb mRNAs (Purcell and Martin, 1993). Figure 1.6, part 8) The 2kb mRNAs are then exported to the cytoplasm via cellular RNA export pathways, independent of HIV-1 Rev protein. Figure 1.6, part 9) From the 2kb mRNAs, HIV-1 Tat, Rev and Nef protein can be translated utilizing cellular ribosome complexes. Figure 1.6, part 10) Tat and Rev both contain nuclear localization signals within their amino acid sequences, and they re-enter the nucleus to execute their primary functions. Re-entry of Tat and Rev effectively ushers in the late phase of the HIV-1 replication cycle.

1.3.4 Gene expression in the late phase.

Figure 1.6, part 6) Tat binds to nascent viral RNA at the LTR promoter and recruits P-TEFb to phosphorylate serine residues on the CTD of RNA polIII, dramatically increasing its elongation capabilities, and allowing for efficient transcription of viral RNA (Ott et al., 2011). Figure 1.6, part 11a & b) With Rev now present within the nucleus of the infected cell, the larger 9kb and 4kb mRNAs are able to be shuttled out of the nucleus into the cytoplasm. Rev achieves this by binding to a secondary structure in the viral RNA, the Rev response element (RRE), then recruiting cellular export pathways (Fritz and Green, 1996). Figure 1.6, part 12a & b) Once the 9kb and 4kb mRNAs are exported to the cytoplasm, the Gag/Pol and Env structural proteins can be translated by cellular ribosomes, and the accessory proteins Vif Vpr and Vpu can execute (or prepare to execute) their functions in modulating the host immune response. Nef and Vpu dampen the host adaptive immune

response by down-regulating the surface expression of CD4, MHC-I and the TCR-CD3 complex (Meusser and Sommer, 2004; Schwartz et al., 1996b).

1.3.5 Budding and maturation.

Figure 1.6, part 13) The structural precursor proteins Gag and Gag/Pol assemble at the inside surface of the cells plasma membrane with the 9kb viral RNA genome (Berkowitz and Goff, 1994; Lener et al., 1998; Murakami and Freed, 2000). The p6 portion of Gag protein facilitates recruitment of cellular protein for endosomal sorting complex required for transport (ESCRT)-dependent budding of virions from the infected cell, taking with them an envelope of the host cell membrane. Vif prevents the activity of the innate immune effector APOBEC3G, protecting the viral genome from deamination (Sheehy et al., 2002). Figure 1.6, part 14) Protease (PR) then mediates the maturation of the newly formed virion, which takes on the characteristic cone shaped structure (Kohl et al., 1988). Protease represents the last target for cART. The now mature virions can then find new cells to infect and begin the cycle anew.

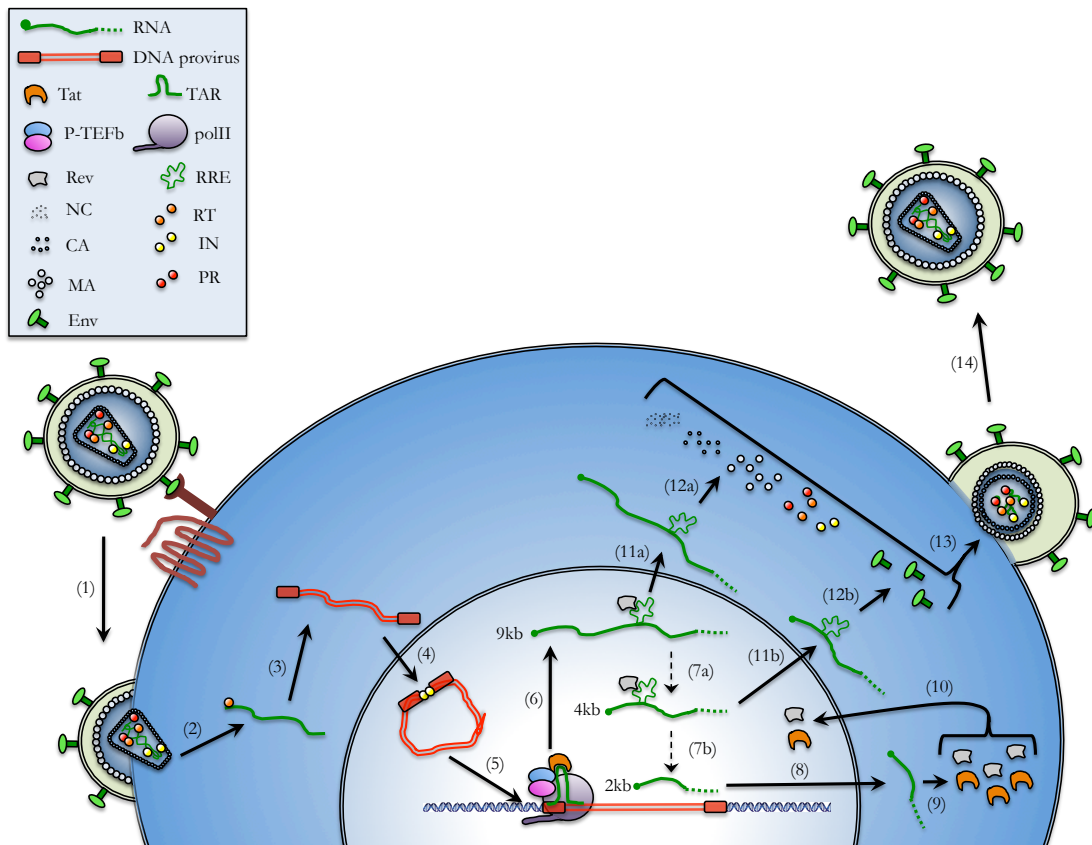


Figure 1.6 The HIV-1 lifecycle. HIV-1 uses its Env glycoprotein to binds to CD4 on the surface of susceptible cells. Further binding of co receptors CCR5 and CXCR4 brings the viral envelope in close proximity to the host cell membrane and facilitates fusion. The viral payload is deposited into the host cell and the capsid shed while the viral Reverse Transcriptase enzyme converts the (+) ss RNA genome into dsDNA. The viral DNA complexes with host factors and viral Integrase enzyme which catalyses the integration of the viral sequence into the host cell genome. Cellular RNA polIII is recruited to transcribe viral RNA initiating at the LTR promoter. 2kb fully spliced mRNA is exported to the cytoplasm to express Tat and Rev, which function in the nucleus to enhance transcription and export of viral RNA respectively. Rev mediated export of the 4kb and 9kn RNAs bring about the late phase of the lifecycle and allow for the translation of the structural proteins encoded by *gag-pol* and *env*. Finally, the 9kb RNA and structural proteins assemble at the cell membrane, and are packaged into new virions that bud from the cell. Protease functions to proteolytically mature the virion particles to a form that may infect new cells and repeat the process anew.

1.4 An Overview of HIV-1 latency and cure.

1.4.1 HIV-1 latency.

The advent of combinational antiretroviral therapy (cART) in 1995 and the development of improved chemotherapies saw HIV-1 infection turn from a near certain death sentence to a manageable chronic illness, saving millions of lives (Gulick et al., 1997). While the implementation of cART undoubtedly turned the tide in the battle against the HIV-1 pandemic, it was quickly realized in the late 1990's that, while progression to AIDS could be delayed indefinitely, HIV+ patients were not cured by cART. The establishment and persistence of a highly stable reservoir of latently infected cells mandated lifelong adherence to cART, lest the latent reservoir reseed infection (Chun et al., 2000). As such, elimination of the latent reservoir has been subject of intense investigation worldwide in the efforts to develop a functional HIV-1 cure (defined below). In the past 20 years, a developing picture of the latent reservoir and the highly diverse and highly complex molecular mechanisms that contribute to it has become clarified. A complete understanding of HIV-1 latency remains elusive however. The reservoir constitutes of as few as a single cell harboring a replication competent provirus per 1 million CD4+ T cells (Finzi et al., 1997). HIV-1 latency is likely a continuum of viral gene expression, from cells that do not express HIV-1 RNA (Lassen et al., 2004; Lassen et al., 2006), to cells that show low levels of HIV-1 RNA, to cells that produce HIV-1 proteins, but not infectious virions. The remainder of this introductory chapter is devoted to summarizing several of the molecular mechanism of HIV-1 latency, specifically those that would be investigated later in the results chapters. While effort has been taken to separate these mechanisms into discrete sections for the purposes of structuring this thesis, these mechanisms are rarely isolated and are more often highly interconnected, occurring simultaneously to drive HIV-1 latency. These mechanisms are grouped into:

- Integration site
- Activation of cellular transcription factors
- Acetylation (of histone)
- Methylation (of histone and DNA)
- Positive transcription elongation factor b (P-TEFb)
- Post translational modifications of HIV-1 Tat protein

To consolidate these diverse mechanisms, a brief overview is also included to summarize, with an explanation of the new approach in the shock and kill method using compound synergy and its possible use in HIV-1 cure.

1.4.2 HIV-1 suppression, viral rebound and a functional cure.

The course of HIV-1 infection and progression to AIDS are broadly outlined in section 1.2.1 and Figure 1.1. The development and widespread use of cART has seen this progression from transmission to inevitable death by AIDS related complications change to one outlined in Figure 1.7. For HIV+ patients, transmission is followed by a sharp peak in viral load, followed by a decrease to the viral set point (Figure 1.7, part 1). Within this time period, the patient receives a diagnosis as being HIV+ and commences their regime of cART. (Figure 1.7, part 2) Adherence to cART typically sees near total suppression of viral replication, where viremia fails to be detected by conventional diagnostic assays. This decay typically occurs in two phases. In the first phase, infected activated CD4+ T cells die rapidly (half-life of days), and during the second decay phase, macrophages and other infected cells die off (half-life of weeks) (Perelson et al., 1996). At this stage, however, the latent reservoir has already established itself, in the GALT, periphery and in sanctuary sites like the CNS. At this point, Figure 1.7 diverges into two of three possible scenarios, the “rebound” scenario (Figure 1.7, parts 3a & 4a) and the “functional cure” scenario (Figure 1.7, parts 3b & 4b), which at the time of writing this thesis remains hypothetical. The latent reservoir has been calculated to be stable up to 60 years despite adherence to cART, the population of (Figure 1.7, part 3a) shows this latent reservoir persisting until cART is interrupted, whereupon the latent reservoir is able to reseed infection (red line) and drive the depletion of CD4+ T cells (yellow line) and the progression to AIDS (Figure 1.7, part 4a). Elimination of the latent reservoir using Latency Reversing Agents (LRAs) has been hypothesized as being a viable method for achieving a functional cure (Figure 1.7, part 3b). A functional cure refers to elimination of all cells that contain an inducible-infectious provirus (and also viremia, blue line), or as many of these cells that the patient will not risk rebound and T cell loss when they cease taking cART (Figure 1.7, part 4b) (green line). This is not to be confused with a sterilizing cure, where all cells containing a HIV-1 provirus, inducible or not inducible (hypermutated/containing major deletions), would be eradicated, which poses a much greater challenge. The third scenario follows lifelong adherence to cART and would therefore be contained entirely within the grey area.

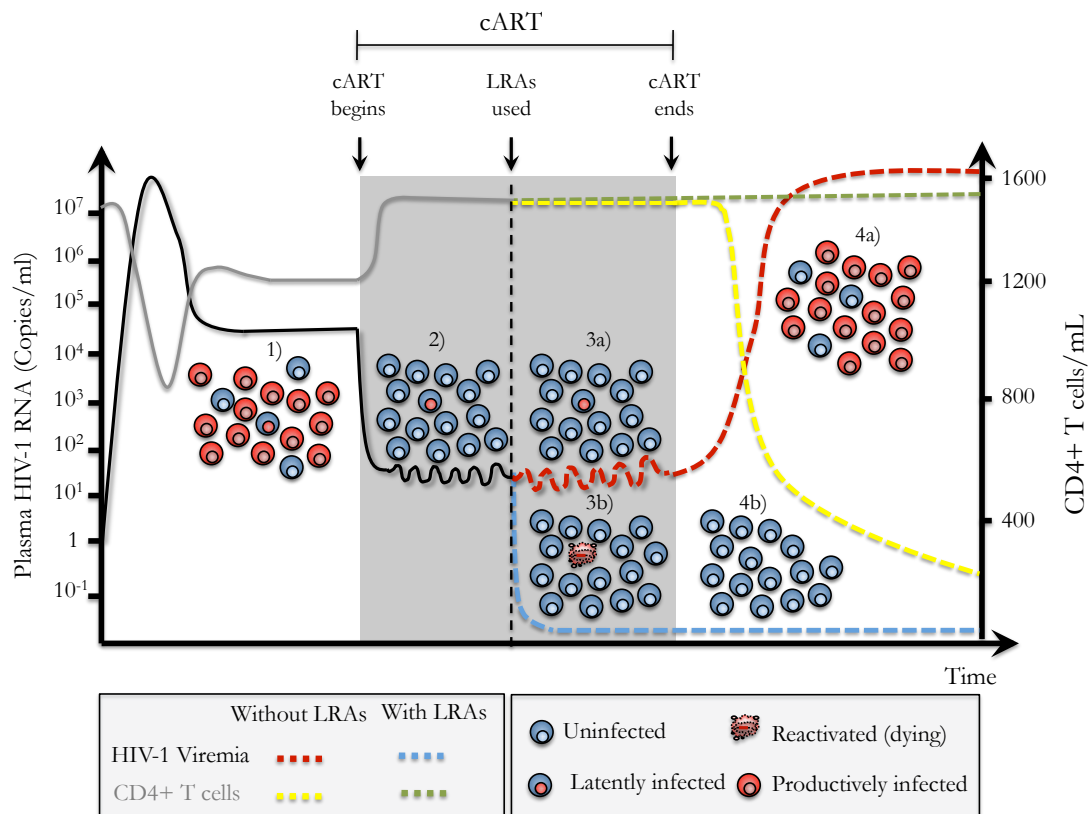


Figure 1.7 HIV-1 suppression, viral rebound and a functional cure. HIV-1 infection sees an early spike in viral load, which is typically controlled to a viral set point within the first few weeks post infection (1). Implementation of combinational antiretroviral therapy (cART) effectively prevents the replication cycle of HIV-1, and brings about a sharp decrease in viral load to below detectable limits and restoration of the CD4+ T cell population (2). At this stage, however, the latent reservoir has been established, and persists in infected patients on cART indefinitely. The figure then branches into two scenarios, with and without eradication of the latent reservoir using LRAs, followed by an interruption of cART. Without eradicating the latent reservoir using LRAs, the latent reservoir persists indefinitely (3a). When cART is interrupted in this scenario, full viral rebound occurs typically within weeks, reseeded from the latent reservoir (4a). Hypothetically, if an effective LRA(s) existed, it could be used to eradicate the latent reservoir while cART was being administered, eradicating cells that contained an inducible, replication-competent provirus (3b). In this scenario, the patient could cease cART and would not suffer viral rebound, effectively becoming HIV- through this functional cure (4b). In reality, a successful functional cure strategy is immensely more complicated, however this figure provides an overview of the worldwide effort at a HIV-1 cure.

1.4.3 The shock and kill method.

The shock and kill method for eradication the latent reservoir is being attempted worldwide to mostly disappointing results. Simplified in Figure 1.8, the model follows treatment with a LRA to “shock” the virus into reactivation, where viral gene expression can recommence. With the expression of viral proteins, the cell would either die due to virus propagation or immune effectors would then recognize the infected cells and target them for eradication. Under the protective cover of continued cART, new infections would be prevented. In this overly simplified, very optimistic model, all of the cells containing inducible provirus (or at least enough for the immune system to keep the remaining reservoir in check) would be reactivated and eradicated. In reality, the challenge of HIV-1 latency is infinitely more complicated and nuanced. A solution will require attempts at a shock and kill approaches, but these have been disappointing for various reasons.

1) The latent reservoir is heterogeneous

The latent reservoir is highly heterogeneous. Is it likely that within a HIV+ patient on cART, no two infected cells will have the exact same integration site and latency scenario (with the exclusion of clonally expanded infected cell). This demonstrates the multiplicity of molecular mechanisms, which govern HIV-1 latency (Darcis et al., 2017). Additionally, the latent reservoir is made up of a number of cell types and locations throughout the body, from peripheral blood, to tissue blocks such as the GALT, to cells protected by the blood brain barrier.

2) Insufficient reactivation

Clinical trials using single LRA treatment regimens have shown disappointing results in the ability of the shock and kill method to deplete the latent reservoir (HIV-1 DNA). This is most probably due to insufficient reactivation of a large enough proportion of the latent reservoir using single LRA agents. It is a major theme of this thesis and has recently been shown in the literature that combinations of mechanistically diverse LRAs may help overcome this hurdle (see section 1.5.11) (Laird et al., 2015).

3) Reactivation is stochastic

Reactivation of HIV-1 using maximum T cell activation, with antigen or mitogen, leaves some inducible provirus in a silent state, where it was potentially inducible by subsequent rounds of reactivation, demonstrating that multiple rounds of LRA treatment is likely necessary (Ho et al., 2013).

Following the shock, was the kill which in itself is a highly complex issue. Reactivation and restoration of viral replication is not likely to be sufficient at eradicating the reactivated cells, rather, macrophages which contribute to the latent reservoir are quite resistant to the cytopathic effects of HIV-1 replication. It would therefore be essential that a robust CTL immune response be mounted against reactivated cells displaying viral peptides on their MHC complexes (Shan et al., 2012). As a multi-pronged approach to the shock is clearly necessary, likewise, a similar multi-pronged approach to the kill will be necessary. A future “kill” strategy will likely include: a therapeutic vaccine (Margolis et al., 2016) broadly neutralizing antibodies (Stephenson and Barouch, 2016) and immune checkpoint inhibitors (Leth et al., 2016).

To date, attempts at using the shock and kill method have not proven successful in a functional cure. The continued push to discover new mechanistically diverse LRAs and synergistic combinations shows promise that effective regimes may be possible in the near future. The work contained in this thesis aims to build on these efforts.

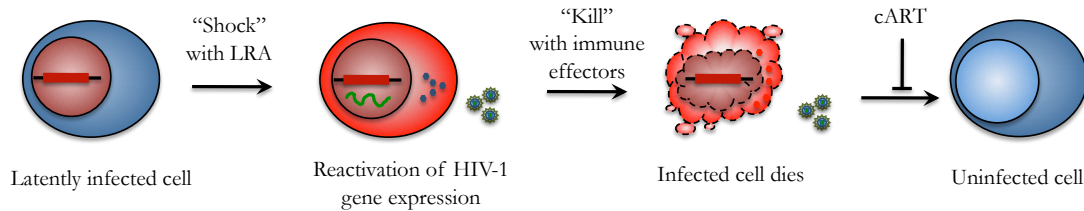


Figure 1.8. The shock and kill model. The shock and kill model was conceived as a possible mechanism to eradicate the pool of latently infected cells that persist during cART. As the name suggests, the mechanism is two pronged. Firstly, for the “shock” component, a LRA, or synergistic combination of LRAs, would be used to induce viral gene expression from the silenced provirus within the latently infected cells. The production of viral proteins within the infected cell would lead to presentation of viral peptides, complexed with MHC-I on the cell surface, allowing for recognition by immune effectors. Additionally, the viral replication within the cell would trigger cell death pathways, killing the infected cell simply through the cytopathic effects of viral replication. Together, these two factors contribute to the “kill” component. Importantly, new infection of susceptible cells is prevented by cART. As with the model presented in Figure 1.7, this represents a overly simplified, highly optimistic approach to clearing the latent reservoir, considering each latently infected cell is unique in the molecular restrictions imposed on the integrated provirus and therefore present many unique challenges within a single patient. Additionally, the ability or inability of different drugs to access the many different latent reservoirs (ie different tissues) is also likely to be very challenging to overcome.

1.5 The molecular mechanisms of HIV-1 latency.

1.5.1 Integration sites and HIV-1 latency.

At very low frequencies, HIV-1 infected activated CD4⁺ T cells result in latently infected cells, where viral gene expression is significantly or totally suppressed through various mechanisms. While the availability of cellular and viral transcription factors and the chromatin architecture surrounding the integrated provirus all contribute to HIV-1 latency in a significant way, they are all reliant firstly upon the site at which the virus integrates within the host cell genome. Following reverse transcription of the viral genome into cDNA, host factors, along with viral proteins, bind the viral DNA genome thereby guiding integration (Section 1.2.3), which predominantly targets intronic regions of actively transcribed cellular genes (~93% in CD4⁺ T cells from HIV⁺ patients on cART (Han et al., 2004). Once integrated, the provirus can be silenced by a range of integration site-dependent mechanisms, summarized in Figure 1.9. While integration events that result in a latent infection occur typically within actively transcribed regions of the genome, integration events are not specific to a single gene or set of genes, although “integration hotspots” have been reported (Schröder et al., 2002). As such, with each infection of a unique cell that results in latency, a unique scenario is presented, where it is unlikely that any two cells will be alike, discounting clonal expansion which may occur later. As some cellular genes expressed constitutively, some sporadically and some not at all, depending on the stage cell development and activation state, the gene targeted is the first broad contributor to HIV-1 latency (Figure 1.9). Steric hindrance is another contributing factor to HIV-1 latency. In this scenario, integration occurs downstream of a strong cellular promoter. Transcription initiates from this cellular promoter and the transcription machinery, RNA polII, elongates along the cellular gene into the integrated LTR sequence, where transcription initiation factors (TFs) are assembling to initiate a second HIV-1 transcription event. The progress of the polII complex through the LTR displaced the TFs through steric hindrance, preventing HIV-1 transcription events. Of great importance for this thesis, this scenario would generate a preRNA that contained the entire HIV-1 sequence embedded with the cellular RNA sequence (Figure 3.1). Interruption of the native splicing pattern of the cellular gene and incorporation of HIV-1 exonic sequence into the mature cellular mRNA would then producing a chimeric mRNA from which HIV-1 gene expression could possibly occur.

This mechanism of HIV-1 gene expression lead to the hypothesis that began the work contained in this thesis and is summarized in Figure 3.1. Integration not only occurs in a largely non-specific manner in terms of its gene target, but also in terms of its orientation, relative to the cellular gene into which it integrates. As such, a random proportion of integration events result in a “backwards” provirus. This presents an interesting scenario, as successful transcription initiation/elongation events occurring simultaneously at the cellular promoter and viral LTR may result in a “collision event”, leading to premature termination of RNA transcription for both the cellular gene and HIV-1 RNAs. Enhancer trapping: Proximity of the integrated LTR to the cellular promoter could potentially lead to the phenomenon of enhancer trapping, where assembly of transcription factors at the viral LTR’s enhancer region enhance the cellular promoters transcription efforts and counteract transcription from the LTR.

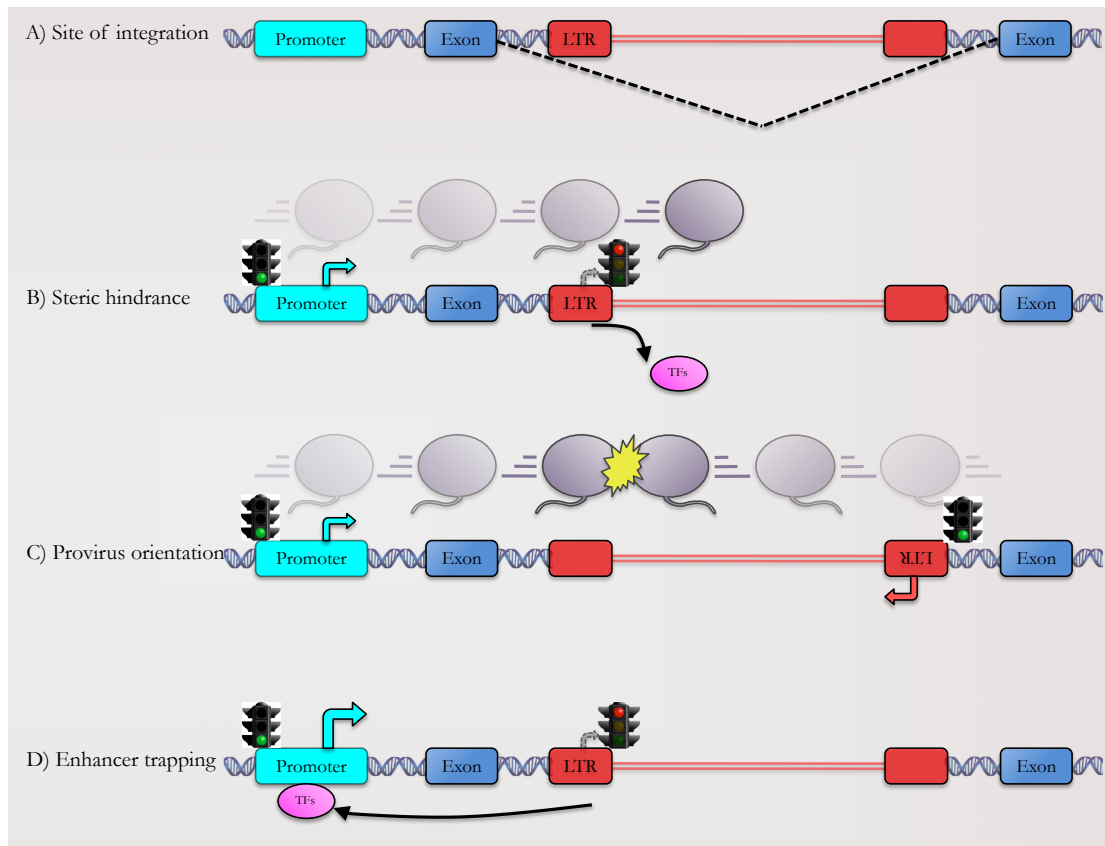


Figure 1.9 Transcriptional interference and HIV-1 latency. HIV-1 integration occurs predominantly within the intronic sequences of actively transcribed genes, with each integration event providing a unique set of possible restrictions on viral gene expression. Following integration, several factors relating simply to the site of integration can contribute to HIV-1 latency. A) This condition is highly dependent on the specific gene (or intron of the gene) where HIV-1 integrates, where some genes will have a very low level of constitutive expression. B) Steric hindrance refers to the phenomenon where transcription events initiate from a strong upstream cellular promoter, elongate through the proviral LTR and displace the transcription factors (pre-initiation complex) assembling at the viral promoter. Of note, the RNA produced will contain the entire viral sequence embedded within the RNA transcribed from these cellular genes (Figure 3.1). C) The orientation of the integrated provirus, relative to the cellular gene in which it has integrated, can also play a part in latency. If integrated in the reverse orientation, Transcription events initiation at the cellular promoter and viral LTR can lead to collision events of the elongating RNA polIII complex. D) Proximity of a strong cellular promoter upstream of the viral LTR can lead to enhancer trapping, where the enhancer (NF- κ B binding region) of the U3 can enhance cellular transcription events in preference of HIV-1 transcription events.

1.5.2 Activation of cellular transcription factors.

As an obligate intracellular parasite, HIV-1 is highly dependent on numerous cellular transcription factors for mediating viral gene expression. As such, the viral LTR promoter is littered with the binding sites of many important transcription factors including NF- κ B, NFAT, STAT, SP-1 and AP-1 (Figure 1.5). Activation of these transcription factors drives efficient transcription from the viral LTR, and is necessary for reversing HIV-1 latency, with the aid of HIV-1 Tat protein. Overcoming restrictions on several diverse activation pathways is therefore required, these are summarised in Figure 1.10. NF- κ B represents one of the master regulators of cellular transcription and is activated via the activity of protein kinase C θ (PKC), which assumes centre stage in the T cell supramolecular activation cluster, a complex interwoven network of proteins that result from extracellular stimuli. Following stimulation, production of diacylglycerol (DAG) in the plasma membrane, results in translocation of PKC from the cytosol to the plasma membrane. At the plasma membrane, PKC phosphorylates a protein named CARD (Caspase recruitment domain)-containing MAGUK protein 1 (CARMA1), which functions as a molecular scaffold for the assembly of a multiprotein complex comprising of Bcl10, MALT1 and the I κ B kinase (IKK). The IKK in turn is made up of the heterodimer IKK α and IKK β with the NF- κ B essential modulator (NEMO), and function by phosphorylating serine 32 and serine 36 on the inhibitory I κ B molecule that sequesters the NF- κ B p50/p65 heterodimer inactive in the cytoplasm. As a result, the I κ B molecule is subsequently polyubiquitinated, and degraded by the proteasome, freeing the NF- κ B p50/p65 heterodimer, and allowing for its translocation to the nucleus and displacement of the inhibitory p50:p50 homodimer (Williams et al., 2006) (Figure 1.10 A). Following stimulation, an influx of calcium ions (Ca²⁺) into the cell allows for binding to the serine/threonine protein phosphatase calmodulin-calcineurin complex, inducing a conformational change that results in the dephosphorylation of NFAT. NFAT may then translocate into the nucleus to execute its function (B). The JAK/STAT pathway transmits information from extracellular chemical signals (cytokines) through the use of three major components: the cell receptor on the cell surface, the Janus kinase (JAK) and a dimerised signal transducer and activator of transcription (STAT) protein. Following cytokine-receptor binding, associated JAK proteins are activated, allowing for the phosphorylation

of tyrosine residues located on the cytoplasmic region of the receptor molecule. STAT proteins can now dock to the newly phosphorylated receptor molecule by their SH2 domains, allowing for subsequent phosphorylation of tyrosine residues by JAK. The activated STAT molecules then undergo dimerisation and translocation to the nucleus (C). The mitogen activated protein kinase (MAPK) pathway results in the activation of cFos-cJun (AP-1). The cascade commences when a receptor comes into contact with its specific ligand (eg a cytokine), resulting in the recruitment of small G proteins and the phosphorylation of a MAPKKK, which phosphorylates MAPKK, which in turn phosphorylates MAPK. In the case of AP-1 activation the MAPK involved is the Jun N-terminal kinase (JNK), which phosphorylates serine 63 and serine 73 on cJun. cFos then dimerises with the phosphorylated cJun, forming the AP-1 transcription factor, which can translocate into the nucleus (D). Interaction between the viral protein Tat and cellular DNA-dependent protein kinase (DDPK) results in the subsequent phosphorylation of serine 121 of SP-1, resulting in increased transcription mediated by SP-1 (E). For this thesis, three compounds were chosen to serve as representative transcription factor activators: TNF α , PMA and Bryostatin-1. TNF α is a cell signaling protein cytokine which functions primarily in the regulation of immune cells. TNF α functions by binding to the TNF receptor and triggers the activation of NF- κ B and AP-1 through the PKC/ NF- κ B and MAP kinase pathways respectively. PMA (phorbol 12-myristate 13-acetate) has a structure analogous to that of diacylglycerol (DAG), and as such is a potent activator of the PKC pathway. Bryostatin-1 is also a potent modulator of the PKC pathway.

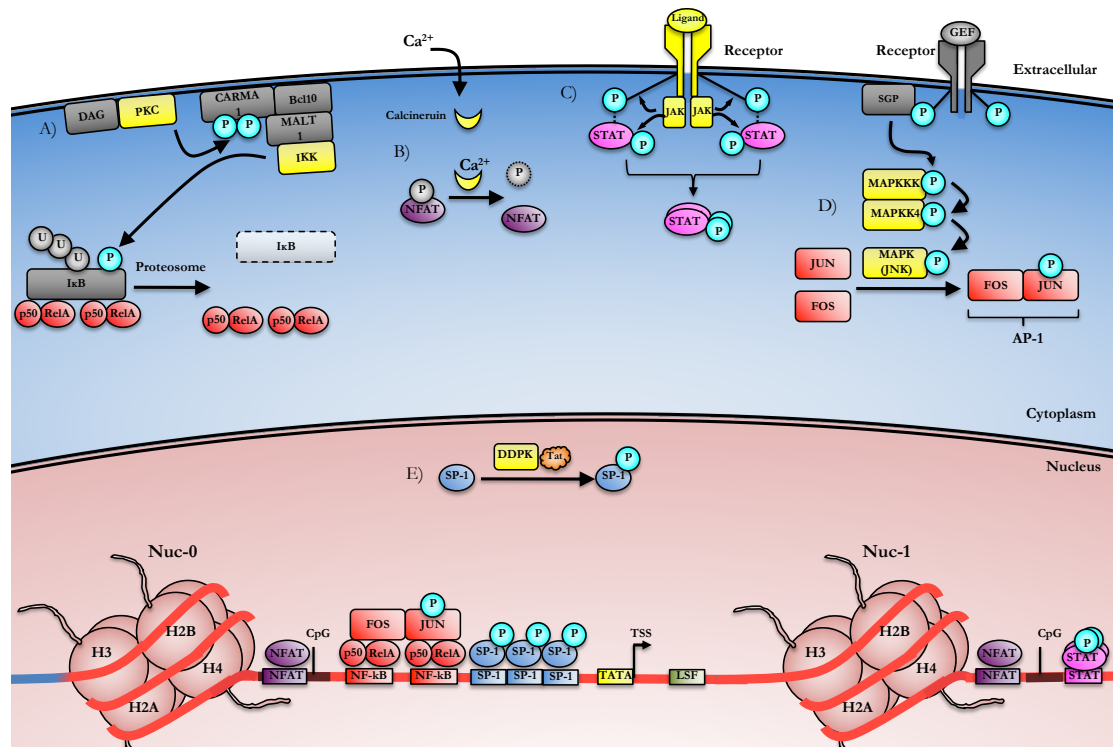


Figure 1.10 Activation of cellular transcription factors. The integrated provirus is dependent of several cellular transcription factors for efficient transcription initiation. A) Recruitment of PKC promotes phosphorylation scaffold protein CARMA1, resulting in the recruitment of the IκB kinase (IKK), phosphorylation of IκB and release of NF-κB. NF-κB then translocates into the nucleus. B) Influx of calcium (Ca^{2+}) allows the phosphatase calmodulin-calcineurin complex to dephosphorylate NFAT in the cytoplasm, allowing translocation into the nucleus. C) Stimulation of cell surface signal translocation receptors causes dimerisation, which allows JAK to bind and phosphorylate tyrosine residues, forming a docking site for STAT proteins, which are in turn phosphorylated by JAK. Once phosphorylated, these STAT proteins dimerise and are translocated into the nucleus. D) Activation of the MAP kinase cascade follows stimulation of a small G protein by a guanine-nucleotide exchange factor (GEF), phosphorylating MAPKKK, which phosphorylates MAPKK, which sequentially phosphorylates MAPK. MAPK (JNK) can then phosphorylate c-Jun, where it can dimerize with c-Fos, forming AP-1, which translocates into the nucleus. E) HIV-1 Tat protein can bind to the DNA-dependent protein kinase (DDPK) to phosphorylate the ubiquitous SP-1 transcription factor.

1.5.3 Chromatin structure.

In eukaryotic cells, genomic DNA is packaged in the nucleus by the formation of a complex structure called chromatin. Chromatin comprises of repeating units called nucleosomes, made up of 146bp of DNA wrapped around a histone octamer (containing two copies of four histone proteins: H2A, H2B, H3 and H4). Histone protein 1 (H1) is recruited for the formation higher order chromatin, but does not make up the “bead on a string” structure that is the nucleosome. The nucleosome is a stable DNA-protein complex, however is also highly dynamic, tightly controlling DNA replication, DNA repair and access of transcription factors to the underlying genes for gene expression (Li et al., 2007). This tight regulation of gene expression (epigenetics) is achieved through post-translational modifications of histone amino-terminal tails include acetylation, methylation, phosphorylation, ubiquitination/sumoylation ((Fischle et al., 2003; Schotta et al., 2004) and is referred to as the histone “code” (Jenuwein and Allis, 2001). These modifications mediate the transition of chromatin between two states: euchromatin, a decondensed form that readily allows for expression of the underlying genes and heterochromatin, a tightly packed form where access to the underlying genes is more restricted.

Hyperacetylated histone is typically associated with euchromatin and gene expression (Hodges et al., 2009), as the acetyl group neutralizes the histone net-positive charge, destabilizing the histone-DNA interaction (Hong et al., 1993) (Figure 1.11). Conversely, deacetylated histone is typically associated with heterochromatin and a lack of gene expression (Lin et al., 2011). Regions of the chromosome that are associated with low levels of transcription, i.e. at the centromeres and gene deserts, are constitutively in the heterochromatin state. Within the nucleus, histone acetylation results in the recruitment of nucleosome remodeling SWI/SNF complexes containing the ATP-dependent helicase BRG1 (SMARCA4). Other notable members of the ATP-dependent remodeling family are the INO80, ISW1 and CHD complexes. As acetylation and methylation of histones plays a large role in the transitions between these two states, and therefore also on gene expression, they are of great interest in the field of HIV-1 latency. During HIV-1 latency, p50:p50 homodimers bind to the NF- κ B binding site within the viral LTR and recruit CBF-1 and HDAC-1 (Tyagi and Karn, 2007). Likewise HDAC-1 and HDAC-2 are recruited to the LTR via SP-1 and the SP-1 binding site. The recruitment of HDACs to the LTR promotes the removal of acetyl groups from Histone H3K9, and prevent transcription by RNA polIII through repressive chromatin structure (Williams et al., 2006) (Figure 1.11 and

1.15a). Activation of the PKC and the NF- κ B pathway results in the presence of p50:p65 heterodimers and displacement of the p50:p50/HDAC complex at the LTR, resulting in acetylation of histone, relaxing of chromatin structure and alleviation of transcriptional repression. Blocking histone deacetylation using HDAC inhibitors can lead to reactivation of viral gene expression from purified resting CD4⁺ T cells and is at the heart of several clinical trials in the HIV-1 cure field. For this thesis, three compounds were chosen to represent the HDAC inhibitors: Vorinostat (panHDACi), Panobinostat (panHDACi) and Romidepsin (HDAC1 and HDAC2 inhibitor).

1.5.4 Acetylation and deacetylation.

Acetylation of histone and other protein substrates is controlled by two groups of enzymes: the histone acetyltransferase (HATs), which add acetyl groups to the lysine residues within histone tails and histone deacetylase (HDACs), which counteract HATs by removing these acetyl groups. The HAT enzymes grouped based on their structure, action and subcellular localization.

- Gcn5-related N-acetyltransferase (GNAT) family (hGCN5, PCAF, ELP3)
- MYST family (TIP60, MYST1-4)
- p300/CBP
- TFIIIC90, TAF1
- SRC1, ACTR, p160

Type A HATs are located in the nucleus, whereas the Type B enzymes are located in the cytoplasm where they modify histones newly translated at the endoplasmic reticulum (Neuwald et al., 1997; Richman et al., 1988; Torchia et al., 1998). Outside of their role in modulating the histone code, CBP/p300, GCN5 and PCAF can also acetylate HIV-1 Tat and other cellular proteins to modulate its function dramatically (Figure 1.14a), and therefore these HAT enzymes are more correctly termed lysine acetyltransferase enzymes (KATs), as they may act upon numerous non-histone substrates (Ott et al., 1999). Acetylation of histone proteins is a reversible process, which is counteracted by the function of deacetylase enzymes. HDACs have been divided into several classes (Hayakawa and Nakayama, 2010):

- Class I (HDAC1/2/3/8)
- Class II (HDAC4/5/7/9)
- Class IIa (HDAC6/10)
- Class III (Sirtuins)
- Class IV (HDAC 11)

HDACs commonly form multiprotein complexes to perform their deacetylation function. Such complexes include: the nuclear remodeling and deacetylation complex (NuRD), which contains ATP-dependent chromatin remodeling and deacetylation functions, the Sin3 complex, which binds to DNA-binding proteins and functions broadly as a transcriptional repressor, the Co-REST and N-CoR complexes which also function in gene repression. The Sirtuin HDAC (SIRT1) functions in a NAD⁺ dependent manner,

removing acetyl residues from H4K16 (Vaquero et al., 2007). SIRT1 ties histone acetylation to methylation by activating Suv39H1.

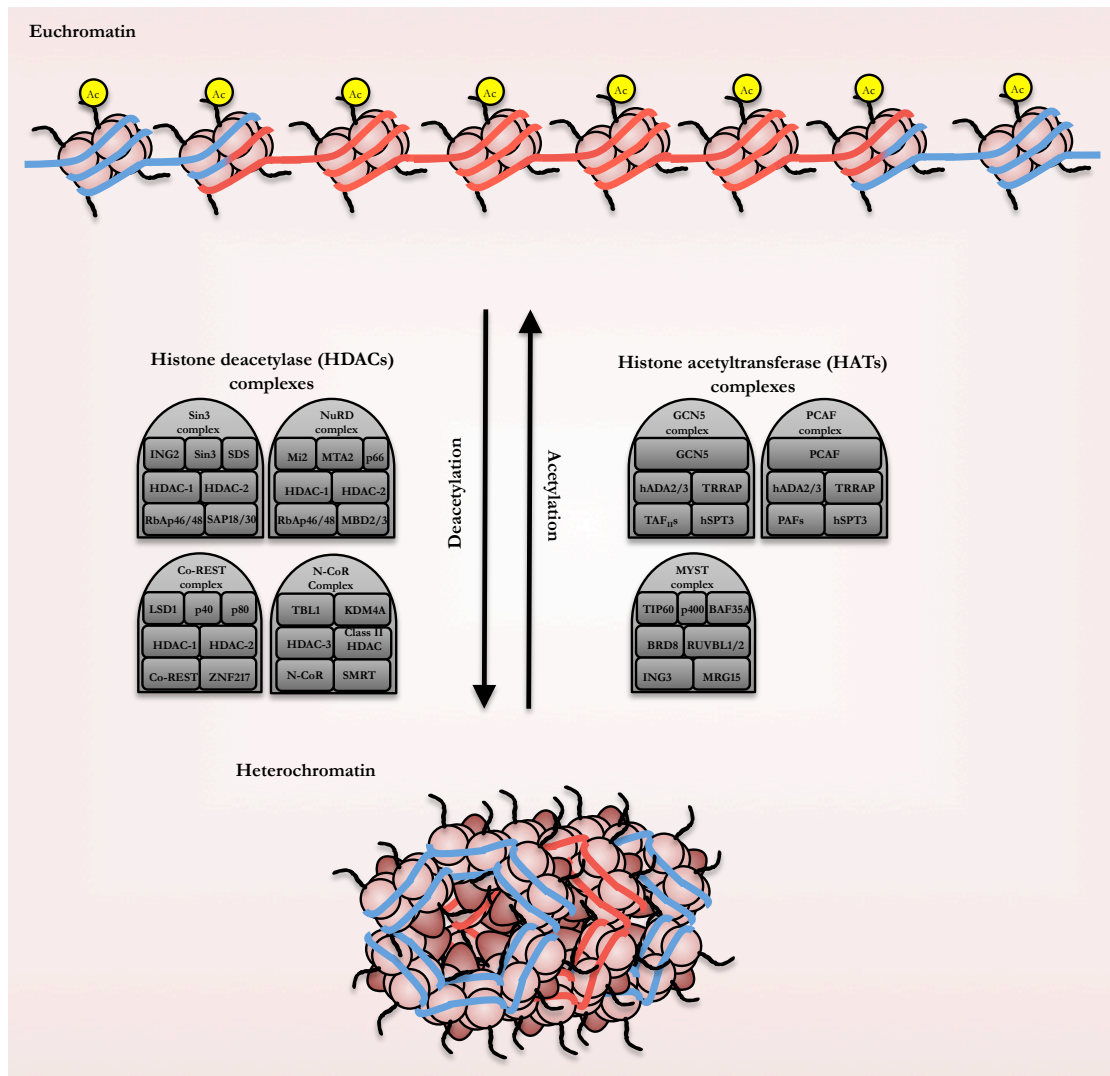


Figure 1.11 Chromatin structure, acetylation and deacetylation. In eukaryotic cells, DNA is packaged as chromatin, a highly dynamic DNA-protein complex that tightly controls DNA replication, DNA repair and access of transcription factors to the underlying genes for gene expression. Chromatin exists in one of two states, euchromatin, a decondensed form that readily allows for expression of the underlying genes and heterochromatin, a tightly packed form where access to the underlying genes is more restricted. Transition between these two states is controlled by post-translational modifications of histone proteins. Histone deacetylase (HDAC) complexes strip acetyl groups from histone, driving heterochromatin formation, whereas histone Acetyltransferase (HAT) complexes add acetyl groups to histones in the formation of euchromatin.

1.5.5 Methylation.

Acetylation and methylation of lysine residues (K) within histone 3 (H3) and histone 4 (H4) proteins play key roles in chromatin structure and gene expression/repression. These modifications are tightly controlled by a suite of histone acetyl and methyl transferase enzymes HATs and HMTs, as well as histone deacetylase and demethylase enzymes HDACs and HDMs. All acetylation modifications of histones are activating in terms of gene expression. Several of the key histone residues that are acetylated are: K9, 14, 27 and 36 on H3 and K5 and 16 on H4. Methylation modifications, on the other hand, are a more complex pattern or posttranslational modifications. Methylation (of a single histone) can be either activating or repressing, depending on if the histone is mono-, di- or tri- methylated. Figure 1.12 shows the modifications of histone 3 and histone 4, however, acetylation and methylation do not occur simultaneously.

Activating methylation markers

-H3K4: Mono-, di- and trimethylation of lysine 4 by SET1 results in the recruitment of chromodomain-helicase-DNA-binding protein 1 (CHD1) and the nucleosome-remodeling factor subunit BPTF to open chromatin and allow for gene expression, as well as inhibiting the NuRD (HDAC) complex. (Flanagan et al., 2005; Kuzmichev et al., 2002; Li et al., 2006)

-H3K9: monomethylation of lysine 9 by G9a/Suv39h1 is a hallmark of activation, commonly associated with the promoters of active genes (Imai et al., 2010; Karmodiya et al., 2012).

-H3K27: While di- and trimethylation of histone 27 are strong marks of gene repression, monomethylation is associated with active promoters.

-H3K36: Methylation of H3K36 in yeast occurs on nucleosomes that are displaced in preparation for passage of RNA polIII (Carrozza et al., 2005)

-H3K79: Mono- and dimethylation of H3K79 is associated with activation of gene expression, whereas, interestingly, trimethylation has been shown to be both activating and repressive.

-H4K20: Lysine 20 of histone 4 is not acetylated but exclusively methylated. Monomethylation is present at active promoters, and is only catalysed by PR-set7 (Beck et al., 2012).

Repressive methylation markers

-H3K9: Di- and trimethylation on histone 9 involving COUP-TF interacting protein (CTIP-2) and Suv39h1 assembling with SP-1 and HDAC1/2 at the LTR (Marban et al., 2005) can recruit heterochromatin protein 1 (HP1) (Cheutin et al., 2003) which plays an important role in the process of HP1 spreading, termed position effect variegation (PEV) and heterochromatin formation.

-H3K27: Di- and trimethylation of H3K27 is strongly associated with gene repression. While most histone methylations are catalyzed by several enzymes, the EZH2 methyltransferase component PRC2 complex is alone implicated in controlling all 3 forms of H3K27 methylation (Ferrari et al., 2014; Kuzmichev et al., 2002)

-H3K79: see above

-H4K20: Trimethylation of lysine 20 of histone 4 by PR-set7 is a repressive marker (Wu et al., 2010).

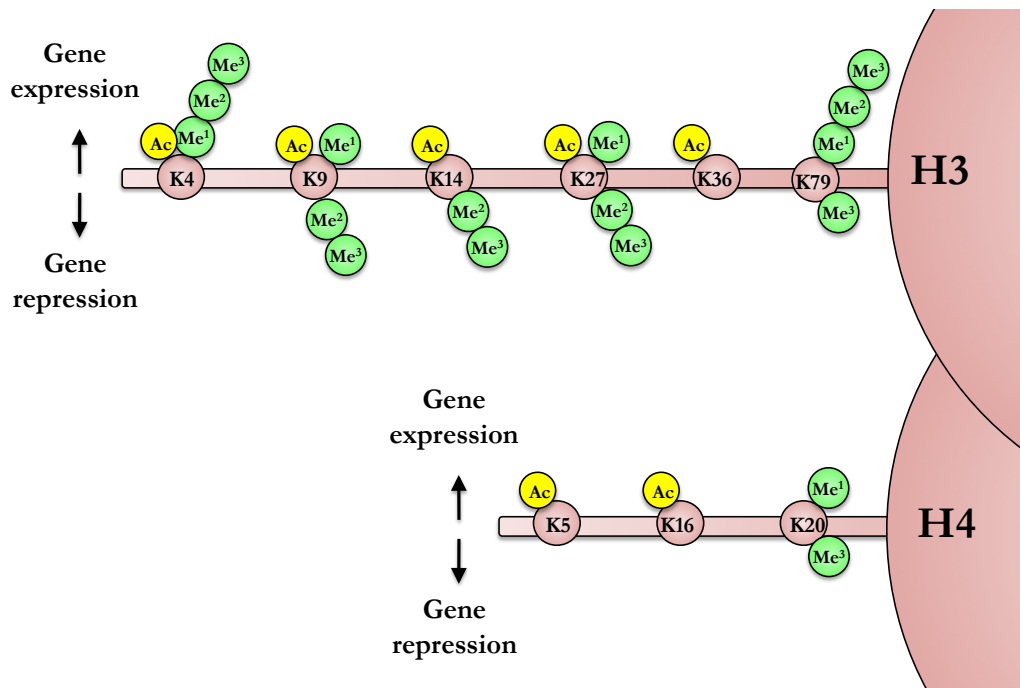


Figure 1.12 Posttranslational modifications of histone tails. The post translational modifications of the N-terminal tails of histone 3 and histone 4 play a major role in chromatin structure and gene expression, known as the histone code. Acetylation events are always marks of activation, euchromatin and gene expression from the underlying DNA. Methylation is a more dynamic modification and can be either activating or repressing, even within the same histone. Trimethylation of H3K4, in combination with acetylation of H3K9 an H3K14 are hallmarks of an active gene promoter, whereas trimethylation of H3K9 with H3K14 and H3K27 is a sign that the underlying gene is repressed.

1.5.6 DNA methylation.

Histone modification, acetylation and methylation, are tightly interconnected in the greater process of writing the histone code and modulating gene expression, however the histone code contributes to the higher level of gene expression regulation called the epigenetic code, which includes DNA methylation. Unlike histone modifications, which are highly dynamic and may be modified readily when gene expression is required or if gene expression needs to cease, DNA methylation represents a less readily reversible modification, commonly used for long term gene silencing (Jones 2001). Cytosine (C) residues linked to an adjacent downstream guanine (G) by a single phosphate form a CpG dinucleotide, which act as a site for DNA methylation. CpG sites are commonly methylated in eukaryotes, however CpG islands, sequences enriched for CpG dinucleotides, are generally unmethylated (Brandeis et al. 1994). DNA methylation occurs following histone deacetylation and di- and trimethylation. For the HIV-1 promoter during latency, HDACs complex with centromere-binding-protein 1 (CBF-1), heterochromatin protein 1 (HP1), CTIP-2 resulting in the removal of acetyl groups from H3K9 and H3K27. Methylation by Suv39h1, G9a and EZH2 methyltransferases follows (Epsztejn-Litman et al., 2008; Lehnertz et al., 2003) (Figure 1.13). DNA methyltransferase enzymes (DNMTs) are then recruited and hypermethylate the CpG island located adjacent to Nuc-1, which in turn recruits the Methyl-CpG Binding Protein 2 (MBD2) and the NuRD remodeling complex (Kauder et al., 2009). DNA methylation also introduces steric hindrance which interferes with the native bending of the double helix structure in the major groove, which also affects nucleosome positioning and chromatin structure (Nathan and Crothers, 2002). Finally, DNA methylation can occlude the binding sites of many important transcription factors: NANOG, SOX2, KLF4, OCT4, TAF1 and p300, contributing to gene repression (Lister et al., 2009).

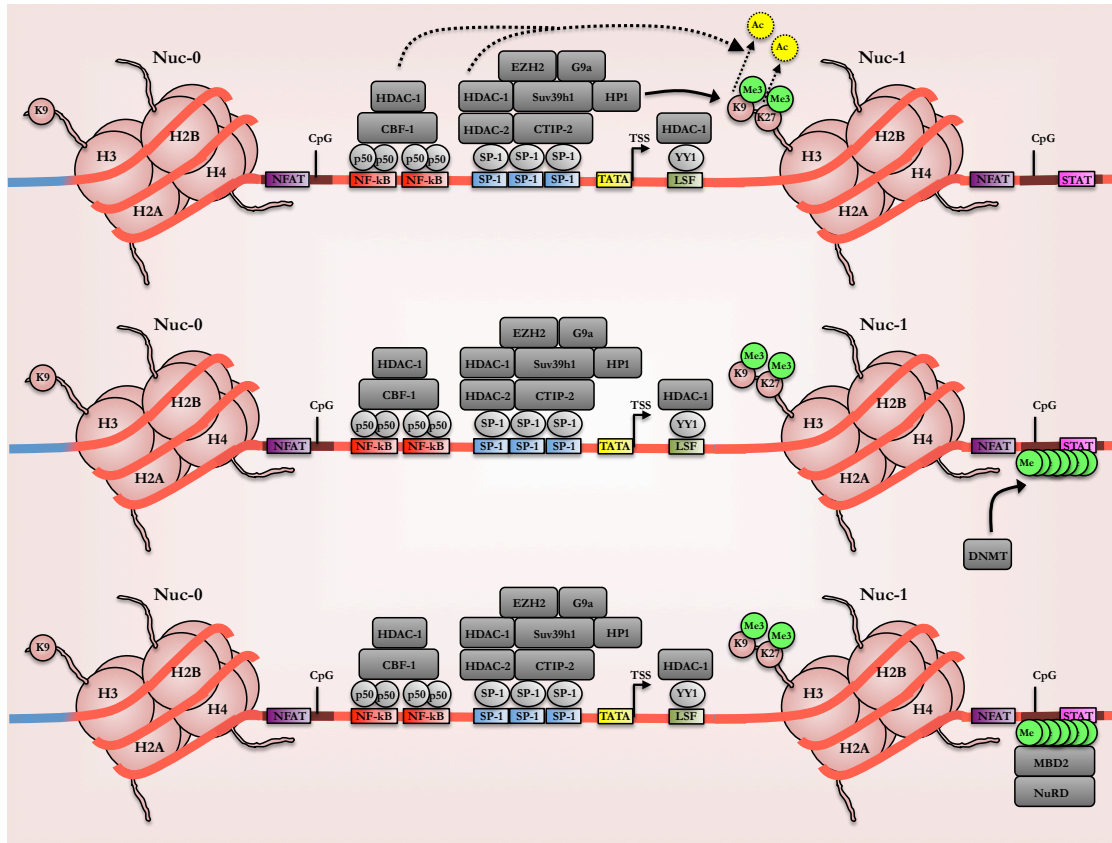


Figure 1.13: DNA methylation in HIV-1 latency. Deacetylation and methylation of histone proteins can be associated with methylation of DNA CpG islands, which also contributes to gene silencing. At the LTR promoter, HDAC complexes bind to p50:p50 homodimer at the NF-κB binding site and to SP-1 at the SP-1 binding sites. Acetyl groups are stripped from H3K9 and H3K27 residues and subsequently trimethylated by histone methyltransferases Suv39h1, G9a and EZH2. DNA methyltransferase complexes are recruited and hypermethylate CpG dinucleotides adjacent to the Nuc-1, allowing for the recruitment of Methyl CpG binding protein (MBD2) and the chromatin remodelling complex NuRD. The provirus is then tightly wrapped up within heterochromatin structure, and viral gene expression is repressed.

1.5.7 The Positive Transcription Elongation Factor b (P-TEFb).

HIV-1's transactivator of transcription (Tat) protein is the master regulator of HIV-1 gene expression through its role in promoting efficient transcription elongation (Kao et al., 1987a), and is the protein of single most importance in reactivating viral gene expression from latency and for this thesis. As such, the following three sections are devoted to the interactions Tat has with the essential transcription factor positive transcription elongation factor b (P-TEFb), the post translational modifications of Tat and their effects on the many roles Tat plays in viral gene expression, and finally how Tat overcomes transcriptional pausing to drive efficient transcription elongation. Cellular gene expression is tightly controlled at several levels, but perhaps none more so than at the transcription level. One of the ways eukaryotic cells regulate their gene expression at the transcription level is by the interplay of positive and negative transcription factors, the abundance of which depends on the cell's global transcriptional demands.

P-TEFb is a cyclin dependent kinase that acts by hyperphosphorylating serine residue 5 (with CDK7) and serine residue 2 (with CDK9) within YSPTSPS heptapeptides on the C-terminal domain (CTD) of RNA polymerase II (polII) (Garriga 2004); (Price, 2000) which greatly enhances polIIs transcription elongation capabilities (Zhu et al., 1997) P-TEFb consists primarily of heterodimers of Cyclin T1 and its Cyclin dependent kinase CDK9, however other combinations of cyclins (T1 & K) and CDKs are possible (Fu et al., 1999). When not immediately needed, P-TEFb is sequestered in the cytoplasm in an inactive complex composed of the 7SK small nuclear RNA (snRNA) (Nguyen et al., 2001); (Yang et al., 2001), and HEXIM1 (Jeronimo et al., 2007; Krueger et al., 2008; Markert et al., 2008) (Figure 1.14). The complex contains two additional protein partners to further ensure its stability. At the 5' end of the RNA, the 7SK-capping enzyme MePCE is located, which serves to methylate the 5' end of the RNA, protecting it against exonuclease activity. (Bayfield et al., 2010). At the 3' end of the RNA, the La-related protein 7 (LARP7) binds to confer additional stability. While bound in this 7SK snRNP complex, the kinase activity of P-TEFb is effectively neutralized. The exact mechanism Tat exploits to recruit P-TEFb remains unclear, however Tat binds to Cyclin T1 with higher affinity than its structurally related competitor HEXIM1 (Dames et al., 2007; Schulte et al., 2005) potentially resulting in a transition form where Tat has replaced HEXIM1 in the 7SK snRNP complex (Krueger et al., 2010).

Following the synthesis of a TAR stem loop at the nascent HIV-1 RNA, the Tat/P-TEFb complex may disassociate from the 7SK snRNP and phosphorylate polIII (Sobhian et al., 2010). When required for cellular gene expression, P-TEFb is recruited through its binding to bromodomain containing protein 4 (BRD4) a member of the bromodomain and extra terminal domain (BET) family (Jang et al., 2005; Yang et al., 2005). As HIV-1 requires P-TEFb for efficient transcription elongation, Tat must compete with BRD4 for P-TEFb. As a result of this competition, bromodomain inhibitors have recently gained wide use in HIV-1 reactivation and synergy studies around the world and are represented in this thesis by the following LRAs: JQ1 (+) (BRD2/3/4), PFI-1 (2/4) and LY-303511 (BRD2/3/4).

The heat shock protein 90 (Hsp90) has been identified as yet another possible participant in the establishment and control of HIV-1 latency. The heat shock proteins act as chaperone proteins in normal cell functions and have been implicated in several steps in the HIV-1 lifecycle. Hsp90 also acts as a chaperone for newly synthesized CDK9, the kinase component of the essential P-TEFb (O'Keeffe et al., 2000). Compounds that modulate Hsp90 function may therefore have a part to play in future LRA studies. For this thesis, CCT-018159 serves as the representative Hsp90 inhibitor.

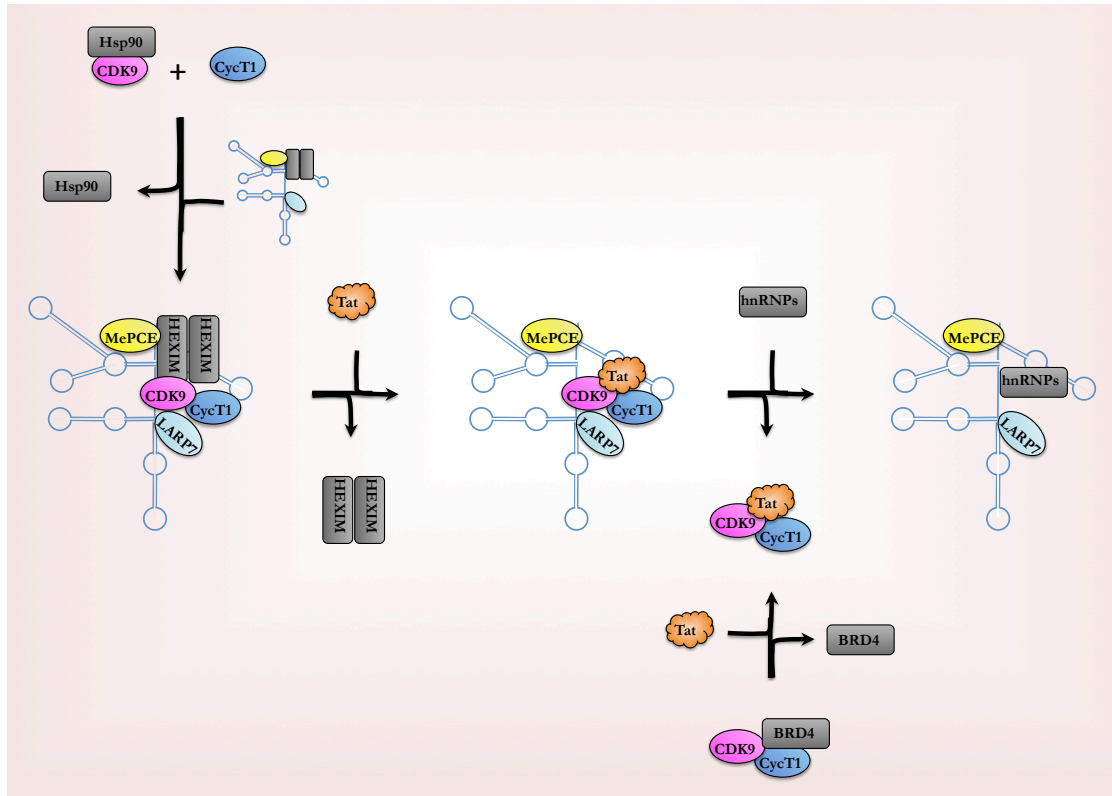


Figure 1.14 P-TEFb extraction from 7SK snRNP by HIV-1 Tat. The heat shock protein 90 (Hsp90) serves as a molecular chaperone for newly synthesized CDK9, in the formation of the P-TEFb heterodimer. For efficient transcription and viral gene expression, HIV-1 required P-TEFb to hyperphosphorylate the C terminal domain of RNA polIII. P-TEFb exists in an inactive form bound by 7SK snRNP. Tat binds to the CycT1 in the 7SK snRNP complex, resulting in a conformational change that displaces HEXIM, creating a transition complex. Binding of Tat/P-TEFb to the TAR stem-loop of nascent HIV-1 RNA is believed to catalyze the liberation of the Tat/P-TEFb from the snRNP complex, allowing for the assembly of the superelongation complex (SEC). Tat must compete for P-TEFb with cellular BRD4.

1.5.8 Posttranslational modifications of Tat.

Tight regulation of the nucleosome occurs through posttranslational modifications, and in a similar manner HIV-1 Tat protein is controlled by acetylation, methylation, phosphorylation and ubiquitination. The majority of these modified residues (K50, K51, R52, R53) are located within the arginine rich motif (ARM) of Tat, with the inclusion of lysines K28 and K72. Together these residues are targeted by writer and eraser enzymes which work to modulate Tat between the early and late phase of its transactivation role. Broadly speaking, the early (TAR dependent) phase involves the binding of Tat to the TAR stem loop for the recruitment of P-TEFb, whereas the late (TAR independent) stage occurs when polIII must leave the TAR stem-loop and progress through the viral sequence that is to be transcribed. Note, the early (TAR dependent) and late (TAR independent) phases of transcription are not to be confused with the early (Rev independent) and late (dependent) phases of HIV replication.

Early (TAR dependent) phase:

While bound to the TAR stem-loop, the cellular methyltransferase SET7/9 monomethylates K51 of Tat, strengthening Tat-TAR bonding, an important step in the assembly of the super elongation complex (SEC) in the early phase of transactivation. (Pagans et al., 2010). To later facilitate transition into the late phase, lysine specific demethylase (LSD1) and its cofactor CoREST remove the methyl group from K51, allowing it to be subsequently acetylated to dissociate from TAR in the late phase (Sakane et al., 2011). Lysine 28, located in the cysteine rich region of Tat is acetylated by the PCAF acetyltransferase complex likewise enhancing the binding of Tat to the TAR stem-loop, (Kiernan et al., 2002; Tagami et al., 2002). K28 is deacetylated by the class II HDAC6, destabilizing the Tat-TAR interaction (Huo et al., 2011a; Huo et al., 2011b). With K51 monomethylated and K28 acetylated, the Tat-TAR binding is sufficient to allow for the assembly of P-TEFb and the super elongation complex (SEC), a complex of cellular transcription factors that regulate the transition to highly efficient transcription elongation through the phosphorylation of RNA polIII. With the early stage complete, these modifications are removed, allowing for the late phase to begin (Figure 1.15 & 1.16).

Late (TAR independent) phase:

The newly demethylated K51, with its neighboring K50 residue are acetylated by the p300/CBP and Gcn5-related N-acetyltransferase (GCN5) Acetyltransferase enzymes, neutralizing the positive charge of the arginine rich motif of Tat and disrupting the Tat-TAR interaction. (Kiernan et al., 1999). Acetylation of K50 recruits SWI/SNF nucleosome remodeling complexes, allowing for enhanced passage of polIII and transcription elongation of viral RNA and the end of the late phase. An important modification for the recycling the Tat protein to begin the early phase again in a new round of transcription is the deacetylation of K50 and K51 by the class III deacetylase SIRT1 (Sakane et al., 2011).

Tat inactivation:

In addition to the reversible cycling between the early and late phase of transactivation, di and trimethylation modifications of K50 and K51 by SETDB1 as well as neighboring arginine residues R52 and R53 by PRMT6 introduce steric hindrance, which prevents the Tat-TAR interaction. These modifications differ in that no demethylase (eraser) enzymes are known exist to reverse the process, potentially resulting in long term inactivation of Tat protein, which may have implications for HIV-1 latency (Anand et al., 2008). Interestingly Harrich *et al* showed that overexpression of PRMT6 increased the stability of Tat, but did not suppress transactivation in the A549 human alveolar adenocarcinoma cell line, which naturally lacks PRMT6 expression (Sivakumaran et al 2013).

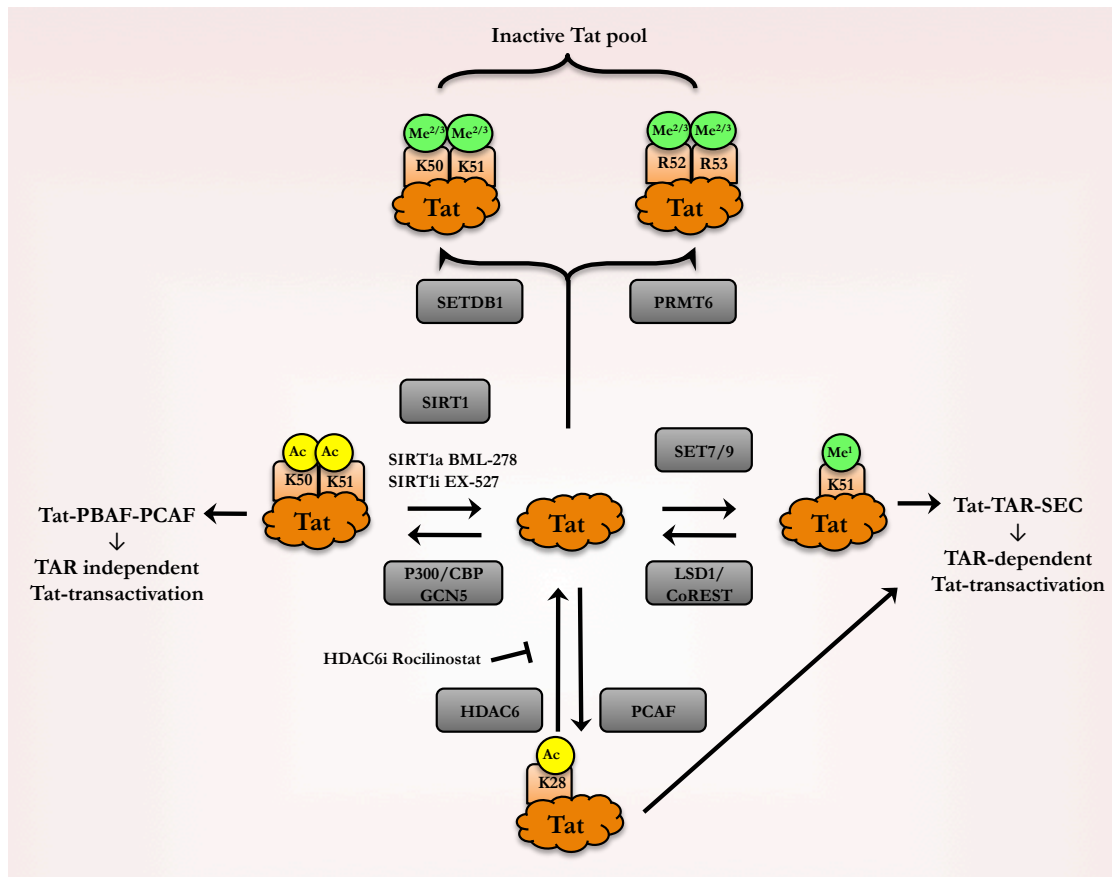


Figure 1.15 (4.2): Post-translational modifications of HIV-1 Tat protein. Tat function is elaborately controlled at the post-translational level, allowing the Tat protein to cycle between two different states, early and late, depending on the role the protein must perform. Initially, the early Tat (K51^{Me1}) state is formed by mono-methylated of K51 by SET7/9, to allow for TAR binding and the formation of the super elongation complex (SEC). LSD1/CoRest demethylate K51, which is in turn acetylated with neighboring K50 by p300/CBP to form the late state form of Tat (K50^{Ac}/51^{Ac}), involved in dissociating from the TAR stem-loop and elongating RNA transcription by polIII. To recycle the Tat protein back to the early state, so new rounds of transcription elongation can be aided, SIRT1 deacetylates K50 and K51, and the process can begin again. Acetyltransferase PCAF acetylates the key K28 residue, contributing to the formation of the Tat-TAR-SEC complex. This modification can be reversed by HDAC6, which can be targeted by the HDAC6 inhibitor Rocilinostat. Additionally, SETDB1 and PRMT6 can methylate K50/K51 and R52/R53, modifications that render the protein inactive and may occur during the establishment of HIV-1 latency.

1.5.9 Tat mediated transactivation of HIV-1 transcription.

To this point, this review has covered the recruitment of P-TEFb by Tat to the TAR RNA stem loop from the inhibitory 7SK snRNP complex, as well as the post translational modification of Tat and their role as a molecular switch between early and late transactivation. The following section attempts to tie these more detailed sections to the larger events that govern HIV-1 transcription. Transcription from the HIV-1 LTR promoter, as well as the promoters of approximately 30% of human genes, undergoes the phenomenon of promoter-proximal pausing of the polII complex (Core et al., 2008). This sees the assembly of the pre-initiation complex of general transcription factors with polII, the initiation of RNA transcription and the synthesis of a short stretch of RNA, followed by pausing of polII and cessation of elongation. For HIV-1, this pause occurs after the TAR RNA stem loop has been transcribed (Kao et al., 1987b), and is mediated by NELF and DSIF (Sehgal et al., 1976) and a lack of Tat/P-TEFb. NELF is a heteropentamer composed of 5 peptides (NELFA-E), and DISF is composed of p160 and p14. The two molecules work cooperatively to repress polII elongation, leading to the paused state. (Yamaguchi et al., 1999) (Figure 16).

With these negative regulatory elements in place, transcription through the entire ~9kbp viral genome is very inefficient, and only rarely produces a full-length transcript. The transcription events that do produce these rare full-length mRNAs are referred to as the pioneer rounds (as Tat is not yet present). These rare 9kb mRNAs are subsequently spliced fully to the 2kb mRNAs, where they are free to leave the nucleus and are used to express HIV-1 Tat, Rev and Nef proteins, the former two of which re-enter the nucleus to usher in the late phase of viral replication (Figure 1.6).

Tat protein undergoes post translational modifications (Figure 1.15) to commandeer P-TEFb from the 7SK snRNP complex and bind the TAR stem-loop at the paused polII complex. NELF and DISF are then phosphorylated, displacing NELF and converting DISF to a positive elongation factor (Yamada et al., 2006), alleviating their repressive control of polII (Yoh et al., 2008). RNA polII is hyperphosphorylated at key serine residues within its C-Terminal Domain, while Tat undergoes a change in post translational modifications, recruiting nucleosome remodeling complexes (SWI/SNF) and allowing the Tat/PTEF-b/polII complex to detach from the TAR and for polII to efficiently elongate transcription.

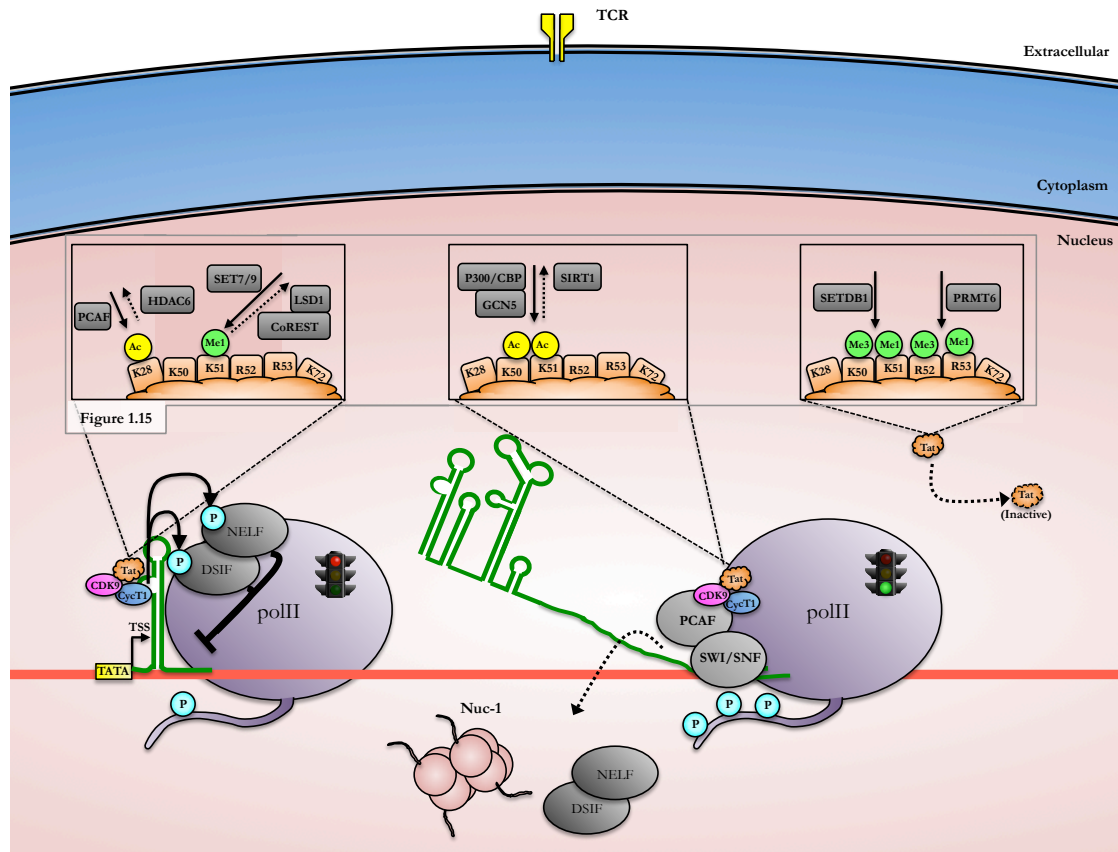


Figure 1.16: Tat mediated transactivation of transcription. Negative factors NELF and DISF cause polII to stall shortly after initiation transcription, producing a short RNA containing the TAR stem loop. Tat (K28Ac & K51Me¹) recruits P-TEFb to the TAR stem loop, resulting in the phosphorylation of NELF, DISF and polII. Tat undergoes a change of posttranslational modifications (K50Ac & K51Ac), allowing the Tat/P-TEFb/polII complex to dissociate from the TAR stem-loop, recruiting nucleosome remodeling complexes (SWI/SNF), allowing for efficient transcription elongation.

1.5.10 Overview.

HIV-1 latency is clearly a multifaceted and highly complex combination of factors that each warrant investigation. While sections 1.5.2 to 1.5.9 of this review attempt to give a working introduction to each of the molecular mechanisms of HIV-1 latency of interest in this thesis, this overview as well as Figure 1.17 attempt to distill these points and tie these mechanisms together in a brief summary. In Figure 1.17a, we see the restrictive mechanisms that contribute to a silenced provirus. In quiescent CD4⁺ resting memory T cells, the need for cellular transcription factors in cellular gene expression is greatly reduced, which in turn reduces the pool of factors available for HIV-1 gene expression. As a result, the virus may be starved of these transcription factors to a point where viral gene expression is completely suppressed, only to be alleviated upon some cell-stimulating event.

Chromatin structure plays a large role in the accessibility of underlying genes to cellular transcription machinery, and therefore gene expression. The histone code, comprising of acetylation and methylation of the N-terminal tails of histones H2, H3 and H4, allows for the highly dynamic transition between restrictive heterochromatin to permissive euchromatin and is written and erased by acetyltransferase and deacetylase complexes as well as methylase and demethylase complexes. Finally, methylation of histones within the HIV-1 associated nucleosomes can result in hypermethylation of CpG islands within the viral LTR promoter sequence, resulting in a less readily reversible restriction on viral gene expression.

Following an activation stimulus, viral gene expression from a previously silenced provirus may recommence as the cell becomes more metabolically active again (Figure 1.17b). Activation of the host cell results in recommencement in critical cell signaling pathways (PKC and MAP kinase) and renewed expression of important cellular transcription factors. Binding of these cellular transcription factors to their binding sites within the LTR results in the subsequent recruitment of acetyltransferase complexes and favorable chromatin remodeling (Lusic et al., 2003). HIV-1 Tat undergoes a set of post translational modifications that allow it to free P-TEFb from the inhibitory 7SK snRNP complex and recruit it to the TAR stem-loop. A switch in the post translational modifications of Tat and CDK9 mediated phosphorylation of negative factors DSIF, NELF and the C-terminal

domain of RNA polII coincides with the recruitment of acetyltransferases and nucleosome remodeling complexes (SWI/SNF), and efficient HIV-1 gene expression.

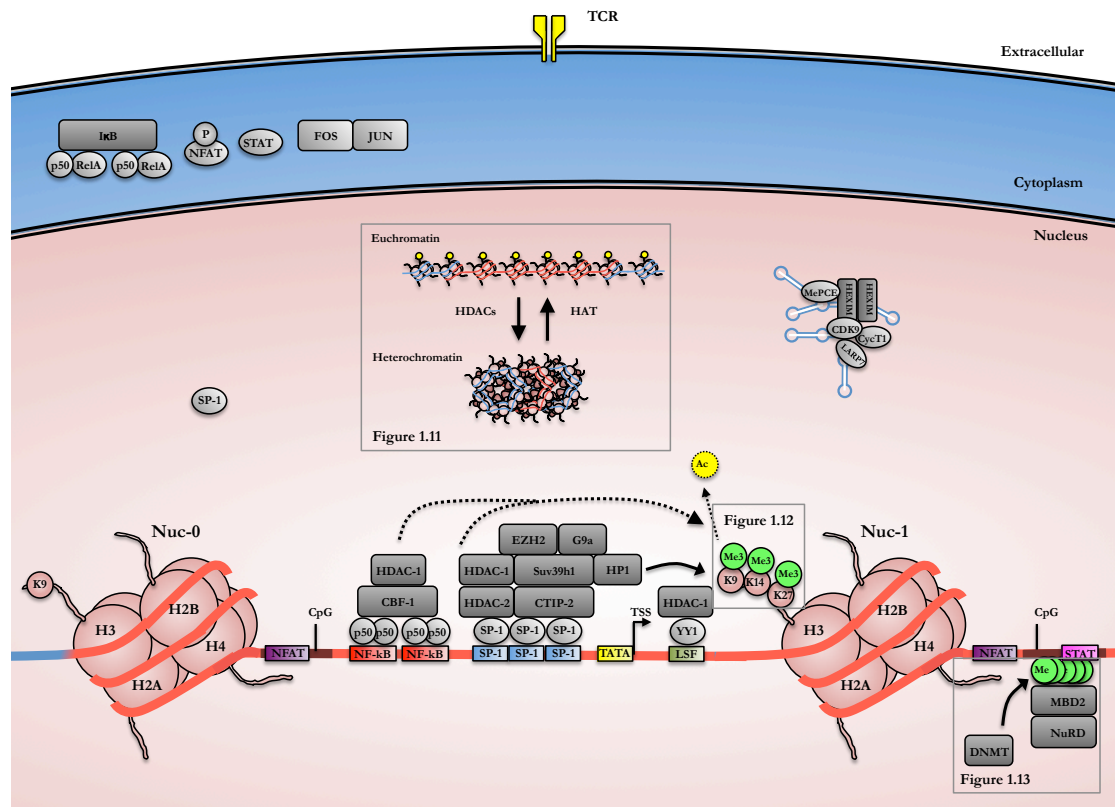


Figure 1.17a: The molecular mechanisms of HIV-1 latency: Silenced provirus. For the silenced provirus, the integrated provirus is tightly associated with histone proteins in the heterochromatin state, preventing access of transcription factors and inhibiting viral gene expression. Deacetylation and methylation of histone tails, as well as methylation of adjacent CpG dinucleotides within the LTR contribute to this state. A lack of cellular transcription factors and P-TEFb also prevents transcription from the LTR. Taken together, these inhibitory molecular mechanisms contribute to a lack of viral gene expression and HIV-1 latency.

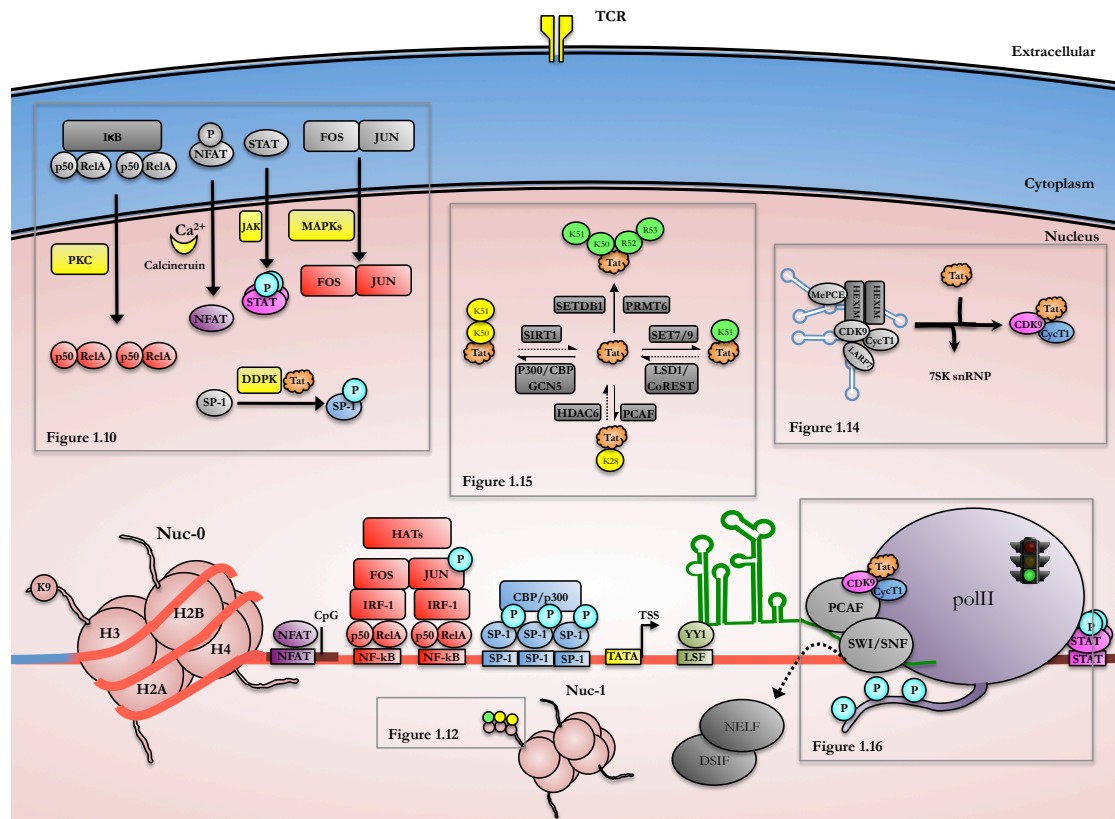


Figure 1.17b: The molecular mechanisms of HIV-1 latency: Activated provirus. Following stimulation, cellular transcription factors become available for exploit. Binding of these factors to the LTR results in recruitment of acetyltransferase complexes and a conversion to euchromatin. RNA polII initiates transcription where Tat recruits P-TEFb to phosphorylate and remove negative factors DISF and NELF, and dramatically increase polII processive. Transcription elongation coincides with the recruitment of nucleosome remodeling complexes and reactivation of viral gene expression.

1.5.11 Compound synergy.

As HIV-1 latency is such a multifaceted phenomenon, involving the interplay of several distinct molecular mechanisms, it seems likely that no single “silver bullet” will be able to reactivate latent infection to the level required for a functional cure. It is also likely due to this fact that clinical trials using a single latency reversing agent have returned disappointing and inconsistent results. This may be expected as effectively treating one of the restrictions may have no effect on the many others. Rather, it is much more likely that a multifaceted strategy will be required, targeting each of these mechanisms in turn. For this reason, we consider compound synergies for answers, by targeting several molecular restrictions (roadblocks), we may achieve what a single latency reversing agent cannot (Figure 1.18). Synergy not only involves targeting more than one mechanism, but because the mechanisms are so interdependent, it is likely that targeting two pathways simultaneously will result in a greater outcome than the sum of their parts. With synergistic reactivation of HIV-1, $1+1>2$. The mechanisms discussed here in this introduction are investigated throughout the results chapters of this thesis. Understanding the precise interplay between the molecular mechanisms governing HIV-1 latency may take some years from the time of writing this thesis, however, it is the authors beliefs that the LRA synergy approach will be necessary for a functional HIV-1 cure.

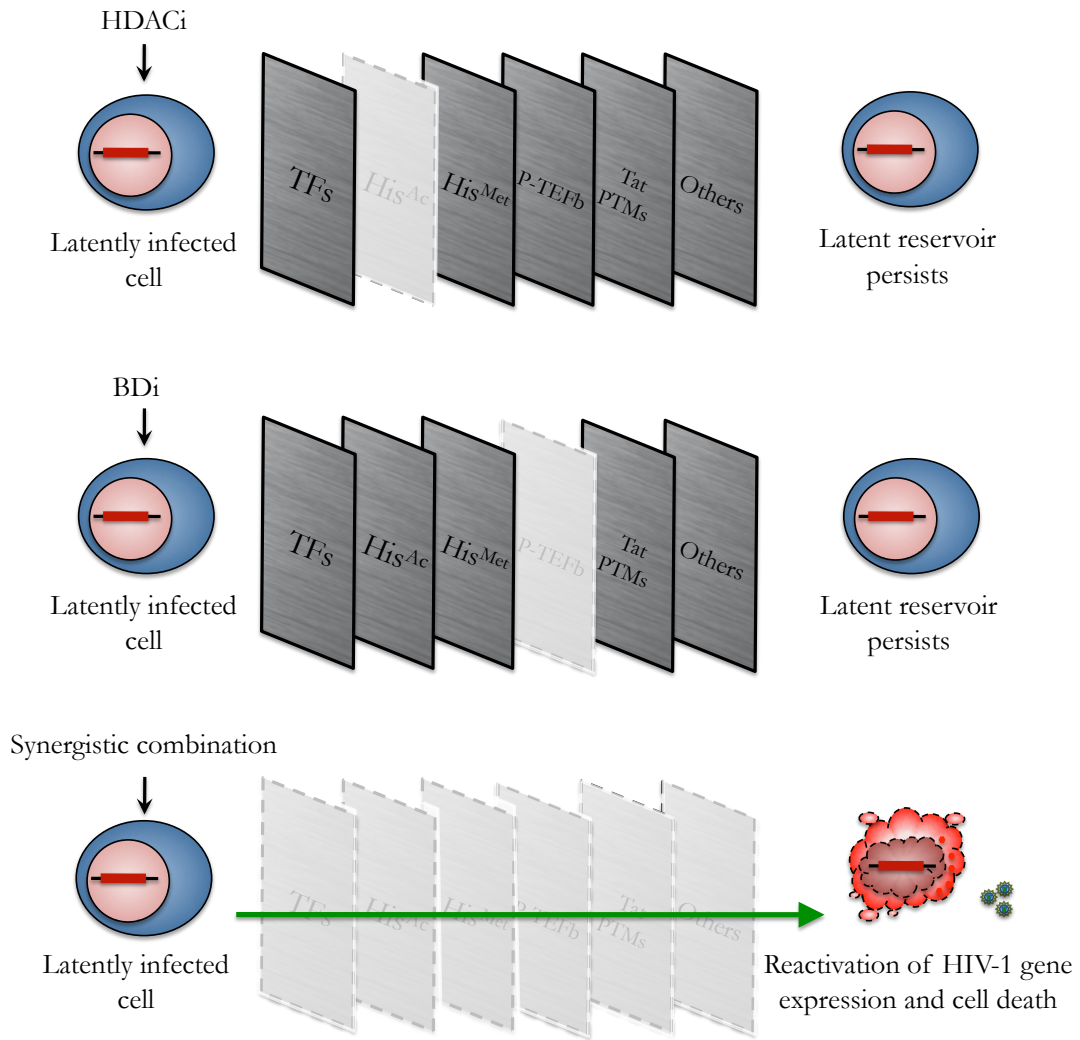


Figure 1.18 Using synergistic combinations to overcome HIV-1 latency. Targeting one of the many mechanisms that govern HIV-1 latency is unlikely to result in efficient reactivation of HIV-1 gene expression, as numerous other restrictions may still be in place. The use of a combination of mechanistically different LRAs that cooperate together in a synergistic combination may, however, prove much more efficient at HIV-1 reactivation in a future HIV-1 cure regimen.

1.6 Project Aims

The long-term persistence of a latent reservoir in HIV+ people taking successful combinational antiretroviral therapy (cART), and the inevitable rebound of viral replication following therapy interruption has seen worldwide attention given to the development of strategies for eradicating the latent reservoir (Alexaki et al., 2008) (Chun, Davey et al. 2000)(Laird et al., 2015).

Today, much is known regarding the complex interconnected set of molecular mechanism that work to silence the integrated provirus within latently infected cells yet to date, all early efforts at eliminating the latent reservoir have produced disappointing results (Lin et al., 2011, Kauder et al. 2009, Pagans et al., 2010, Rasmussen et al., 2013). It is now appreciated that it is unlikely that a single “silver bullet” therapy will achieve effective reactivation of viral gene expression and clearance of the latent reservoir. Here we set out to better understanding the molecular mechanisms of HIV-1 latency and contribute to developing a HIV-1 specific therapeutic strategy that may lead to a functional HIV-1 cure. Whereas many previous attempts at developing latency reversing agents adopted heavily from other fields of research (e.g. cancer), resulting in therapies that lack specificity for HIV-1, we sought to develop the next generation of highly HIV-1 specific compounds. To this end, we sought to:

- 1) To generate an *in vitro* model that recapitulates HIV-1 post integration latency and contained a novel pathway of HIV-1 Tat expression which could be targeted in High Throughput Chemical Screening (Chapter 3).
- 2) To use a panel of mechanistically diverse latency reversing agents with predictable behavior to validate the model (Chapter 4).
- 3) To screen a library of >114,000 small drug like compounds and discover novel LRAs which reactivate HIV-1 gene expression in a highly specific manner for further validation (Chapter 5).
- 4) To discover any synergistic combinations that might exist between any novel LRAs found and those known drugs at the frontier of HIV-1 cure research (Chapter 6).

Chapter 2 Materials and Methods

2.1 Reagents.

2.1.1 Chemicals.

All reagents and chemicals used throughout this thesis were of analytical grade and obtained from Sigma-Aldrich, MO, USA, unless stated otherwise.

2.1.2 Oligonucleotides.

All oligonucleotides used throughout this thesis were obtained from Sigma-Aldrich (MO, USA) at a concentration of 20 μ M unless stated otherwise.

Table 2.1 Oligonucleotides used for plasmid construction.

Oligo Number	Oligo Name	Nucleotide Sequence (5'-3')
Using splice overlap extension PCR to replace <i>hGH</i> with <i>tat</i> exon 2, making T4+CChGH (introns)		
A) Odp 2559	XbaI- <i>hGH</i> (nested cDNA on RTPCR) Fw	GGGCCCTCTAGAGGATCCCAAGG
A) Odp 2396	Tat-+CC- <i>hGH</i> exon4 Rv	TGTCGACACCCAATTTGGCCCCATCAGCGTTTG
B) Odp 2395	<i>hGH</i> exon4-+CC-Tat Fw	CAAACGCTGATGGGGCCAATTTGGGTGTCGACA
B) Odp 2342	<i>hGH</i> exon5-Tat Rv	GCCATCTTCCAGCCTTGCTTTGATAGAGAA
C) Odp 2341	Tat- <i>hGH</i> exon5 Fw	TTCTCTATCAAAGCAAGGCTGGAAGATGGC
C) Odp 2560	EcoRI- <i>hGH</i> (nested cDNA on RTPCR) Rv	GTCCAGTGTGGTGGAAATTTCTGCAG
Amplifying <i>hGH</i> (cDNA) from whole cell RNA after reverse transcription		
Odp 2559	XbaI- <i>hGH</i> (nested cDNA on RTPCR) Fw	GGGCCCTCTAGAGGATCCCAAGG
Odp 2560	EcoRI- <i>hGH</i> (nested cDNA on RTPCR) Rv	GTCCAGTGTGGTGGAAATTTCTGCAG
Introducing CBR luciferase in frame with <i>nef</i>		
Odp 2525	Nef-+G-CBR (KpnI) Fw	ACACCTCAGGTACCGATGGTAAAGCGTGAG
Odp 2526	CBR-+G-Nef (KpnI) Rv	TCTTAAAGGTACCCGCTAACCGCCGCCTT
Introducing CBG68 luciferase in frame with <i>nef</i>		
Odp 2611	XhoI-+CC-CBG Fw	NNNNNNCTCGAGCCATGGTAAAACGCG
Odp 2595	CBG-+G-Nef (KpnI) Rv	TCTTAAAGGTACCCGCTAGCCGCCAGCTTT
qPCR primers for detecting HIV-1 DNA		
MH353	First round Unspliced Fw qPCR	AACTAGGGAACCCACTGCTTAAG
SL20	First round Unspliced Rv qPCR	TCTCCTTCTAGCCTCCGCTAGTC
SL19	Second round Unspliced Fw qPCR	TCTCTAGCAGTGGCGCCCGAACA
SL20	Second round Unspliced Rv qPCR	TCTCCTTCTAGCCTCCGCTAGTC
SL28	First round Multiply Spliced Fw qPCR	CTTAGGCATCTCTATGGCAGGAA
Odp3115	First round Multiply Spliced Rv qPCR	CCGTTCACTAATCGAATGGA
Odp3113	Second round Multiply Spliced Fw qPCR	CAGAACAGTCAGACTCATCAA
SL29	Second round Multiply Spliced Rv qPCR	TTCTTCGGGCCCTGTCGGGTCCC

2.1.3 Plasmids.

All DNA plasmids used throughout this thesis are listed below.

Table 2.2 DNA plasmids used throughout this thesis.

Plasmid Name/No	Description	Source
pcDNA3.1-	Eukaryotic expression plasmid containing multiple cloning site. CMV driven	Invitrogen, CA, USA
pcDNA5/FRT	Contains Flpase Recombination Target sequence (FRT). Contains (Δ ATG) Hygromycin ^R . Must be "Flipped in" for resistance. CMV driven	Invitrogen, CA, USA
pØhGH	Contains the human growth hormone (hGH) gene cassette. Promoterless.	Nichols Institute Diag.
pcDNA3.1-hGH (WT)	Contains hGH cassette inserted using XbaI/SspI (compatible with EcoRV). CMV driven.	Jonathan Jacobson
pEGFP.N1	Contains the enhanced green fluorescent protein (EGFP) ORF. CMV driven.	Clontech, CA, USA
pcDNA3.1-GFP	Contains EGFP ORF inserted using XhoI/NotI. CMV driven.	Jonathan Jacobson
pJ344.GFP	Synthesized <i>de novo</i> containing: SD1- Δ gag/pol-nc2/5 fusion- Δ env(RRE ⁺)-nef/EGFP. Inserted into pDRNL with BssHIII-BspEI. Promoterless.	DNA2.0
pDRFM.nef/GFP	WT LTR, splices to form a <i>nef</i> mRNA (1/2/5/7) with GFP(ORF) in frame with Nef using KpnI/KpnI.	Jonathan Jacobson
pGEM.Ds.Red ^{Ex}	Contains the double stranded red fluorescent protein express (Ds.Red ^{Ex}) ORF. Promoterless.	James Mcklusky Lab
pLenty6.Ds.Red ^{Ex}	Self-inactivating LTR lentiviral construct. Ds.Red ^{Ex} ORF inserted using EcoRI/XhoI. CMV driven.	Jonathan Jacobson
pPromegaCBR(basic)	Contains the click beetle red luciferase (CBR) ORF. Promoterless.	Promega
pPromegaCBR(control)	Contains the CBR ORF behind an SV40 promoter.	Promega
pcDNA5/FRT.CBR	CBR ORF inserted using XhoI/EcoRI. Contains Flpase Recombination Target sequence (FRT).	Jonathan Jacobson
pDRFM.nefCBR	WT LTR, splices to form a <i>nef</i> mRNA (1/2/5/7) with CBR(ORF) in frame with Nef using KpnI/KpnI.	Jonathan Jacobson
pPromegaCBG68(basic)	Contains the click beetle red luciferase (CBG) ORF. Promoterless.	Promega
pPromegaCBG68(control)	Contains the CBG ORF behind an SV40 promoter.	Promega
pcDNA5/FRT.CBG	Contains Flpase Recombination Target sequence (FRT) CMV driven.	Jonathan Jacobson
pDRFM.nefCBG	WT LTR, splices to form a <i>nef</i> mRNA (1/2/5/7) with CBG(ORF) in frame with Nef using XhoI/KpnI.	Jonathan Jacobson
pMDLg/pRRE	Contains Gag and Pol ORFs. Used for lentiviral construction. CMV driven.	Didier Trono (Addgene)
pRSV.Rev	Contains Rev cDNA expressing plasmid in which the joined second and third exons of HIV-1 rev are under the transcriptional control of RSV U3 promoter.	Didier Trono (Addgene)
pMD2.G	Contains the Vesicular Stomatitis Virus G glycoprotein (VSV-G). CMV driven.	Didier Trono (Addgene)

Plasmid Name/No	Description	Source
pcDNA3.1-.Tat72(WT) aka pTat(WT)	Contains tat exon 2 (first ORF) from NL _{4,3} , lacks a stop codon. Protein is slightly larger than 72aa. Inserted using XhoI/BamHI. CMV driven.	Jonathan Jacobson
pcDNA3.1:T4+CC hGH	Contains the hGH cassette with tat exon2 between hGH exons 4 and 5 (replacing intron 4). CMV driven.	Jonathan Jacobson
pcDNA3.1:T4+CC hGH cDNA	hGH/ <i>tat</i> cassette is cDNA (no introns). CMV driven.	Jonathan Jacobson
pcDNA3.1:CBG.T4+CC hGH (introns)	Bicistronic, with CBG(ORF) upstream of the hGH/ <i>tat</i> cassette. Contains hGH introns. CMV driven	Jonathan Jacobson
pcDNA3.1:CBG.T4+CC hGH (cDNA)	Bicistronic, with CBG(ORF) upstream of the hGH/ <i>tat</i> cassette. hGH/ <i>tat</i> cassette is cDNA (no introns). CMV driven	Jonathan Jacobson
pcDNA5FRT.CBG.T4+CC hGH (cDNA)	Bicistronic, with CBG(ORF) upstream of the hGH/ <i>tat</i> cassette. hGH/ <i>tat</i> cassette is cDNA (no introns). Contains Flpase Recombination Target sequence (FRT) CMV driven.	Jonathan Jacobson
pcDNA5FRT.CBR	Contains the CBR(ORF). Contains Flpase Recombination Target sequence (FRT) CMV driven.	Jonathan Jacobson
pcDNA3.1:CBR.T4+CC hGH (cDNA)	Bicistronic, with CBR(ORF) upstream of the hGH/ <i>tat</i> cassette. hGH/ <i>tat</i> cassette is cDNA (no introns). CMV driven.	Jonathan Jacobson
pcDNA5FRT.CBR.T4+CC hGH (cDNA)	Bicistronic, with CBR(ORF) upstream of the hGH/ <i>tat</i> cassette. hGH/ <i>tat</i> cassette is cDNA (no introns). Contains Flpase Recombination Target sequence (FRT) CMV driven.	Jonathan Jacobson
pcDNA5FRT.CBG	Contains the CBG(ORF). Contains Flpase Recombination Target sequence (FRT) CMV driven.	Jonathan Jacobson
pDRFM.nef/CBR	WT LTR, splices to form a <i>nef3</i> mRNA (1/2/5/7) with CBR(ORF) in frame with <i>nef</i> . Cloned into pDRNL using BssHIII/BspEI	Jonathan Jacobson
pDRFM.nef/CBG	WT LTR, splices to form a <i>nef3</i> mRNA (1/2/5/7) with CBG(ORF) in frame with <i>nef</i> . Cloned into pDRNL using BssHIII/BspEI	Jonathan Jacobson
pLenti6.T4+CC hGH	Self-inactivating LTR lentiviral construct. hGH cassette using NheI/KpnI. CMV driven.	Jonathan Jacobson

2.1.4 Drugs, compounds and molecular probes.

All drugs, compounds and molecular probes used throughout this thesis are listed below.

Table 2.3 Drugs used throughout this thesis.

Drug Name	Drug Class/Target	Source	Cat/WEHI/WECC
BML-278	Sirt 1 activator	Abcam Biochem	AB144536
Bryostatins-1	PKC activator	Sigma-Aldrich	B 7431
CCT018159	HSP90 inhibitor	Cayman Chemical	10012591
DZNep	HMTi	Cayman Chemical	13828
EX527	Sirt 1 inhibitor	Cayman Chemical	10009798
JQ1(+)	Brd2, 3, 4 inhibitor	Cayman Chemical	11187
LY303511	LY294002 neg. ctrl. Brd2, 3, 4 inhibitor	Tocris Bioscience	2418/5
Panobinostat	HDAC (pan) inhibitor	TRC	P180500
PFI-1	Brd2, 4 inhibitor	Cayman Chemical	11155
PMA	PKC activator	AdipoGen	AG-CN2-0010
Rocilinostat	HDAC class6&8 inhibitor	Selleck Chemicals	S8001
Romidepsin	HDAC class1&2 inhibitor	TRC	R425060
TNF α	NF- κ B	Sigma-Aldrich	SRP3177
UNC-0638	Selective G9a & GLP HMT inhibitor	Tocris Bioscience	4343
Vorinostat	HDAC (Pan) inhibitor	Cayman Chemical	10009929
DP#2	Triazolopyridazine/BDi†	WEHI§	WEHI-0015915
DP#3	Oxoindole/BDi†	WEHI§	WEHI-0118034
DP#4	Diazapine/BDi†	WEHI§	WEHI-0009016
DP#5	Imidazolopyridazine/BDi†	WEHI§	WEHI-0095576
DP#7	Quinazoline/BDi†	WEHI§	WEHI-0085584
DP#8	Amidopyridine/Unknown‡	WEHI§	WEHI-0142183
DP#6	Amidothiazole/Unknown‡	WEHI§	WEHI-0078085
DP#14	Amidothiazole/Unknown‡	WEHI*	WECC-1248349
DP#16	Amidothiazole/Unknown‡	WEHI*	WECC-1250191

§ Acquired as part of the WEHI HTCS library.

* Synthesised by collaborators at the WEHI.

† Probable mechanism of action (not published)

‡ Unknown mechanism of action.

2.2 Cloning.

2.2.1 Splice overlap extension PCR.

Splice overlap extension (SOE) PCR was used to generate chimeric gene sequences, where hGH and *tat* were arranged in a context modeling HIV-1 integration into a eukaryotic gene and subsequent alternative splicing. Reactions were run at 95°C 2min, [95°C 10sec, 50°C 10sec, 72°C Xsec]_{x2}, [95°C 10sec, Y°C 10sec, 72°C Xsec]_{x30}, 72°C 5min, where X is dependent on the fragment size and enzymes nucleotide (nt) polymerisation rate and Y on the primer annealing temperature T_m. Phusion high fidelity polymerase was purchased from ThermoFischer.

Table 2.4 Splice overlap extension (SOE) PCR setup.

Primary (1°) PCR reaction		Secondary/Tertiary (2°/3°) PCR reactions	
dNTP [10mM]	1µL	dNTP [10mM]	1µL
Mg ²⁺ [50mM]	0.5µL	Mg ²⁺ [50mM]	0.5µL
PhusionPol (2U/µL)	0.5µL	PhusionPol (2U/µL)	0.5µL
HF buffer x5	10µL	HF buffer x5	10µL
DNase free H ₂ O	36µL	DNase free H ₂ O	Up to 50µL
Primer Fw [20µM]	0.5µL	Primer Fw [20µM]	0.5µL
Primer Rv [20µM]	0.5µL	Primer Rv [20µM]	0.5µL
Plasmid DNA	50ng (1µL)	Product A/AB	20ng (XµL)
		Product B/C	20ng (XµL)

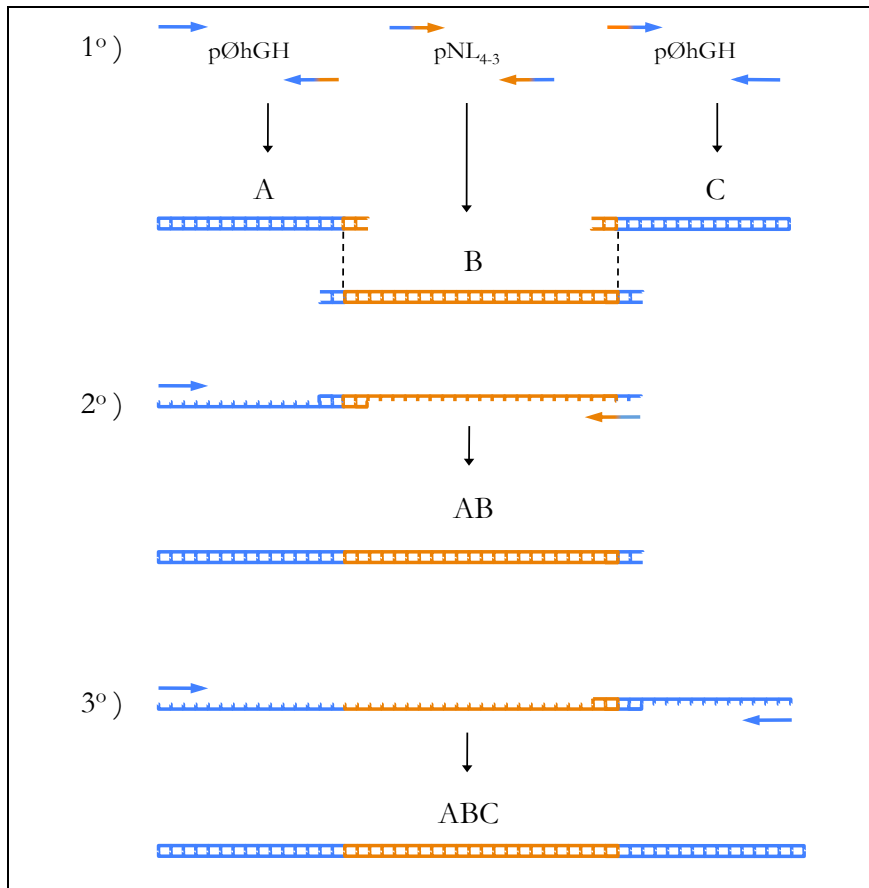


Figure 2.1 Splice overlap extension (SOE) PCR. Splice overlap extension (SOE) PCR was used to stitch two sequences together, for hGH (blue, fragments A and C) and *tat* exon 2 (orange, fragment B), modeling integration of HIV-1 into a eukaryotic gene intron and subsequent alternative splicing. Primers comprise 15nt from both of the two sequences to be stitched together. Primary (1°) PCR products A, B and C therefore contain 15nt overhangs at their termini of the soon-to-be adjacent exon. Two primary PCR products (A and B) can then be stitched together in a secondary reaction (2°), using the 5' and 3' flanking primers from the primary reactions, to form the product AB. The final product ABC is formed in a tertiary (3°) PCR reaction, using AB and C as templates.

2.2.2 DNA gel electrophoresis.

Ten times concentrate (x10) loading dye (50% 0.05% bromophenol blue & 0.05% Xylene cyanol in PBS with 50% glycerol (v/v)) was added DNA sample and loaded into 1% agarose gels, prepared in 1x TAE (40mM Tris, 20mM acetic acid and 1mM EDTA, pH adjusted to 8.0) + x1 RedSafe™ DNA stain (iNtRON Biotechnologies). Electrophoresis was carried out at 135V for 45min using a Bio-Rad Powerpac 200 (Bio-Rad, CA, USA). DNA was visualized, and images taken using a Syngene G:Box gel documentation station with GeneSnap image acquisition software (Synoptics Ltd, Cambridge, UK).

2.2.3 Gel purification of DNA.

DNA bands were excised using a sterile scalpel, and purified through a column using the Qiaquick DNA Gel Extraction Kit (QIAGEN, Dusseldorf, Germany) as per manufacturer's instructions.

2.2.4 Restriction digestion of DNA.

Restriction enzymes (RE) were sourced from New England Biolabs (NEB), MA, USA with reaction conditions according to the manufacturer's instructions. Typically, RE digests were carried out in 20µL volumes, cutting between 500ng-5µg of DNA with 1µL (5-20U) of each enzyme in the appropriate buffer provided at x1 concentration with x1 bovine serum albumin (BSA) if needed. Reactions were incubated at the appropriate temperature for 1hr-4hr and resolved using DNA gel electrophoresis 2.2.2.

2.2.5 DNA ligation.

DNA fragments were ligated using T4 DNA ligase (Fermentas, ON, Canada) in a final volume of 20µL, according to the manufacturer's instructions. For sticky-ended ligations, reactions were incubated at 37°C for 1hr-2hr. For blunt-ended ligations, reactions were incubated at 16°C overnight. Best results were found using a ratio of insert:vector DNA ends between 10:1-20:1.

2.2.6 Transformation of chemically competent *E. coli*.

20µL ligation reactions were carefully added to 50µL of chemically competent *E. coli*, incubated on ice for 1hr-3hr, heat shocked at 37°C for 60sec then allowed to recover on ice for 5min. 400µL of SOC media (super optimal broth with catabolite repression and added glucose) was added and the bacteria were allowed to recover shaking at 37°C 1hr before plating on pre-warmed Luria broth (LB)-agar plates, augmented with an appropriate antibiotic, Ampicillin 100µg/ml or Kanamycin 30µg/ml (Media Prep Unit, Doherty Institute) and incubated overnight at 30°C-37°C. Chemically competent *E. coli* strains used in this thesis include: TOP10 (for blue/white colony screening), HB101 (for plasmids containing repeated sequences including HIV-1 LTRs) and SCS110 (*dam*-/*dcm*-methylation knockouts for pairing with RE inhibited by DNA methylation).

2.2.7 Plasmid DNA preparation.

For small (mini) scale DNA isolation, cultures were grown overnight in 3mL LB broth containing Ampicillin 100µg/ml (Sapphire Bioscience) or Kanamycin 30µg/ml (Life Technologies). 2mL of bacterial suspension was pelleted for 1min at 11,000g at 4°C. DNA was isolated using the Wizard® Plus SV Miniprep kit (Promega, WI, USA) as per manufacturer's instructions. For large (maxi) scale DNA isolation, starter cultures were grown overnight in 20mL LB broth, transferred to 250mL LB broth and grown overnight. Bacterial suspensions were balanced and pelleted in a GSA rotor (Du Pont Instruments) using a Sorvall RC-5C centrifuge for 15min at 6000g at 4°C. DNA was isolated using the QIAGEN plasmid MAXI (QIAGEN Dusseldorf, Germany) as per manufacturer's instructions. DNA pellets were resuspended in 200µL – 1,000 µL TE buffer (Tris-Cl 10mM + EDTA 1mM pH=8.0).

2.2.8 DNA quantification.

DNA concentration was measured by absorbance using the Nanodrop 1000 spectrophotometer (Thermo Scientific, MA, USA) at 230nm, 260nm and 280nm.

2.2.9 Sequencing.

DNA plasmids were sequenced using the BigDye® v3.1 cycle sequencing kit (ThermoFischer Scientific). 20µL reactions used 500ng plasmid template, 2µL BigDye master mix, 4µL x5 BigDye buffer and 1µL oligonucleotide primer [5µM], and were run in a thermocycler at 95°C 5min, [95°C 10sec, 50°C 5sec, 60°C 3min]_{x30}, 60°C 5min. Unincorporated nucleotides were removed from the reaction using the DyeEx 2.0 spin kit (QIAGEN, Dusseldorf, Germany), boiling off any remaining liquid and sequenced at the Applied Genetics Diagnostic Laboratory, Dept Pathology, University of Melbourne for analysis using an ABI 3100 Automated capillary DNA sequencer (Applied Biosystems, CA, USA). Sequence reads were analyzed using Sequencher v4.10.1. (Gene Codes Corp).

2.2.10 Whole RNA extraction using TRIzol® reagent.

1x10⁶ HEK293T cells were seeded into a 6 well plate (giving ~80% confluency) and transfected 24hrs later with 2µg of pcDNA3.1.T4+CChGH, using Lipofectamine2000 (ThermoFisher) according to the manufacturer's instructions. 48hrs post transfection, cells were washed with PBS and pelleted in a 1.5mL tube. All residual phosphate buffer saline (PBS) was removed and the pellet resuspended in 1mL of TRIzol® reagent (ThermoFisher). The lysate was frozen before phase separation and phenol chloroform extraction of whole RNA.

2.2.11 Phenol Chloroform extraction.

Cell debris was pelleted at 12,000g for 10min at 4°C, the TRIzol transferred to a fresh tube, and 200µL chloroform added. The mix was vortexed vigorously and the organic and aqueous layers separated by spinning at 12,000g for 15min at 4°C. The upper clear (aqueous) layer was carefully removed and RNA precipitated as described below.

2.2.12 Alcohol precipitation of DNA and RNA.

For DNA precipitation, bacterial cell lysate was mixed with 0.1 volume of Sodium Acetate [3M] and 0.7 volumes of 100% isopropanol and precipitated at 12,000g for 30min at 4°C. DNA washed with 500µL of 75% ethanol to remove excess salt and resuspended in TE buffer. For RNA precipitation, 500µL 100% isopropanol was added to the aqueous fraction of Phenol Chloroform extracted RNA and incubated at room temperature for

10min. RNA was precipitated at 12,000g for 10min at 4°C, the isopropanol removed, and RNA washed with 1mL of 75% ethanol. RNA was resuspended in RNase free water.

2.2.13 Reverse Transcription PCR from whole RNA.

Table 2.5 Reverse Transcription PCR setup.

First strand cDNA synthesis		Nested PCR for cDNA amplification	
dNTP [10mM]	1µL	dNTP [10mM]	1µL
DNase free H ₂ O	10µL	Mg ²⁺ [50mM]	0.5µL
Oligo(dT) ₂₀ [50µM]	1µL	PhusionPol (2U/µL)	0.5µL
Whole cell RNA	3.5µg (1µL)	HF buffer x5	10µL
65°C 5 min then on ice 1 min		DNase free H ₂ O	36µL
First Strand Buffer x5	4µL	Primer Fw [20µM]	0.5µL
DTT [0.1M]	1µL	Primer Rv [20µM]	0.5µL
RNase Inhibitor	1µL	Whole cDNA	2µL
Superscript III RT	1µL		
50°C 1hr, 70°C 15min			

DTT = dithiothreitol

RT = reverse transcriptase

dNTP = deoxynucleotide

HF = high fidelity

2.3 Culturing Mammalian Cell Lines.

2.3.1 Cell Lines.

All adherent cell lines were maintained in DF10 (Dulbecco's modified eagle media DMEM + Fetal Bovine Serum (FBS) 10% (v/v) + Pen/Strep 100U/mL(Life Technologies)). Suspension cells (lines and primary) used RF10 (RPMI + FBS 10% (v/v) + Pen/Strep 100U/mL) unless otherwise stated. OPTI-MEM was used serum/antibiotic free unless otherwise stated. PBS(-/-) denotes Calcium and Magnesium free x1 Phosphate Buffer Saline. Cells were sourced from the American Type Culture Collection (ATCC) and the NIH AIDS Research Program (NIH ARP).

Table 2.6 Mammalian cell lines used throughout this thesis.

Line Name	Description	ATCC	Source
HeLa	Human epithelial (cervical carcinoma) derived adherent cells.	CCL-2	
TZM-bl (JC53-bl)	HeLa based, express CD4/CCR5. Stable LTR-IRES.Firefly <i>luc</i> / β <i>Gal</i> cassette.		NIH ARP Cat#8129
HEK 293T	Human embryonic kidney derived adherent cells. Highly competent for transfection, suitable for virus production. SV40-T+.	CRL-3126	
FlpIn™-293	293 based, contain a single FRT sequence for Flpase mediated recombination and stable cell generation.		Invitrogen R750-07
Jurkat	Human T cell (acute T cell leukemia) suspension cells.	CRL-2899	
J-Lat6.3	Jurkat cells infected with HIV-R7/Env-/GFP. Maximal TNF α stimulation 18-25% GFP+.		NIH ARP Cat#9846
J-Lat10.6	Jurkat cells infected with HIV-R7/Env-/GFP. Maximal TNF α stimulation 80-85% GFP+.		NIH ARP Cat#9849

2.3.2 Transient DNA plasmid transfection of adherent stable cell lines.

For transient transfections in 24, 48 and 96 well formats (Nunc, Foskilde, Denmark), cells were seeded at 2.0×10^5 , 1.1×10^5 or 2.5×10^4 cells per well respectively in DF10, to allow for an ~80% confluent cell monolayer after 24hrs. Transfections were performed using Lipofectamine2000 (ThermoFischer) transfection reagent. DNA and Lipofectamine2000 were hydrated separately in plain OPTI-MEM (Gibco) for 5min, DNA drop-wise added to Lipofectamine2000, allowed 20min to complex, then drop-wise adding the complex to the cell monolayer. A DNA:Lipofectamine2000 ratio of $1\mu\text{g}:1.25\mu\text{L}$ was used unless otherwise stated.

2.3.3 Drug treatment of adherent stable cell lines.

Cells were seeded directly into white 96 well plates (Costar, Corning) at 2.5×10^4 cells per well in a volume of 50 μ L of DF10 and were allowed to form a monolayer overnight. 24hrs post-seeding, 50mM drug stocks were titrated 2-fold across 7 points in DMSO (Millipore), and 0.8 μ L of each dilution transferred to 1000 μ L OPTI-MEM, giving a x2 preparation (0.8% DMSO). 50 μ L of the x2 mix was added to wells, giving x1 (0.4% DMSO) and incubated for 48hrs before assaying for luciferase activity.

2.3.4 Drug treatment of suspension cell lines.

J-Lat suspension T cells were seeded into flat-bottomed 96 well plates at 4×10^4 cells per well in a volume of 50 μ L of RF10 and incubated overnight. 24hrs post-seeding, 50mM drug stocks were titrated 2-fold across 7 points in DMSO, and 0.8 μ L of each dilution transferred to 1mL OPTI-MEM, giving a x2 preparation (0.8% DMSO). 50 μ L of the x2 mix was added to wells, giving x1 (0.4% DMSO) and incubated for 48hrs before by flow cytometry analysis.

2.3.5 Firefly luciferase assay of adherent stable cell lines.

Luciferase assays were performed 48hrs post transfection/drug treatment unless otherwise stated. For 24 and 48 well format experiments, media was removed by aspiration, cells washed with PBS(-/-) and 100 μ L or 50 μ L (respectively) of a x1 passive lysis buffer PLB \emptyset (Promega, WI, USA) added. Cells were incubated at room temperature for 20min with gentle agitation. 10 μ L of the cell lysate was transferred to white polystyrene 96 well plates (Corning), and combined with 25 μ L SteadyGlo (Promega, WI, USA) luciferase reagent. For 96 well format experiments, cells were seeded directly into white polystyrene 96 well plates, 48hr post transfection, media was removed by aspiration, cells washed with PBS(-/-), and 25 μ L x1 PLB \emptyset added and incubated for 20min at room temperature. 25 μ L SteadyGlo luciferase reagent was then added to each well. Luciferase activity was measured 5-30min after addition of luciferase reagent on a FLUOstar Omega multiplate reader (BMG LABTECH) without wavelength filters.

2.3.6 Click Beetle luciferase assay of adherent stable cell lines.

Click beetle luciferase assays were all performed in 96 well format, unless otherwise stated. 48hr after transfection (or drug treatment for stable cell lines), media was removed by aspiration and 25 μ L ChromaGlo dual-luciferase reagent was added to each well, without the need for a lysis step. Dual-luciferase activity was measured <5min after addition of luciferase substrate on a FLUOstar Omega multiplate reader (BMG LABTECH), reading initially using the 610nm/20nm filter for CBR luciferase activity, followed by a second read using the Em520 (520nm) filter for CBG luciferase activity (gains of 3600 for both readings).

2.4 Creating stable cell lines.

The major accomplishment of this thesis was the generation of stable cell lines that permit the detection of novel LRAs that specifically modulate expression from a proviral HIV-reporter (Chapter 3), while minimizing undesired non-specific gene activation. The HEK derived FlpIn™-293 (Life Technologies) based cell lines (FlpIn.FM and FlpIn.RV) comprise of 3 stably integrated constructs to achieve this (Chapter 3), whereas the J-Lat6.3FM and J-Lat10.6FM cells were adapted from previously established stable clones (Verdin *et al.*).

2.4.1 Transfection for Flpase mediated (FlipIn) recombination.

Two 75cm² flasks were seeded with the parental FlpIn™-293 cells (Life Technologies) at 80% in DF10 and incubated overnight to form a monolayer. For FlpIn.FM and FlpIn.RV stable cell lines, 2µg of the pcDNA5/FRT-Click Beetle Luciferase plasmid (Green and Red respectively), containing the Flpase recombinase target (FRT) sequence, were co-transfected with 18µg of pOG44 Flpase recombinase expression plasmid (Life Technologies) using Lipofectamine 2000 (Invitrogen) as per manufacturer's instructions. At 48hrs after transfection, Hygromycin selection commenced for 10 days at 250µg/mL (474µM), replacing media as needed until resistant foci emerged. As the FlpIn™-293 parental cells contain a single FRT site, resistant "Flipped-In" cells were clonal.

2.4.2 Pseudovirus production.

75cm² flasks were seeded with HEK293T cells at 80% in DF10 and incubated overnight to form a monolayer. Before transfection, media was replaced with a minimum volume of DF10 to maximize transfection efficiency and pseudovirus concentration. Pseudovirus was produced by co transfection of the following plasmids: 1) pseudoviral genome (pDRFM.nef/CBR, pDRFM.nef/CBG or pLenti6.T4+CChGH) : 2) pRSV.Rev : 3) pMDLg/RRE : 4) pMDG (VSVG) : 5) pcDNA3.1-Tat(WT) in a ration of 12µg : 2µg : 2µg : 2µg : 2µg using Lipofectamine2000 as per the manufacturer's instructions. At 48hrs after transfection, the media was collected and passed through a 0.45µm Minisart® syringe filter (Sartorius) before applying to target cells for lentivector transduction.

2.4.3 Transduction of cells.

Flipped In cells were transduced with pFM.nef/CBR and pFM.nef/CBG derived LTR-reporter viruses (Figure 3.4 & 3.8) by replacing culture media with media containing pseudovirus. Pseudovirus media was replaced with fresh growth media after 4hrs. 48hrs after transduction, single clone preparations were made using a limiting dilution of 1 cell/100 μ L (for 500 wells, 50mL). At 9 days post transduction, wells with a single cell foci were observed and subsequently passaged in a fresh 96 well plate. At 16 days post transduction, surviving clones were split into 2 identical 96 well plates, one for culturing and the other lysed during the assay for dual luciferase expression. To enhance the baseline of the LTR-driven luciferase reporters (CBR and CBG respectively), IRES mediated Tat expression was introduced by pLenti6.T4+CChGH (Figure 3.5) derived pseudovirus transduction, as above, followed by a second round of limiting dilutions and clone selection. Surviving clones were assayed for efficient dual luciferase activity and the FlipIn.FM (clone C2) and FlipIn.RV (clone B6) obtained.

2.5 Flow cytometry.

Investigation of cell size, granularity and reporter gene expression (fluorescence) was measured using flow cytometry analysis on a FACSCalibur (BD Immunocytometry systems, CA, USA), using Cell Quest V6.0. LRA activity was determined using the percentage of fluorescently positive cells within a population, compared to unstimulated controls, using FlowJo v7.6.3 software.

2.5.1 Preparation of J-Lats for flow cytometry.

For suspension T cell lines, 100 μ L of a x2 FACS fix solution, PBS(-/-) + 2% FBS + 2mM EDTA + 2% formaldehyde (v/v), was added directly to wells to chemically fix cells 48hrs post activation. Cells were then mixed thoroughly by multichannel pipetting and transferred to 1.5mL Titrertube[®] micro test tubes FACS tubes (Bio-Rad) for cytometry analysis.

2.5.2 Flow cytometry of J-Lats using FACSCalibur.

For gating on live non-fluorescent T cells, parental Jurkat cells were passed through the FACSCalibur and forward-scatter and side-scatter gates drawn around the bulk of viable, single cells within the sample. For gating GFP and DS.Red positive cells, GFP+ (J-Lat10.6) and DS.Red+ (Jurkat^{DS.Red}) cells were maximally activated with 20ng/mL of TNF α . Gates were then drawn for each fluorescent reporter gene. For reactivated experimental samples, 10,000 total events were captured and GFP/DS.Red expression analyzed using FlowJo v7.6.3.

2.5.3 Preparation of leukapheresis cells for flow cytometry.

72hrs after addition of an LRA, 50 μ L (unknown number of cells) from each condition from the leukapheresis experiments were pelleted at 400g for 5min at room temperature, washed with PBS(-/-) + 1mM EDTA, re-pelleted and stained with Live/Dead[®] fixable near-IR cell stain (Thermo Fischer) as per manufacturers instructions. Cells were then fixed using FACS fix solution, PBS(-/-) + 1% FBS + 1mM EDTA + 1% formaldehyde (v/v) and analysed using the BD LSR II flow cytometer to determine cell viability.

2.5.3 Flow cytometry of leukapheresis cells using LSR II.

Cells were measured for viability where the Live/Dead® fixable near-IR cell stain used was actively transported out of viable cells, leaving dead cells brightly stained at 780nm/60nm. 25,000 total events were captured, and live/dead staining analyzed using FlowJo v7.6.3.

2.6 Primary cell experiments.

2.6.1 Isolation of PBMCs from buffy coats.

25mL of buffy coat was mixed with 25mL PBS(-/-) and 25mL slowly layered onto 15mL Ficoll-Plaque™ Plus (certified endotoxin free, GE Healthcare), before spinning at 800g for 20min (acceleration slow, deceleration OFF) at room temperature. All spins thereafter were done at 4°C and cells were stored on ice. The PBMCs were collected from the interface and transferred to a new 50mL tube, topped with PBS^E(PBS(-/-) +2mM EDTA) and centrifuged at 400g for 10min (acceleration high, breaks ON). PBS^E was aspirated, cells gently resuspended in 2mL PBS^E and pooled. Tubes were topped with PBS^E and cells pelleted at 400g for 10min. To lyse residual erythrocytes, PBS^E was aspirated and cells incubated in 3mL ammonium chloride 0.83% (w/v) for 5min on ice. Cells were washed in PBS^E and pelleted again. PBMCs were resuspended in 20mL RF10 (RPMI +10% FBS +Pen/Strep) then counted.

2.6.2 Isolation of CD4+ T cells form PBMCs.

Tubes were topped with FACS wash (PBS(-/-) + 1mM EDTA 1% FBS (v/v)) and centrifuged at 400g for 10min at 4°C. The cells were then washed with 50mL of FACS wash before being resuspended in 50mL of fresh FACS wash before counting using a haemocytometer. 2×10^8 PBMCs were pelleted and resuspended in a hybridoma supernatant cocktail that allows for the negative selection of resting memory CD4+ T cells. The required volume of each supernatant was determined by flow cytometry analysis. 4,375 μ L(Purcell lab stocks) or 1,909 μ L(Lewin lab stocks) of the hybridoma supernatant cocktail was used to resuspend the PBMCs and incubated for 1hr on ice.

Table 2.7 Hybridoma supernatant cocktail for resting CD4+ T cell negative selection.

Hybridoma S/N	Target	Vol (μ L) for a 2×10^8 cell sort	
		Purcell	Lewin
OKT8	CD8	700 μ L	250 μ L
OKM1	CD11b	700 μ L	313 μ L
FMC17	CD14	700 μ L	235 μ L
3G8	CD16	200 μ L	313 μ L
FMC63	CD19	400 μ L	300 μ L
2.06	HLA-DR	1250 μ L	313 μ L
GlyA	GlyA	400 μ L	160 μ L
CD69(L78)Pure (BD)	CD69	25 μ L	25 μ L
		$\Sigma = 4,375\mu$ L	$\Sigma = 1,909\mu$ L

Cells were washed in 48mL FACS wash, pelleted and resuspended in 120 μ L anti mouse IgG-MicroBead (Miltenyi Biotec) and incubated at 4°C for 15min. Cells were washed with FACS wash, pelleted and unbound beads removed by aspiration. Cells were resuspended in 2mL FACS wash and run through a LD MACS column (Miltenyi Biotec), allowing for negative selection of resting memory CD4⁺ T cells (CD8⁻/CD11b⁻/CD14⁻/CD16⁻/CD19⁻/HLA-DR⁻/GlyA⁻/CD69⁻). The CD4⁺ fraction was counted and resuspended in RF10 + IL-2 1U/mL at 2x10⁶ cells/mL. To assess the purity of the negatively selected population, the following samples were prepared and stained with PE mouse anti-human CD3 and FITC mouse anti-human CD4 antibodies (BD Pharmigen) for 20min at 4°C:

Table 2.8 antiCD3 and antiCD4 staining for resting CD4⁺T cell purity check.

	antiCD3-PE	antiCD4-FITC
5x10 ⁵ PBMCs (Donor 1)	-	-
5x10 ⁵ PBMCs (Donor 1)	2 μ L	-
5x10 ⁵ PBMCs (Donor 1)	-	2 μ L
5x10 ⁵ rCD4 ⁺ (Donor 1)	2 μ L	2 μ L
5x10 ⁵ rCD4 ⁺ (Donor 2)	2 μ L	2 μ L
5x10 ⁵ rCD4 ⁺ (Donor 3)	2 μ L	2 μ L
5x10 ⁵ rCD4 ⁺ (Donor 4)	2 μ L	2 μ L

Purity was assessed using the FACScalibur flow cytometer.

2.6.3 MTS cell viability/proliferation assay.

MTS reagent is a tetrazolium inner salt which is used to determine the relative viability of a sample by measuring bulk metabolism. Viable cells metabolize the MTS tetrazolium molecule to its formazan product, which is readily detectable by colorimetric analysis. 5×10^4 resting memory CD4⁺ T cells were seeded in 50 μ L RF10 + IL-2 2U/mL, and 50 μ L each LRA concentration prepared also in RF10 + IL-2 2U/mL, added. Media lacking an LRA served as an untreated “live cells” control, and sodium arsenite [200 μ M] treated “dead cells” served as a negative control for normalizing results. PMA[10nM]+PHA[10 μ g/mL] served as an additional “activated cells” positive control. 56hrs post drug addition, 20 μ L MTS reagent (Cell Titre 96® Aqueous One Solution Cell Proliferation Assay (Promega, WI, USA) was added to cells in 100 μ L of growth media and allowed to incubate for 16hrs. Bulk cell metabolism (a surrogate for viability and cell activation) was measured 72hrs post drug treatment as per the manufacturer’s instructions with a Thermo Multiskan Ascent plate reader (Thermo Fischer) at 492nm. For presenting data, each sample is normalized between dead cell wells (negative control at 0%) and untreated/no drug “cell only” wells (positive control at 100%). If a drug is toxic, the readout will be between 0% and 100%, whereas if the drug induces proliferation, the value will be proportionally above 100%. Because the MTS assay can only measure bulk metabolism of a well, it cannot show how many cells are present or dead, as a live/dead stain like propidium iodide does during flow cytometry. This presents a significant limitation to the assay and highlights the need for additional measurements regarding toxicity and proliferation before making a definitive conclusion on drug toxicity.

2.7 Reactivation of HIV from patient leukapheresis samples.

2.7.1 Isolation of CD4+ T cells form leukapheresis samples.

Vials of frozen PBMCs (from leukapheresis of HIV+ patients on long term suppressive cART) were thawed at 42°C in a water bath and 1mL of warm FBS was added dropwise. Cells were then transferred to a 15mL tube and another 4mL FBS added dropwise, then 6mL of RF10. Cells were pelleted at 400g for 10min at room temperature. Following aspiration, the cells were resuspended in RF10, pooled into a 50mL tube which was topped up with RF10. Cells were pelleted again at 400g for 10min at room temperature. Following aspiration of supernatant, the cells were resuspended in PBS(-/-) and counted using a hemocytometer. CD4+ T cells (CD8⁻/CD14⁻/CD15⁻/CD16⁻/CD19⁻/CD36⁻/CD56⁻/CD123⁻/GlyA⁻/TCRγδ) were then negatively selected for using the antibody cocktail and magnetic microbead preparations in the CD4+ T cell isolation kit (Miltenyi Biotec) as per manufacturer's instructions. CD4+ T cells were then counted before being diluted to 5x10⁶cells/1mL in RF10, and 1mL seeded for each condition in a 24 well plate. Cell purity was analysed as described in section 2.6.2.

2.7.2 Reactivation of leukapheresis samples.

Integrase inhibitor (Raltegravir) was made to 2μM in RF10 + IL-2 (2U/mL), and used to make 1mL preparation of each LRA, then added to the appropriate wells containing the CD4+ T cells. Cells were transported to PC3 and incubated for 72hrs.

2.7.3 Harvesting reactivated leukapheresis cells.

Cells were resuspended, 100uL transferred for live/dead staining (section 2.5.3), and the remaining volume pelleted at 400g for 10min. 1mL of TRIzol® reagent was used to resuspend the cell pellet for phase separation, phenol chloroform RNA extraction and alcohol precipitation (section 2.2.11). RNA pellets were resuspended in 50μL RNase free water.

2.7.4 DNase treatment of whole RNA.

To remove any carry-over genomic DNA, RQ1 DNase (Promega) was added to the whole RNA preparation and incubated at 37°C for 30min. 2μL of the DNase stop solution was added and incubated at 65°C for 10min.

2.7.5 cDNA synthesis.

cDNA was synthesized using the SuperScript III Reverse transcription kit (ThermoFisher). 2 μ L oligo dT [50 μ M], 2 μ L random hexamer [50ng/mL] and 2 μ L dNTP [10mM] were added to 500ng whole RNA and the volume brought to 20 μ L with water. For annealing, this was incubated at 65°C for 5min then on ice for 2min. 8 μ L first strand buffer [x5], 8 μ L MgCl₂ [25mM], 4 μ L DTT [0.1M], 0.5 μ L RNase inhibitor [10U/ μ L] and 1 μ L Superscript III RT enzyme [2000U/ μ L] were then added and the samples incubated at 25°C for 10min, 50°C for 50min and finally 85°C for 5min.

2.7.6 First round PCR.

Amplification of multiply spliced (MS) and unspliced (US) HIV-1 DNA was performed by first round PCRs using the Phusion high fidelity polymerase system (New England Biolabs). 0.25 μ L Phusion Pol [2U/ μ L], 0.5 μ L dNTP [10mM], 5 μ L Phusion buffer [x5], 5.5 μ L water and 0.625 μ L of each oligonucleotide primer [20 μ M] were mixed with 12.5 μ L of cDNA and HIV-1 DNA amplified in a thermocycler as follows: 95°C for 10min to allow DNA melting, then 15 cycles of 94°C for 10sec, 55°C for 10sec, 72°C for 10sec. Final elongation was allowed 5min at 72°C for completion. The primers for first each first round PCR can be found in Table 2.1.

2.7.7 qPCR of HIV DNA.

HIV-1 DNA was quantification using quantitative PCR (qPCR) using the Brilliant II SYBR® Green qPCR system. 10 μ L of SYBR Green master mix [x2] was mixed with 1 μ L of each oligonucleotide primer [20 μ M], 3 μ L water and 5 μ L of the first round PCR product. qPCR runs were performed according to the following conditions: 95°C for 10min to allow DNA melting, then 60 cycles of 94°C for 20sec, 58°C for 20sec, 72°C for 20sec. Dissociation curves were generated by increasing the temperature from 60°C to 90°C at a rate of 0.5°C/read.

2.8 Data presentation and statistical analysis.

2.8.1 Data presentation and statistical analysis.

Prism v7.0 (GraphPad) was used for the plotting of data and statistical analyses throughout this thesis. Data typically displayed sample means, with (+/-) error bars representing standard deviation (SD). For determining statistically significant differences, unpaired two-tailed *t*-tests were performed unless otherwise stated and deemed to be significant if $p < 0.05$. Where $n=3$ is presented, this represents 3 independent experiments, where at least 3 side-by-side replicates were included. The exception to this is the leukapheresis experiments, where n = the number of donors included for each condition, each done in single.

Chapter 3: Platforms to assess specific reactivation of HIV-1 from latency.

3.1 Aim.

Most of the current chemotherapeutic HIV-1 latency reversing agents also modulate the expression of a vast array of bystander cellular genes that may have detrimental effects. The first aim of this thesis was to generate reporter cell lines that accurately model HIV-1 latency *in vitro* and can distinguish HIV provirus-specific gene activation from non-specific cellular-gene activation. The objective is to generate a platform for high throughput chemical screening and the discovery of novel compounds that specifically reactivate HIV-1 gene expression, while avoiding global cell activation and cell toxicity.

3.2 Introduction.

Early during the course of infection, HIV-1 establishes pools of latently infected cells (Alexaki, Liu et al. 2008), many of which harbor a replication-competent integrated provirus, held in a “silenced” state, where viral gene expression is inhibited due to a range of constraints including site of integration (Schröder et al. 2002), a lack of requisite cellular factors (Mbonye 2014), chromatin structure (Hodges et al. 2009)(Lin et al. 2011) and a lack of HIV-1 Tat protein (Karn 2011). While viral gene expression is silenced in a latent state, the provirus within the infected cell remains invisible to the immune system, persisting for the life of the cell. Upon some form of stimulation however, the virus can be “re-awoken” and commence viral gene expression, virion production and new rounds of replication, which can subsequently reseed the infection if combinational antiretroviral therapy (cART) is interrupted (Chun et al. 2000). This necessitates the need for lifelong therapy. Collectively, the pools of latently infected cells are known as the latent reservoirs and represent a major roadblock in current attempts at a functional HIV-1 cure.

To address the persistence of the latent reservoir, many attempts are underway to identify potentially useful therapeutics, both among existing drugs for other diseases such as cancer therapies, as well as newly identified drug-like compounds. Such drugs would act to re-awaken the silenced provirus within latently infected cells and ultimately prompt the death and clearance of HIV-1 provirus containing cells. These compounds are commonly known as Latency Reversing Agents (LRAs). To date this approach, coined the “shock and kill”

strategy has focused primarily on compounds targeting the epigenetic regulators of gene expression. Some popular epigenetic targets include the Histone Deacetylase (HDAC) (Rasmussen 2016) and Bromodomains (BD) proteins (Li et al. 2013), which play an important role in chromatin architecture and RNA transcription events, both critical for the cells own gene expression and maintenance. While these approaches have shown some promise to “shock” the provirus into recommencing rounds of RNA synthesis, many of these LRAs do so in a largely indiscriminate manner, often affecting global cellular gene expression, an undesired side effect of their non-specific mechanisms of action (Gray et al. 2016). The non-specific activity of many trialed LRAs has rendered several candidates, developed for chemotherapy for terminal cancer, as too dangerous for further development as potential leads for latent HIV-1 activating drugs where the current antiviral drugs can safely prolong health. Theoretically, the ideal LRA would have an effect on only the infected cells harboring an HIV-1 provirus, while having minimal effect on uninfected bystander cells. Such an LRA would therefore need to exploit some distinction between an infected and uninfected cell, that is, a druggable pathway unique to the infected cell due to the presence of the provirus, but absent in the uninfected cells. We hypothesize that during HIV-1 latency a novel pathway of HIV-1 gene expression occurs that does not require LTR driven transcription, and results in the production of HIV-1 Tat protein (Figure 3.1). Tat plays the role of master regulator of HIV-1 gene expression (Kao et al. 1987), potentially acting as an ON/OFF switch for HIV-1 latency (Singh 2009). Targeting this pathway of Tat protein expression is therefore at the center of our attempts at developing novel LRAs. Our model of Tat expression during proviral silencing (HIV-1 latency) follows integration of the proviral DNA into an intron of an actively transcribed cellular gene, where the viral RNA is degraded as a lariat intron of the target gene during RNA splicing. As the infected cell returns to a quiescent state, both cellular and viral gene expression are silenced bringing about a latent infection. The lack of essential host transcription factors, such as NF- κ B, together with the dominance of the cellular genes own promoter excludes the viral LTR promoter from driving HIV-1 transcription events, a phenomenon termed promoter occlusion (Van Lint, Bouchat et al. 2013). Readthrough transcription events initiating at the upstream cellular promoter would, however, generate a preRNA that included the entire HIV-1 sequence hidden embedded within the intronic sequence of the host gene (Han, Lin et al. 2008) (Figure 3.1). The presence of the viral sequence in the preRNA, including all of the HIV-1 splice donor and acceptor sites (Purcell 1993), could potentially alter the native splicing pattern of the maturing RNA to

incorporate viral sequence, such as the first coding exon of *tat*, into a mature “chimeric” mRNA containing *tat* within the now joined cellular exons. In previous work (manuscript in preparation) the Purcell group extensively examined these chimeric mRNAs and showed that Tat protein can be expressed from them by an internal ribosome entry site (IRES) mechanism of cap-independent protein translation, as detailed in Jonathan Jacobson, honors thesis 2011, University of Melbourne & Michelle Lee, PhD thesis 2018, University of Melbourne and below (Figure 3.5 & Appendix 1). For several other virus families, such as the *Picornaviridae*, the IRES circumvents antiviral defenses that prevent viral gene expression by lowering global cap-dependent protein translation (Plank et al. 2013). The IRES pathway of Tat expression therefore presents a potentially “druggable” pathway that is unique to infected cells and would therefore leave uninfected bystander cells unaffected by such drug treatment strategies. Tat protein acts positively to drive its own expression, by dramatically increasing the efficiency of successful LTR-driven transcription events, creating an LTR/Tat positive feedback loop (Verhoeef, Tijms et al. 1997). This suggests that drug-mediated induction of the initial pioneer rounds of Tat protein expression, by novel LRAs tailored to target the IRES pathway, may be sufficient in reestablishing the LTR/Tat positive feedback loop, reactivating HIV-1 gene expression.

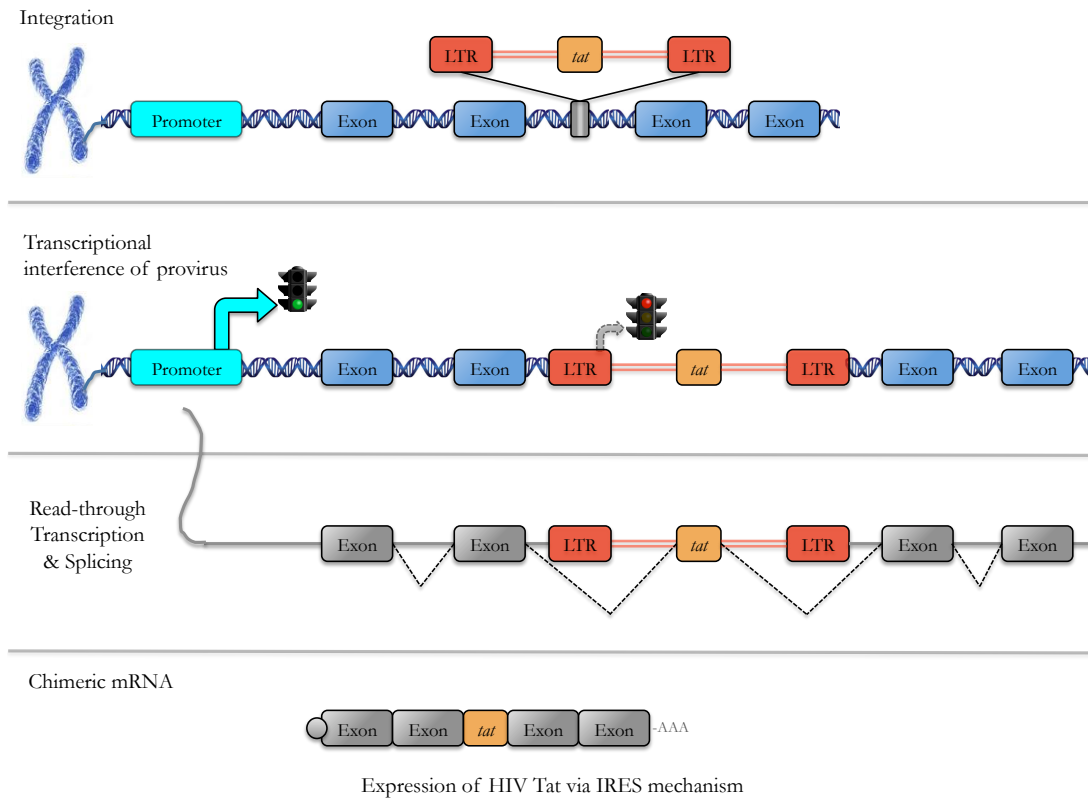


Figure 3.1: Expression of HIV-1 Tat protein during viral latency.

Following infection of a suitable cell and reverse transcription of the viral genome into dsDNA, integration within an actively transcribed cellular gene takes place, depicted here within an intron separating two cellular exons. The combination of several inhibitory factors that result from the infected cell returning to a resting quiescent state render the viral LTR promoter unable to drive its own transcription events, resulting in a silenced provirus, and viral latency. Transcription events from an upstream cellular promoter would result in pre-mRNA that includes the entire viral sequence, which, due to its complex arrangement of splice donor and acceptor sites, may allow the incorporation of HIV-1 sequence into the maturing cellular mRNA. The result is a chimeric mRNA that contains both cellular and viral sequence. Chimeric mRNAs containing the first coding exon of *tat*, which contains enough sequence to express a fully functional 72aa isoform of the Tat protein, may then express Tat protein in the cytoplasm via an IRES mechanism that underlies the *tat* exon. The Tat protein, having a multitude of roles in viral gene expression, may then initiate the Tat-mediated positive feedback loop to dramatically increase viral gene expression, effectively breaking the latent state.

3.3 Results.

The first objective of this thesis was to produce reporter cell lines that could discriminate compounds that could specifically reactivate latent HIV-1 while avoiding activating bystander cellular genes.

3.3.1 Construction of FlipIn.FM dual reporter cell line.

3.3.1.1 CBG luciferase expression from bicistronic constructs.

A reporter cell platform capable of assessing specific reactivation of HIV-1 from latency must exclude potentially toxic compounds using an “off target” reporter by measuring the stable expression levels of a constitutive marker gene. The off-target reporter gene would readily show any change in cell homeostasis due to global cell activation or drug toxicity, that was not HIV-1 specific. The initial reporter cell lines were designed to contain this off-target reporter in a 1:1 ratio with the Tat expression cassette, introduced together as a bicistronic construct. To achieve this, the Click Beetle Green68 luciferase (CBG) open reading frame (ORF) was cloned into pcDNA5/FRT.T4+CChGH, which contained the second exon of *tat* within the *human Growth Hormone (bGH)* gene cassette, replacing intron 4, but which retained its other native introns, *bGH* introns 1, 2, and 3 (Figure 3.2 Ai). We elected to express Tat from within the chimeric *tat/bGH* gene cassette, as opposed to a discrete *tat* ORF, to preferentially screen drugs that modulated Tat expression through its native IRES mechanism. This mechanism of translation initiation relies on structured RNA underlying the *tat* coding sequence and cannot be expressed by the cap-dependent ribosome scanning. As a result of this engineering, IRES-mediated expression is the only mechanism supporting Tat translation within the context of the T4+CChGH reporter (Figure 3.2). Transient plasmid transfection of the bicistronic pcDNA5/FRT.CBG-T4+CChGH (introns) construct was used to confirm CBG luciferase expression but was shown to be relatively low, 10% of the positive control pCBG (Figure 3.2B), suggesting that the intermediate bicistronic RNA transcript was highly unstable. This instability may have resulted from nonsense-mediated decay (NMD) of the RNA (Chang et al. 2007), due to exon-exon junctions forming within *bGH* downstream of the CBG stop codon. NMD serves as a protective cellular mechanism detecting exon-exon junctions downstream of an in-frame termination codon to avoid expressing potentially toxic truncated proteins from RNAs that contain premature termination codons, which may aberrantly arise by mutation (Wilusz, Wang et al. 2001).

To simply overcome this, an alternate version pcDNA5/FRT.CBG-T4+CChGH (cDNA) was used (Figure 3.2Aii). This bicistronic construct lacked the *bGH* introns, and was therefore not subjected to NMD, which was reflected in the rescued high level expression of CBG expression, at 74% of the positive control (Figure 3.2B)). The cytomegalovirus immediate-early promoter (CMV-IE or simply CMV) was used to drive constitutive high levels of RNA transcription for the off-target reporter constructs.

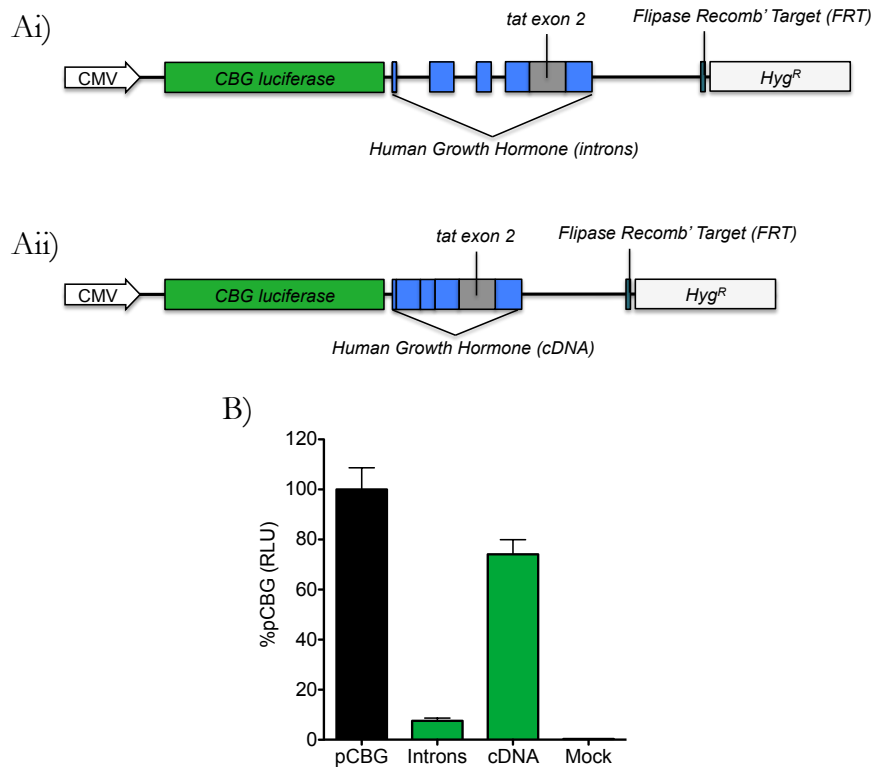


Figure 3.2: CBG expression from pcDNA5/FRT.CBG.T4+CChGH bicistronic constructs. Schematic of two versions of bicistronic plasmid containing the Click Beetle Green68 luciferase ORF upstream of the *tat*/human growth hormone chimeric gene cassette; (Ai) pcDNA5/FRT.CBG-T4+CChGH (introns) contains a genomic (intron containing) *bGH* gene cassette, with *tat* exon 2 between exons 4 and 5 of *bGH*, downstream of the CBG open reading frame. Aii) pcDNA5/FRT.CBG-T4+CChGH (cDNA) contains a similar arrangement, however, the *tat*/*bGH* cassette has been converted to cDNA (lacking introns). These plasmids use the CMV-IE promoter for RNA transcription to ensure constitutive expression of CBG this “off target” reporter. (B) HEK293 cells were transiently transfected with the control construct, as well as the intron containing construct and cDNA construct, with CBG expression measured at the 48hr time point. A CMV-driven CBG plasmid, pCBG, was used as the positive control plasmid and an empty pcDNA3.1- plasmid used as a mock transfection control to provide the background level of expression. Induction is shown as percentage of the pCBG control with the error bars representing standard deviation of n=3.

3.3.1.2 HIV-1 Tat expression from bicistronic construct.

Following observation of efficient CBG expression from the upstream open reading frame (uORF) from the bicistronic cDNA construct, it was then necessary to likewise examine IRES-mediated Tat protein expression from the downstream open reading frame (dORF). HEK293 cells were transiently co-transfected with pcDNA5/FRT.CBG-T4+CChGH (cDNA) to drive Tat expression and a second Tat-responsive LTR-driven *gfp* reporter plasmid. LTR transactivation and GFP expression measured by flow cytometry was used as a surrogate for Tat expression (Figure 3.3). We observed modest GFP expression, at 15% of the control plasmid pGFP when pcDNA5/FRT.CBG-T4+CChGH (cDNA) was co-transfected, demonstrating consistent coordinated levels of Tat expression from a dORF while Luc was synchronously expressed from the uORF. For reference, co-transfection with a wild type *tat* plasmid (pTat(WT)) produced 70% GFP expression, relative to the control. Empty pcDNA3.1- plasmid was used as a mock transfection and provided an experimental background level of expression. Taken together with the data in Figure 3.3, we have shown that the bicistronic construct pcDNA5/FRT.CBG-T4+CChGH (cDNA) expresses CBG luciferase efficiently from uORF and also expresses modest levels of Tat from the *tat/human growth hormone* chimeric gene cassette dORF.

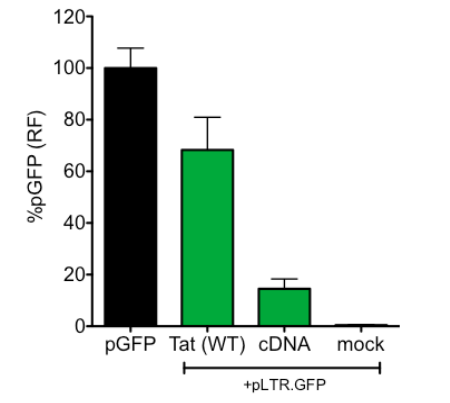


Figure 3.3: Tat expression from the pcDNA5/FRT.CBG.T4+CChGH (cDNA) bicistronic construct. HEK293 cells were co-transfected with either pTat(WT) or pcDNA5/FRT.CBG-T4+CChGH (cDNA) and an LTR-driven *gfp* reporter plasmids, and GFP expression as a reporter for Tat-mediated transactivation of LTR-directed expression measured at the 48hr time point. GFP expression, at 15% of the pGFP control, was observed when the pLTR.GFP reporter plasmid was co-transfected with pcDNA5/FRT.CBG.T4+CChGH (cDNA). Co-transfection with wild type Tat plasmid pTat(WT) produced 70% of the positive control plasmid. Induction is shown as percentage of the pGFP control with the error bars representing standard deviation of n=3.

3.3.1.3 Hygromycin B selection of FlipIn.CBG.T4+CChGH⁺ cells.

The FlpIn® recombinase system (Invitrogen), allows for the quick establishment of stable cell lines by utilizing Flpase mediated recombination into a defined genomic location of a candidate cell line, in this case HEK293 derived cells. The cell line genome contains a single Flpase Recombinase Target (FRT) sequence that serves as the specific destination sequence for “Flipping-In” of the pcDNA5FRT plasmid that contains the matching recombination sequence, to generate a clonal population of stable genome-modified cells. Successful Flip-In events of the plasmid into the cell chromosome confer Hygromycin B resistance, whereas unFlipped-In cells remained susceptible. Co-transfection of pcDNA5/FRT.CBG.T4+CChGH (cDNA) plasmid with the pOG44 recombinase coding plasmid was followed 48hrs later with selection of Flipped-In cells using Hygromycin B. To serve as a control, untransfected cells were also treated with Hygromycin B, and a kill curve created over 7 days. Untransfected cells were shown to be 100% dead after 7 days cultivation in hygromycin containing media at concentrations of above 175µg/mL, whereas recombination of the pcDNA5/FRT.CBG.T4+CChGH (cDNA) plasmid into the cell genome had conferred Hygromycin B resistance to Flipped-In cells at all concentration (Table 3.1).

Table 3.1: Hygromycin B kill curve of FlipIn.CBG.T4+CChGH⁺ cells.

FlipIn.CBG ⁺ cells (Hygromycin B Resistant)								Untransfected cells (Hygromycin B Susceptible)							
µg/mL	1	2	3	4	5	6	7	µg/mL	1	2	3	4	5	6	7
300	+++	+	+	+	+	+	+	300	+++	++	---	---	---	---	---
275	+++	+	+	+	+	+	+	275	+++	++	+	---	---	---	---
250	+++	+	+	+	+	+	+	250	+++	++	+	---	---	---	---
225	+++	++	+	+	+	+	+	225	+++	++	+	+	+	---	---
200	+++	++	+	+	+	+	+	200	+++	++	++	+	+	---	---
175	+++	++	++	+	+	+	+	175	+++	+++	++	+	+	---	---
150	+++	+++	++	+	+	+	+	150	+++	+++	++	++	+	+	+
125	+++	+++	++	++	+	+	+	125	+++	+++	+++	+++	++	+	+
100	+++	+++	+++	+++	++	+	+	100	+++	+++	+++	+++	+++	+	+
75	+++	+++	+++	+++	+++	++	++	75	+++	+++	+++	+++	+++	+++	+++
50	+++	+++	+++	+++	+++	+++	+++	50	+++	+++	+++	+++	+++	+++	+++
25	+++	+++	+++	+++	+++	+++	+++	25	+++	+++	+++	+++	+++	+++	+++

+++ All cells are adherent and healthy

++ Majority of cells are adherent and healthy

+ Some cells remain adherent (foci of resistant cells)

--- All cells are dead and floating

3.3.1.4 Dose dependent expression from LTR-driven CBR reporter.

To model HIV-1 latency as closely as possible within the artificial background of immortalized cell lines, it was of key importance that the reporter provirus utilizes all the processes involved in native HIV-1 gene expression, while including features for easy use in high throughput assays. The LTR-driven Click Beetle Red Luciferase (CBR) reporter provirus, pFM.nef/CBR, was prepared to fulfill these properties. The reporter provirus contains native HIV-1 LTRs (NL_{4.3}) and extended 5' untranslated leader sequence, allowing for tightly restricted expression that is sensitive to Tat-mediated transactivation, deletions to remove HIV-1 *gag/pol* and *tat* genes, as well as an internal deletion within *env*. The reporter provirus retains non-coding exons 2 and 5, with appropriate splice signals, allowing for authentic HIV-1 splicing of the *Nef* β (1/2/5/7) mRNA, from which a Nef/CBR fusion reporter is expressed (Figure 3.4A). The *Nef* β mRNA was specifically chosen to serve as HIV-1 reporter as the 5' RNA secondary structure tightly restricts protein translation, resulting in a desirably low baseline. To assess the responsiveness of the reporter plasmid to Tat transactivation, and also its baseline level of expression in the absence of Tat, pFM.nef/CBR was transiently co-transfected with either pTat or a mock plasmid into HEK293 cells. At 48hrs the cells were assayed for CBR luciferase activity as a surrogate for HIV-1 gene expression. We observed a tightly dose-dependent response ($r^2=0.96$) in the presence of a constant amount of pTat (Figure 3.4Bi), while showing very low amounts of CBR luciferase expression without pTat co-transfection. LTR-mediated Nef/CBR reporter expression was shown to increase 20-fold across all concentrations of reporter plasmid in the presence of pTat over the mock co-transfected counterparts (Figure 3.4Bii).

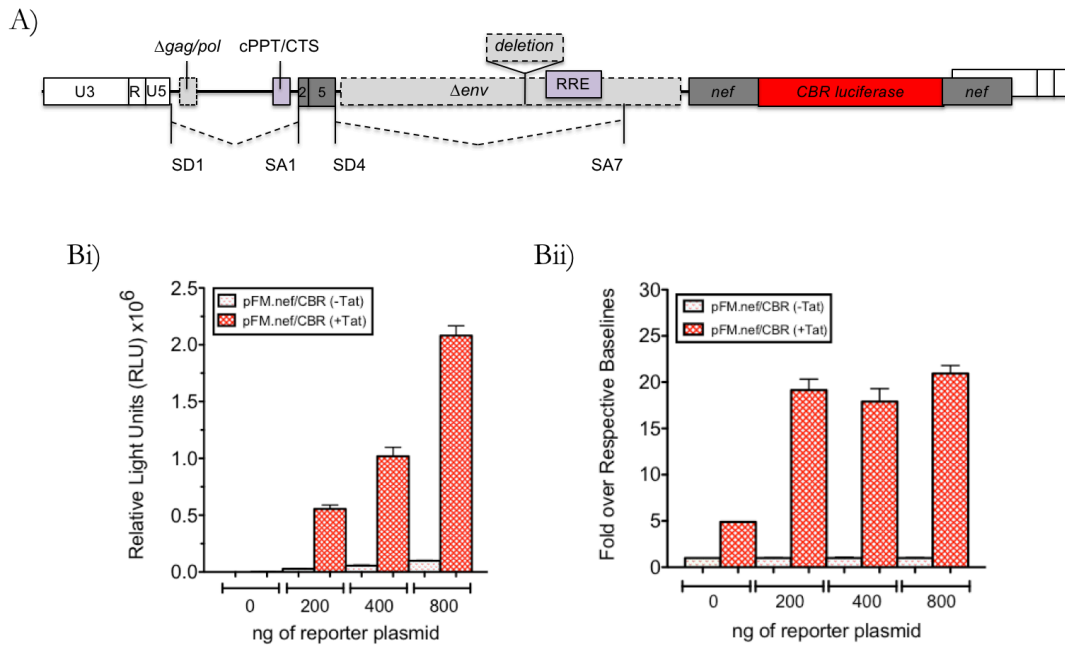


Figure 3.4: Dose dependent CBR expression from LTR-driven pFM.nef/CBR. (A) Schematic of the LTR-driven CBR reporter construct pFM.nef/CBR. The proviral reporter lacks HIV-1 *gag/pol* and *tat* genes, but retains the authentic splice donor (SD) and splice acceptor (SA) sites, SD1, SA2, SD4, and SA7 and authentically joins non-coding exons 2 and 5, allowing for splicing of the *Nef3* (1/2/5/7) mRNA. The pFM.nef/CBR reporter construct introduces wild type LTR sequences and flanking proviral host DNA from the pNL4-3 proviral clone that replicates the integrated proviral landscape of the pNL_{4.3} when recombined into the target sequence within FRT-transduced HEK293 cells. After recombinant HEK293 cells were transiently transfected with and either pTat(WT) or a Mock plasmid and the LTR-driven expression was measured at the 48hr time point. (Bi) Nef/CBR expression was shown to have a tightly dose dependent relationship when co-transfected with a constant amount of pTat ($r^2=0.96$), where doubling the amount of reporter plasmid transfected produced a proportional increase in CBR expression. (Bii) When titrating the amount of reporter plasmid, we observed a similar 20-fold transactivation of Nef/CBR reporter expression over the mock transfection (baseline) control. Induction was shown as raw RLU or fold-change over the untreated cell baseline with the error bars representing standard deviation from three independent experiments ($n=3$). Note in part Bii where 0ng of reporter plasmid was transfected, only 1-fold levels of luciferase was expected. The elevated levels detected were caused by bleed through from neighboring wells, giving the erroneous higher values that we attribute to experimental error inherent to the detection machinery (Section 2.3.3 and 2.3.6).

3.3.1.5 Augmenting Tat expression within reporter cell lines.

In addition to seeking compounds that activate HIV-1 LTR-mediated gene expression, a cell-based drug screening platform would also seek novel compounds that decreased LTR-driven expression through inhibiting Tat expression or function. For inhibitor detection the reporter cell lines require a sufficiently high level of Tat-mediated expression so that decreases could be accurately measured. Tat-mediated Nef/CBR reporter expression from the original bicistronic construct described above was not sufficient for this purpose. Therefore, a second *tat/bGH* gene cassette was introduced to increase the level of Tat expression in the cell line via lentivector transduction a CMV-driven T4+CChGH (intron containing) chimeric gene cassette introduced within a lentivector backbone (Figure 3.5A). As there was no upstream open reading frame in this case, the presence of introns within *bGH* would not induce nonsense mediated decay in the same fashion as the bicistronic construct (Figure 3.2A). Previous work had demonstrated the efficiency of Tat expression from the chimeric T4+CChGH (IRES only) context was only 13% efficient relative to wild type Tat expression from pTat(WT), similar to the results obtained from the Tat IRES in the bicistronic construct (Figure 3.3). In these experiments, the pLenti6.T4+CChGH plasmid was transfected into the HeLa derived TZM-bl cell line, a HeLa cell derivative expressing high levels of CD4, CXCR4 and CCR5 receptors for HIV-1. The TZM-bl cell line is used widely in HIV-1 research as an LTR-driven *firefly* luciferase (*Fluc*) reporter for HIV-1 infection using Fluc. While the TZMbl cell line itself could potentially be used for drug screening, it does have several drawbacks for screening LRAs which will be covered in the chapter discussion below. It is for these reasons that the FlipIn dual reporter cell lines were designed as a superior platform for assessing agents that modulate HIV-1 latency. Introduction of the pLenti6.T4+CChGH construct into the FlipIn cell lines by lentivector transduction that uses authentic HIV integration aimed to increase the steady state expression of Tat to a level high enough to detect a drug-induced decrease in LTR-driven expression of the Nef/CBR reporter of provirus.

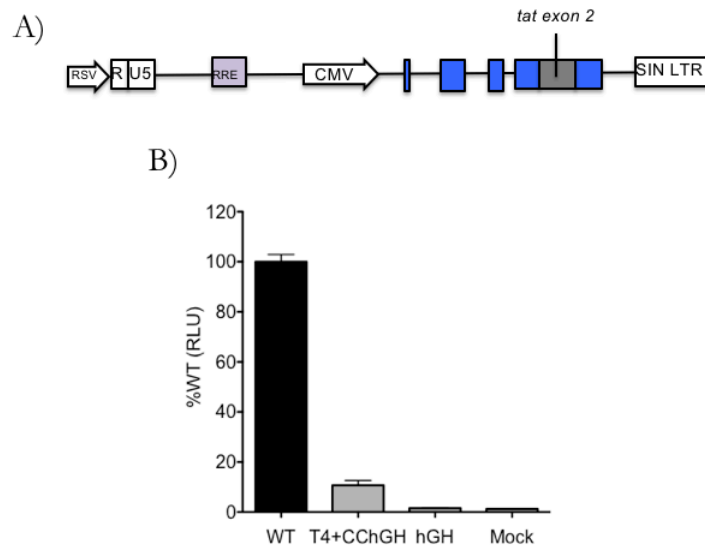


Figure 3.5: Expression of Tat from *tat/hGH* gene cassette. (A) Schematic diagram of pLenti6.T4+CChGH plasmid insert. The pLenti6 lentivector was constructed to express *tat/hGH* (intron containing) chimeric gene cassette under the CMV promoter after integration into the reporter cell line. When introduced into the FlipIn cells transduced cells would be expected to display augmented Tat expression through the IRES mechanism. (B) Firefly luciferase (Fluc) activity obtained in TZMbl cells transfected with the T4+CChGH plasmid that expresses Tat through the IRES mechanism and compared to positive control wild type pTat(WT) plasmid expressing Tat by conventional translation initiation. Wild type *hGH* served as an experimental negative control to ascertain the baseline level of Firefly luciferase expression in TZMbl cells. Induction is shown as percentage of the pTat(WT) control with the error bars representing standard deviation (n=3).

3.3.1.6 Selection of completed FlipIn.FM (clone C2).

After validating the three component plasmids for expression and reporter function by transient transfection, a stable cell line was generated as a platform for assessing HIV-1 LRAs. The process of clone generation for the FlipIn.FM reporter cell line occurred following three distinct steps. Firstly, Parental HEK293 derived FlipIn.Empty cells were “Flipped-In” with the CMV-driven off target reporter pcDNA5/FRT.CBG.T4+CChGH (cDNA) bicistronic plasmid and selected using Hygromycin B. Since only a single Flpase Recombination Target (FRT) sequence site exists within the cell genome, the resulting resistant cells were considered clonal. Selected cells were expected to coordinately express a constitutive level of CBG luciferase as well as a low level of Tat protein through the *tat* IRES mechanism. Secondly, the now CBG⁺, Hygromycin B resistant cells were transduced with the pFM.nef.CBR lentivirus. Due to random nature of the lentivector integration events, and the need to isolate a clone for reproducibility in High Throughput Chemical Screening, single cell dilutions and clone screening was performed to find a clone that was CBG⁺ and CBR^{LOW}. Clones that were CBG⁺/CBR⁻ were discarded. Thirdly, additional Tat expression was enhanced by a second transduction event with pLenti6.T4+CChGH, a lentivector expressing CMV-driven T4+CChGH, and a second round of single cell dilutions performed to find CBG⁺ and CBR^{HIGH} clones. Clones were tested head to head and a ratio of LTR-driven expression versus CMV-driven expression calculated. Clone C2, giving an LTR/CMV ratio of 1.4 : 1 (Figure 3.6), was chosen for expansion and became the FlipIn.FM dual reporter cell line for use in high throughput chemical screening (HTCS) for HIV-1 LRAs and other subsequent experiments.

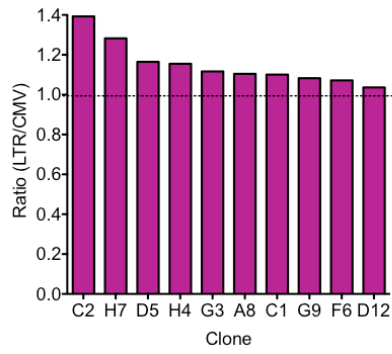


Figure 3.6: LTR/CMV ratios of FlipIn.FM clones. Following single cell selection and assaying for the relative expression of both LTR-driven and CMV-driven reporters, an LTR/CMV ratio was calculated and the clone C2, which showed ratio of 1.4 : 1 was chosen to become the FlipIn.FM dual reporter cell line.

3.3.2 Construction of FlipIn.RV dual reporter cell line.

3.3.2.1 CBR luciferase expression from bicistronic construct.

To ensure that the compounds identified in the HTCS were not simply interfering with the luciferase enzyme activity, giving a “false hit”, a second reverse-orientation or dye-swap control cell line was needed to confirm any hits. To achieve this the procedure described above was repeated starting with the FlipIn.Empty cells, but using modified constructs that switched the CBG and CBR reporter genes. During counter screening, results with a reporter-swap cell line should give matching results to the original FlipIn.FM dual-reporter cell line, both with toxicity profile and LTR-activation profile. However it is worth noting that, while the “flipped-in” CMV-driven off-target reporter would be at identical locations in both cell lines due to the site directed recombination process at the single FRT site, the lentivector transductions using pFM.CBR and pFM/nefCBG and pLenti6.T4+CChGH would result in different random integration events, which could potentially lead to different responses between the reporter-swapped cell lines. The first inclusion into the FlipIn.RV cell line was therefore the pcDNA5/FRT.CBR.T4+CChGH (cDNA) bicistronic off target reporter. This construct was made by simply removing the Click Beetle Green ORF from the original construct replacing it with the Click Beetle Red (CBR) ORF at the exact same position (Figure 3.7A). CBR luciferase expression from the uORF was similarly validated by transient transfection into HEK293 cells (Figure 3.7B). At 48hrs post transfection, the pcDNA5/FRT.CBR.T4+CChGH (cDNA) bicistronic construct produced only 48% of the CBR expression obtained from the pCBR positive control plasmid. While adequate, this was significantly lower than the level seen in the CBG counterpart shown in Figure 3.2 (74%). Tat expression from this construct mirrored that seen from the CBG counterpart in Figure 3.3 (data not shown).

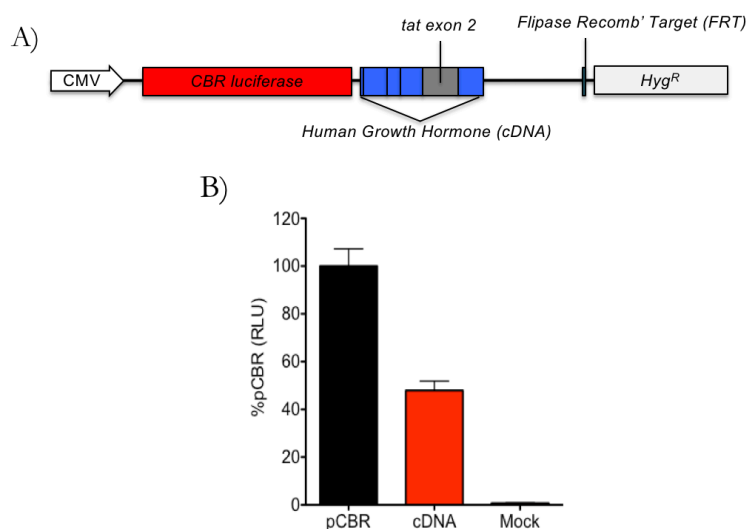


Figure 3.7: CBR expression from pcDNA5/FRT.CBR.T4+CChGH (cDNA) bicistronic construct. (A) Schematic diagram of the bicistronic plasmid containing the Click Beetle Red luciferase gene upstream of the *tat/human growth hormone* chimeric gene cassette. This construct was made by replacing the original CBG ORF with the CBR ORF using the *XbaI* and *KpnI* restriction sites. (B) HEK293 cells were transfected with pcDNA5/FRT.CBR.T4+CChGH (cDNA) and CBR expression measured after 48hr. Interestingly, CBR expression from this bicistronic construct was shown to reach only 48% of the control pCBR plasmid. Empty pcDNA3.1- plasmid was used as a negative mock transfection control that provided an experimental background level of expression. Induction is shown as raw percentage of pCBR control with the error bars representing standard deviation (n=3).

3.3.2.2 Hygromycin B selection of FlipIn.CBR.T4+CChGH⁺ cells.

The FlpIn® site specific recombination system was again used to generate this stable cell line by co-transfection of pcDNA5/FRT.CBR.T4+CChGH (cDNA) with the recombinase coding plasmid pOG44 and selection using Hygromycin B 48hrs later. A kill curve was created over 7 days. Untransfected cells were 100% dead 7 days after cultivation at concentrations above 75µg/mL with a different batch of Hygromycin B to that used in Table 3.1. Transfected cells were also 100% dead at concentrations above 200µg/mL, but showed resistant foci at concentrations between 100µg/mL-200µg/mL, which were pooled for further use.

Table 3.2: Hygromycin B kill curve of FlipIn.CBR.T4+CChGH⁺ cells.

µg/mL	FlipIn.CBR ⁺ cells (Hygromycin B Resistant)							µg/mL	Untransfected cells (Hygromycin B Susceptible)						
	1	2	3	4	5	6	7		1	2	3	4	5	6	7
300	++	+	---	---	---	---	---	300	++	+	---	---	---	---	---
275	++	+	+	+	+	+	---	275	++	+	---	---	---	---	---
250	+++	+	+	+	+	+	---	250	++	+	---	---	---	---	---
225	+++	+	+	+	+	+	---	225	++	+	---	---	---	---	---
200	+++	++	+	+	+	+	+	200	++	++	+	---	---	---	---
175	+++	+++	+++	+	+	+	+	175	+++	+++	+++	+	+	+	---
150	+++	+++	+++	+	+	+	+	150	+++	+++	+++	++	+	+	---
125	+++	+++	+++	+	+	+	+	125	+++	+++	+++	+++	++	+	---
100	+++	+++	+++	+++	+++	+++	++	100	+++	+++	+++	+++	++	+	---
75	+++	+++	+++	+++	+++	+++	++	75	+++	+++	+++	+++	+++	++	+
50	+++	+++	+++	+++	+++	+++	+++	50	+++	+++	+++	+++	+++	++	+
25	+++	+++	+++	+++	+++	+++	+++	25	+++	+++	+++	+++	+++	+++	+++

- +++ All cells are adherent and healthy
- ++ Majority of cells are adherent and healthy
- + Some cells remain adherent (foci of resistant cells)
- All cells are dead and floating

3.3.2.3 Dose dependent expression from LTR-driven CBG reporter.

To construct the FlipIn.RV reporter swap cell line an LTR-driven reporter containing CBG within *nef* was prepared by replacing the original CBR ORF with the CBG ORF using the unique *XhoI* and *KpnI* restriction sites located within *nef*. The pFM.*nef*/CBG construct also contains native HIV-1 LTRs (NL₄₋₃) and major deletions of *gag/pol* and *tat* genes as well as an internal deletion within *env*, while preserving splicing to produce a *Nef3* mRNA, from which a Nef/CBG fusion reporter is expressed (Figure 3.8A). Likewise, to assess the responsiveness of the counter-screen reporter plasmid to Tat transactivation, and also its baseline level of expression in the absence of Tat, pFM.*nef*/CBG was transiently co-transfected with either pTat(WT) or a Mock plasmid. Again, we observed a tightly dose-dependent expression response ($r^2=0.89$) in the presence of a constant amount of pTat(WT) (Figure 3.8Bi). LTR induction was again shown to increase approximately 20-fold in the presence of Tat across all concentrations of reporter plasmid (Figure 3.8Bii). The results seen using this counter screen reporter closely mirror those seen in the original pFM.CBR reporter, suggesting that this counter screen cell line would prove to be a stringent validation for potential novel LRAs.

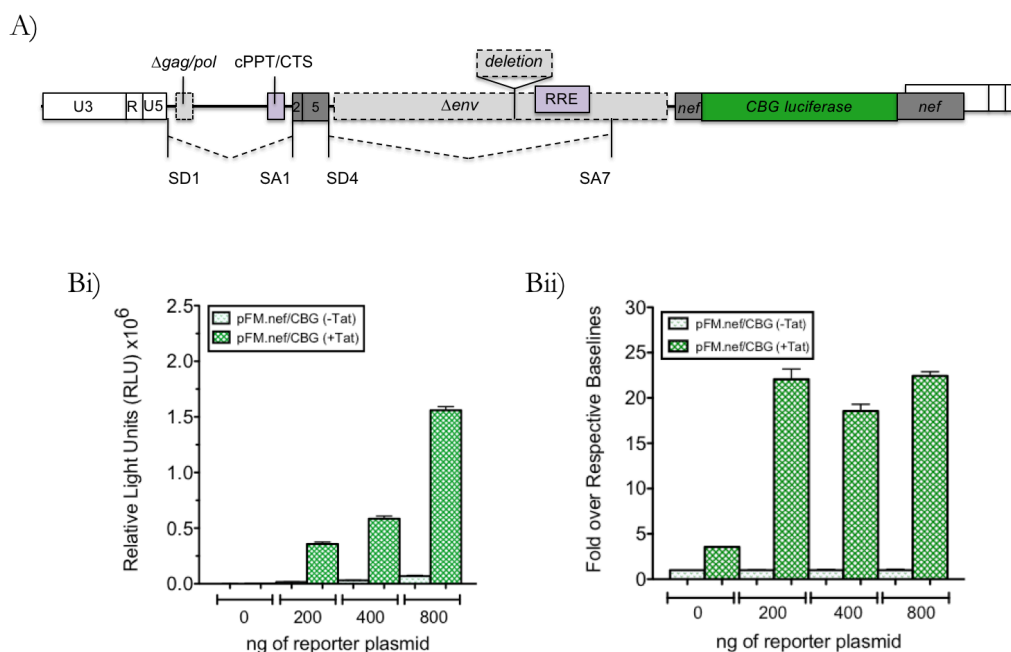


Figure 3.8: Dose dependent CBG expression from LTR-driven pFM.nef/CBG. (A) Schematic of the LTR-driven CBG reporter construct pFM.nef/CBG. As with the CBR counterpart, the proviral reporter lacks HIV-1 *gag/pol* and *tat* genes, but retains the authentic splice donor (SD) and splice acceptor (SA) sites, SD1, SA2, SD4, and SA7 and authentically joins non-coding exons 2 and 5, allowing for splicing of the *Nef3* (1/2/5/7) mRNA. The pFM.nef/CBG reporter construct introduces wild type LTR sequences and flanking proviral host DNA from the pNL₄₋₃ proviral clone that replicates the integrated proviral landscape of the pNL₄₋₃ plasmid when recombined into the target sequence within FRT-transduced HEK293 cells. After recombinant HEK293 cells were transiently transfected with pFM.nef/CBG and either pTat(WT) or a Mock plasmid and the LTR-driven expression measured at the 48hr time point. (Bi) Similarly to the CBR counterpart, expression from the LTR-driven Nef/CBG reporter showed a tightly dose dependent relationship ($r^2=0.89$) when co-transfected with a constant amount of pTat and (Bii) showed a 20-fold activation over mock transfection (baseline) across all amounts of reporter plasmid used. Induction is shown as raw RLU or fold change over the untreated cell baseline with the error bars representing standard deviation from three independent experiments ($n=3$). Note in part Bii where 0ng of reporter plasmid was transfected, only 1-fold level of luciferase was expected. The elevated levels detected were caused by bleed through from neighboring wells, giving the erroneous higher values that we attribute to experimental error inherent to the detection machinery (Section 2.3.3 and 2.3.6)..

3.3.2.4 Selection of completed FlipIn.RV (clone B6).

Having swapped out the luciferase genes in the reporter constructs, an identical three-step process used for the original FlipIn.FM cell line was followed to generate the completed FlipIn.RV counter screen line. Parental FlipIn.Empty cells were “Flipped-In” with the pcDNA5/FRT.CBR.T4+CChGH (cDNA) CMV-driven off target reporter and selected for using Hygromycin B. The resulting CBR⁺ cells were transduced with the pFM.nef/CBG reporter lentivirus and single cell dilutions performed to detect any CBR⁺/CBG^{LOW} clones. Again, to augment endogenous Tat expression via the IRES mechanism, this clone was then further transduced with a CMV.T4+CChGH lentivirus and a CBR⁺/CBG^{HIGH} clone was detected and selected based on the LTR/CMV ratio. Clone B6 showed the highest ratio of 1.2 (Figure 3.9) and was chosen as the FlipIn.RV counter screen cell line

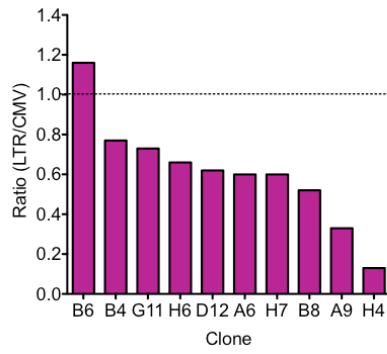


Figure 3.9: LTR/CMV ratios of FlipIn.RV clones. Following single cell selection and assaying for the relative expression of both LTR-driven and CMV-driven reporters, an LTR/CMV ratio was calculated and the clone B6, which showed a ratio of 1.2 was chosen to become the FlipIn.RV counter screen cell line.

3.3.3 Validating FlipIn.FM and FlipIn.RV dual reporter cell lines.

3.3.3.1 Dose dependent responses to Tat plasmid in cell lines.

The two completed HIV-1 latency reporter cell lines each contained three distinct constructs that together attempt to model the molecular events that control gene expression during latency as closely as possible in an immortalized cell line (Figure 3.10A). The limitations for these models include the cell type being immortalized, the use of a truncated splicing construct, and the use of a CMV promoter for the non-specific reporter. Potential problems with these issues are addressed in the discussion below. With the *tat* IRES pathway being the only mechanism possible for Tat expression (and therefore Tat-mediated LTR activation), the cell lines would also selectively pull out compounds that modulated our mechanism of interest, meaning desirable hits should potentially show little or no non-specific activity. Any non-specific activity would also be clearly evident through the off-target reporter. Interestingly, at steady state, that is, without activation from exogenous Tat or drug treatment, the CMV-CBG level in the FlipIn.FM cells was shown to be 23-fold greater than that of the LTR-CBR level, despite the ratio seen in Figure 3.6. However, why this change occurred after a few weeks of passaging remains unclear. In contrast, the CMV-CBR and LTR-CBG levels seen in the FlipIn.RV cell line (Figure 3.10B) showed only a 3-fold difference. This high level of CMV-CBG expression in the FlipIn.FM cells becomes evident in later experiments where a fold change achieved with strong activators like PMA appears to be very modest. Before the cell lines could be cleared for use in HTCS to assess the potential of over 114,000 small drug-like molecules to specifically reactivate LTR-driven expression (Chapter 4), it was necessary to fully validate the response of their respective LTR-driven reporter proviruses, as well as their ability to detect drug candidates that function with high specificity for the LTR. To assess this, both completed cell lines were transiently transfected with increasing amounts of pTat(WT) and their LTR and CMV responses measured for dual luciferase activity (Figure 3.10C and D). Induction was graphed as fold over the respective luciferase baseline levels when transfected with mock plasmid. These data showed a tight dose dependent level of LTR induction, $r^2=0.92$ for FlipIn.FM and $r^2=0.99$ for FlipIn.RV, while the respective CMV reporters remained unchanged. Importantly, the level of LTR induction was consistent across cell lines, with a 12 fold change obtained when transfected with the maximum amount of pTat(WT).

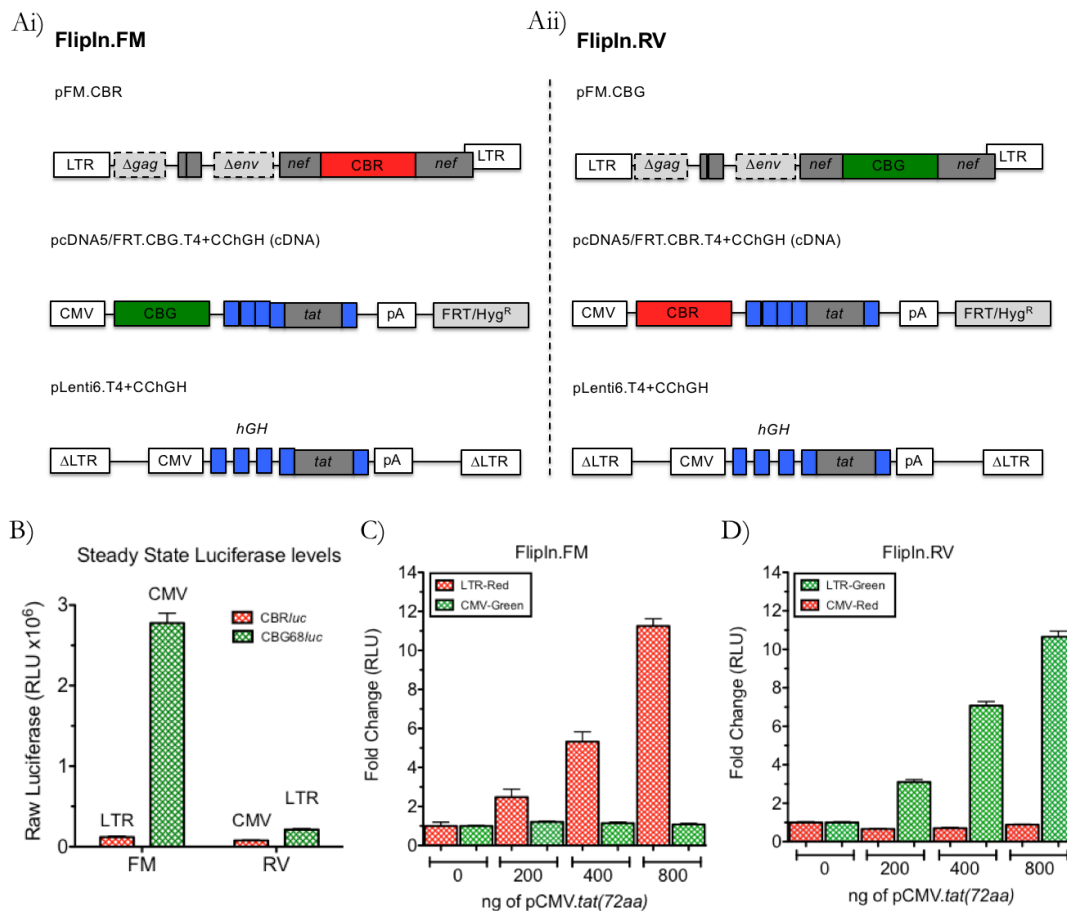


Figure 3.10: Response of completed FlipIn.FM and FlipIn.RV dual reporter cell lines to Tat expression plasmids. The completed (Ai) FlipIn.FM and (Aii) FlipIn.RV cell lines consist of 3 discrete constructs that attempt to model HIV-1 latency in primary cell infection, but allow for high throughput experiments as a cell line model. They each contain an LTR driven luciferase reporter (CBR and CBG respectively) which shows a very low baseline of leaky expression but is highly responsive to HIV-1's native transactivator Tat. Each reporter includes a complimentary off-target reporter, driven by the CMV promoter to screen out toxic or non-specific drugs. Finally, to provide enough endogenous Tat to allow for detection of inhibitor drugs, a third Tat expression cassette was included into each cell line. Transfection of the pCMV.tat(72aa) Tat encoding plasmid into the (C) FlipIn.FM and (D) FlipIn.RV cell lines validated that LTR-driven expression could be induced independently of activating the off target CMV control. Induction was assayed at the 48hr time point and is shown as fold change over the untreated cell baseline with the error bars representing standard deviation of n=3.

3.3.3.2 Dose dependent responses to Tat protein in cell lines.

Another experiment to further test the LTR response to transactivation was to transiently transfect the completed FlipIn.FM and FlipIn.RV dual reporter cell lines with biologically active recombinant Tat protein (rTat). Of note, Tat86aa is the two exon isoform of Tat protein expressed by the NL_{4.3} strain of HIV-1, as opposed to the 72aa isoform expressed from the pTat(WT) plasmid used to confirm Tat-responsivity above. Tat86aa, contains an additional 14 amino acids from the second coding exon of HIV-1 NL_{4.3} that is a more stable form of the Tat protein, and is therefore marginally more efficient at transactivating the LTR. Recombinant Tat protein was titrated across a wide range of concentrations from 1 μ M (10⁶pM) down to 15pM in a 2-fold series. Cells were transfected following the same protocol and time frame used with the plasmid experiments and assayed at 48hr post transfection. Figure 3.11 showed the lower end of a characteristic drug-like curve for each cell line, although the maximum level of induction (plateau) was not achieved within the concentration window used. The minimal concentration required to separate the LTR and CMV reporters was \sim 1nM (10³pM) in both cell lines. Interestingly, the maximum induction (at 1 μ M) was 6-fold in the FlipIn.FM cells, but only 3.5-fold in the FlipIn.RV cells.

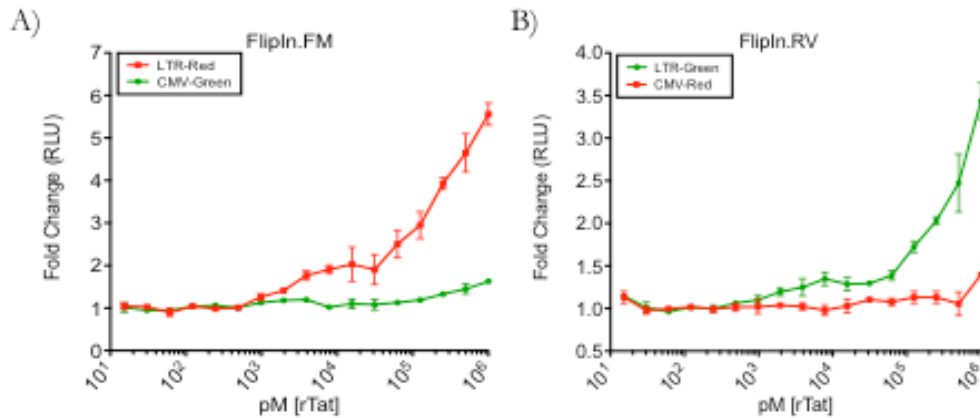


Figure 3.11: Response of completed FlipIn.FM and FlipIn.RV dual reporter cell lines to recombinant Tat protein.

Recombinant Tat 72aa protein (rTat) was transfected into FlipIn.FM and FlipIn.RV dual reporter cell lines and induction of LTR-driven and CMV-driven expression measured at the 48hr time point. We observed 6-fold induction of the LTR reporter in the FlipIn.FM cell line at the highest concentration of rTat used, 1 μ M (10⁶pM), but interestingly only 3.5 fold in the FlipIn.RV cell line. We also observed that the minimal concentration of rTat required to separate the LTR and CMV reporters in both cell lines was \sim 1nM (10³pM). Induction is shown as fold change over the untreated cell baseline with the error bars representing standard deviation of n=3.

3.3.4 Modifying J.Lat latently infected Jurkat T cell line.

3.3.4.1 Generating T cell derived J.LatFM dual reporter populations.

Different models of HIV-1 latency were used in this thesis for the development of our novel LRAs to balance of two major properties: (1) the suitability for high throughput screening for a large number of compounds, and (2) modeling HIV-1 post integration latency *in vitro* that matches as close as possible what occurs in a patient. While the FlipIn cells are ideal for HTCS, as will be discussed in Chapter 4, they are derived from the Human Embryonic Kidney (HEK293) cell line. As such, they do not represent the CD4+ T cells that contain the HIV-1 reservoir, and, being immortalized, differ significantly in their metabolism from primary CD4+ cells. The FlipIn.FM and FlipIn.RV cell models therefore serve as an ideal first-step on the path of drug discovery, but any hits found in this model must be further validated in additional HIV latency models. The next model and step along the path were two of the Latently infected Jurkat T cell line (J.Lat) clones (Jordan *et al* 2003). While these are still immortalized cell lines, they represent a more relevant cell of origin, the CD4+ T cell. Additionally, the J.Lat clones are infected with a replication deficient full-length provirus capable of expressing both Tat spliced isoforms, which more closely resembles wild type HIV-1 than the FlipIn reporter provirus. With these factors, the J.Lat clones were considered here as an appropriate next step on the path of drug development for the “hits” from the FlipIn model. Interestingly, despite these two original clones being generated in the same experiment by Jordan *et al*, and sharing the same reporter provirus, they respond very differently to LRA treatment. This is due to their different integration sites within their respective host cells and therefore the two clones are subject to different restriction mechanisms for HIV-1 gene expression, although there are certainly many more factors contributing to the difference seen. Two clones, representing a highly inducible provirus (J.Lat10.6) and very difficult to induce provirus (J.Lat6.3) were chosen for further studies. To generate the adapted J.Lat models used here, J.Lat10.6 cells, clonal for a single HIV-R7/E/GFP reporter virus integration site, were transduced with a CMV-*DS.Red*^{EXP} lentivirus to add an off-target reporter system (Figure 3.12). The same process was repeated with the J.Lat6.3 clone. Unlike the FlipIn model, however, which has a single recombination site for the CMV-driven off-target reporters (through the Flip-In process), the J.Lat10.6FM and J.Lat6.3FM populations are heterogeneous in their CMV-driven *DS.Red* reporters, due to random integration of the lentivirus. An advantage of this random integration, is that a more global view of the off-

target effects of LRAs can be gained as opposed to a clonal context as with the FlipIn model. For this reason, the dual reporter J.Lats are termed populations rather than clones.

FlipIn (HEK293 line) → J.Lat (Jurkat line) → CD4+ T cells (primary)

Simple manipulation High Throughput ✓ ✓ ✓	Simple manipulation Medium throughput ✓	Labour intensive Low throughput ✗
Clonal LTR-reporter provirus lacks Tat/TAR loop but allows for splicing. ✓	Clonal LTR-reporter provirus contains Tat/TAR loop and allows for splicing. ✓ ✓	Latently infected cells selected for using cART represent natural infection ✓ ✓ ✓
Luciferase system	Flow Cytometry	qPCR
HEK 293: Unrelated cell type & Immortalised ✗	Jurkat: Appropriate T cell type but Immortalised ✓	Primary: Appropriate T cell type and primary ✓ ✓ ✓
Non-specific reporter is clonal ✗	Non-specific reporter is heterogeneous ✓	Latency integration sites selected for using cART ✓ ✓ ✓

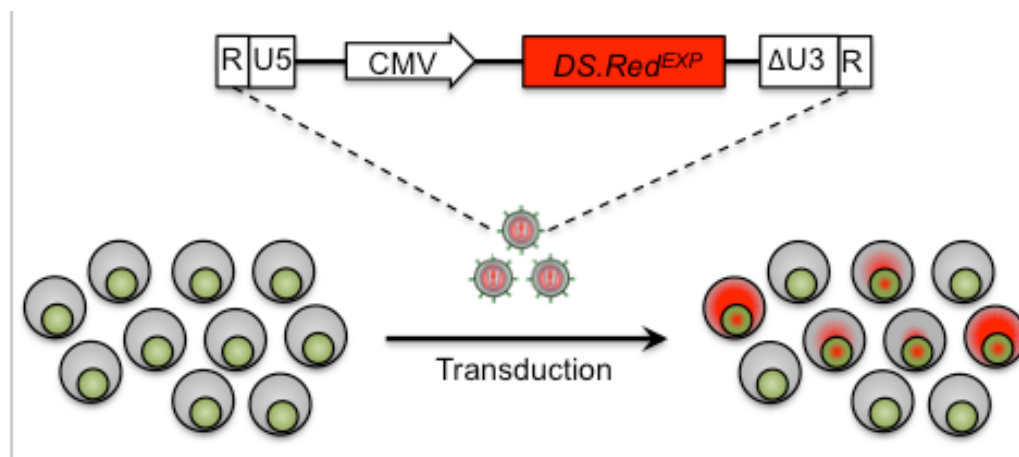


Figure 3.12: Generating J.LatFM populations. Cells from the pre-established J.Lat10.6 and J.Lat6.3 cell lines, which each have a unique clonal HIV-R7/E⁻/GFP provirus, were transduced with a lentivirus to introduce a CMV-driven *DS.Red^{EXP}* red fluorescent protein gene. Integration would occur randomly within infected cells, generating a heterogeneous population in terms of the off-target reporter. Of note, not all cells were successfully transduced by an inducible CMV-*DS.Red* reporter. For both J.Lat10.6FM and J.Lat6.3FM modified cell lines, ~45% of the cells were transduced, as seen after maximum activation using PMA, whereas their steady state expression without activation was ~5% GFP positive (Figure 3.13).

3.3.4.2 Validating J.LatFM populations.

Although the J.Lat10.6 and J.Lat6.3 clones were originally created under the same conditions within the same experiment in the Verdin laboratory by Jordan *et al*, they exhibit very different behavior when treated with a strong stimulant such as PMA, due most likely to the different integration sites of their respective HIV-R7/E/GFP reporter proviruses. Although for each case, 100% of the cells contain the LTR-*gfp* reporter provirus, maximal activation typically shows ~85% GFP positive for the J.Lat10.6 clone and ~20% GFP positive for the J.Lat6.3 clone. Transduction of the two clones with a lentivirus encoding a CMV-driven *DS.Red^{Exp}* reporter gene generated a heterogeneous population of Red+ cells containing random lentivector integrations. For both the newly created J.Lat10.6FM and J.Lat6.3FM populations, ~5% of the cells were Red+ without stimulation (from expression driven off the constitutive CMV promoter) whereas after stimulation with PMA at 8nM, both showed ~45% Red+ (Figure 3.13). The advantage of a heterogeneous population in terms of the CMV-driven non-specific reporter, is that we gain a broader view of global cell activation, as each CMV-*DS.Red^{Exp}* reporter is likely to have integrated into a unique position within each host cell, and therefore each reporter provirus will be subject to different restrictions on gene expression.

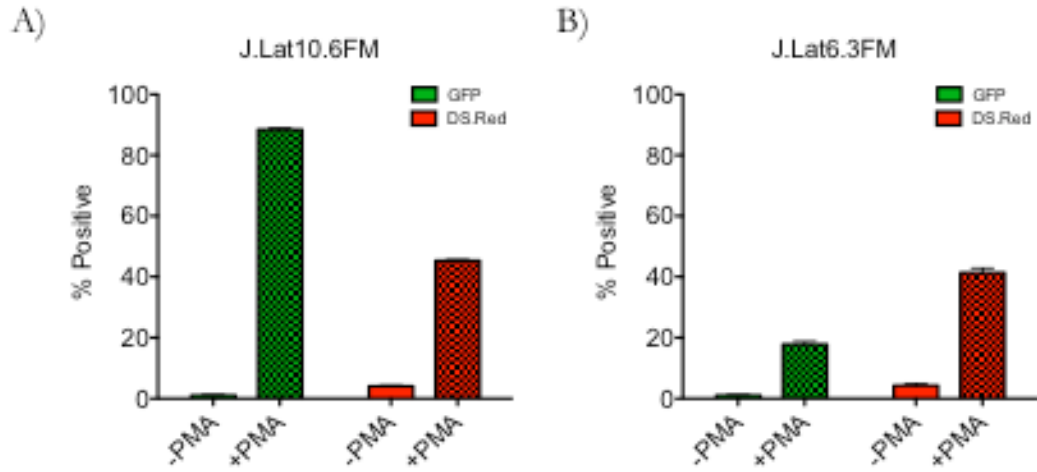


Figure 3.13: Validation of J.LatFM transductions. Following transduction of J.Lat10.6 and J.Lat6.3 clones with a CMV- *DS.Red^{Exp}* lentivirus, bulk transduced cells were stimulated with 8nM PMA, and assayed at 48hrs post treatment. GFP positive and Red positive cells were harvested, fixed and analyzed by flow cytometry under PC3 level biocontainment. Induction is shown as percentage positive with the error bars representing standard deviation (n=3).

3.4 Discussion.

The introduction of cART proved highly successful in decreasing HIV-1 related morbidity and mortality (Gulick et al. 1997, Harrison et al. 2010). Due to the risk of viral rebound from the latent reservoir of infected cells, cART must be adhered to for life, leaving the patient vulnerable to cART related toxic effects as well as social stigma (Dahl et al. 2010). Additionally, with each new infection that is able to receive therapy, the global financial burden increases. Finding a cure for HIV-1 is therefore an important challenge for mankind. The ultimate goal for this thesis was to discover and develop novel LRAs that specifically targeted HIV-1 infected cells, while leaving uninfected bystander cells unaffected. To do this the novel LRA must specifically reactivate HIV-1 gene expression, while avoiding non-specific or off-target global gene activation. Due to the very rare occurrence rate of an inducible latent infection arising, approximately 1 in 1 million CD4+ T cells (Finzi et al. 1997), efforts to study HIV-1 latency have relied heavily on the use of model systems. Detailed descriptions of the currently used cell lines, primary cell models and *in vivo* models of HIV-1 latency can be found in Appendix 2. The drawbacks for each model for drug screening, however, necessitated the development of the FlipIn model of HIV-1 latency.

The following discussion will outline how the FlipIn model was designed to overcome the specific shortcomings of the current HIV-1 latency models, and how the model was designed to detect novel LRAs specifically targeting the *tat*/IRES pathway. The limitations to the FlipIn model are also considered. The main advantage of cell line models is the ease in which they can be cultured and expanded, allowing for high throughput assays with a high degree of reproducibility. The main disadvantage of cell line models is that they are continually dividing and metabolically active, which differs to the natural HIV-1 reservoir that is predominantly in resting memory T cells. Three more considerations must be raised:

1. The tissue/progenitor from which the cell line is derived and how faithfully this host cell represents that native setting of latent HIV-1 infection.
2. The reporter construct, i.e. does it mimic a full-length or truncated provirus and how faithfully it recapitulates HIV-1 gene expression.
3. Is the cell line homogeneous for the integrated reporter?, i.e. will the cell line represent a single latency scenario?

As discussed in the introduction to this chapter, we sought to recapitulate the molecular events that occur during HIV-1 latency: 1) Generation of chimeric *cellular/tat* mRNAs capable of expressing Tat protein from an IRES following HIV-1 integration and LTR silencing by a cellular gene (Figure 3.1). 2) Tat mediated LTR trans-activation, polIII driven transcription and RNA processing, including native HIV-1 splicing (Figure 1.16). 3) Re-establishment of the Tat-TAR feedback loop necessary to sustain HIV-1 gene expression and result in the death of the infected cell. The FlipIn model also includes the following features, making this system preferable to many other models for the specialized task of discovering novel specific LRAs (listed in Appendix 2).

1. **Novel target pathway for HIV-1 specificity:** The FlipIn cells include the novel pathway of IRES mediated Tat expression in the chimeric *tat/bGH* mRNA construct (Section 3.2), which may allow for detection of novel LRAs that specifically target this pathway. Work done on these chimeric *tat/bGH* genes was adapted from the authors honors thesis: Mechanisms controlling the translation of HIV-1 Tat protein, Jonathan Jacobson 2011, and is summarized in Appendix 1.
2. **High fidelity, high throughput proviral reporter:** Unlike the TZMbl's LTR reporter construct (Figure A.3), the pFM.nef/CBR and pFM.nef/CBG (Figure 3.4 and 3.8 respectively) requires native HIV-1 RNA splicing, more faithfully modeling HIV-1 gene expression. To allow for truly high throughput (as would be needed for library screening) the FlipIn model uses luciferase assay technology, rather than the flow cytometry based method of the J.Lat model. The FlipIn cells also do not require PC3 level containment.
3. **Avoiding off target effects.** The inclusion of the non-specific reporter constructs allowed for immediate elimination of compounds that induced global gene activation. This important feature is lacking in all other models of HIV-1 latency discussed in Appendix 2. It was for this reason that the J.Lat cells were modified to include a CMV-driven DS.Red non-specific marker, to confirm that the compounds found in Chapter 5 did not show off target effects.

Generation the bicistronic pcDNA5/FRT.CBG.T4+CChGH (introns) construct were initially confounded by a very low level of CBG expression, seen at only 10% of the control pCBG construct when transiently transfected (Figure 3.2). Review of the construct design indicated that the presence of a stop codon within the CBG ORF, upstream of where the *tat/bGH* cassette was predicted as a trigger of a rapid degradation of the mRNA by the

process of nonsense-mediated decay (NMD)(Chang, Imam et al. 2007). This activity may explain the low level of gene expression. To rectify this, the intron containing *tat/bGH* portion was exchanged with a cDNA version, making the pcDNA5/FRT.CBG.T4+CChGH (cDNA) construct, which immediately overcame the potential problem of NMD and restored CBG gene expression to 74% of the control.

Interestingly, in Figure 3.7 when the counterpart pcDNA5/FRT.CBR.T4+CChGH construct was made and tested in an identical manner, it achieved only 48% of the pCBR control. This may be due to subtle differences in the two luciferase reporter genes that confer different stability at the RNA level, but these experiments were not pursued over moving forward with a drug discovery program. What is known is that the CBR luciferase enzyme itself has a rapid rate of decay (half-life = 45min) when compared to the relatively stable CBG luciferase (Figure 3.14).

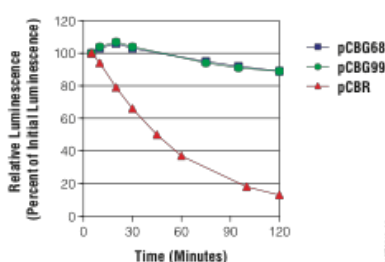


Figure 3.14: Activity-Decay profiles of CBG and CBR luciferase reporters.

Chroma-Glo™ Luciferase assay system Technical Manual 2008/9 (Promega®)

Analysis of Tat expression from the downstream ORF of pcDNA5/FRT.CBG.T4+CChGH (cDNA) in Figure 3.3 showed 15% of the GFP expression seen with the pTat(WT) plasmid when co-transfected with a pLTR.GFP reporter plasmid. This number, ~13% of the pTat(WT), has been highly conserved across many experiments that use the *tat/bGH* constructs and is likely due to the *tat* IRES structure (Appendix 1). While HIV-1 is known to contain an IRES at the 5' untranslated region (UTR) of all its mRNAs, located within the 5' LTR (Amorim, Costa et al. 2014) and contain an IRES within the *gag* sequence, either a distinct element or an extension of the 5'UTR IRES (Buck, Shen et al. 2001) the *tat* IRES has not been previously described in the literature, although the Purcell lab have manuscripts in preparation/submission. One important consideration for the non-specific reporters of the FlipIn and J.Lat models is the promoter involved. While the CMV promoter used is not HIV-1 related, it is possible that a constitutively active human gene promoter, such as the *ef1a* promoter for the

eukaryotic translation initiation factor 1a (EIF1a), may have been suitable alternative to a viral promoter like the CMV-IE. Future experiments will benefit from using different promoters to detect non-specific LRA activity.

The pFM.nef/CBR and pFM.nef/CBG reporters (Figure 3.4 and 3.8 respectively) contain wild type 5' and 3' LTR sequences, allowing for integration and Tat mediated transactivation and allow for native RNA splicing to produce the *Nef3* (1/2/5/7) mRNA (Purcell and Martin 1993). Complimentary experiments in Figure 3.4 and 3.8 showed that both of the LTR-driven reporters responded to Tat transactivation in a tight dose-dependent manner ($r^2=0.96$ and $r^2=0.89$ respectively) when co-transfected with pTat(WT). Likewise, the same LTR reporter constructs, now integrated as a proviral reporter in the completed FlipIn.FM and FlipIn.RV cell lines responded to pTat(WT) transfection in an identical, tight dose-dependent manner ($r^2=0.92$ and $r^2=0.99$ respectively). No CMV induction was observed. (Figure 3.10 D & E). The cell line response to recombinant Tat protein closely mirrored these plasmid transfection results, as seen in Figure 3.11.

The J.Lat model, described by the Verdin laboratory (Jordan et al. 2003) are widely used in the HIV-1 field, therefore we sought to compare latency reactivation from these valuable reagents, after modifying the J.Lat10.6 and J.Lat6.3 full-length clones to better suit our purposes. The CMV.DS.Red^{Express} reporter forms a heterogeneous population within the two clones, each showing 5% Red positive populations before activation and 45% Red positive populations following maximal activation (figure 3.13).

With the FlipIn.FM and FlipIn.RV models generated and validated, and the J.Lat clones modified to include a marker of non-specific activation, the models needed for the discovery and development of novel HIV-1 LRAs were completed and ready for high throughput chemical screening. While having limitations, the FlipIn dual reporter cell lines attempt to account for both the rapid expansion and experimental reproducibility that a cell line affords, while presenting a druggable Tat-IRES pathway which recapitulates HIV-1 latency. Including a second non-HIV reporter measuring coordinate expression of other genes permits the screening out of potentially harmful non-specific compound hits.

Chapter 4 Validating dual reporter cell lines using a panel of mechanistically diverse known HIV-1 Latency Reversing Agents

4.1 Aim.

To further validate the dual reporter cell lines that model HIV-1 latency *in vitro* using panel of 15 known Latency Reversing Agents which span a diverse range of mechanisms of action and have predictable defined behavior.

4.2 Introduction.

Within latently infected T cells, viral gene expression is significantly or totally suppressed due to a range of molecular mechanisms (Van Lint, Bouchat et al. 2013). These occur both at the transcriptional level, involving the site of integration, transcriptional interference (Greger, Demarchi et al. 1998), chromatin architecture (Agosto, Gagne et al. 2015) and accessibility of host transcription factors (Williams and Greene 2007), as well as at the post-transcriptional level, involving processing/export of viral RNA and post-translational modifications of cellular and viral proteins including HIV-1 Tat (Tripathy, Abbas et al. 2011).

With the newly generated clones of both FlipIn cell lines isolated and their responses to Tat transactivation assessed (Chapter 3), our HIV-1 latency model required further validation using a range of mechanistically diverse known LRAs before use in library screening. Various drugs and molecular probes were available from commercial vendors, with published diverse mechanistic activities and some used in ongoing clinical trials. Useful compounds with well-defined mechanisms of action (MOA) are summarized in Appendix Table A.1. Fifteen known LRA candidates were picked to cover a diverse range of MOAs for use as single LRA treatments (Chapter 4), or in combination for synergistic effect with novel LRA hits from our drug screen (Chapter 6). Their ability to induce LTR-driven transcription, as a marker of viral gene expression, was assessed as well as their effect on an off-target reporter gene driven by an unrelated promoter (CMV-IE) using both the FlipIn and J.Lat models. To compliment the reactivation experiments, each compound had its associated toxicity assessed to determine if the compound was suitable to proceed to the next step on the path of drug discovery. Toxicity was measured in a cell line (HEK293 cells) and primary CD4+ resting memory T cells in parallel assays.

The mechanisms of HIV-1 latency are covered in detail in Chapter 1, but the relevant LRAs chosen can be grouped according to each targeted mechanism (Figure 4.1):

Activation of cellular transcription factors: Tumor necrosis factor α (TNF α), phorbol 12-myristate 13-acetate (PMA) and Bryostatin-1 are all involved in the activation of the cellular transcription factor NF- κ B p50:p65 heterodimer through the activation of PKC. NF- κ B is essential for the pioneer rounds of transcription necessary for expressing Tat at a level high enough to sustain its positive feedback loop (Williams and Greene 2007), and is also involved in the recruitment of Acetyltransferase complexes at the LTR promoter.

Chromatin organization: The restrictive heterochromatin environment (Grewal and Moazed 2003) can be relaxed into a more permissive euchromatin state (Hodges, Bintu et al. 2009) with the intervention of the HDACis Vorinostat (panHDACi), Panobinostat (panHDACi) and Romidepsin (HDACi class I and HDACi class II). Due to their wide use in the HIV-1 latency field and their predictable behavior, they have been chosen for use in this thesis.

Protein and DNA methylation: Methylation presents a highly dynamic factor in viral gene expression, depending on which residue and which methylation pattern occurs. For example, monomethylation of histone 3 lysine 9 (H3K9) is associated with euchromatin and a permissive state, whereas di-methylation and tri-methylation of the same residue by methyltransferase enzymes G9a and SUV39H1, respectively, is associated with heterochromatin and a lack of viral gene expression (Karmodiya, Krebs et al. 2012). Likewise, tri-methylation of H3K27 is brought about by EZH2, which has also been shown to play a role in maintaining HIV-1 latency (Carrozza, Li et al. 2005). For this thesis, DZNep (EZH2 inhibitor) and UNC-0638 (G9a inhibitor) were chosen as representative histone methyltransferase inhibitors (HMTi) as they target these two methyltransferase complexes implicated in HIV-1 latency.

P-TEFb: Efficient transcription of viral RNA from the proviral LTR promoter is mediated by Tat protein and is dependent of cellular P-TEFb (Kao, Calman et al. 1987). Tat must therefore recruit P-TEFb, which is often sequestered in an inactive form with the inhibitory 7SK snRNP complex, where the kinase activity of P-TEFb is inhibited (Yang, Zhu et al. 2001). Additionally, Tat must compete with bromodomain containing proteins

(including BRD4) for P-TEFb (Yang, Yik et al. 2005). To address this restriction, bromodomain inhibitors (BDi) JQ1 (+), PFI-1 and LY-303511 have been chosen to examine this mechanism. CCT-018195 was also used to inhibit Hsp90, which is may also make more free P-TEFb available for recruitment by Tat.

Post-translational modifications of Tat: Tat naturally cycles between two phases, a TAR binding form (K28^{Ac}/K51^{Me1})(Pagans, Kauder et al. 2010) and the elongating form (K50^{Ac}/K51^{Ac})(Kiernan, Vanhulle et al. 1999). SIRT1 and HDAC6 function by stripping activating acetyl groups from key lysine residues on Tat, allowing for cellular methyltransferase complexes SETDB1 and PRMT6 to add inhibitory di and trimethylation modifications, rendering Tat inactive (Anand, Schulte et al. 2008). This thesis utilized the compounds BML-278 and EX-527, which are marketed as SIRT1 activators and inhibitors respectively, as well as Rocilinostat, a specific HDAC6 inhibitor.

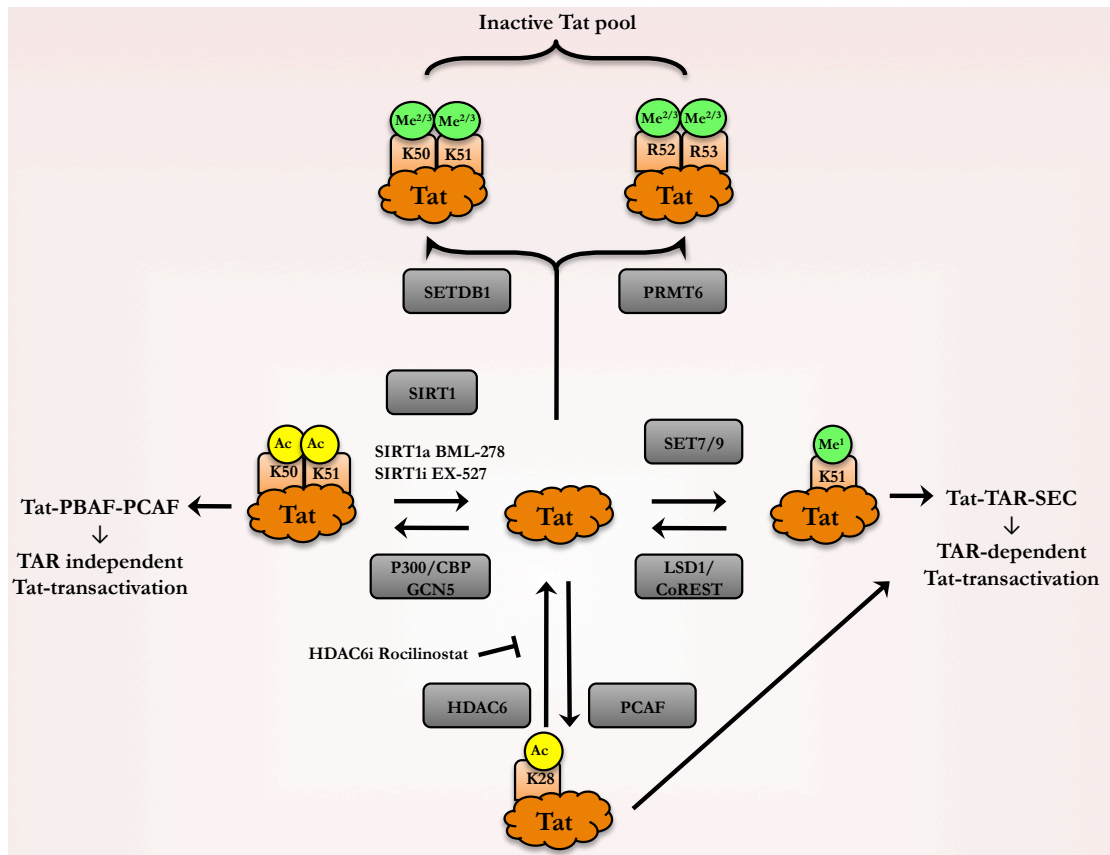


Figure 4.2: Post-translational modifications of HIV-1 Tat protein. Tat function is elaborately controlled at the post-translational level, allowing the Tat protein to cycle between two different states, early and late, depending on the role the protein must perform. Initially, the early Tat (K51^{Me1}) state is formed by mono-methylation of K51 by SET7/9, to allow for TAR binding and the formation of the super elongation complex (SEC). LSD1/CoRest demethylate K51, which is in turn acetylated with neighboring K50 by p300/CBP to form the late state form of Tat (K50^{Ac}/51^{Ac}), involved in dissociating from the TAR stem-loop and elongating RNA transcription by polIII. To recycle the Tat protein back to the early state, so new rounds of transcription elongation can be aided, SIRT1 deacetylates K50 and K51, and the process can begin again. Acetyltransferase PCAF acetylates the key K28 residue, contributing to the formation of the Tat-TAR-SEC complex. This modification can be reversed by HDAC6, which can be targeted by the HDAC6 inhibitor Rocilinostat. Additionally, SETDB1 and PRMT6 can methylate K50/K51 and R52/R53, modifications that render the protein inactive and may occur during the establishment of HIV-1 latency.

4.3 Results.

The goal for Chapter 4 was to further validate the two new FlipIn dual reporter cell lines by comparison with the well-established J.Lat models of HIV-1 latency and with experiments using primary CD4⁺ T cells. The reason for this was to have confidence that results generated using these artificial HEK293-based models did in fact model HIV-1 latency in a T cell. For easy comparison between the 6 sets of experiments: Reactivation in FlipIn.FM, FlipIn.RV, J.Lat10.6FM and J.Lat6.3FM as well as toxicity in a cell line and in primary CD4⁺ T cells, data from at least three independent experiments (each with triplicate wells) are shown in figures placed “side by side” comparing each cell substrate used (vertically in columns A-O) as well as a side by side between each drug (horizontally in rows I-V). As the FlipIn models use luciferase technology, reactivation is plotted as fold change over untreated baseline. As the J.Lat models use fluorescence and flow cytometry, reactivation was plotted using the percentage of the population that was positive for a fluorescent protein. Finally, the MTS toxicity assay measures bulk metabolism through a colorimetric assay, where data was plotted normalized between lysed (dead) cell controls and untreated (live) cell controls.

4.3.1 Assessing known Transcription Factor Activators.

The panel of 15 known latency reversing agents was divided based on their proposed mechanism of action. The first set covered were the NF- κ B and PKC activators TNF α (A), PMA (B) and Bryostatin-1 (C) and is shown in Figure 4.3. Bryostatin-1 also serves as a PKC activator.

4.3.1.1 (A) TNF α .

TNF α activates HIV-1 gene expression as it is a potent activator of the NF- κ B pathway through activation of PKC. At the plasma membrane PKC activates the membrane associated protein CARMA1. This interaction forms a scaffold to which multiple proteins can bind, including the I κ B kinase (IKK) which phosphorylates the inhibitory molecule I κ B, allowing the NF- κ B p50:p65 heterodimer to enter the nucleus and bind to the LTR promoter. In the FlipIn.FM (I) and FlipIn.RV (II) cell lines, the NF- κ B activator TNF α induced high levels of LTR-driven luciferase, achieving 36-fold and 40-fold over the untreated baseline respectively (AI & AII). Interestingly, despite NF- κ B being such a widely used transcription factor, no change was seen in the respective homogeneous off-target CMV reporters. Jordan *et al* (2003) used TNF α to achieve maximal activation of their J.Lat full-length clones in their paper describing the generation of the models. Here we likewise see high levels of LTR activation from both the J.Lat10.6FM (AIII) and J.Lat6.3FM (AIV), achieving GFP positive populations of 79% and 21% respectively. Of note, 31% and 30% CMV-DS.Red populations were seen in from the heterogeneous off-target reporter constructs in the J.Lat populations respectively, demonstrating a marked difference from the FlipIn cell lines. Regarding toxicity in the FlipIn cell line (AV) and primary CD4⁺ T cells (AVI), TNF α showed a small increase in bulk metabolism in the cell line experiments, approximately 110% of the unstimulated cell control, but, interestingly, no change in the primary cells.

4.3.1.2 (B) PMA.

PMA mimics diacylglycerol (DAG), activating the PKC pathway, which serves as a central player in supramolecular activation cluster. As PMA acts in such a promiscuous

manner, it will never be safe in a clinical setting, however it does serve as a useful positive control (rather than a true LRA) for proof-of-principle experiments such as these *in vitro* experiments. In a similar fashion to TNF α in the FlipIn.FM and FlipIn.RV cell lines PMA achieved a high level of LTR reactivation, achieving 21-fold increases in both cell lines at 4nM (BI & BII). PMA also induced CMV-driven off target effects, showing 3.5-fold and 10-fold activation respectively. A similar result was seen in the two J.Lat10.6FM and J.Lat6.3FM models. LTR-GFP induction was seen to plateau at 8nM, inducing a 90% GFP positive population and 17% GFP positive population respectively, with high off target effects seen in 44% and 37% CMV-DS.Red induction respectively (BIII & BIV). PMA showed very different results in the two toxicity experiments in the cell line (BV) and primary cells (BVI). While the cell line is immortalized, and therefore constantly metabolically active, treatment with such a potent activator as PMA led to a decrease in bulk metabolism at 48hrs, decreasing to 60% at 4-8nM. Conversely, with the primary resting memory CD4+ T cells, PMA achieved potent activation, inducing bulk metabolism to 390% of the unstimulated control.

4.3.1.3 (C) Bryostatin-1.

Serving as an additional PKC activator, Szallasi (1994) showed that Bryostatin-1 activated only a subset of the responses that PMA activates, and subsequently blocks those that it does not activate. Unlike PMA, the FlipIn.FM and FlipIn.RV cell lines did not respond to Bryostatin-1 whatsoever at either the LTR or CMV promoter (CI & CII). The J.Lat (CIII & CIV) and MTS toxicity experiments (CV & CVI) confirmed that the concentration window used was appropriate to induce activation, concluding that the FlipIn cells simply were not inducible by this drug. The J.Lat10.6FM and J.Lat6.3FM both responded to Bryostatin-1, producing 24% GFP positive and 2.3% GFP positive populations. As with PMA, non-specific induction as again seen with PKC activation here, producing 23% and 33% DS.Red positive respectively. The results with Briostatin-1 mirror those with PMA, showing that the heterogeneous CMV-off-target reporter of the J.Lat models is superior in sensitivity and breadth, compared to the clonal CMV-off-target reporter within the FlipIn models, which did not respond to either LRA. In the toxicity assays, Bryostatin-1 had no effect in the cell line experiments, but was a potent activator of the primary CD4+ cell metabolism, achieving 181% induction at 800nM. Taken together these results show general consistency between the FlipIn and J.Lat models in

HIV-1 reactivation, however an important difference between the heterogeneous (J.Lat) and clonal (FlipIn) CMV-drive “off target” reporters in these four cell lines.

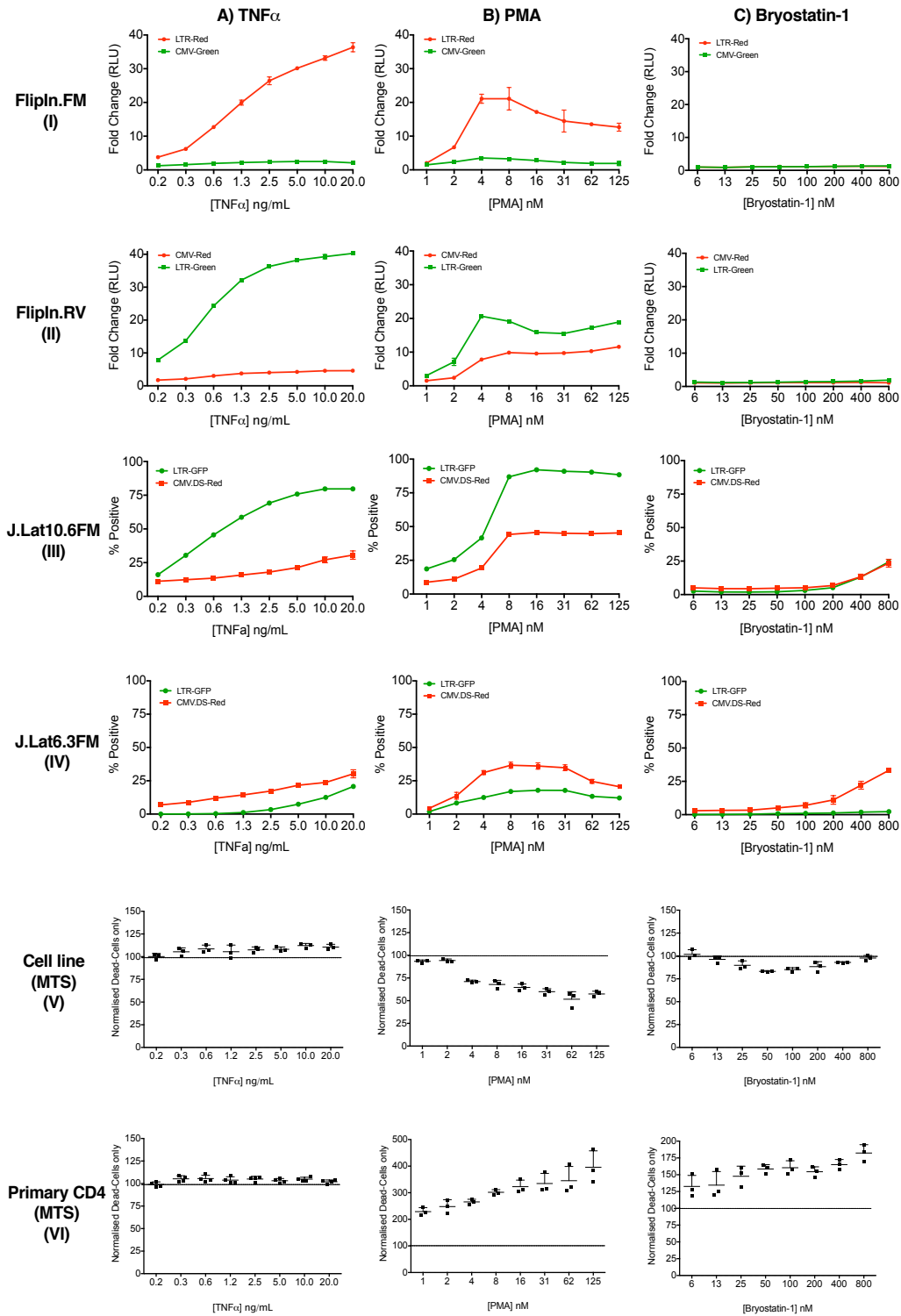


Figure 4.3: Induction of gene expression using known Transcription Factor activators. Treatment of reporter FlipIn and J.Lat cell lines for 48hrs and primary CD4+ T cells for 72hrs with known Transcription Factor activators TNF α , PMA and Brypstatin-1 across an 8-point concentration gradient. Induction is shown as fold change (FlipIn), percentage positive (J.Lat) and percentage survival (MTS) with the error bars representing standard deviation of n=3.

4.3.2 Assessing known Histone Deacetylase Inhibitors.

The second set of compounds assessed were the histone deacetylase inhibitors Vorinostat (D), Panobinostat (E) and Romidepsin (F). The hydroxamic acid compounds Vorinostat and Panobinostat serve as pan HDACis, targeting HDACs of Class I and Class II, and possibly others. Romidepsin, which has an unrelated chemical structure and function serves as a more specific HDAC inhibitor, targeting HDAC-I and HDAC-2 of Class I. An important distinction to remember is that the FlipIn clones (C2 for FlipIn.FM Figure 3.6 and B6 for FlipIn.RV Figure 3.9) were chosen as they had the highest level of LTR-driven expression of all the surviving clones. The J.Lat clones on the other hand were all chosen based on their lack of expression (and their ability for that expression to be induced). So the two models differ in that the FlipIn cells have a high baseline of expression and the J.Lats have a very low level of baseline expression. These differences likely include the chromatin environment that surrounds the LTR-reporters in each model, euchromatin/permissive for the FlipIn cells and heterochromatin/restrictive for the J.Lats. This lower baseline for the J.Lat models will likely result in them being much more inducible by HDACis than the FlipIn models, as is seen in Figure 4.4

4.3.2.1 (D) Vorinostat.

Vorinostat, by comparison to most other HDACi represents a comparatively impotent HDACi, however, due to its prolific use in HIV-1 latency studies and its highly recognized name in the field, it was included in the calibration of the FlipIn cells. The FlipIn.FM (DI) and FlipIn.RV (DII) showed peak activation with Vorinostat at 10 μ M, achieving 4.5-fold and 11.7-fold induction over baseline respectively. As expected from a HDACi, there was likewise an increase in CMV-driven off-target reporters, achieving 2.8-fold and 11.2-fold induction over baseline respectively. The J.Lat cell lines also showed a non-specific activation profile when treated with Vorinostat. The J.Lat10.6FM (DIII) cells showed a 48% GFP positive and 33% DS.Red population plateauing at 5 μ M, whereas the J.Lat6.3FM (DIV) cell line showed 16% and 39% positive respectively at 5 μ M. HDACis were developed as potential anti-cancer drugs. Perhaps as a result of this Vorinostat (and the other two HDACis) showed considerable toxicity in the cell line toxicity assay (DV). Interestingly toxicity was also seen in the primary CD4+ T cells (DVI) at concentrations of 5 μ M and above. At 20 μ M Vorinostat reduced bulk metabolism to 20% and 50% in the cell line and primary cells respectively.

4.3.2.2 (E) Panobinostat.

Like Vorinostat, Panobinostat belongs to the hydroxamic acid family of pan HDACis, however, Panobinostat is a far more potent compound than Vorinostat. With this in consideration, the concentration window for Panobinostat begins at a maximum of 800nM. Despite the 25-fold difference in potency between Vorinostat and Panobinostat, the two drugs behaved in a strikingly similar way. In the FlipIn.FM (EI) and FlipIn.RV (EII) cells, a 3-fold change and 11-fold change as seen in LTR-driven expression respectively at 200nM. Likewise a 2.3-fold and 9-fold change as seen in the CMV-reporters for both cell lines, again displaying a proportional level of no-specific activation when using pan HDAC inhibitors. In the J.Lat10.6FM cells (EIII), 51% of the population was induced to become GFP positive, and a nearly identical 48% became CMV-DS.Red at 200nM. For the J.Lat6.3FM cells (EIV), a 15% GFP and 44% DS.Red positive population was induced. In the cell line toxicity assay (EV), Panobinostat was toxic at and above 50nM, reducing viability to 15% at 800nM. In the primary CD4+ T cell experiments, Panobinostat proved toxic at and above 25nM reducing viability to 52% at 800nM.

4.3.2.3 (F) Romidepsin.

Romidepsin is another highly potent HDACi Romidepsin acting through a different mechanism to the hydroxamic acid HDACi, targeting HDAC-I and HDAC-II. Romidepsin is approximately 3-logs more potent than Vorinostat. The starting concentration was adjusted to begin at 20nM in these experiments. Romidepsin showed nearly identical responses to Vorinostat and Panobinostat in all 6 experiments. In the FlipInFM (FI) and FlipIn.RV (FII) cells, Romidepsin induced 3.4-fold and 9-fold increases in LTR-driven expression at 5nM and proportional increases in the CMV-driven expression. In the J.Lats (FIII & IV), 52% and 19% GFP positive populations were detected, associated with 38% and 44% DS.Red positive populations (10.6FM and 6.3FM respectively) at 10nM. Romidepsin was toxic in the cell line model (FV) at and above 2.5nM (totally toxic at 10nM), and at 1.25nM and above in the primary cells (FVI), with 33% the normalized value at 20nM.

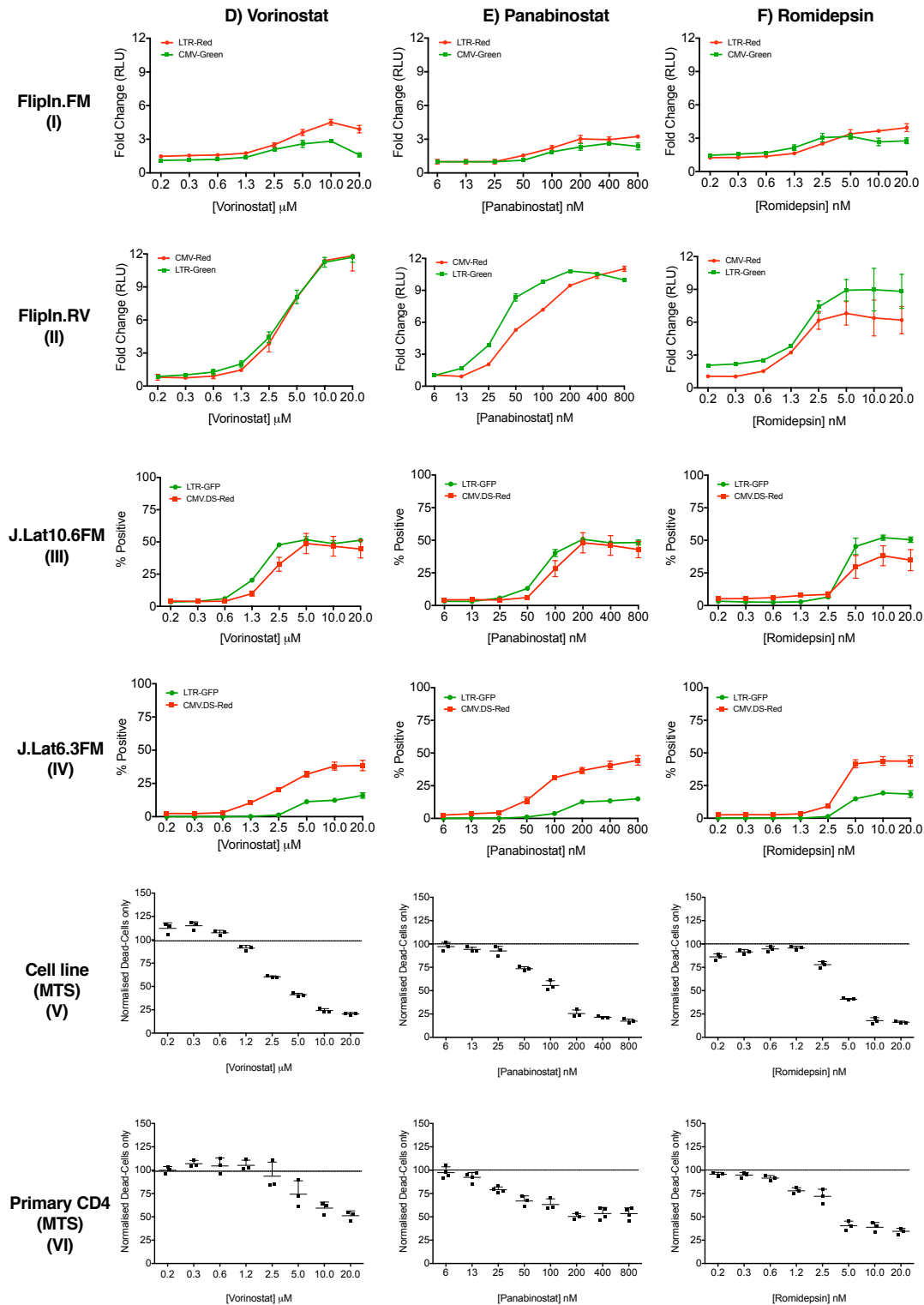


Figure 4.4: Induction of gene expression using known histone deacetylase inhibitors. Treatment of reporter FlipIn and J.Lat cell lines for 48hrs and primary CD4+ T cells for 72hrs with known Histone deacetylase inhibitors Vorinostat, Panabinostat and Romidepsin across an 8-point concentration gradient. Induction is shown as fold change (FlipIn), percentage positive (J.Lat) and percentage survival (MTS) with the error bars representing standard deviation of n=3.

4.3.3 Assessing known Histone Methyltransferase Inhibitors.

The third set of compounds assessed here are the histone methyltransferase inhibitors DZNep and UNC-0638. DZNep is marketed as an inhibitor EZH2, a component of the PCR2 complex implicated in the di- and trimethylation of histone 3 lysine 27 (H3K27), a known marker of repressive heterochromatin. UNC-0638 is a selective histone lysine methyltransferase inhibitor targeting only G9a and GLP. G9a is involved in restrictive methylation of H3K9. Methylation of H3K27 and H3K9 is associated with silencing of HIV-1 gene expression and latency.

4.3.3.1 (G) DZNep.

DZNep showed encouraging results in several models and proved to be one of the most interesting compounds both as a single agent and in synergistic combination with several other compounds (Chapter 6). In the FlipIn.FM (GI) and FlipIn.RV (GII) cells, DZNep induced 11-fold and 22-fold increases in LTR-driven gene expression, with 2.2-fold and 5.4-fold changes in the CMV-driven reporters, representing a largely LTR-specific mode of action. DZNep performed only modestly in the J.Lat10.6FM (GIII) cells. At 10 μ M a GFP positive population of 10.3% and a DS.Red population of 6.6% was detected. DZNep was not able to induce LTR-driven expression in the J.Lat6.3FM cells (GIV). DZNep proved to reduce bulk metabolism in the cell line (GV) to 75% of the normalized control at and above 2.5 μ M, but had no effect on primary CD4+ T cells(GVI).

4.3.3.2 (H) UNC-0638

An interesting trend was conserved across all 6 experiments using UNC-0638. Maximal activation of both LTR and CMV reporters was seen at 10 μ M, followed by a sharp drop off (toxicity) above 10 μ M. 8-fold and 13.5-fold increases were seen in the LTR reporters in the FlipIn.FM (HI) and RV (HII) cells. 2.8-fold and 6-fold increases were seen in their respective CMV-driven off-target reporters, portraying only low level specificity for HIV-1 reactivation. In the J.Lat10.6FM cells (HIII), a 22% GFP⁺ population was seen (11.3% DS.Red positive). The J.Lat6.3FM cells (HIV) showed minor induction to 1.3% GFP positive and 13% DS.Red positive. As mentioned, UNC-0638 showed toxicity at 20 μ M, reducing bulk metabolism to 0% (ie completely toxic) in both cell line and primary experiments (HV & HVI).

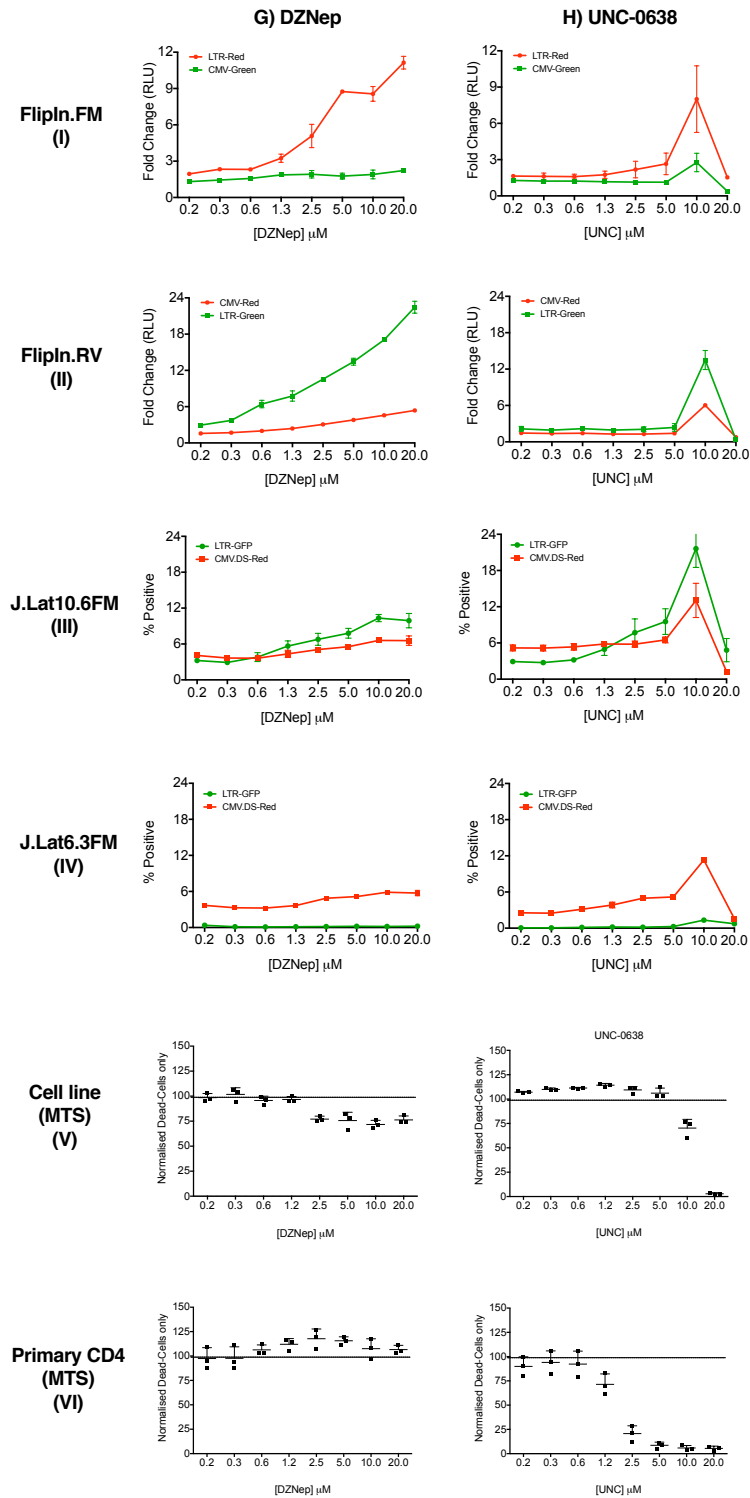


Figure 4.5: Induction of gene expression using known Histone methyltransferase inhibitors. Treatment of reporter FlipIn and J.Lat cell lines for 48hrs and primary CD4+ T cells for 72hrs with known Histone methyltransferase inhibitors DZNep and UNC-0638 across an 8-point concentration gradient. Induction is shown as fold change (FlipIn), percentage positive (J.Lat) and percentage survival (MTS) with the error bars representing standard deviation of n=3.

4.3.4 Assessing known Bromodomain Inhibitors.

The fourth class of LRAs to be covered were the bromodomain inhibitors JQ1 (+) (I), PFI-1 (J) and LY-303511 (K). The bromodomain inhibitors are also extensively investigated in the cancer therapy field and have been adapted with some success in the HIV-1 latency field. The rationale for using them for HIV-1 latency reversal in this thesis is that the bromodomain containing protein BRD4 is known to compete with HIV-1 Tat protein for the essential cellular positive transcription elongation factor b (P-TEFb), which HIV-1 requires for efficient transcription of the proviral genome.

4.3.4.1 (I) JQ1 (+).

JQ1 (+) is an inhibitor of several bromodomain-containing proteins including BRD2, BRD3 and BRD4 and belongs to the Diazapine family. JQ1 (+) showed promising results in all but one of the six cell-evaluation platforms used, with consistent highly specific activation of the LTR and low toxicity and off target effects seen. JQ1 (+) also performed well as a synergy partner with many other non-mechanistically-related compounds (Chapter 6). In the FlipIn cells, JQ1 (+) induced 9-fold and 5.3-fold increases in LTR-driven gene expression from the FM (I(I)) and RV (I(II)) cell lines respectively. Very low off-target effects were seen, <2-fold for either cell line. In agreement with these encouraging results, the J.Lat10.6FM (I(III)) responded well, showing a 33% GFP positive population at 20 μ M, where the CMV-DS.Red population did not change from <5% positive. In contrast to the three cell lines mentioned above, the J.Lat6.3FM cells (I(IV)) were not reactivated with JQ1 (+) (or any other BDi), showing no change in LTR-driven or CMV-driven activation. This contrast clearly demonstrates the difference between the two J.Lat clones used in this thesis. In the toxicity experiments, JQ1 (+) showed a small amount of toxicity (>75% remained viable) in the cell line (I(V)) and likewise similar results in the primary cells (I(VI)) where >75% of the cells remained viable.

4.3.4.2 (J) PFI-1.

The second bromodomain inhibitor tested was PFI-1, an inhibitor of BRD2 and BRD4. 7-fold and 9-fold changes in LTR-driven expression were seen in the FlipInFM (JI) and RV (JII) cell lines respectively. A 1.4 and 3.7-fold change in the CMV-driven off target reporters was detected, suggesting a LTR-specific mechanism of action similar to JQ1 (+). While PFI-1 also induced a modest level of LTR-GFP expression in the J.Lat10.6FM cells (JIII), achieving 26% GFP positive, PFI-1 was found to have no effect on LTR activity below 2.5 μ M, in contrast to JQ1 (+). No change was seen in the CMV-DS.Red level in this model. PFI-1 failed to induce any change in LTR-driven expression in the J.Lat6.3FM cells (JIV), confirming that the provirus within these cells is not inducible by BDis. PFI-1 had no effect on bulk metabolism in the cell line toxicity experiments (JV), however was shown to increase the bulk metabolism in primary cells, achieving 120% of the unstimulated primary cells. Taken together, these results generally mirror those seen with JQ1 (+).

4.3.4.3 (K) LY-303511.

LY-303511 is marketed as the negative control compound for a similar compound called LY-294002, a PI3-kinase inhibitor. LY-303511, however, also acts as an inhibitor of BRD2, BRD3 and BRD4. The structure of LY-303511 differs substantially from JQ1 (+), and the two compounds therefore likely have different secondary target proteins. The FlipInFM and FlipIn.RV cells responded predictably to this BDi, with 4.6-fold and 6.3-fold changes above baseline in LTR-driven expression respectively. The CMV-reporters showed a 1.4-fold and 2.7-fold change respectively (KI & KII). In the J.Lat10.6FM cells (KIII), an 11% GFP positive population as detected, whereas no change as seen in the J.Lat6.3FM cells (KIV). For both J.Lats, a small increase in CMV.DS.Red expression was seen from a baseline of 4.5% positive to 6.5% positive in both cases. LY-303511 also had little effect on cell metabolism with no significant deviation from the untreated control (KV & KVI).

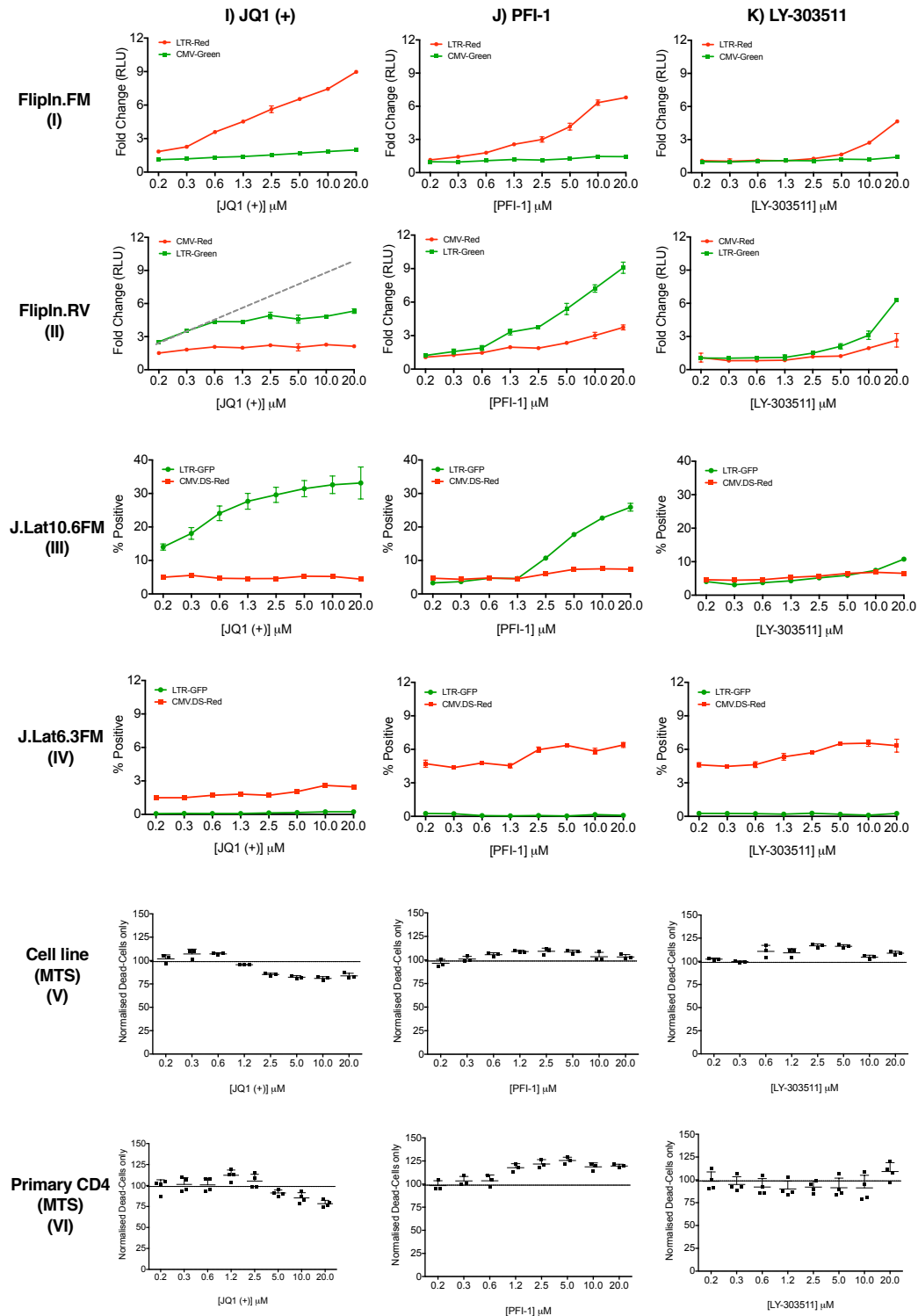


Figure 4.6: Induction of gene expression using known Bromodomain inhibitors. Treatment of reporter FlipIn and J.Lat cell lines for 48hrs and primary CD4⁺ T cells for 72hrs with known Bromodomain inhibitors JQ1 (+), PFI-1 and LY-303511 across an 8-point concentration gradient. Induction is shown as fold change (FlipIn), percentage positive (J.Lat) and percentage survival (MTS) with the error bars representing standard deviation of n=3. The dashed line, expected LTR reactivation in I(II), is discussed below.

4.3.5 Assessing a known Heat Shock Protein 90 Inhibitor.

The Hsp90 inhibitor, CCT-018159, could potentially group with the bromodomain inhibitors under a more general “activators of P-TEFb”. This compound may have effects outside of P-TEFb, as its target Hsp90 is believed to play many roles within the cell and within the HIV-1 lifecycle as a highly expressed chaperone protein. CCT-018159 however, is selective for Hsp90 over Hsp72 and topoisomerase II.

4.3.5.1 (L) CCT-018159.

This inhibitor of the Hsp90 showed generally very modest activity across all of the assays performed. In the FlipIn.FM (LI) cells, a 2-fold change was seen in LTR-driven expression, with a 3.7-fold change seen in the FlipIn.RV cells (LII). For both cell lines, no change was seen in the CMV-driven reporters. The J.Lat10.6FM cells (LIII) were induced by CCT-108159 (LTR or CMV-driven expression). Again, no change was seen in the J.Lat6.3FM cells (LIV). Despite its inability to modulate high levels of reporter gene expression in any cell line model, CCT-018159 did prove to be quite toxic in both the cell line and primary cell experiments. In the cell line, CCT018159 was toxic at and above 2.5 μ M, and at 20 μ M reduced the bulk metabolism to 38% of the normalized control. Likewise, in the primary cells, toxicity was seen at and above 10 μ M, reducing bulk metabolism to 61% of the normalized control at 20 μ M. Toxicity may be expected as Hsp90 is one of the most highly expressed proteins within eukaryotic cells (Csermely, Schneider et al. 1998), and fulfills a host of roles as a protein chaperone, assisting the proper folding, stability and degradation of other proteins. Inhibition of such a prolific protein may therefore be expected to prove toxic.

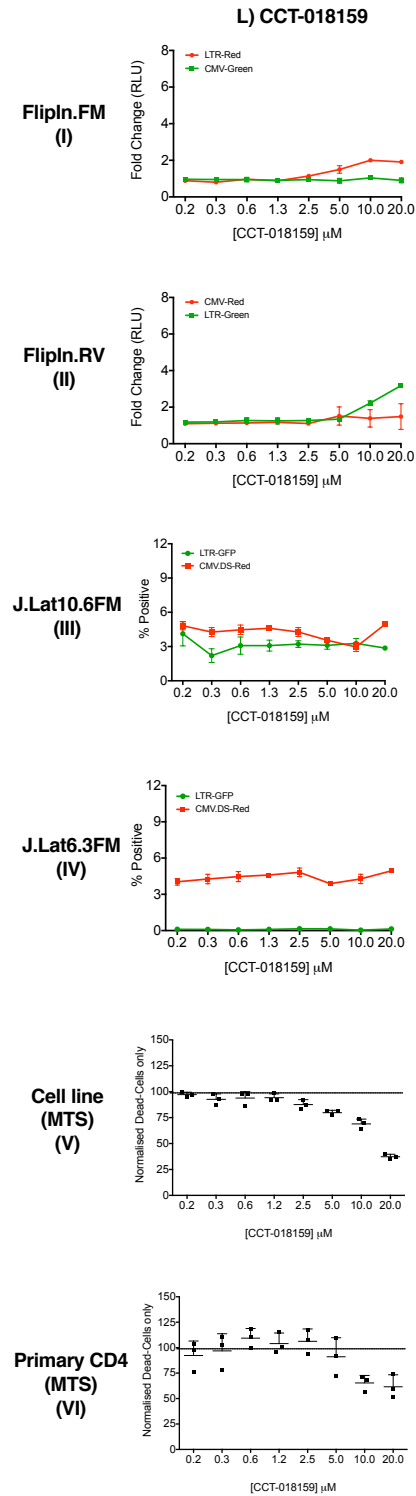


Figure 4.7: Induction of gene expression using known Heat shock protein 90 inhibitor. Treatment of reporter FlipIn and J.Lat cell lines for 48hrs and primary CD4+ T cells for 72hrs with known Heat shock protein inhibitor CCT-018159 across an 8-point concentration gradient. Induction is shown as fold change (FlipIn), percentage positive (J.Lat) and percentage survival (MTS) with the error bars representing standard deviation of n=3.

4.3.6 Assessing known modulators of Tat Posttranslational Modifications.

The sixth and final set of LRAs modulate the posttranslational modifications of proteins including HIV-1 Tat. Coincidentally, all three are also HDAC inhibitors, however their role is not in chromatin remodeling through histone modifications. BML-278 acts as an activator of the Class III HDAC Sirtuin 1 (SIRT1), which may remove the Lysine 50 and Lysine 51 acetyl groups from Tat, a posttranslational modification associated with the late phase of Tat mediated transactivation required for inducing efficient RNA transcription. Conversely EX-527 is a SIRT1 inhibitor, preventing the deacetylation of Tat and keeping it in a acetylated state. The third HDAC inhibitor, which modulated Tat posttranslational modifications, is the HDAC6 inhibitor Rocilinostat. This compound prevents the removal of the lysine 28 acetyl group, a marker that strengthens the Tat-TAR interaction.

4.3.6.1&2 BML-278 (M) & EX-527 (N)

As neither the SIRT1 activator or inhibitor showed any effect in any of the reactivation assays tested, their results have been briefly summarized together here. Neither BML-278 or EX-527 had any effect on LTR or CMV-driven expression in any of the 4 cell lines tested either as single agents (Figure 4.8) or as in any synergy combination (Chapter 6). Toxicity from either BML-278 was seen in the primary CD4+ T cells (MVI), decreasing bulk metabolism to 77% of the normalized control levels. EX-527 decreased bulk metabolism to 80% of the normalized value in the cell line experiments (NV).

4.3.6.3 Rocilinostat (O)

The HDAC6 inhibitor Rocilinostat, however, did show interesting results across the board. In the FlipIn.FM cells, Rocilinostat induced a 4.3-fold change in LTR-expression and a 2.9-fold in off target CMV-expression (OI). In the FlipIn.RV cells, a 11.5-fold change was achieved with an associated 7.4-fold increase in the CMV-driven reporter (OII). Similar to the HDACi compounds above, Rocilinostat achieved a 55% GFP positive population in the J.Lat10.6FM model with a 29% DS.Red positive population (OIII). In the J.Lat6.3 cells, a 10.2% GFP positive was seen with a 22.5% DS.Red positive population (OIV). Rocilinostat did prove toxic at 20µM. In the cell line, the bulk metabolism was reduced to 50% of the normalized value at 20µM, however the rug was toxic at 5µM and

above (OV). In the primary cells, a reduction to 73% of the normalized value was detected at 20 μ M (OVI).

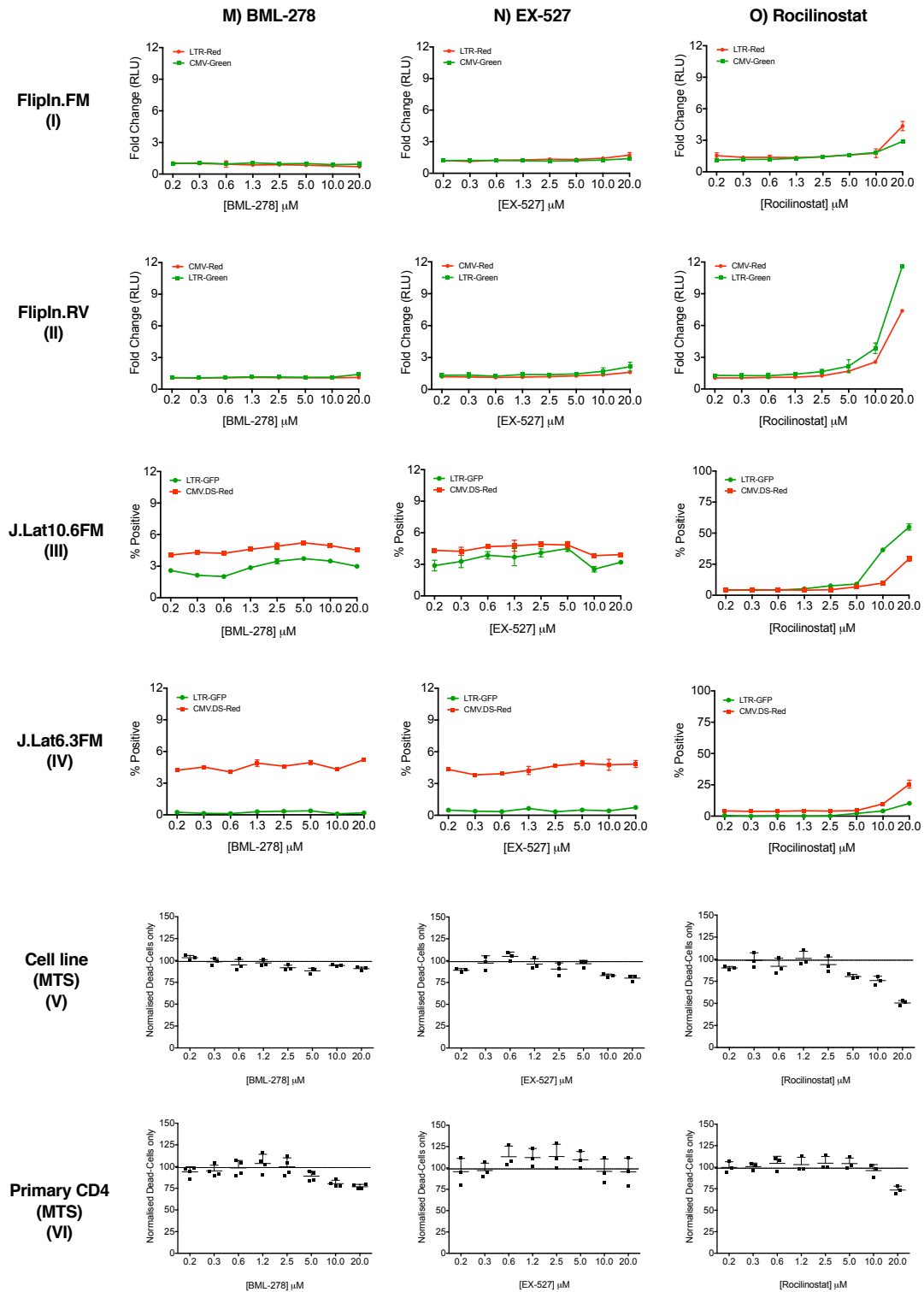


Figure 4.8: Induction of gene expression using known modifiers of Tat Posttranslational Modifications. Treatment of reporter FlipIn and J.Lat cell lines for 48hrs and primary CD4⁺ T cells for 72hrs with known modifiers of Tat Posttranslational modifications BML-278, EX527 and Rocilinostat across an 8-point concentration gradient. Induction is shown as fold change (FlipIn), percentage positive (J.Lat) and percentage survival (MTS) with the error bars representing standard deviation of n=3.

4.4 Discussion.

HIV-1 is reliant on cellular transcription factors for efficient expression of its genes, and these factors are often a limiting in quiescent T-cells promoting HIV-1 latency. Reactivation of viral gene expression through T cell signaling pathways may seem like an attractive target for potential therapy. Caution must be taken however, as activation by T cell stimuli will likely bring about prolonged activation of multiple cellular pathways, resulting in undesired side effects, such as global cell activation and autoimmune reaction. Similarly, caution must be taken when considering the use of broadly non-specific chromatin remodeling drugs like the pan HDACis. While this class of drugs may be successful at alleviating the restrictive heterochromatin environment surrounding the HIV-1 promoter, they may, and most likely would, likewise trigger gene expression from other areas of the genome. A more attractive target would involve the viral transactivator Tat, because a hypothetical therapy targeting only this protein may prove much more specific for only cells containing the Tat protein, i.e. predominantly cells containing a provirus. An alternative approach to a HIV-1 functional cure, termed the “Block and Lock” method. In this method, rather than reactivating the virus and killing the cell as with the shock and kill method (section 1.4.3), the cortistatin compound Didehydro-Cortistatin A (dCA) has been shown to suppress the activity of Tat protein (Kessing and Valente et al; Mousseau and Valente et al) thereby “locking” the provirus into latency, and preventing viral rebound. This method does show interesting potential in adding to already established cART, however, this thesis is interested only in the activators of HIV-1 gene expression.

In this chapter our goal was to further validate the newly generated FlipIn cell lines as appropriate models that attempt to recapitulated HIV-1 latency in a cell line before committing to their use in high throughput chemical screen (Chapter 5). The question from the onset of this chapter was: did the FlipIn model closely match the well established J.Lat model in its HIV-1 reactivation profile?, and did it match the toxicity profile of primary CD4+ T cells. To achieve this, 15 known LRAs were studied in the FlipIn and the HIV-1 reactivation profiles compared to the J.Lat cell lines, which are well established in the field. The 15 LRAs were also tested in cell line (HEK293 based) and primary CD4+ T cell toxicity assays. Each LRA is briefly discussed below and the FlipIn cells response and use as a model for HIV-1 latency critically assessed to conclude the chapter.

Transcription factor activators

TNF α performed as a strong inducer of LTR-driven gene expression across all 4 models: the FlipIn.FM, FlipIn.RV, J.Lat10.6FM and J.Lat6.3FM dual reporter cell lines. TNF α also induced CMV-driven gene expression in all 4 models, with non-specific gene activation being more evident in the J.Lat models, possibly due to their CMV-reporter constructs being heterogeneous within the population (section 3.3.4.1). TNF α induced only a modest increase in cellular metabolism from the HEK293 cell line and the primary CD4⁺ T cells in the MTS assay. These results are in general agreement with those in the literature that TNF α is a potent activator of HIV-1 gene expression in immortalised cell lines (Folks and Fauci et al 1989), however Yang et al show that it does not necessarily hold true for HIV-1 reactivation in primary cells, unless paired with other stimuli (Yang and Siliciano et al 2009). Likewise, PMA proved a very potent PKC activator and, while PMA is excessively potent as a pan T-cell activator to be used clinically in a LRA based cure strategy, it did serve as an expedient proof of principle control compound in this study. The isoforms of PKC are: Conventional (α , β 1, β 2 and γ) which require Ca²⁺ influx and diacylglycerol (DAG), Novel (δ , ϵ , η and θ), which require DAG but do not require Ca²⁺ influx and Atypical (ι and ζ), which do not require Ca²⁺ influx or DAG, but require phosphatidyl serine. As the cells treated with PMA in these experiments were not also treated with an agent to induce calcium influx (eg ionomycin), it is most likely that the Novel PKC isotypes are responsible for the activation seen. In the literature PKC θ is known to play a uniquely important role in HIV-1 gene expression (Lopez-Huertas and Coiras et al 2016). To better define the FlipIn cell lines, future studies should include PMA +/- ionomycin to further study which isotypes of PKC may be involved. While PMA induced massive proliferation in primary resting CD4⁺ T cells, it proved toxic in the HEK293 cell line MTS assays above 4nM. Diaz et al 2015 describes HIV-1 activation by Bryostatin-1 through activation of the NF- κ B pathway, however the FlipIn cell lines showed no such activation, despite being highly sensitive to TNF α . The J.Lat10.6FM model, however, did respond well to Bryostatin-1 treatment, with the J.Lat6.3FM model responding to a very low degree. Additionally, as with NF- κ B with TNF α the CMV-driven reporters of the J.Lats were induced, whereas those of the FlipIn cell lines were not. This clear disparity between FlipIn and J.Lat models, warrants further investigation. As with PMA, PKC activation through Bryostatin-1 induced proliferation in primary resting CD4⁺ T cells, but had only minor effects on HEK293 cell metabolism.

Chromatin architecture modulators

As might be expected from three compounds which act through similar MOAs, the data raised using the three HDACi compounds were essentially identical, with the exception of their potency. For each Vorinostat, Panobinostat and Romidepsin, the respective LTR and CMV-driven reporters were induced in a near super-imposed fashion, across all four cell lines. This highly proportional induction, where LTR~CMV, demonstrated the generally non-specific mechanism with which HDACis act indiscriminately throughout the genome. This is in agreement with a recent clinical trial involving Vorinostat, where cellular gene upregulation was sustained to 70 days post treatment (Elliot and Lewin 2014 ; Mota and Lewin et al 2018). As might be expected from compounds frequently used in clinical trials as anti-cancer agents, the HDACis were highly toxic in the cell line experiments. What is interesting, however, is that the death of the cells seen in the MTS assays seems to be inversely proportional to the activation of LTR and CMV-driven gene expression seen in both luciferase and flow cytometry assays. This suggests that LTR-driven and CMV-driven expression continues, and peaks, even as the cells are stressed and dying. Taken together, the HDACi compounds add support the FlipIn cells ability to demonstrate non-specific activation, however, their use in accurately measuring toxicity is questionable.

Methylation inhibitors

DZNep and UNC-0638 inhibit EZH2 and G9a respectively, both of which are implicated in the methylation of H3K9 and H3K27, inducing latency. DZNep induced a dose dependent response in both of the FlipIn cell lines and modest induction in the J.Lat10.6FM model, but was unable to induce LTR-reporter expression within the J.Lat6.3FM cells. DZNep showed only low levels of toxicity in the cell line experiments and was not found to be toxic in primary cell experiments. DZNep has also been described as an inhibitor of the s-adenosylhomocysteine (SAH) hydrolase enzyme, which is involved in the synthesis of adenosine (Lee and Kim 2013). Why blocking this activity would have an effect on viral gene expression remains unclear, although it may account for the toxicity seen in the constantly dividing cell line, which is missing from the non-dividing resting memory CD4+ T cells. In contrast UNC-0638 behaved in a largely non-specific manner. UNC-0638 showed a sharp peak in LTR and CMV-driven gene expression at 10 μ M, across both FlipIn and J.Lat models, but was highly toxic above this concentration, leading to

total cell death in all six experiments including in the primary CD4⁺ T cells (at 2.5 μ M). Several other members of the UNC family exist (-0224, -0642 and 0646) and should be explored to further understand the FlipIn models response to methyltransferase inhibitors.

P-TEFb activators

The FlipIn cell lines were designed to detect novel LRAs that synergised with the low level of HIV-1 Tat protein that they express via the *tat/bGH* chimeric gene and *tat* genes IRES. As may be expected by their involvement in freeing P-TEFb, the bromodomain inhibitors performed well in these models. JQ1 (+), PFI-1 and LY-303511 all target BRD4 and all activated LTR-driven gene expression in a highly specific, dose dependent manner in the FlipIn models. These data mirrored that of the J.Lat10.6FM model, adding to the body of evidence that the FlipIn models closely resemble this particular J.Lat clone. JQ1 (+) proved to be the most potent inhibitor of the three, however, this LRA showed an unexpected plateau effect in the FlipIn.RV LTR reporter, for reasons yet unknown. JQ1 (+), nor any of the other BDis were able to induce LTR-driven gene expression from the J.Lat6.3FM clone, suggesting that the either P-TEFb is not a constraining actor in HIV-1 gene expression in this model, or that multiple other restrictions exist. PFI-1 was able to reactivate LTR-driven expression in the J.Lat10.6FM cell line, but only at 2.5 μ M and above, being approximately 10-fold less potent than JQ1 (+). LY-303511 was again less potent than the former two BDis, inducing LTR-driven gene expression above 2.5 μ M. None of the bromodomain inhibitors proved to be toxic in the cell line and primary cell experiments (the toxicity cut off being 75% of the normalized value and below). PFI-1 was shown to induce and increase in primary CD4⁺ T cell metabolism. CCT-018159 inhibits Hsp90 binding the P-TEFb subunit CDK9. Of note, the members of the Heat shock protein family are among the most highly expressed proteins within the cell, and perform a number of roles. Inhibiting Hsp90 may inadvertently have affected a number of different regulatory pathways within the models tested. CCT-018159 induced only modest LTR-driven activation in the FlipIn cell lines, but none in the J.Lat models. As the FlipIn cells express constitutive levels of Tat via a CMV-driven *tat/bGH* chimeric gene cassette, whereas the J.Lat cells undergo the native Tat-TAR feedback loop and therefore express a lower level of Tat when unstimulated, the FlipIn cells may be more sensitive to this LRA. Interestingly, and possibly as a result of inhibiting such a widely used protein, CCT-018159 proved toxic in both cell line and primary cell experiments.

Tat posttranslational modifications

The representatives of this group includes the SIRT1 activator BML-278, SIRT1 inhibitor EX-527 and HDAC6 inhibitor Rocilinostat. Modulating the SIRT1 lysine deacetylase by either activation (BML-278) or inhibition (EX-527) had no effect whatsoever. This brings into question the possibility that IRES expressed Tat protein and the Tat protein made following the normal RNA-cap dependent manner may have different post translational modifications, which warrants further investigation. Further studies, possibly utilising mass spectrometry, looking at the protein and its modifications directly may raise some interesting results and are being considered for the near future. The Class III (HDAC6) inhibitor Rocilinostat, is expected to block the removal of acetyl modifications on the lysine 28 residue of Tat. Rocilinostat showed interesting results across all four cell lines. In the FlipIn models, Rocilinostat induced LTR-driven gene expression at 20 μ M, which was associated with off target activation of the CMV-driven reporters. Likewise, both clones of the J.Lats were reactivated. HDAC6 is not believed to be involved in chromatin remodelling like the Class I HDACs, yet inhibition of HDAC6 was able to induce LTR-driven expression in the J.Lat6.3FM model. This interesting result raises many questions regarding the exact action of Rocilinostat, and therefore it was used in synergy combinations in the J.Lat cells in Chapter 6.

Taken together, the response to the panel of 15 LRAs were generally similar between the FlipIn and J.Lat models of HIV-1 latency. The FlipIn models, however, utilized several properties that make more suitable than the J.Lats for high throughput detection of novel LRAs. These include the dual luciferase system also allows for high throughput experiments, and no requirement for PC3 level security. The responses seen in the FlipIn also match those seen in many other latency studies in the literature, yet the FlipIn cells ability to precisely track toxicity in primary resting CD4+ T cells is questionable. For this reason, the FlipIn.FM cell line provides a good first step in on the road to drug discovery, where a more manageable number of hit compounds could then be progressed into primary models of HIV-1 latency.

Chapter 5 Discovery of seven novel families of highly specific HIV-1 Latency Reversing Agents.

5.1 Aim.

To now use the validated dual reporter cell lines that model HIV-1 latency *in vitro* to screen a library of small drug-like compounds by high throughput chemical screening and discover novel compounds that specifically modulate HIV-1 gene expression while avoiding global cell activation and cell toxicity.

5.2 Introduction.

With the development of combination antiretroviral therapy (cART), and the realization that prolonged cART was unable to cure HIV+ patients due to the persistence of the latent reservoir, attention turned to strategies to clear the latent reservoir. The approach tried most extensively to date is the shock and kill approach, where a latency reversing agent(s) (LRAs) are used to reactivate HIV-1 gene expression in latently infected cells, leading to their death, clearance, and eradication of inducible provirus from the patient. Despite many attempts at formulating an effective treatment regime, and advancement to clinical trials with several well-characterized LRAs already with FDA approval, results have been inconsistent and largely disappointing. (Table 5.1)

Table 5.1: Known Latency Reversing Agent used in advanced trials.

Target mechanism	LRA investigated	References
Transcription factor activators	TNF α (NF- κ B)	(Saleh, Wightman et al. 2011)
	Bryostatin-1 (PKC)	(Perez, de Vinuesa et al. 2010)
Chromatin architecture modulators	Vorinostat* (panHDAC)	(Burnett, Lim et al. 2010; Archin, Liberty et al. 2012)
	Panobinostat* (panHDAC)	(Rasmussen et al. 2013)
	Romidepsin* (HDAC1/2)	(Ying, Zhang et al. 2012)
Methylation inhibitors	BIX-01294 (G9a)	(Bouchat, Gatot et al. 2012)

Target mechanism	LRA investigated	References
P-TEFb activators	JQ1 (+) (BRD4)	(Banerjee, Archin et al. 2012)
	Disulfiram* (HEXIM1)	(Xing, Bullen et al. 2011)
Immune activation therapy (IAT)	IL-2* and IFN- γ *	(Davey, Bhat et al. 1999; Stellbrink, van Lunzen et al. 2002)
	IL-7*	(Wang, Xu et al. 2005)
	Anti-PD1*	(Dafonseca, Chomont et al. 2010)

LRA* used in advanced primary latency models or clinical trials*

While these early compounds are being investigated for their anti-HIV-1 capabilities as LRAs, many have been repurposed from cancer research field that smoothed out many regulatory and ethical hurdles associated with clinical trials in the HIV-1 latency field as they already have FDA approval. Therefore, several compounds that had sufficient safety data were tested in clinical trial for HIV latency reversal without the cost and long waiting periods required for approval of a “first in man” trial. Unfortunately, simply repurposing these drugs from the cancer field, rather than using new compounds that have been tailor made for specifically targeting HIV-1, has resulted in the use of drugs that have high levels of non-specific gene activating activity (Chapter 4). At the onset of this PhD project (February 2012) we wished to address the lack of highly specific LRAs, tailor made to reactivate HIV-1 in a specific manner. For this reason, we set out to utilize the FlipIn.FM cell line model of HIV-1 latency generated in Chapter 3 and validated in Chapter 4 to screen a library of >114,000 small drug like compounds to discover the next generation of LRAs that reactivate HIV-1 gene expression in a highly specific manner.

Collaborators at the Walter and Eliza Hall Institute (WEHI) and Children’s Cancer Institute Australia (CCIA) have generated a library of compounds, the Stage 6 (2010) WECC set, containing ~114,000 highly diverse “lead-like” small molecules sourced from 10 commercial vendors, stored within the Queensland Compound Library (QCL). The library has been rigorously filtered to remove molecules that have been found previously to give false positive “hits” in many assay systems tested. These molecules are appropriately named pan assay interference compounds (PAINS). 89% of the molecules within the WECC library contains comply with Lipinski’s 4 “rules of five” (Benet et al 2016), which is usually necessary for a drug to be orally active in humans. These rules specify that new drug leads should ideally:

- Have a molecular weight of less than 500 Daltons (Fig 5.1)
- Have no more than 5 hydrogen bond donors
- Have no more than 10 hydrogen bond acceptors
- Have a lipophilicity $\log P < 5$

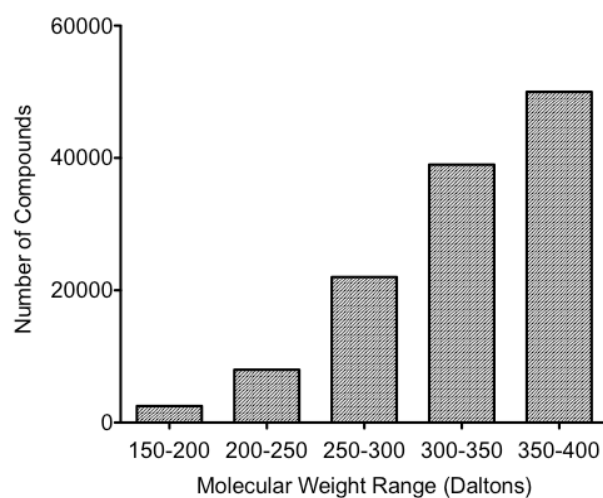


Figure 5.1: Molecular weight range within the WECC compound library.

The Stage 6 WECC set has a molecular weight cutoff of 400 Daltons, with an average molecular weight of 328 Daltons. (Data provided by the Walter and Eliza Hall screening laboratory)

Intellectual Property rights for molecules within the library are also available (see Series E below). Our collaborators at the WEHI also had access to three smaller boutique compound libraries including: epigenetic (95 compounds), kinase (276 compounds) and known drug (3,700 compounds) collections which were included in a HTCS process.

The drug discovery strategy here was to use the screening platforms developed and validated in earlier chapters in a step-wise iterative screening approach. The primary screen would be in a miniaturized assay in FlipIn.FM cells, then hits curated through the 11 point dose titration then counter screen in the FlipIn.RV cells. Final selections were made after screening through two J-Lat cell lines, then activity confirmation in primary leukapheresis from multiple donors.

The cell based screening strategy adopted for this thesis ultimately yielded seven families of highly specific HIV-1 LRAs summarized in Figure 5.2.

1) **High Throughput Chemical Screening:** The HEK293 based FlipIn.FM dual reporter cell line described in Chapter 3 was used to screen the Stage 6 WECC set library of ~114,000 small “lead-like” compounds at a single concentration of 10 μ M with 10,000 cells in 20 μ l volumes in 384 well plates. The 10 μ M drug concentration, while relatively high, was considered an acceptable “sweet spot” in the balance between toxicity and potency for the compounds used for assay validation in Chapter 4. An emphasis was placed on detecting the maximum number of initial hits by using the highest concentration possible. Medicinal chemist collaborators from WEHI advised that potency would most likely be poor until extensive medicinal chemistry had taken place. At the end of the FlipIn.FM screen 512 compounds were classed as “hits” chosen for their specific reactivation of LTR-driven gene expression over the non-specific CMV-driven gene expression. Screened hits showed at least a 3 standard deviation fold increase in the ratio of LRT/CMV of untreated cells (>Ave + 3SD). Compounds that did not achieve this level of LTR activity, relative to the CMV control, were deemed too non-specific and were not progressed to further stages. *This work was carried out by collaborators (Dr Kate Jarmen) at the WEHI, and not by the author.

2) Confirmation: The 512 screened hits found were re-assayed in triplicate at 10 μ M for confirmation in the same Flipin.FM cell line. From this, 152 compounds became “confirmed hits” exhibiting acceptable reactivation profiles and these progressed to 11-point dose response experiments. *This work was carried out by collaborators (Dr Kate Jarmen) at the WEHI, and not by the author.

3) Counter screens: To ensure that the 152 confirmed hits were not producing false positive results by simply interfering with the luciferase system, the FlipIn.RV reverse orientation cell line was used to confirm hit compounds by directly proceeding to a single 11-point dose response experiments. Seven individual compounds, belonging to seven distinct chemical series, that demonstrated the most LTR-specific reporter activation and but low toxicity behavior were pulled out of this shortlist. *This work was carried out by collaborators (Dr Kate Jarmen) at the WEHI, and not by the author.

4) Latency models: Seven individual compounds, each belonging to a distinct chemical series, were re-purchased fresh from vendors supplying the screening array, then independently tested in 8-point dose response experiments (triplicate) by the author at the Doherty Institute in the FlipIn.FM and FlipIn.RV cell lines. These seven compounds were also assayed in the J.Lat T cell line models of HIV-1 latency. Additionally, the first rounds of medicinal chemistry were commenced with these seven compounds by collaborators Dr Brad Sleebs and Dr William Nguyen at the WEHI. The chemistry studies generated >100 structural analogues within one of these series (Series E) that encompassed composition of matter towards a full patent, and from these two were selected for presentation in this thesis.

5) Synergy: Finally, 2 of the seven novel series, which showed the best synergistic reactivation with multiple known LRAs (Chapter 6), were taken forward for reactivation experiments from primary leukapheresis samples.

High Throughput Chemical Screening:

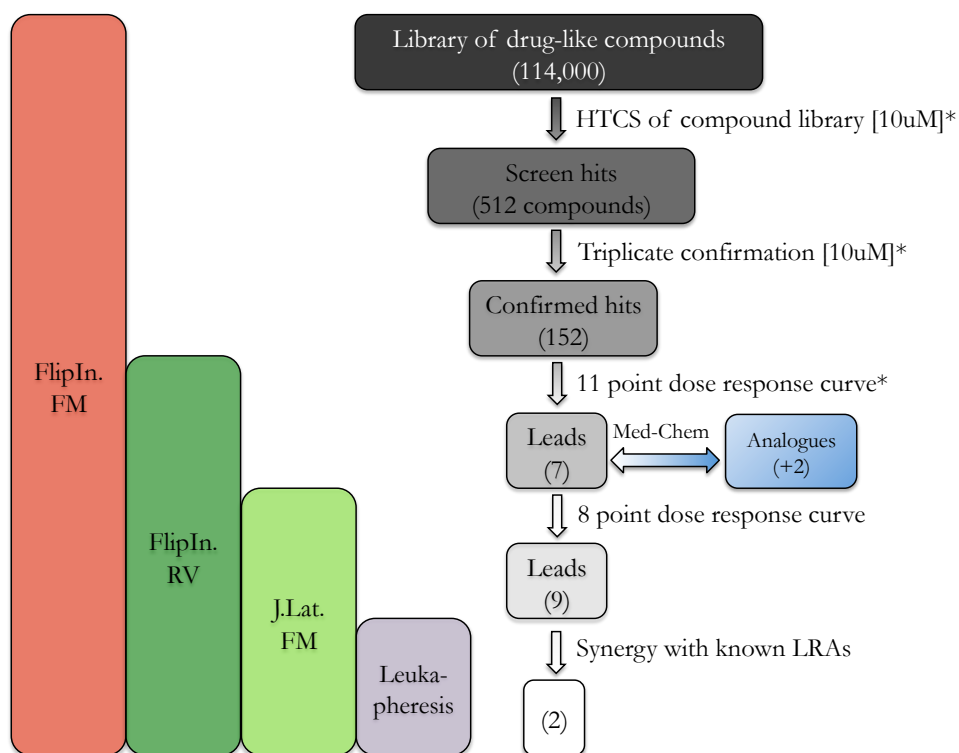


Figure 5.2: Overview of drug discovery screening matrix. The progression of hit compounds through four distinct stages including: initial screening of the compound library, confirmation of screened hits, counter screening in the reverse orientation FlipIn.RV and J.Lat T cell lines and finally synergy studies in primary leukapheresis experiments.

* This work was carried out by collaborators at the WEHI.

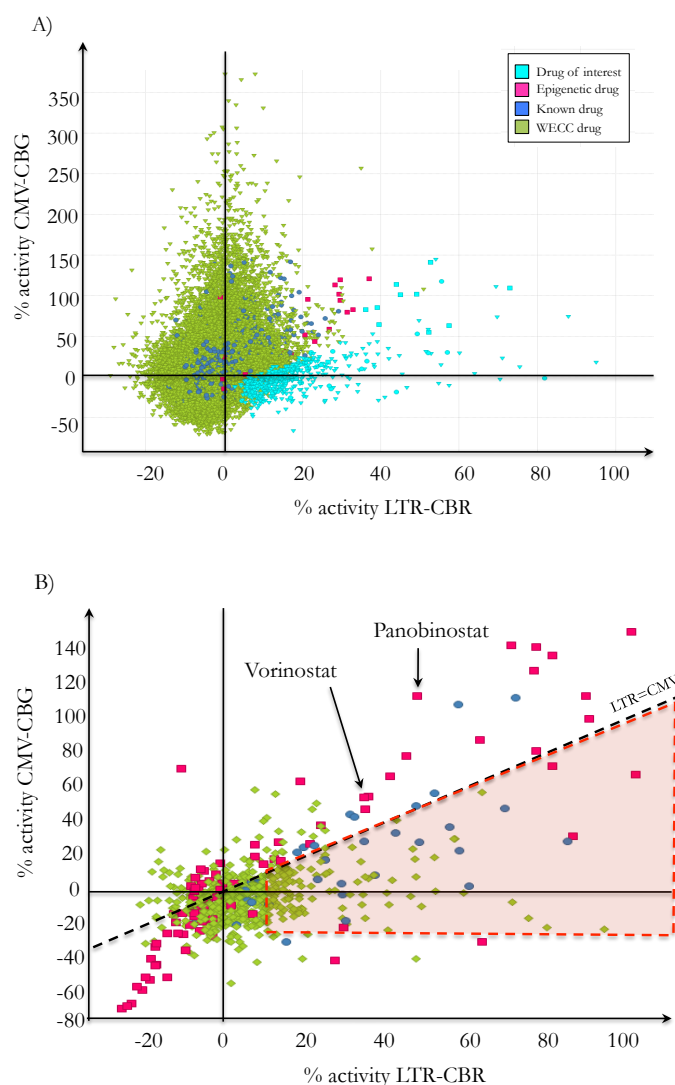


Figure 5.3: Primary High Throughput Chemical Screen and triplicate confirmation screen. A) A scatter plot showing the entirety of the compounds screened in HTCS, including ~114,000 compounds of the Stage 6 WECC set (Green triangle), 95 epigenetic modulator compounds (pink square) and ~3700 known drugs (Dark blue circle). Compounds of interest (512 screened hits) from these three libraries are shown in light blue and displayed when run in triplicate in part B). B) The black dashed line represents activation where LTR=CMV (where activation is shown to be non-specific and affects the two reporters equally). Compounds on or above this line were therefore classed as non-specific. Compounds within the red shaded area, however, showed specificity for the LTR over the CMV and were advanced onto the net stage of LRA discovery. Compounds showing a >25% decrease in CMV-CBG level were discounted as too toxic (as the CMV reporter acted as a surrogate for toxicity). HDACis Vorinostat and Panobinostat are shown, note they sit above the LTR=CMV, showing their nonspecific activity.

5.3 Results.

5.3.1 Characterizing the seven series of novel Latency Reversing Agents.

5.3.1.1 Characterizing the seven series of novel Latency Reversing Agents.

The structures of the seven chemically distinct of compound families (series) that were discovered via HTCS to specifically reactivate LTR-driven expression are shown in Figure 5.4. Also included within Series E are two additional compounds, DP#14 and DP#16, created through subsequent rounds of medicinal chemistry to increase the potency of the original compound DP#6. Each compound has a WECC identification number for reference within the library, or a WEHI number assigned to the novel composition of matter analogue compounds synthesized in the medicinal chemistry program that occurred after the library screen. For simplicity, these numbers will be not be used throughout this thesis, rather a simpler Damian Purcell (DP) laboratory numbering system will be used. Notably, this numbering system begins with #2, as DP#1 is not present in the shortlist. This is due to DP#1 coincidentally belonging to the same series as DP#2 (the Triazolopyridazine series), but being less potent than DP#2, was abandoned in place of the latter. Each compound was also allocated an arbitrary identification name: series A-G. These series names were used for convenience rather than frequently using the seven-digit compound name. Extensive studies of the seven chosen compound series carried out by collaborators at the WEHI and the author at the Doherty institute, as well as invaluable input by the chemistry team at the WEHI, prioritized Series E as the most interesting for their ability to synergize strongly with several known classes of LRAs (Chapter 6) and the free IP space surrounding the Amidothiazole series. In 2016, a provisional patent was filed around the IP of the Amidothiazole, and subsequently a full patent was filed in 2017.

Table 5.2: Novel Latency Reversing Agent hit summary table.

WECC/WEHI number	Core drug name	DP number	Series
0015915	Triazolopyridazine	2	B
0118034	Oxindole	3	C
0009016	Diadapine	4	A
0095576	Imidazopyrazole	5	G
0085584	Quinazoline	7	D
0143183	2-Amidopyridine	8	F
0078085	Amidothiazole	6	E (Gen1)
1248349	Amidothiazole	14	E (Gen2)
1250191	Amidothiazole	16	E (Gen3)

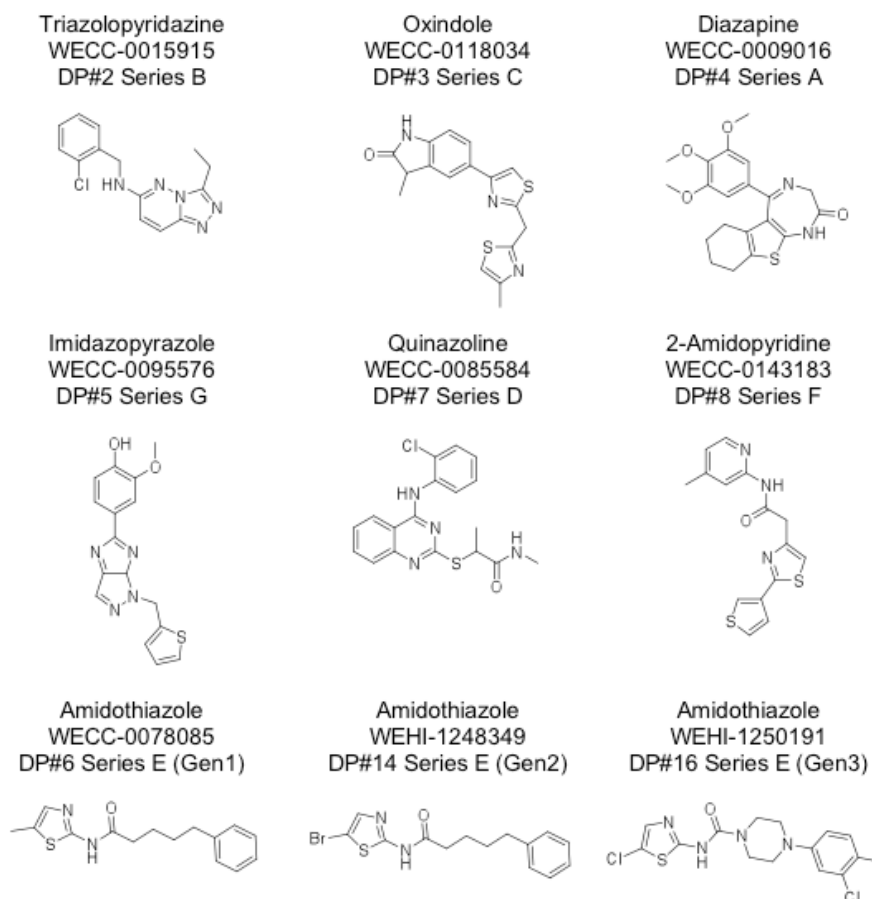


Fig 5.4 Structures of the seven novel latency reversing agent hits and analogues.

The structures above show seven LRA compounds that were “hits” in the FlipIn.FM model discovered through the drug screening process. Each belongs to chemically distinct families and several potentially novel latency reversing agents. Also included are two analogues of the original Series E compound, the result of medicinal chemistry to increase potency. Each compound was codified with the Stage 6 WECC set number, or, in the case of the two compounds produced through medicinal chemistry, a WEHI number. Each compound has also been assigned a DP (Damian Purcell Laboratory) number, as an arbitrary series letter code.

5.3.1.2 Bromodomain inhibition alpha screen.

*This work was carried out by collaborators (Dr Kate Jarmen) at the WEHI, and not by the author. As described in Chapter 3, the FlipIn.FM cell line was engineered to express a low level of HIV-1 Tat protein, by modeling an IRES mediated mechanism that may occur during post integration latency, and which the Purcell laboratory is studying from other angles. As such, the cell line was designed with a bias for finding compounds that synergized with this pathway of Tat expression or compounds targeting the Tat-TAR positive feedback loop. Extensive reports in the literature indicate that bromodomain containing proteins such as BRD4 play an important role in controlling the levels of free P-TEFb, a host transcription factor critical for processive HIV-1 transcription and subsequent gene expression. BRD4 competes with HIV-1 Tat protein and hinders its role in recruiting the transcription factor to the stalled RNA polymerase II at the viral promoter. Bromodomain inhibitors such as JQ1 (+), yielded encouraging results in the FlipIn models (Chapter 4). It was therefore probable, that the cell-based screening tools biased the detection of compounds that synergize with Tat protein, and “hits” from the library screen may target bromodomain containing proteins. With this in mind, bromodomain protein-interaction assay alpha screens were performed at WEHI using our seven novel LRAs (DP#2-DP#8).

Two sets of assays were used, one targeting BRD4 domain 1 and the second targeting domain 2 (Figure 5.5). Surprisingly, 5 of the 7 novel series interacted, at least in part, with bromodomain domain 1 and 2 of BRD4 to inhibit its activity. The compounds are listed here in order of decreasing potency: DP#4, DP#3, DP#2, DP#5 and DP#7, giving EC₅₀s against domain 1 at 827.9nM, 1399.6nM, 2523.5nM, 4355.1nM and 5224.0nM respectively. For reference, the potent bromodomain inhibitor, JQ1 (+), has an EC₅₀ in the literature of 77nM, 10.8-fold to 67.8-fold more potent than any of the novel compounds listed. The compounds hit domain 2 in the same sequence, but with slightly increased potency at 406.4nM, 895.4nM, 1358.3nM, 2387.8nM and 3104.6nM respectively. Again for reference, in the literature, JQ1 (+) has an EC₅₀ of 33nM for domain 2, 12.3-fold to 94.1-fold more potent than the novel compounds. Interestingly, the DP compound with the highest affinity for BRD4 (DP#4) is a Diazapine compound like JQ1 (+). DP#6 (Series E) and DP#8 (Series F), however, were unable to inhibit either domain of BRD4, and, to the date of writing this thesis, their mechanism of action remains novel and are the subject of continuing investigation.

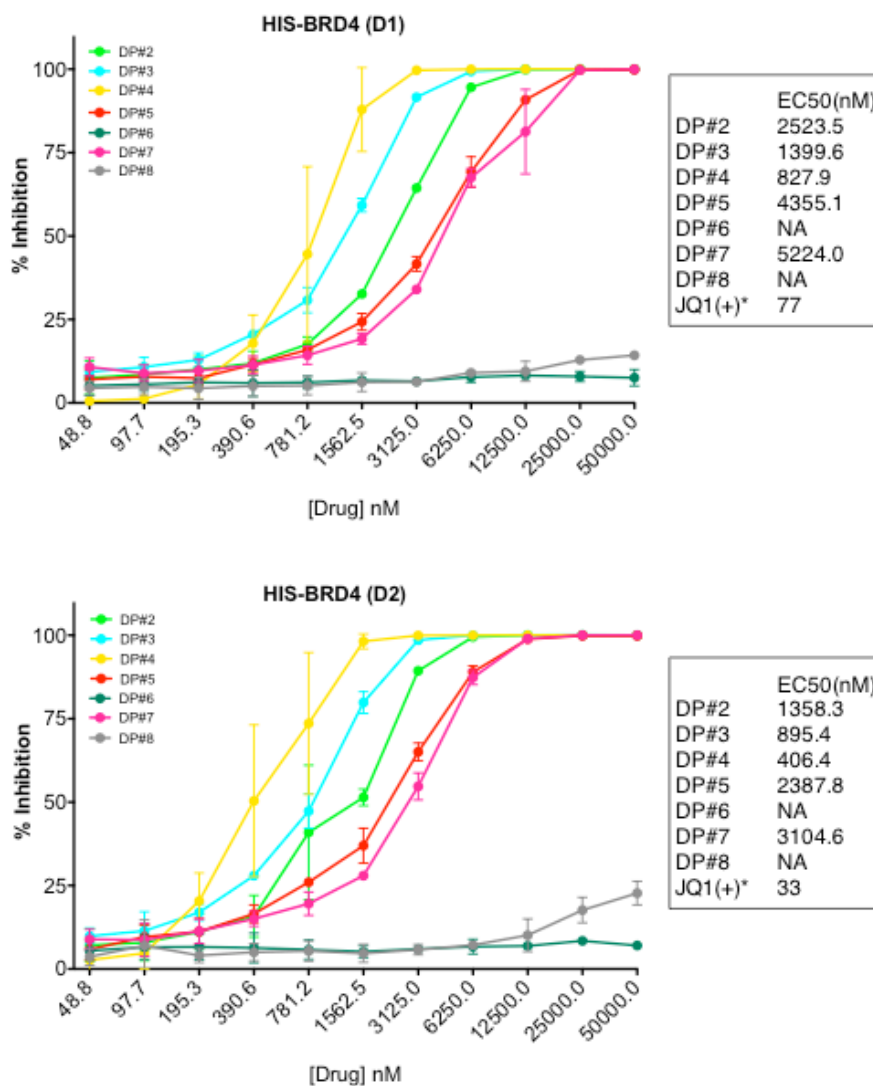


Figure 5.5: BRD4 Bromodomain inhibition alpha screen. Domains 1 and 2 of the BRD4 protein were targeted using the seven novel latency reversing agents found through the HTCS process. Of the seven unique series, five targeted BRD4 (both domain 1 and 2), with EC₅₀ values spanning from 827nM – 5224nM for domain 1, and 406nM – 3104nM for domain 2. For context, the EC₅₀ values for the potent BDi JQ1 (+) are 77nM and 33nM for domains 1 and 2 respectively. DP#6 of Series E and DP#8 of Series F showed minimal to no inhibition of either domain. This work was carried out by collaborators at the WEHI.

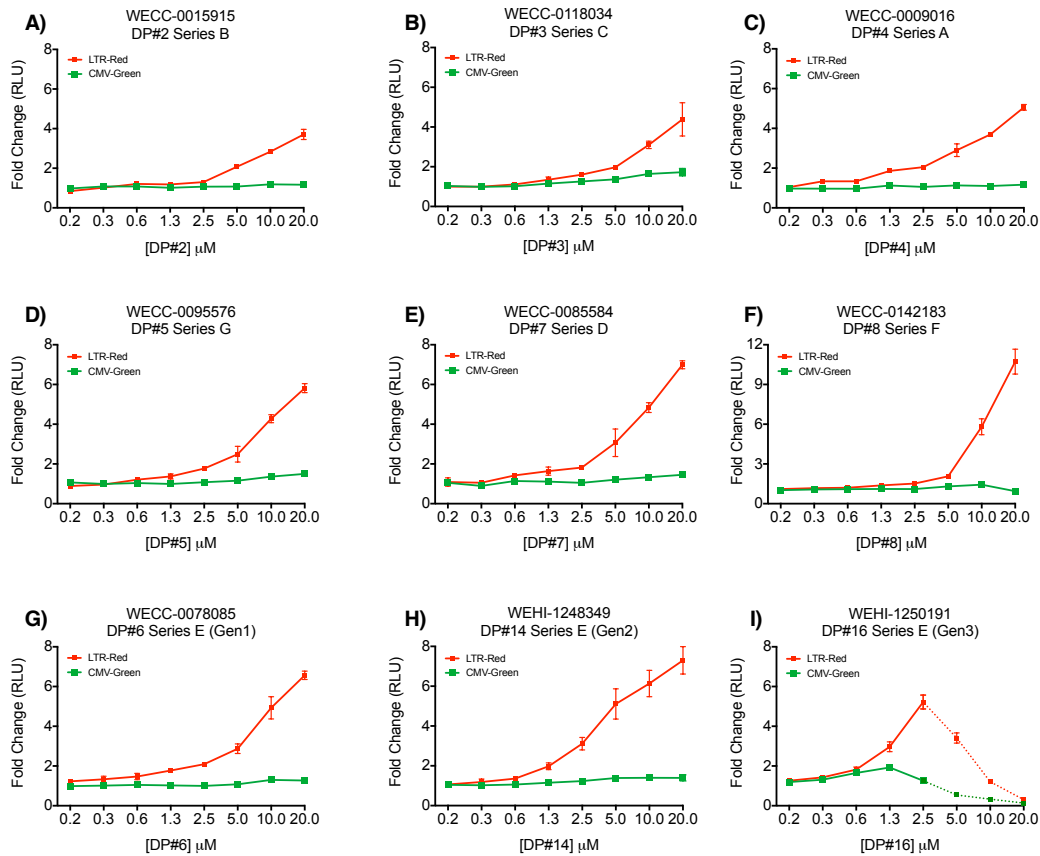
5.3.2 Assessing novel Latency Reversing Agents in the FlipIn cell lines.

5.3.2.1 FlipIn.FM response to novel LRAs.

With the HEK293 and Jurkat based models of HIV-1 latency constructed (Chapter 3) and subsequently validated using the panel of 15 known latency reversing agents (Chapter 4), it was possible to likewise assess the novel latency reversing agent “hits” and analogue compounds found by HTCS and subsequent medicinal chemistry (above). These compounds, showed high levels of LTR-driven gene expression in conjunction with desired low levels CMV-driven gene expression in the HTCS process. They then progressed through triplicate confirmation and a pioneer (n=1) 11-point dose response experiment, all conducted by collaborators at the WEHI. These compounds were transferred to the Purcell laboratory for further in-depth assessment across the various platforms for testing LRA activity and specificity upon HIV-1 latency.

For the FlipIn.FM dual reporter cell line, HIV-1 reactivation was modeled by increased LTR-driven Click Beetle Red (CBR) luciferase reporter expression. Non-specific activation, due to off-target drug effects, were modeled by increased CMV-driven Click Beetle Green (CBG) reporter expression. For these experiments, a 2-fold series dilution was set up in 100 μ L in a 96 well plate across 8-points, beginning with a highest concentration of 20 μ M and ending with 0.156 μ M (156nM) (Figure 5.6). Cells were incubated in the presence of each compound for 48hrs before harvesting. Interestingly, each compound from DP#2-DP#14, although being chemically distinct from each other, all showed remarkably similar reactivation profiles, with maximum reactivation being achieved at 20 μ M (except for DP#16 as outlined below). Viewing the shape of the curves, however, suggests that higher drug concentrations may result in yet higher levels of LTR-driven gene expression, as the plateau was not reached for most compounds within this concentration window. The table in Figure 5.6 summarizes the data in two formats: The first format (fold) shows the fold changes over the unstimulated baseline for both the LTR and CMV-driven reporters. The second format is a comparison of the area under the curve (area), also included as some compounds begin to show activity at lower sub-toxic concentrations, which would be missed by simply looking at the maximum level of reactivation achieved. Additionally, a specificity ratio, LTR specific reactivation over CMV non-specific reactivation has been calculated for both data sets. JQ1 (+) has been included for comparison, as most of the novel DP compounds also targeted BRD4. In terms of

induction of LTR-driven gene expression, the achieved levels ranged from 3.7-fold (DP#2) to 10.7-fold (DP#8). Individually, in order of increasing maximum reactivation, they were: DP#2 (3.7-fold), DP#3, (4.4-fold), DP#4 (5.1-fold), DP#5 (5.8-fold), DP#6 (6.6-fold), DP#7 (7-fold), DP#14 (7.3-fold) and DP#8 (10.7-fold). The exception to this trend was DP#16, the generation 3 compound from Series E, which achieved 5.2-fold induction over baseline, but at 2.5 μ M. Also of note for DP#16 is the apparent toxicity seen at concentrations above 2.5 μ M (denoted by a dotted line), where both the LTR and CMV-driven expression can be seen to drop sharply in a dose dependent manner. As expected, due to the strict selection criteria in HTCS, only low-level changes in CMV-driven Click Beetle Green (CBG) expression levels were seen (all were <2-fold over baseline), displaying each compounds specific activity at the proviral LTR. To compare the three members of Series E, LTR-reactivation was measured at 2.5 μ M, above which DP#16 became toxic. For DP#6, DP#14 and DP#16, these values were 1.7, 2.5 and 4.9 respectively, demonstrating the increased potency medicinal chemistry had introduced with each subsequent generation.

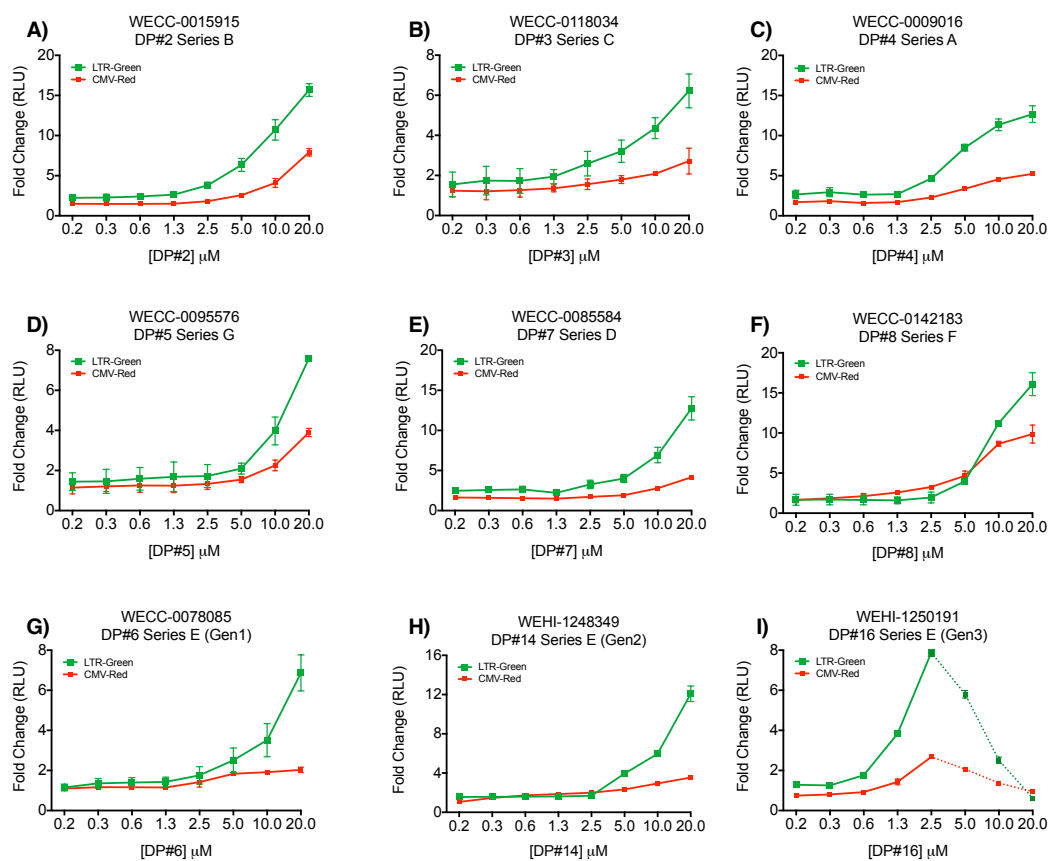


Drug	LTR (fold)	CMV (fold)	Ratio (fold LTR/CMV)	LTR (area)	CMV (area)	Ratio (area LTR/CMV)
DP#2	3.7	1.2	3.2	32.2	2.7	11.8
DP#3	4.4	1.7	2.5	37.9	10.5	3.6
DP#4	5.1	1.2	4.3	50.7	2.4	21.4
DP#5	5.8	1.5	3.9	56.1	6.0	9.4
DP#7	7.0	1.5	4.8	68.8	5.8	11.8
DP#8	10.7	0.95	11.3	90.1	4.6	19.7
DP#6	6.6	1.3	5.2	67.4	4.0	17.1
DP#14	7.3	1.4	5.3	90.5	7.0	12.9
DP#16	5.2	1.3	4.1	NA	NA	NA
JQ1 (+)	9.0	2.0	4.5	122.6	15.42	8.0

Figure 5.6: Induction of gene expression in FlipIn.FM cells using novel LRAs. FlipIn.FM cells were treated with each DP novel LRA over an 8-point 2-fold dilution series and assayed 48hrs post addition of drug. In each case, with the exception of DP#16, reactivation peaked at 20 μ M and ranged from 4-fold over baseline (DP#2 and DP#3) to as high as 10-fold over baseline (DP#8). Induction is shown as fold change over the untreated cell baseline with the error bars representing standard deviation of n=3. The table summarized the fold change over unstimulated (fold) for both LTR and CMV-driven reporters at maximal activation, as well as the area under the curves of each (area). Ratios (LTR/CMV) have also been included for comparison.

5.3.2.2 FlipIn.RV response to novel LRAs.

To confirm the results seen in the original FlipIn.FM screening cell line, the FlipIn.RV reverse orientation cell line was likewise utilized to assess each novel LRA. The experimental procedure was identical to that of the FlipIn.FM cell line experiments outlined above, with a 2-fold dilution series set up over 8 points beginning at 20 μ M. The main difference between the two FlipIn models is the site of integration of the LTR-driven reporter proviruses. The integration site difference of the FlipIn.RV LTR-driven reporter cell line showed, on average, greater levels of LTR induction, however the same trends were conserved across the two cell lines. In Figure 5.7 each of DP#2-DP#14, showed maximal induction of LTR-driven expression at 20 μ M. In terms of induction of LTR-driven gene expression, the achieved levels ranging from 6.2-fold (DP#3) to 16.1-fold (DP#8). Individually, in order of increasing maximum activation, they were: DP#3 (6.2-fold), DP#6 (6.9-fold), DP#5 (7.6-fold), DP#14 (12.1), DP#4 (12.7-fold), DP#7 (12.8-fold), DP#2 (15.7-fold) and DP#8 was again the best performer at 16.1-fold. Again DP#16, the third-generation compound from series E, showed maximal induction (8-fold) at 2.5 μ M and toxicity at concentrations above 2.5 μ M (as seen by a drop in CMV expression). Encouragingly, similar trends were mostly conserved between the two models with DP#3 (Series C) performing relatively poorly and DP#8 (Series F) performing the best in terms of cross assay consistency. Interestingly, an important difference between the two cell lines was the induction of CMV-driven reporter expression by the FlipIn.RV cell line with some compounds that was not seen in the FlipIn.FM cell line. Of note was the 7.9-fold induction seen with DP#2 and the 9.9-fold change seen with DP#8, will all compounds inducing at least 3-fold increases in CMV-driven non-specific activation. These observations were unexpected as the site of both CMV-reporter genes will be identical between both cell lines due to them being introduced using the FlpIn recombination system. Again, to compare the three members of Series E, the area under the curve was calculated up to 2.5 μ M, above which DP#16 became toxic. For DP#6, DP#14 and DP#16, these values were 1.2, 1.5 and 7.4 respectively, demonstrating the increased potency medicinal chemistry had introduced with each subsequent generation. Taken together, the results of the two FlipIn cell lines are in general agreement with each other, however, being a HEK293 derived cell line, further validation was required in the J.Lat Jurkat T cell derived cell line.



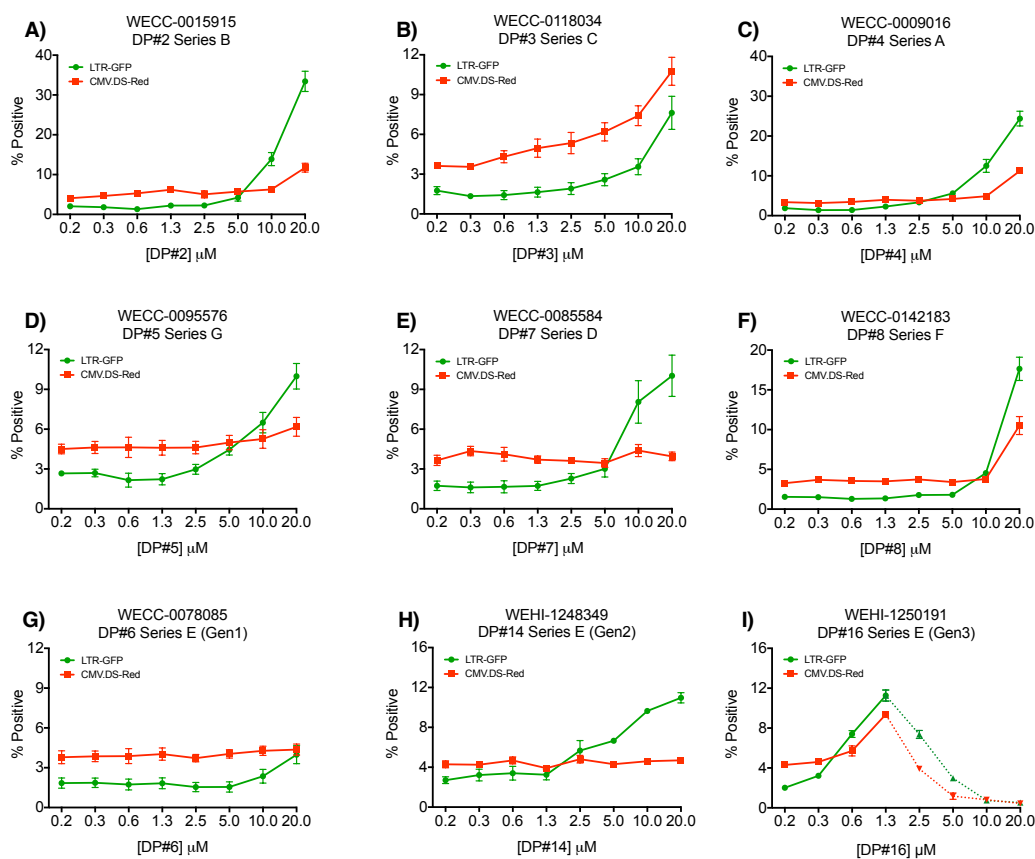
Drug	LTR (fold)	CMV (fold)	Ratio (fold LTR/CMV)	LTR (area)	CMV (area)	Ratio (area LTR/CMV)
DP#2	15.7	7.9	2.0	174.1	66.2	2.6
DP#3	6.2	2.7	2.3	64.0	21.3	3.0
DP#4	12.7	5.2	2.4	174.0	60.3	2.9
DP#5	7.6	3.9	1.9	61.8	27.0	2.3
DP#7	12.8	4.2	3.0	121.2	34.9	3.5
DP#8	16.1	9.9	1.6	166.2	122.1	1.4
DP#6	6.9	2.0	3.5	56.0	16.2	3.5
DP#14	12.1	3.5	3.5	106.0	35.4	3.0
DP#16	7.9	2.7	2.9	NA	NA	NA
JQ1 (+)	5.3	2.1	2.5	76.6	23.0	3.3

Figure 5.7: Induction of gene expression in FlipIn.RV cells using novel LRAs. RV cells were treated with each DP novel LRA over an 8-point 2-fold dilution series and assayed 48hrs post addition of drug. With exception of DP#16, reactivation peaked at 20μM. Unlike the original cell line however, there was a marked increase in CMV-driven expression seen for all compounds. Induction is shown as fold change over the untreated cell baseline with the error bars representing standard deviation of n=3 experiments. The table summarizes the fold change over unstimulated (fold) for both LTR and CMV-driven reporters at maximal activation, as well as the area under the curves of each (area). Ratios (LTR/CMV) have also been included for comparison.

5.3.3 Assessing novel Latency Reversing Agents in the J.Lat cell lines.

5.3.3.1 J.Lat10.6.FM response to known LRAs.

Showing promising signs in the FlipIn.FM and FlipIn.RV cell lines, the 9 compounds were advanced into the more relevant J.Lat models of HIV-1 latency. The advantages of the J.Lat cell lines over the FlipIn models are outlined in detail in Chapter 4 and include greater relevance in their cell type (T cell origin) and a more complete reporter provirus with a native Tat-TAR feedback loop. The modified J.Lat cells are also a heterogeneous population for the CMV-driven DS.Red non-specific reporter, more accurately representing global gene expression than the FlipIn models, clonal for their CMV reporters. The J.Lat10.6FM cell line represents a more inducible provirus than the counterpart J.Lat6.3FM clone. As seen with the FlipIn models, the J.Lat10.6FM cells in Figure 5.8 showed maximum reactivation from their LTR-driven reporters at 20 μ M, although the shape of the curves suggest a higher concentration may be required for maximal reactivation. The exception again was DP#16, which showed a peak at 1.25 μ M, rather than 2.5 μ M seen in the FlipIn cells. Again, among the better performers were DP#2, showing a 33.4% GFP positive population, DP#4, showing 24.4% positive and DP#8 showing 17.7% positive. As seen with the FlipIn cells, DP#3 performed relatively poorly, with only 7.6% GFP positive population at 20 μ M. To compare the three members of Series E, reactivation at 1.25 μ M was compared, above this concentration DP#16 became toxic. For DP#6, DP#14 and DP#16, these values were 0.9%, 1.25% and 11.2% GFP positive respectively, demonstrating the increased potency medicinal chemistry had introduced with each subsequent generation. As seen with the FlipIn.RV cell line some non-specific activation of the heterogeneous CMV-DS.Red reporter, most notably for DP#2, DP#3, DP#4 and DP#8, all achieving approximately 12% positive, up from a baseline of 4%. Interestingly, DP#16 from Series E also showed non-specific activity, where DP#6 and DP#14 did not. While these novel compounds all showed the ability to induce LTR-drive gene expression, to varying extents, the levels of induction seen were modest at best when compared to several of the known LRAs tested in Chapter 4, including the HDACi series, averaging around 50% positive (Figure 4.4) as well as the PKC/NF- κ B activators achieving maximal induction levels of >75% positive. With this in mind, the novel compounds shown here may be better suited to act with some of the known LRAs in synergistic combinations than as single agents. This will be explored in Chapter 6.



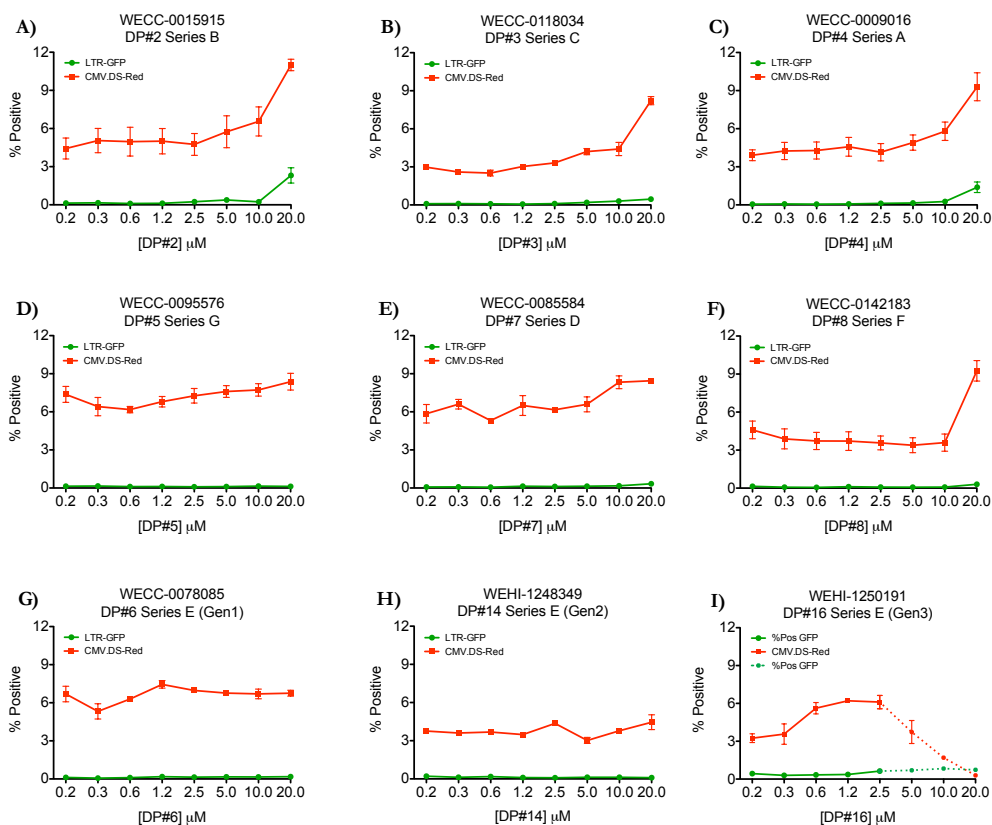
Drug	LTR (%)	CMV (%)	Ratio (% LTR/CMV)	LTR (area)	CMV (area)	Ratio (area LTR/CMV)
DP#2	33.4	11.7	2.9	274.8	67.0	4.1
DP#3	7.6	10.8	0.7	60.9	71.3	0.9
DP#4	24.4	11.3	2.2	226.5	44.4	5.1
DP#5	10.0	6.2	1.6	105.0	26.2	4.0
DP#7	10.0	3.9	2.6	109.2	4.8	22.8
DP#8	17.7	10.5	1.7	114.9	35.6	3.2
DP#6	4.0	4.4	0.9	29.6	4.6	6.4
DP#14	11.0	4.7	2.3	148.5	11.0	13.5
DP#16	11.3	9.4	1.2	NA	NA	NA
JQ1 (+)	33.1	4.4	7.5	606.2	5.0	121.2

Figure 5.8: Induction of gene expression in J.Lat10.6FM cells using novel LRAs.

Treatment of J.Lat10.6FM dual reporter cell line with nine novel LRA hits and analogues, across an 8-point titration gradient and assayed at the 48hr time point post drug addition. LTR induction was measured by Green Fluorescent Protein expression and off target effects (CMV) via DS.Red expression. Induction is shown as percentage positive with the error bars representing standard deviation of n=3. The table summarized the percentage positive (%) for both LTR and CMV-driven reporters at maximal activation, as well as the area under the curves of each (area). Specificity ratios (LTR/CMV) have also been included for comparison.

5.3.3.2 J.Lat6.3.FM response to known LRAs.

In Chapter 4, the J.Lat6.3FM proved exceedingly difficult to reactivate with known LRAs. This relative difficulty in obtaining full LTR-induction across the cell population was also observed here with none of the novel hits and analogue compounds able to achieve efficient reactivation of LTR-driven expression (Figure 5.9). Of note, very low-level expression was seen with DP#2 (2.3% positive) and DP#4 (1.3% positive) at 20 μ M. For all of the other compounds, LTR-driven expression was <0.5% positive, demonstrating an inability to reactivate the deep form of latency exemplified by the J.Lat6.3 provirus. Predictably, the CMV-driven DS.Red expression was seen to be nearly identical to that of the J.Lat10.6FM cells, due to the two clones being transduced with the CMV-DS.Red pseudovirus under identical conditions and with random integration into the Jurkat cell genome. This was also evident in the treatment of each clone with the panel of known LRAs in Chapter 4. Taken together, the lack of reactivation in this clone demonstrates that single agent LRAs are likely to not be sufficient to reactivate all the inducible provirus within the latent reservoir, and that synergistic combinations of LRAs, targeting different restrictions on viral gene expression, will likely be needed.



Drug	LTR (%)	CMV (%)	Ratio (% LTR/CMV)	LTR (area)	CMV (area)	Ratio (area LTR/CMV)
DP#2	2.3	11.0	NA	13.5	55.89	NA
DP#3	<0.5	8.3	NA	<0.5	42.1	NA
DP#4	1.3	9.3	NA	7.9	46.4	NA
DP#5	<0.5	8.3	NA	<0.5	30.3	NA
DP#7	<0.5	8.4	NA	<0.5	46.4	NA
DP#8	<0.5	9.3	NA	<0.5	29.4	NA
DP#6	<0.5	6.7	NA	<0.5	9.5	NA
DP#14	<0.5	4.5	NA	<0.5	6.5	NA
DP#16	<0.5	6.1	NA	<0.5	NA	NA
JQ1 (+)	0.24	2.5	NA	4.0	15.9	NA

Figure 5.9: Induction of gene expression in J.Lat6.3FM cells using novel LRAs. Treatment of J.Lat6.3FM dual reporter cell line with nine novel LRA hits and analogues, across an 8-point titration gradient and assayed at the 48hr time point post drug addition. LTR induction was measured by Green Fluorescent Protein expression and off target effects (CMV) via DS.Red expression. Induction is shown as percentage positive with the error bars representing standard deviation of n=3. The table summarized the percentage positive (%) for both LTR and CMV-driven reporters at maximal activation, as well as the area under the curves of each (area). Specificity ratios (LTR/CMV) have also been included for comparison.

5.3.4 Drug associated toxicity of novel Latency Reversing Agents.

5.3.4.1 FlipIn.FM (HEK293) toxicity response to novel LRAs.

MTS assays were performed to assess the respective toxicity of the novel LRAs both in the FlipIn.FM (HEK293 derived) cell line and in primary CD4+ resting memory T cells. This assay, while informative in many respects, shows the bulk average cell metabolism within each well, and does not directly measure how many viable cells remain after drug treatment. It is therefore possible that a drop in the signal induced by any one compound is due to a decrease in metabolism of the cells within that well, rather than true cell death by apoptosis or necrosis. To address this, live dead staining was performed on key drugs/combinations as detailed in Chapter 6. Interestingly, despite DP#16 being the only novel LRA compound to induce a notable drop in the CMV-drive reporter, which acts as an inbuilt cell health indicator, four of the other series were shown to show some toxicity at 20 μ M. The exceptions to this were DP#5, DP#7 and the two earlier generations of series E DP#6 and DP#14, all of which remained at \sim 100% of the normalized value (ie no toxicity detected). DP#2, DP#3 and DP#4 all reduced the signal output to 60%-65% at 20 μ M, whereas a decrease to 28% of the normalized value was detected with DP#8. Another interesting observation was the drop in signal seen when treating the FlipIn.FM cells with DP#16. In the luciferase system, concentrations above 2.5 μ M were toxic, whereas with the MTS system, the decrease from baseline was seen at concentrations as low as 0.625 μ M (625nM). The discrepancy between the inbuilt CMV reporters and the MTS metabolism assay are yet to be fully resolved.

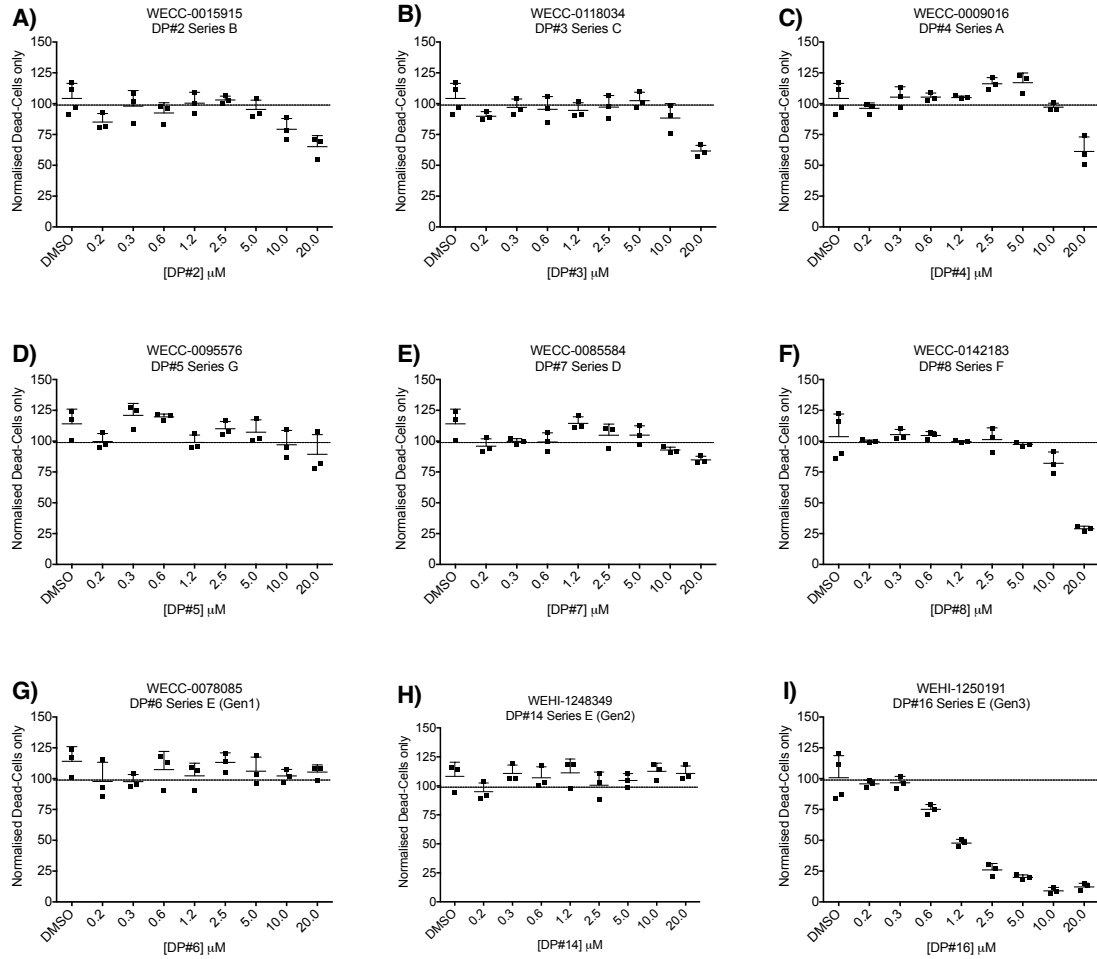


Figure 5.10: Measuring drug associated toxicity of novel LRAs in FlipIn.FM cells. Treatment of HEK293 derived FlipIn.FM cell line with a panel of 15 known LRAs, across an 8-point titration gradient and assayed at the 48hr time point post drug addition. Bulk metabolism by MTS assay was used as a surrogate for detecting global cell activation and cell death by drug associated toxicity. Toxicity is shown normalized to untreated cells (100%) and dead cells (0%) with the error bars representing standard deviation of n=3.

5.3.4.2 Primary CD4⁺ T cell toxicity response to novel LRAs.

While the toxicity data in the FlipIn.FM cells looked generally encouraging, the real test for the novel compounds would be how primary resting memory CD4⁺ T cells performed. To this end, CD4⁺ resting memory T cells were isolated and treated with the novel compounds and their bulk metabolism measured at 72hrs. Encouragingly, the trends seen were very similar to those seen in the FlipIn MTS experiments of Figure 5.10, with DP#8 showing high levels of toxicity, reducing the signal detected to 12% of the untreated baseline, at 20 μ M and DP#16 showing an average of 38% of the untreated baseline at 0.3125 μ M (312.5nM). DP#2 and DP#3 were again shown to decrease the signal output to 57% and 64% respectively. Contrary to the FlipIn MTS experiments, DP#4 showed no toxicity in primary cells. The remaining compounds DP#5, DP#7, DP#6 and DP#14 again showed negligible deviation from the baseline.

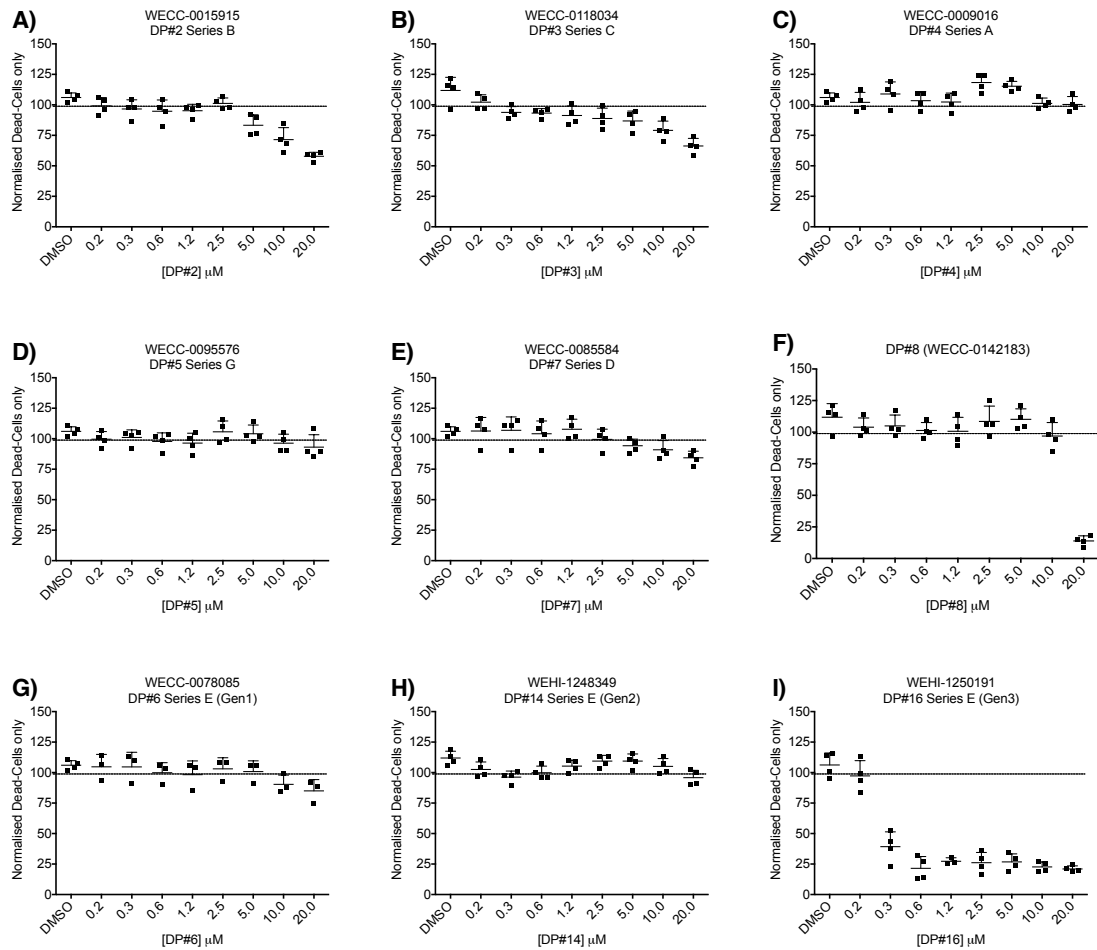


Figure 5.11: Measuring drug associated toxicity of novel LRAs in primary CD4+ resting memory T cells. Treatment of primary CD4+ T cell with a panel of 15 known LRAs, across an 8-point titration gradient and assayed at the 72hr time point post drug addition. Bulk metabolism by MTS assay was used as a surrogate for detecting global cell activation and cell death by drug associated toxicity. Toxicity is shown normalized to untreated cells (100%) and dead cells (0%) with the error bars representing standard deviation of n=4 donors (done in duplicate).

5.4 Discussion.

HIV-1 persists in infected individuals in a long-lived pool of latently infected cells, despite prolonged successful antiretroviral therapy. Attention has now turned to developing therapeutic strategies for clearing the body of inducible, silenced provirus capable of producing replication competent virus and eradicating the relevant latent reservoir. To date, several classes of latency reversing agents have completed, or are currently undergoing trial in advanced primary models of HIV-1 latency, or in early-phase clinical trials with mixed success. The mechanism of action of the compounds enrolled in these past and current strategies are summarized on Table 5.1 below.

Table 5.1: Known Latency Reversing Agent used in advanced trials.

Target mechanism	LRA investigated	References
Transcription factor activators	TNF α (NF- κ B)	(Saleh, Wightman et al. 2011)
	Bryostatins-1 (PKC)	(Perez, de Vinuesa et al. 2010)
Chromatin architecture modulators	Vorinostat* (panHDAC)	(Burnett, Lim et al. 2010; Archin, Liberty et al. 2012)
	Panobinostat* (panHDAC)	(Rasmussen et al 2013)
	Romidepsin* (HDAC1/2)	(Ying, Zhang et al. 2012)
Methylation inhibitors	BIX-01294 (G9a)	(Bouchat, Gatot et al. 2012)
P-TEFb activators	JQ1 (+) (BRD4)	(Banerjee, Archin et al. 2012)
	Disulfiram* (HEXIM1)	(Xing, Bullen et al. 2011)
Immune activation therapy (IAT)	IL-2* and IFN- γ *	(Davey, Bhat et al. 1999; Stellbrink, van Lunzen et al. 2002)
	IL-7*	(Wang, Xu et al. 2005)
	Anti-PD1*	(Dafonseca, Chomont et al. 2010)

* clinical trial

Notably, many of these drugs were advanced for therapy in the cancer research field, and some have been suitable for testing in the HIV-1 latency field. These are well characterized and some have FDA approved indications in cancer therapy, enabling their rapid advancement into clinical trials against latent HIV-1. Some of these drugs may have an important part to play in a future cure regime, but at present there is a lack of a class (or several classes) of LRAs that specifically target HIV-1 infected cells. For this reason, we

set about developing a model screening platform that allowed for detection of HIV-1 specific LRAs, and underwent HTCS to discover these novel HIV-1 LRA compounds.

Unlike the discussion provided in Chapter 4, relating to the fifteen well characterized known latency reversing agents, the seven novel series here are yet to be characterized. Rather, the exact mechanisms of action for the seven novel series are largely unknown. While five of the seven series were shown to inhibit BRD4, these compounds likely also have other molecular targets (either other BRD proteins or unrelated proteins), whereas the mechanisms of action for Series E and Series F, which did not target BRD4, are unknown to date. As a result, the following discussion is a largely speculative review of the data raised in this chapter. The screening cell line was, however, designed to detect compounds that synergized with the low level of Tat protein produced during latency via the IRES pathway detailed in Chapter 3. More insight into the activity of these novel LRAs can be gained by pairing them with the known LRAs in synergistic combinations, as detailed in Chapter 6.

Collaborators at the WEHI used the FlipIn.FM dial reporter cell line to screen the Stage 6 WECC set (compound library of >114,000 compounds) and detected an initial 512 hits. The hit must have a LTR/CMV ratio greater than the Ave+3SD of untreated cells. The hit must not induce a decrease in the CMV-CBG expression level below -25%, relative to the untreated cells (ie too toxic). The hits were found at 10 μ M and fall within the red shaded area of compounds that activated resting provirus, but did not activate a CMV-vector expressing a control reporter protein in Figure 5.3. Triplicate experiments at 10 μ M confirmed 152 of these hits as worthy of further investigation. Following 11-point dilution series, the seven series of new LRA candidates were chosen for deeper analysis in this thesis, with an additional 2 compounds being prepared as the result of medicinal chemistry advancement within series E. The nine compounds were tested in the FlipInFM and FlipIn.RV models, then subsequently in the J.Lat10.6FM and J.Lat6.3FM models. To detect any compound toxicity, MTS assays were performed on cell line and primary resting memory CD4+ T cells following drug treatment.

Collaborators at the WEHI performed BRD4 bromodomain inhibition alpha screen and found five of the seven chemical series acted as bromodomain inhibitors. These include:

Table 5.3: Novel series targeting BRD4.

Core drug name	DP number	Series
Triazolopyridazine	2	B
Oxindole	3	C
Diadapine	4	A
Imidazopyrazole	5	G
Quinazoline	7	D

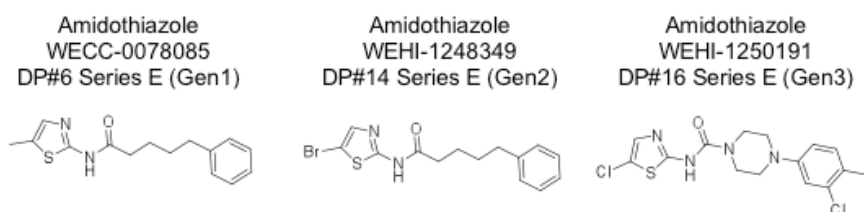
The remaining two series (Series E, Amidothiazole and Series F, Amidopyridine) did not bind to BRD4, and their mechanism of action remains unknown.

In the FlipIn.FM cell line, the nine novel LRAs performed in a similar manner, producing dose-dependent responses, specifically favoring LTR-driven activation over CMV-driven activation. When comparing the ratio of LTR/CMV induction, the nine novel LRAs performed in a highly specific manner reminiscent of the bromodomain inhibitor JQ1 (+). This does not come as a surprise, as five of the nine series were also shown to be bromodomain inhibitors, and, as the FlipIn cell lines constitutively express a low level of Tat protein through the *tal*IRES, P-TEFb activators would be expected to perform well. Similar results were seen in the counter screen FlipIn.RV cell line, however the notable non-specific activation was detected. This is curious, as the CMV-driven off target reporters are in identical locations in the FM and RV cell lines due to the directional FlipIn integration event.

Curiously, while in the FlipIn.FM cells, all of the nine compounds showed dose dependent curves in their LTR-driven reporter. The same held true in the FlipIn.RV cell line with the exception of DP#4, which showed a plateau effect reminiscent of that of JQ1 (+), as seen in Figure 4.6. Additionally, DP#4 belongs to the same chemical family as JQ1 (+) (the Diazepines). Work carried out by others in the Purcell lab has shown that JQ1 (+) may be able to affect HIV-1 splicing (Khoury et al, 2018) which, in this particular cell line, may lead to the spliceosome being directed to a cryptic splice acceptor site that has been identified within the CBG gene. Treatment of this cell line would with Diazepine compounds (JQ1 (+) and DP#4) therefore result in a mRNA that cannot produce CBG luciferase, leading to the unusual plateau curve shape observed. Notable, this splice

acceptor is not present in the Click Beetle Red gene, and as a result, the same phenomenon is not seen in the FlipIn.FM cells with either JQ1 (+) or DP#4.

Medicinal chemistry within Series E, progressing DP#6 as a first-generation compound to DP#14 (Gen2) and subsequently DP#16 (Gen3) resulted in increased potency. Their EC₅₀ values (LTR response in FlipIn.FM cells) are 16.2μM, 4μM and 140nM respectively. Interestingly, the jump from Gen2 to Gen3, which involved the addition of a piperazine ring motif within the structure, introduced new off-target effects as well as toxicity above 1.25μM. Advice from our collaborators in the WEHI chemistry team advised that such a modification may have introduced enough difference to be considered an entirely new class, which will likely now have other targets within the cell. Studies to determine if Gen3 is still within Series E, as well as if they still share a common mechanism of action (MOA) are underway.



As with the known LRAs in Chapter 4, testing the new LRA hits and analogues in the J.Lat10.6FM clone closely resembled the FlipIn models, whereas the J.Lat6.3FM clone proved vastly different. As with the known LRAs, the heterogeneous CMV-driven off-target population of the J.Lats proved superior in detecting off target reactivation than the clonal FlipIn models. These series include DP#2 (Series B), DP#3 (Series C), DP#4 (Series A) and DP#8 (Series F). As with the three bromodomain inhibitors tested in Chapter 4, the novel LRAs struggled to induce LTR-driven gene expression from the J.Lat6.3FM clone. This was also true for the two hit series that were shown not to target BRD4 (Series E and F). These results further confirm that P-TEFb activation by BDis alone is unable to reactivate the 6.3 clone, demonstrating that single LRA therapy is unlikely to address a sufficiently large proportion of the latent reservoir within patients to activate all the provirus capable of initiating emergence of replication competent virus..

Cell line toxicity assays showed toxicity at 20μM when treated for 48hrs with DP#2, DP#3 DP#4 and DP#8. Additionally, DP#16 was toxic above 300nM. Interestingly, these

results are in contrast to those seen in gene expression assays (FlipIn luciferase and J.Lat fluorescence). A recurring trend was that, in the MTS assays, where the bulk metabolism was shown to drop away, the gene expression profiles were peaking at the same concentrations. Finally, in primary resting memory CD4+ T cell toxicity assays, the novel compounds proved non-toxic across the concentration window used. The exception to this were DP#2 which introduced toxicity at 10 μ M and above, DP#8 which proved very toxic at 20 μ M (100% loss of metabolism) and DP#16, which was highly toxic above 200nM.

Taken together, the results of Chapter 5 show encouraging results for the FlipIn dual reporter system serving as a useful platform for detecting novel HIV-1 specific LRAs. While five of the seven novel series of LRAs discovered were shown to be BDi compounds, and therefore already studied as potential LRAs (eg JQ1 (+)), the two remaining series (E and F), which have unknown MOAs continue to be of great interest in our work towards a HIV-1 cure.

Chapter 6 Synergistic reactivation of HIV-1 gene expression using known and novel Latency Reversing Agents

6.1 Aim.

We aimed here to use the same dual reporter cell lines that model HIV-1 latency *in vitro* to test combinations of known and newly screened Latency Reversing Agents and discover synergistic combinations that reactivate HIV-1 from latency both potently and specifically.

6.2 Introduction.

In recent years, attention has turned to the discovery of combinations of mechanistically different LRAs that could cooperate in synergistic partnerships to reactivate viral gene expression greater than what is currently capable with single agent therapies. The idea of using multiple LRAs results from evidence that, while some single LRAs have proved capable of inducing viral RNA transcription, and others are able to induce viral protein expression or extracellular RNA (virions) (Wei, Chiang et al. 2014), a therapy that significantly reduces the level of HIV-1 DNA (i.e. the latent reservoir) remains elusive. The use of multiple LRAs, which each target different restrictions on HIV-1 gene expression, is hoped will deliver a more effective “shock” to the latent reservoir, resulting in more efficient HIV-1 gene expression and clearance of the HIV-1 reservoir.

The hypothetical advantages to using a synergistic combination are two-fold. Firstly, as mentioned, by targeting a number of the distinct molecular mechanisms of HIV-1 latency, we may achieve greater reactivation within a latently infected cell. Moreover, by using multiple LRAs, we are also more likely to achieve reactivation in a greater proportion of the latent reservoir, as each latent provirus likely has different mechanisms suppressing them. Secondly, the idea of a synergistic combination (not simply an additive combination) is to produce a combined effect greater than the sum of their separate effects, i.e. $1 + 1 > 2$. Due to the interconnectedness of many of these molecular pathways, a synergistic combination may in turn allow for using lower doses, or less frequent doses of the individual drugs, potentially minimizing adverse side effects. For a hypothetical example, the use of a transcription factor activator like Prostratin alone, which like Bryostatin-1

activates PKC, may not readily allow for NF- κ B binding at the LTR, due to the maintenance of restrictive chromatin. With high enough dose of Prostratin, some success might be achievable, but likewise the dose required may reach unacceptable toxicity levels for *in vivo* trials. Combined with a HDAC inhibitor, however, which would alleviate the restrictive heterochromatin, NF- κ B could access the binding sites within the LTR, achieving reactivation of viral gene expression. Moreover, a lower dose of Prostratin would be required to achieve this reactivation, potentially avoiding unwanted side effects. There is growing evidence for similar approaches having merit in the HIV-1 cure field. One example from Reuse *et al.* 2009 showed that combining Prostratin and HDACis demonstrated synergy at reactivating HIV-1 gene expression (Reuse, Calao et al. 2009). Darcis *et al.* showed in 2015 that the bromodomain inhibitor JQ1 (+) synergises well with PKC activator Bryostatin-1 and Ingenol-3-angelate PEP005 (Darcis, Kula et al. 2015). Also in 2015, Jiang *et al.* also showed synergy between JQ1 (+) and PEP005 (Jiang, Mendes et al. 2015). Finally Laird *et al.* showed in 2015 that Bryostatin-1 synergised well with JQ1 (+) and the HDACis Vorinostat, Panobinostat, and Romidepsin, heavily influencing the approach adopted for this chapter (Laird, Bullen et al. 2015). While there are no guarantees that the compound synergy approach will prove effective at eradicating the latent reservoir, combinational therapy seems like the next logical step on the path to a therapeutic approach for an HIV-1 cure.

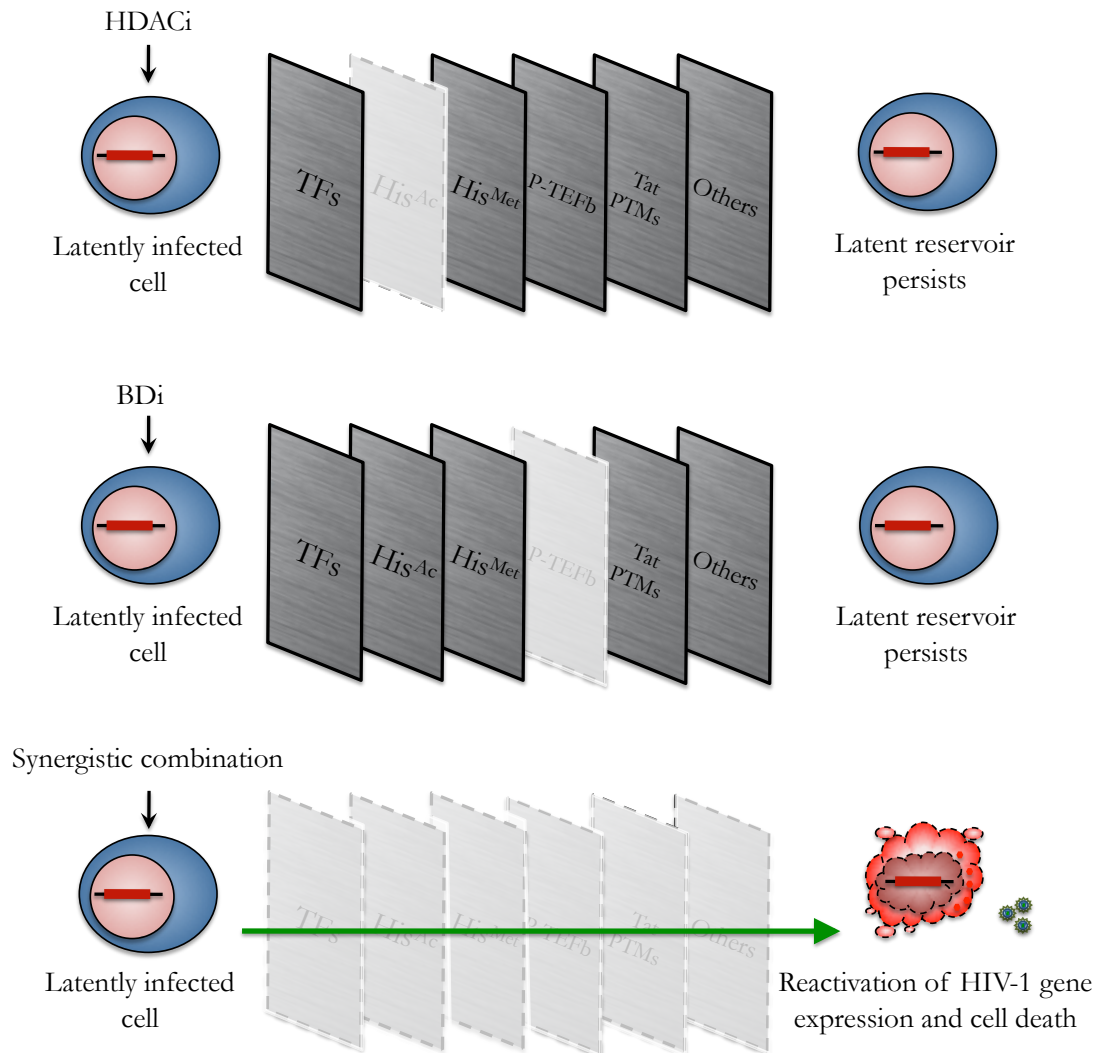


Figure 6.1 (Figure 1.18): Multiple diverse restrictions may prevent reactivation of HIV-1 gene expression within a latently infected cell. While a complete understanding of the some diverse “barriers” silencing HIV-1 gene expression in the context of post integration latency remains unclear, several of the contributing factors have now been well characterized. Despite this, and several clinical trials however, it has become apparent that the entire latent reservoir cannot be addressed using a monotherapy, or a therapy targeting just one of these mechanisms silencing HIV-1 gene expression. It is becoming increasingly clear that a multi-pronged approach, targeting several of the silencing mechanisms simultaneously, will be necessary. This figure includes the 5 different mechanisms addressed in this thesis: Activation of the cellular transcription factors, acetylation and methylation modifications of histone proteins, the availability of P-TEFb for HIV-1 transcription as well as post translational modifications of Tat protein. “Others” includes mechanisms that remain uncharacterized.

In the field of biochemistry, there exists a range of different models of varying complexity to measure possible synergy between combinations of drugs and compounds. The field of HIV-1 latency has widely accepted the Bliss Independence (BI) model, due to its simplicity, relevance in *in vitro* and *ex vivo* models and ease of use in cell-based experiments where strict sigmoidal drug-like curves may not always be achieved. For this calculation, each drug is tested independently as well as in combination alongside a necessary negative control (typically unstimulated cells) and a strong positive control (eg PMA-ionomycin or α CD3/ α CD28). The experimental values obtained are normalized to the negative and positive controls (set to 0 and 1 respectively) to give a set of decimal values, which can then be used in the calculations seen in Figure 6.2.

F_X	= Fraction affected by drug X
F_Y	= Fraction affected by drug Y
$F_{P(XY)}$	= Predicted fraction affected by combination X+Y
$F_{O(XY)}$	= Observed fraction affected by combination X+Y
Drug X affects a fraction	F_X
Drug Y affects a fraction of the unaffected cells	$F_Y*(1-F_X)$
Predicted combination effect	$F_{P(XY)} = F_X + F_Y*(1 - F_X)$ $F_{P(XY)} = F_X + F_Y - (F_Y * F_X)$
Bliss Independence calculation	$\Delta F_{XY} = F_{O(XY)} - F_{P(XY)}$
	>0, synergy
	=0, additive (independent)
	<0, antagonistic

Figure 6.2: The Bliss Independence calculation of compound synergy. For the Bliss Independence calculation, the fraction of cells affected by each drug alone are used to predict the fraction that should be affected by the two drugs used in combination. This prediction is then subtracted from the experimental results observed with this combination, and if the result is greater than zero, the combination is said to be synergistic. If the result is equal to zero, the drugs act independently of each other, and if the result is less than 0, the drugs are antagonistic towards each other.

Table 6.1: Concentrations used for single drug and synergy experiments.

Drug Name	Drug Class	[Single] cell lines	[Synergy] cell lines	[Single] primary	[Synergy] primary
TNF α	NF- κ B activator	20ng/mL	0.3ng/mL	-	-
PMA	PKC activator	10nM	4nM	10nM	10nM
Bryostatin-1	PKC activator	800nM	400nM	800nM	800nM
Vorinostat	HDAC (pan) inhibitor	20 μ M	10 μ M	500nM	500nM
Panobinostat	HDAC (pan) inhibitor	800nM	400nM	30nM	30nM
Romidepsin	HDAC1/2 inhibitor	20nM	10nM	40nM	40nM
JQ1 (+)	BRD2/3/4 inhibitor	20 μ M	10 μ M	1 μ M	1 μ M
PFI-1	BRD2/4 inhibitor	20 μ M	10 μ M	-	-
LY-303511	BRD2/3/4 inhibitor	20 μ M	10 μ M	-	-
CCT-018159	Hsp90 inhibitor	20 μ M	10 μ M	-	-
DZNep	HMT inhibitor	20 μ M	10 μ M	5 μ M (not clinical)	5 μ M (not clinical)
UNC-0638	HMT inhibitor	20 μ M	5 μ M	-	-
BML-278	SIRT 1 activator	20 μ M	10 μ M	-	-
EX-527	SIRT 1 inhibitor	20 μ M	10 μ M	-	-
Rocilinostat	HDAC6 inhibitor	20 μ M	10 μ M	-	-
DP#2	BDR4/other?	20 μ M	10 μ M	-	-
DP#3	BDR4/other?	20 μ M	10 μ M	-	-
DP#4	BDR4/other?	20 μ M	10 μ M	-	-
DP#5	BDR4/other?	20 μ M	10 μ M	-	-
DP#7	BDR4/other?	20 μ M	10 μ M	-	-
DP#8	Unknown	20 μ M	10 μ M	5 μ M	5 μ M
DP#6	Unknown	20 μ M	10 μ M	5 μ M	5 μ M
DP#14	Unknown	20 μ M	10 μ M	5 μ M	5 μ M
DP#16	Unknown	20 μ M	2.5 μ M	100nM	100nM

For cell line single-point synergy experiments, where possible, a concentration was chosen for each known and novel LRA that corresponded to roughly 50% of the maximum induction seen in 8-point titration experiments (Chapters 4 & 5). The concentrations chosen for primary cell experiments from leukapheresis samples were chosen in collaboration with the Sharon Lewin/Paul Cameron laboratory, the suppliers of these valuable cells, to be in agreement with experiments run concurrently with their workgroup. These concentrations best represent the clinically or physiologically relevant concentrations used in various clinical trials, converted for use in these *ex vivo* studies. These concentrations were not significantly toxic in resting memory CD4+ T cells at the 72hr time point, as confirmed in Chapters 4 and 5. Importantly DP#2, DP#3, DP#4, DP#5 and DP#7 were all shown to target BRD4, with far lower potency than JQ1 (+), and therefore did not progress to leukapheresis experiments, whereas DP#6/#14/#16 and DP#8, which have unknown MOAs did progress. DP#14 and DP#8 were also used in combination with JQ1 (+) and DZNep.

6.3 Results.

6.3.1 Synergy in FlipIn cells.

6.3.1.1 Synergy in FlipIn.FM cells.

Having performed detailed studies on the panels of 15 known and 9 novel latency reversing agents (Chapter 4 and 5 respectively), gaining insights into their ability and limitations to reactivate HIV-1 gene expression as single drug “therapies”, their ability to act synergistically with each other was then of key interest. The rationale for these experiments was to ideally produce a greater level of induction than was possible with either drug alone, and potentially avoiding associated toxicity seen at higher concentrations in monotherapy experiments. Table 6.1 shows the (highest) concentrations used for single drug 8-point titration experiments outlined in Chapters 4 and 5, and the sub-maximal concentrations used in the single-point synergy experiments described here. As with Chapters 4 and 5, each of the four FlipIn and J.Lat cell lines were examined individually, first at the level of reactivation, graphed as fold over baseline or percentage positive of the LTR-driven response (CMV-driven responses have been omitted from these data), then by graphing the Bliss Independence scores, more clearly highlighting the synergistic pairs. Figure 6.3 describes the synergistic reactivation seen combining each of the fifteen known LRAs with the nine novel LRA hits and analogues in the FlipIn.FM cell line. For each graph, the dashed horizontal line represents the fold change seen with the each known LRA on its own, the non-striped columns show the effects of each novel DP compound alone and the striped columns show the effects of the novel compounds with the known LRA in question. OPTI refers to OPTI-MEM (drug free media), and a lack of a DP compound. A) TNF α alone at 0.3ng/mL produced a 4-fold change over baseline however performed well in combination with most of the novel compounds, the standouts being DP#2, and DP#8, producing 11-fold and 15-fold changes respectively. B) PMA at 4nM produced an impressive 24-fold change and, while showing no greater effect with any of the bromodomain targeting hit compounds DP#2-DP#7, showed a striking effect when combined with the compounds of unknown MOA, DP#6-DP#16 and DP#8, achieving changes of 42 to 53-fold. C) Interestingly, the other PKC activator, Bryostatin-1, which had only a minimal effect alone and with the bromodomain targeting compounds, reached an 18-fold change in combination with DP#8. The HDAC inhibitors, D) Vorinostat, E) Panobinostat and F) Romidepsin, which as single agents each produce ~4-fold changes

over baseline, showed only modest enhanced reactivation in the presence of DP#5, DP#6 and DP#8. These combinations were subsequently shown to be weakly synergistic (Figure 6.3). The known BDis: G) JQ1 (+), H) PFI-1 and I) LY-303511, all showed only an additive change in the presence of the novel DP compounds that were shown to be BDis (DP#2, DP#3, DP#4, DP#5 and DP#7). In contrast, known BDis synergized well with all members of Series E (DP#6/#14/#16) and Series F (DP#8), achieving induction between 20 to 30-fold for JQ1 (+) and PFI-1, and 10 to 15-fold for LY-303511. For simplicity, the seven novel series of LRAs can now be separated into two categories: the novel BDis (DP#2, DP#3, DP#4, DP#5 and DP#7) and the unknown MOA series (DP#6/14/16 and DP#8) Previous work in the Purcell lab (Leigh Harty honours thesis 2014) has shown a strong synergistic partnership between the BDi JQ1 (+) and the methyltransferase, DZNep. We likewise saw a synergistic relationship between the novel BDis with DZNep. K) Alone DZNep produced a potent 6-fold change alone, which was enhanced to an 11 to 25-fold increase in the presence of the various DP BDis. Additionally, induction with DZNep was also enhanced in the presence of the non-BDis most notably with the third generation Series E compound DP#16, producing a 31-fold change over baseline. These results strongly suggest compound synergy, which will be explored in detail in Figure 6.4. L) The other methyltransferase inhibitor used, UNC-0638, showed a different profile, showing minimal difference in the induction of LTR-driven expression in the presence of the BDi DP compounds. Again, however, the non BDi DP compounds of Series E and Series F enhanced the induction from 1.2-fold for UNC-0638 alone to as high as 13-fold with DP#8. The exception to this trend was with DP#16, although this is possibly due to toxicity issues of this combination. O) The HDAC6 inhibitor Rocilinostat showed no notable change in its 4-fold induction over baseline in the presence of the DP BDi compounds. In contrast, Rocilinostat was yet another known LRA to show an interesting response when combined with the non-BDi compounds, achieving between 11 to 15-fold induction in combination. J) CCT-018159, M) BML-278, N) EX-527 did not show any outstanding results when coupled with any of the novel LRAs.

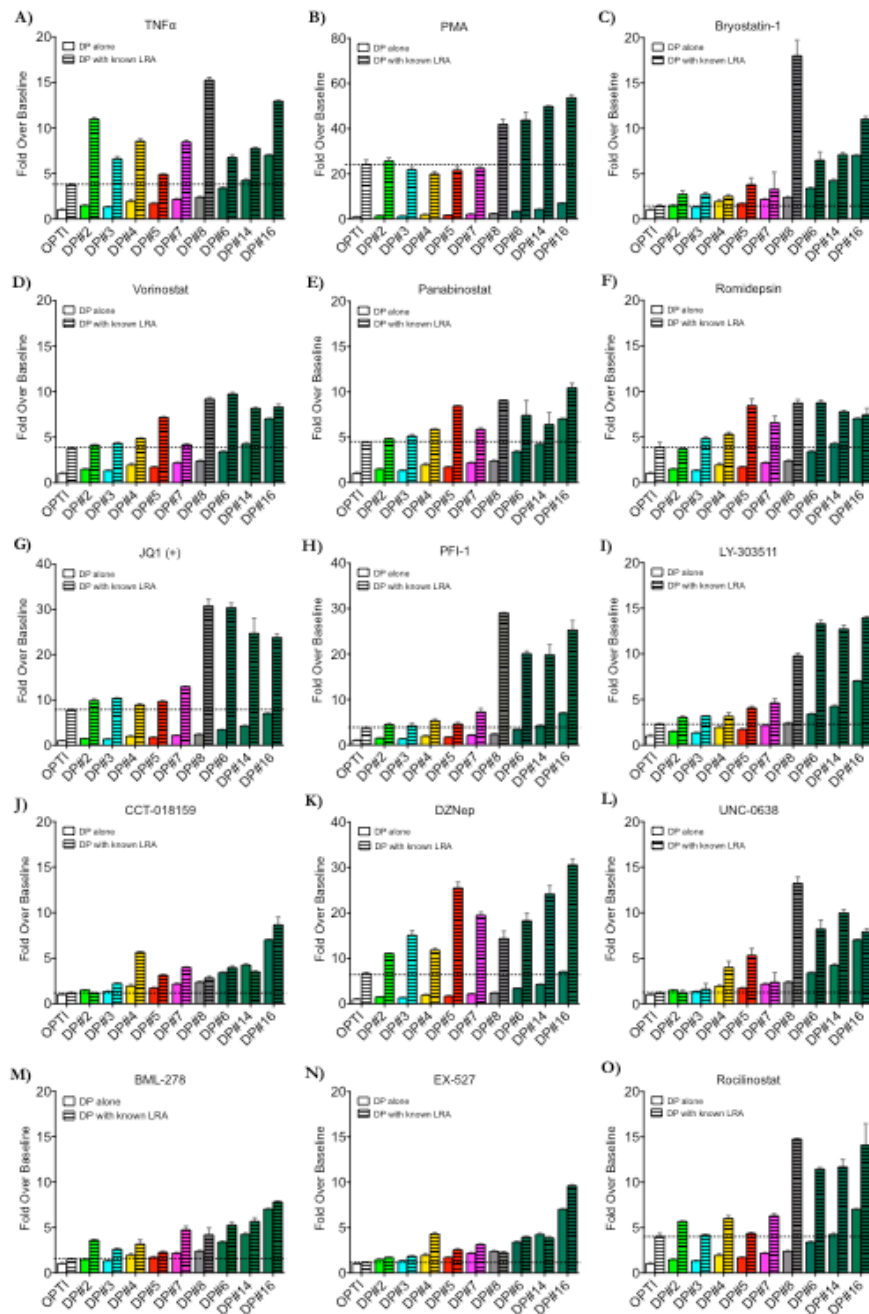


Figure 6.3: Induction of gene expression in FlipIn.FM cells using combinations of known and novel LRA. Treatment of FlipIn.FM dual reporter cell line with each of the 15 known LRAs in combination with all 9 of the novel DP compounds in single point. LTR induction was measured by Click Beetle Red luciferase at the 48hr time point. Induction is shown as fold change over the untreated cell baseline with the error bars representing standard deviation of n=3. Details of each panel is expanded in the text above.

6.3.1.2 Bliss Independence in FlipIn.FM cells.

While Figure 6.3 shows the induction of LTR-driven gene expression in the FlipIn.FM latency reporter cells seen with the known and novel LRAs both alone and side by side in combination, it can be difficult to discern true synergy from a simple additive effect (compound independence) in this format. To make this clearer, Figure 6.4 shows the extent of synergy, as calculated using the Bliss Independence formula found in Figure 6.2. Again, these Bliss Independence scores (BIS) do not show how much induction was achieved, but simply if the combined effect was synergistic (BIS>0), additive/independent (BIS=0) or antagonistic (BIS<0). A) In general, the NF- κ B activator TNF α synergised moderately with some DP compounds, with DP#8 being the most prominent, giving a BIS of +0.19. Members of Series E however, did not synergise well with TNF α . C) A similar profile was seen with the combinations involving the PKC activator Bryostatins-1, where again only DP#8 showed strong synergy, producing a BIS of +0.28. B) In contrast, the other PKC activator PMA showed high levels of synergy with the non-BDi DP compounds of Series E and Series F, synergising to give scores ranging from +0.31 to +0.48. The 5 series of bromodomain targeting DP compounds showed either independence (BIS=0) or possible antagonism (BIS<0), although the latter may be due to cell death from toxicity. The three HDAC inhibitors Vorinostat (D), Panobinostat (E) and Romidepsin (F) did not appear to synergise well with any of the DP compounds, showing an additive relationship where their BIS \approx 0, within +/- 0.1 of the 0 score, across the board. The known BDi drugs JQ1 (+) (G), PFI-1 (H) and LY-303511 (I), as expected, all showed an additive relationship with the mechanistically redundant BDi DP compounds, however they showed a moderate to strong synergistic relationship with the non-BDi DP compounds. JQ1 (+) synergised with members of Series E and F ranging from a moderate BIS of +0.20 with DP#16 to a strong BIS of +0.40 with DP#8. For PFI-1 again DP#8 of Series F produced the strongest synergy, giving a BIS of +0.45. Series E also performed strongly with BIS of \sim 0.26. For LY-303511, the synergy with the members of Series E and F was more modest, with scores ranging from +0.11 to +0.16. K) Methyltransferase inhibitor DZNep produced positive bliss independence scores with all of the novel DP compounds from both the BDi and non-BDi subsets. Within the novel BDi compound set, results ranged from modest levels in combination with DP#2 at +0.07 to a strong synergistic association level with DP#5 at +0.34. Within the non-BDi subset, members of Series E synergised well with DP#16 giving a BIS of +0.34.

In contrast to this, the methyltransferase inhibitor UNC-0638 (L) synergised with the non-BDi compounds but not with the bromodomain targeting DP compounds, which showed a general additive relationship, $BIS \approx 0$. As seen with several other combinations, DP#8 outperformed all other novel compounds, with a BIS of +0.2. O) In contrast the HDACi compounds mentioned above, which did not show a clear trend in terms of synergising with the novel DP compounds, Rocilinostat, the HDAC6 inhibitor synergised with the non-BDi compounds of Series E and Series F, again with Series F being the strongest of these with a BIS of +0.18. Rocilinostat did not however synergise with the bromodomain targeting novel compounds. Finally only additive relationships, where $BIS \approx 0$ were seen when combining any of the DP compounds with either of the known LRAs CCT-018159 (J), EX-527 (M) or BML-278 (N), not surprising perhaps when reviewing their lack of activity as single drug agents shown in Figure 4.3. Taken together, these data show a trend towards synergy between the non-BDi compounds of Series E (DP#6/14/16) and Series F (DP#8) with the known LRAs of the bromodomain inhibitor, methyltransferase inhibitor and HDAC6 inhibitor classes. Novel DP compounds that target bromodomain containing proteins (DP#2, DP#3, DP34, DP#5 and DP#7) only synergized with DZNep, and were simply additive with all other known LRAs.

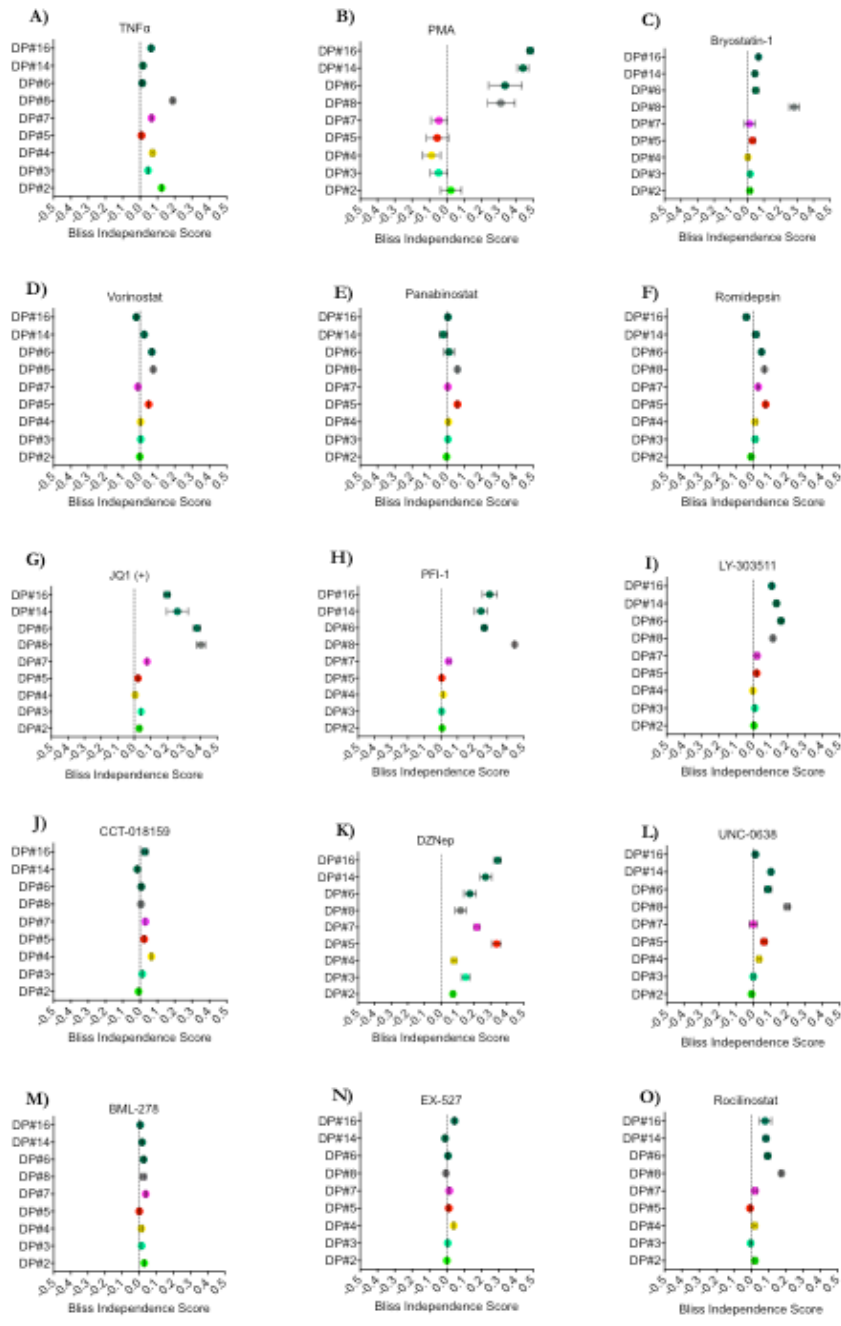


Figure 6.4: Bliss Independence scores seen in the FlipIn.FM cells using combinations of known and novel LRA. Synergy seen following treatment of the FlipIn.FM dual reporter cell line measured using the Bliss Independence (BI) calculation. BI scores on the x-axis show synergy for positive values, independence for $x=0$ and antagonism for negative values. These calculations are performed from induction seen in Figure 6.3, with the error bars representing standard deviation of $n=3$. Details of each panel is expanded in the text above.

6.3.1.3 Synergy in FlipIn.RV cells.

Repeating the same synergy experiments using sub-optimal concentrations in the FlipIn.RV cell line, Figure 6.5 follows the same format where the dashed horizontal line represents the fold change seen with the known LRA alone, the non-striped columns show the effects of each novel DP compound alone and the striped columns show the effects of the novel DP compounds in combination with the known LRA. A) TNF α alone at 0.3ng/mL produced a 4-fold change over baseline however was shown to perform well in combination several of the novel DP compounds, as with the original cell line, the best of these being DP#8, producing a 15-fold change over baseline. B) PMA again performed well as a single agent at 4nM producing a 22-fold change. As with the original cell line, the bromodomain targeting DP compounds, DP#2-DP#7, failed to notably enhance the induction of LTR-driven gene expression whereas when combined with the non-BDi DP compounds, strong synergy was seen, with fold changes reaching 38-fold to 53-fold. C) DP#8 again performed the strongest as a synergy partner with the other PKC activator Bryostatin-1 at 400nM, with a 10-fold change seen with Bryostatin-1 producing a 2-fold change alone. In a data set closely resembling those of the original cell line, coupling the three HDAC inhibitors, D) Vorinostat at 10 μ M, E) Panobinostat at 400nM and F) Romidepsin at 10nM, with the novel DP compounds showed no obvious trends, which was made clear in Figure 6.6 below. Alone the HDACi compounds induced 6-fold, 6-fold and 8-fold changes respectively. At 10 μ M each, the bromodomain inhibitors G) JQ1 (+), H) PFI-1 and I) LY-303511, again did not synergize with the bromodomain inhibiting DP compounds, whereas strong synergy was again seen with all of the non-BDi DP compounds. Alone, JQ1 (+) induced a 4-fold change over baseline, whereas with DP#16, that level was pushed up to 19-fold, with DP#16 producing a 7-fold change alone. With PFI-1, 12-fold to 14-fold changes were seen in combination with the members of Series E and Series F, while alone PFI-1 managed only a 3-fold change. Giving further evidence for this trend was LY-303511, which alone gave a 2-fold change over baseline synergized with DP#16 to give a 16-fold change. K) Methyltransferase inhibitor DZNep appeared to be the most versatile in terms of synergizing with the DP compounds. Not only did DZNep alone at 10 μ M induced a 7-fold change, impressive as a single drug, but it synergized with all DP compounds reaching levels of 25-fold over baseline with DP#2, a bromodomain targeting compounds and 30-fold with DP#16, which has an unknown MOA. L) Results with UNC-0638 did not however reflect those seen in the FlipIn.FM cell line. Where some synergy was seen with members of Series E in the original cell line, no such relationship

appeared evident here, where only an additive result was seen in general. Of note, there may have been some toxicity issues with these experiments, where UNC-0638 shows a reduction in induction when coupled with DP#2, DP#4, DP#7 and DP#6. O) The HDAC6 inhibitor Rocilinostat at 10 μ M showed only additive relationships with the bromodomain targeting DP compounds, and again appeared to synergize with the non-BDi compounds, the best of which was DP#8, giving a 17-fold change and DP#16, giving a 19-fold change over baseline. J) CCT-018159, M) BML-278, N) EX-527 did not show any outstanding results when coupled with any of the novel LRAs.

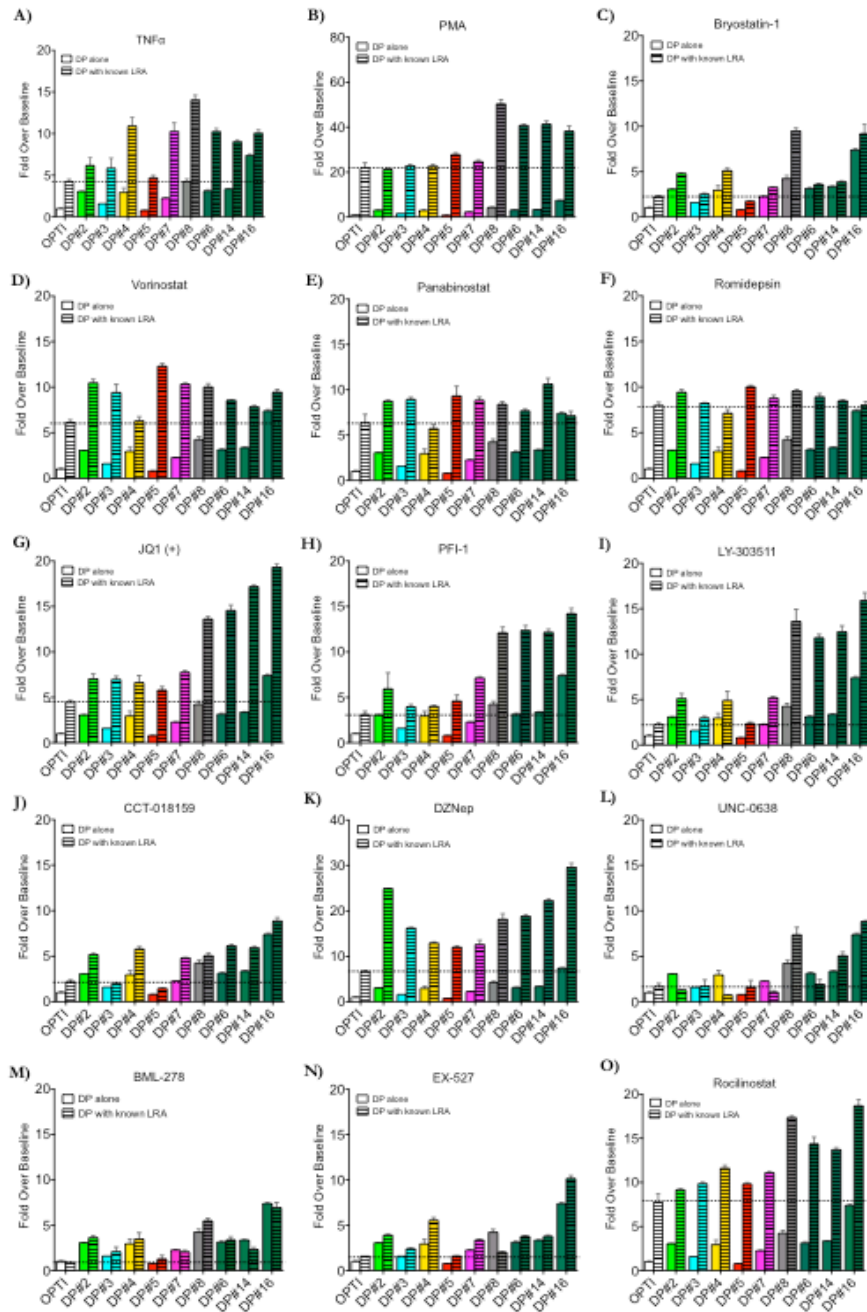


Figure 6.5: Induction of gene expression in FlipIn.RV cells using combinations of known and novel LRA. Treatment of FlipIn.RV dual reporter cell line with each of the 15 known LRAs in combination with all 9 of the novel DP compounds in single point. LTR induction was measured by Click Beetle Green luciferase at the 48hr time point. Induction is shown as fold change over the untreated cell baseline with the error bars representing standard deviation of n=3. Details of each panel is expanded in the text above.

6.3.1.2 Bliss Independence in FlipIn.RV cells.

Figure 6.6 shows the degree of synergy correlating to the LTR-driven induction seen in the dye-swapped FlipIn.RV latency reporter cells, as plotted in Figure 6.5. Many of the results here closely mirror the trends seen in the original FlipIn.FM cell line, although to a slightly lesser extent. The difference again is likely due to the different integration sites of the reporter proviruses within the two cell lines. A) Perhaps the least consistent of all the known LRAs across the two cell lines was TNF α , which showed a general positive association (synergy) with the majority of DP compounds here, however DP#8 again gave the highest positive value of +0.13. C) As with the original cell line, the PKC activator Bryostatin-1 again synergised with DP#8, but to a lesser extent, giving a BIS of +0.08. B) PMA again performed very well in terms of synergising with the non-BDi compounds, with scores ranging from +0.23 with DP#16 to +0.47 with DP#8. The bromodomain targeting DP compounds, however, did not synergise strongly with PMA, rather showing additive interactions. Again, the 5 series of bromodomain targeting DP compounds showed independence (BIS=0), with the possible exception of DP#5, giving a result of +0.11. Combining the novel compounds with the panel of HDAC inhibitors Vorinostat (D), Panobinostat (E) and Romidepsin (F) produced results ranging between -0.10 (possibly due to toxicity) to +0.12 (weakly synergistic), however no clear trends between the three known drugs were seen. JQ1 (+), PFI-1 and LY-303511 results seen in graphs (G), (H) and (I) all neatly replicated their counterparts in the FlipIn.FM cell line, with the non-BDi compounds synergising strongly with JQ1 (+) and PFI-1 and to a lesser extent with LY-303511. The BDi compounds were shown to be only additive in the effect measured with the other known LRAs. JQ1 (+) most strongly synergised with DP#14 of Series E with a BIS of +0.19. Methyltransferase inhibitor DZNep (K) again proved to be the most active in its ability to synergise with other compounds, both from the BDi and non-BDi subsets, producing BIS spanning +0.08 (DP#4, DP#5 and DP#7) to +0.32 (DP#16). UNC-0638 (L) generally showed only an additive response, with a set of results spanning +/- 0.05. In contrast to the result seen with DP#8 and UNC-0638, which suggested a synergistic relationship, the FlipIn.RV cell lines did not corroborate this, with a BIS of +0.05. O) Rocilinostat also similar results in the FlipIn.RV cell line as was seen in the FlipIn.FM, with the non-BDi compounds synergising. The strongest pairing was again with DP#8 at a BIS of +0.13. Again, only additive relationships, where BIS \approx 0 were seen when combining any of the DP compounds with either of the known LRAs CCT-018159

(J), EX-527 (M) or BML-278 (N). Taken together, these data are in general agreement with the replicate experiments performed using the original cell line model.

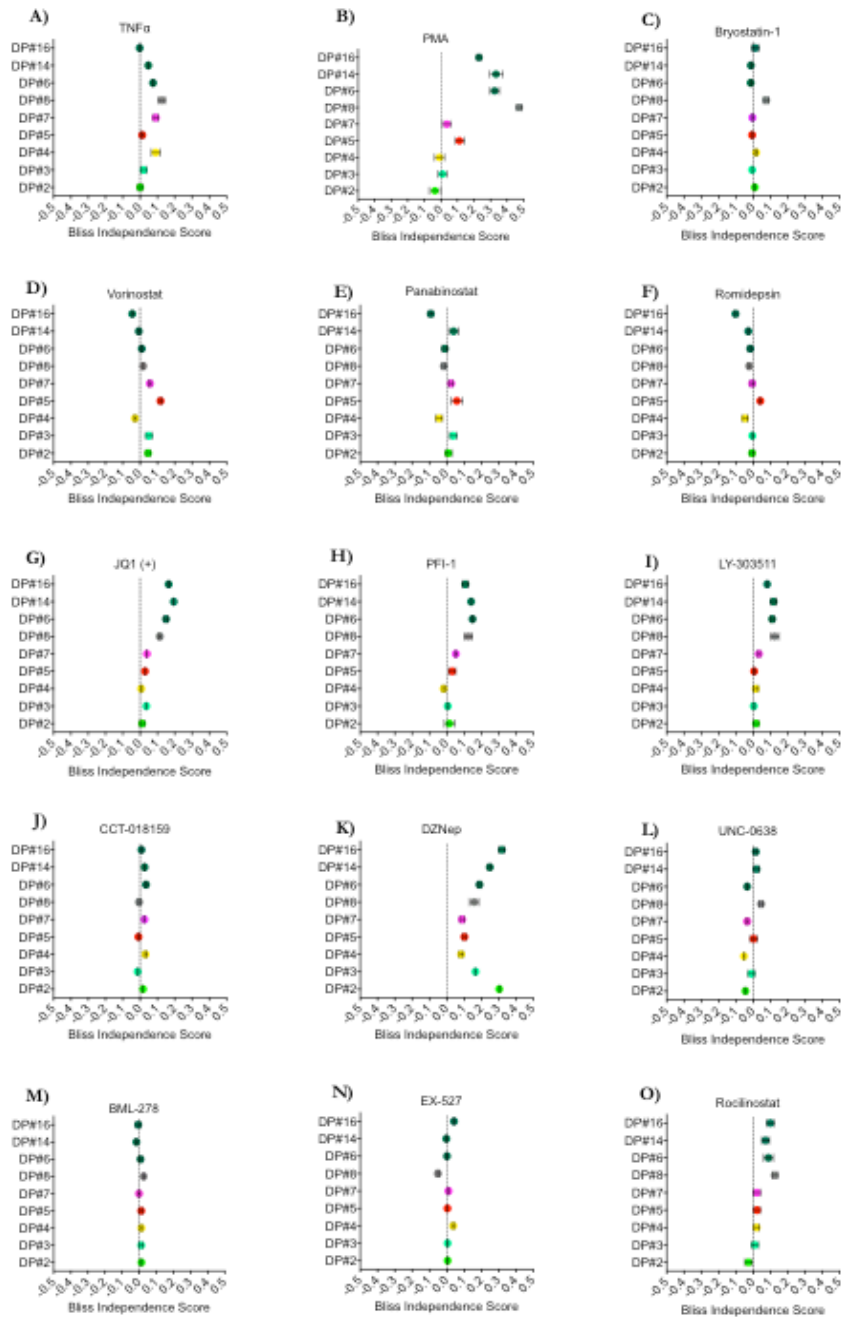


Figure 6.6: Bliss Independence scores seen in the FlipIn.RV cells using combinations of known and novel LRA. Synergy seen following treatment of the FlipIn.RV dual reporter cell line measured using the Bliss Independence (BI) calculation. BI scores on the x-axis show synergy for positive values, independence for $x=0$ and antagonism for negative values. These calculations are performed from induction seen in Figure 6.5, with the error bars representing standard deviation of $n=3$. Details of each panel is expanded in the text above.

6.3.2 Synergy in J.Lat cells.

6.3.2.1 Synergy in J.Lat10.6FM cells.

With the initial synergy experiments completed in the HEK293 based FlipIn models of HIV-1 latency, it was possible to choose the known and novel hit compounds that performed the best in combination and abbreviate the shortlist further before progressing to the J.Lat cell lines and finally, the primary cell experiments. Due to their unknown MOA potentially being novel intellectual property and our great interest in developing new LRAs, including new leads with an ability to synergize strongly with known compounds from several diverse MOAs, members of Series E (DP#6/14/16) and Series F (DP#8) were chosen to progress into the J.Lats. Because the remaining five DP compounds (DP#2, DP#3, DP#4, DP#5 and DP#7), were all bromodomain targeting compounds, and in the FlipIn latency reporter cells they did not synergize with any known LRAs other than DZNep, these did not progress to the more labor-intensive assays. Despite PMA appearing to synergize with the DP compounds stronger than all of the other known LRAs, PMA is toxic *in vivo* and unsuitable for use in any HIV-1 cure regime in a clinical setting due to its induction of global cell activation and has more fittingly served as a positive control throughout this thesis. PMA therefore was not chosen to progress into the J.Lat models. Of the remaining known LRAs, the bromodomain inhibitor JQ1 synergized well with the non-BDi DP compounds, as did the methyltransferase inhibitor DZNep and the HDAC6 inhibitor Rocilinostat. These compounds had performed well and covered 3 distinct MOAs; bromodomain inhibition, methyltransferase inhibition and Tat post translational modifications. Therefore, these three available LRA compounds would make up the shortlist of the known compounds to move forward. As the bromodomain inhibitors showed the most promise as synergy partners, PFI-1 was also included in the hopes of confirming results seen with JQ1 (+). Figure 6.7 shows the induction of HIV-1 gene expression obtained when coupling these known and novel LRAs in the J.Lat10.6FM clone. A) JQ1 (+) alone induced GFP (HIV-1) expression in 23% of cells which was increased to 40% GFP+ with DP#8, 31% with DP#6, 37% with DP#14 and 30% with DP#16. Similar results were also seen in the PFI-1 (B) combinations, increasing the 21% GFP positive levels seen with PFI-1 alone to 49%, 32%, 41% and 31% GFP positive respectively. These results confirm those seen in the FlipIn models where the known BDi compounds synergize well with the non-BDi novel DP compounds. Also consistent with the FlipIn results were those with Rocilinostat (D),

which alone induced GFP expression in 12% of cells, while in combination with DP#8, DP#6, DP#14 and DP#16 induced 20%, 21%, 20% and 25% GFP positive respectively. Conversely, while DZNep performed very well in the FlipIn models, here in the J.Lat10.6 clone only additive, rather than synergistic responses were seen. Again it is possible that the decrease in the GFP positive population seen in the DZNep/DP#16 combination may have been due to toxicity with this

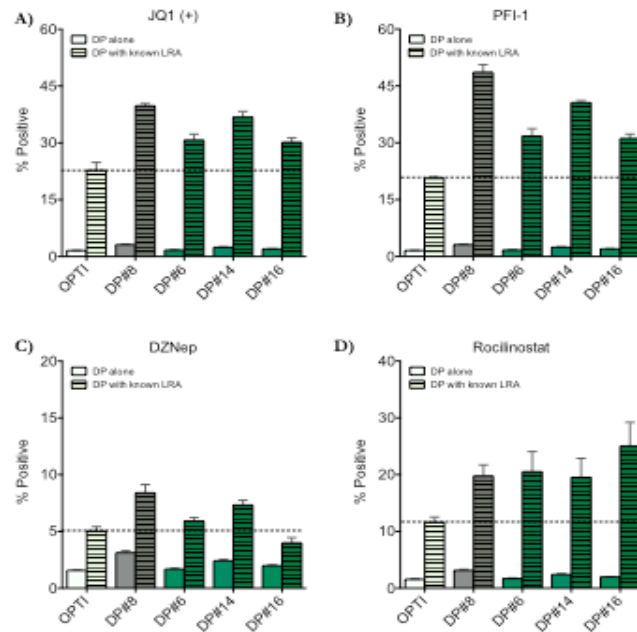


Figure 6.7: Induction of gene expression in J.Lat10.6FM cells using combinations of known and novel LRA. Treatment of J.Lat10.6FM dual reporter cell line with 4 of the known LRAs in combination with all four of the non-BDi novel DP compounds (at a single concentration each). LTR induction was measured by Green Fluorescent Protein expression at the 48hr time point. Induction is shown as percentage positive with the error bars representing standard deviation of n=3. Details of each panel is expanded in the text above.

6.3.2.2 Bliss Independence in J.Lat10.6FM cells.

To confirm that the relationships seen in the combinations tested in Figure 6.7 were indeed synergistic as claimed, it was necessary again to plot the Bliss Independence scores (BIS). A) For JQ1 (+) all the combinations tested were synergistic in this cell line, with BIS ranging from +0.08 with DP#16 to +0.19 with DP#8. These trends were indeed repeated almost identically with PFI-1 (B), where DP#8 proved the strongest partner, with a BIS of +0.31 and the members of Series E giving BIS ranging between +0.12 and +0.31. With Rocilinostat, again positive scores were obtained for all combinations, with DP#16 proving the strongest partner with a BIS of +0.15. In contrast to these results, and also the results seen with DZNep in the FlipIn cell lines, here DZNep did not show any synergy with the members of Series E or Series F, rather showing an additive relationship.

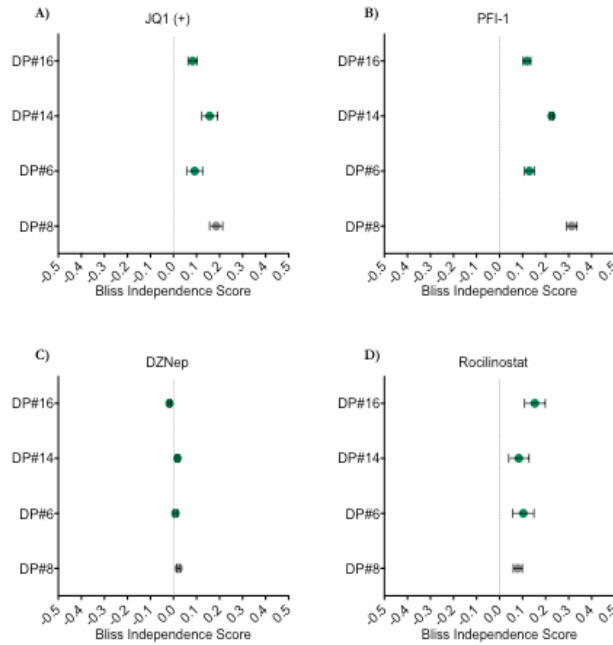


Figure 6.8: Bliss Independence scores seen in the J.Lat10.6FM cells using combinations of known and novel LRA. Synergy seen following treatment of the J.Lat10.6FM dual reporter cell line measured using the Bliss Independence (BI) calculation. BI scores on the x-axis show synergy for positive values, independence for $x=0$ and antagonism for negative values. These calculations are performed from induction seen in Figure 6.7, with the error bars representing standard deviation of $n=3$. Details of each panel is expanded in the text above.

6.3.2.3 Synergy in J.Lat6.3FM cells.

The J.Lat6.3 clone contains a deeply latent provirus that is very hard to induce into HIV-1 gene expression. This cell line had proved unresponsive to many single drug agents either known (Chapter 4) or novel (Chapter 5). In fact, the only drug classes that were shown to induce GFP (HIV-1) expression in this clone were the HDACi as well as the positive control compounds PMA and TNF α . Both of these classes did not progress to the J.Lat synergy experiments due either to a lack of synergy in the FlipIn models, for the HDACi compounds, or not being able to advance to primary cells due to induction of global cell activations (PMA and TNF α). While none of JQ1 (+), PFI-1, DZNep or any of the four novel DP compounds of Series E or Series F were able to induce GFP expression in the J.Lat6.3 clone as single agents, the principle of synergy experiments is that, by targeting multiple distinct restrictions on HIV-1 gene expression with drugs of different MOAs, viral gene expression may yet be achieved. Unfortunately, Figure 6.9 shows that this was not obtained with the combinations mentioned above. All combinations involving JQ1 (+) (A), PFI-1 (B) or DZNep (C) showed no induction of HIV-1 gene expression whatsoever. To add to these underwhelming results, combining any of the DP compounds with Rocilinostat (D), which induced GFP expression in 5% of cells, actually decreased the number of GFP positive cells, likely due to toxicity.

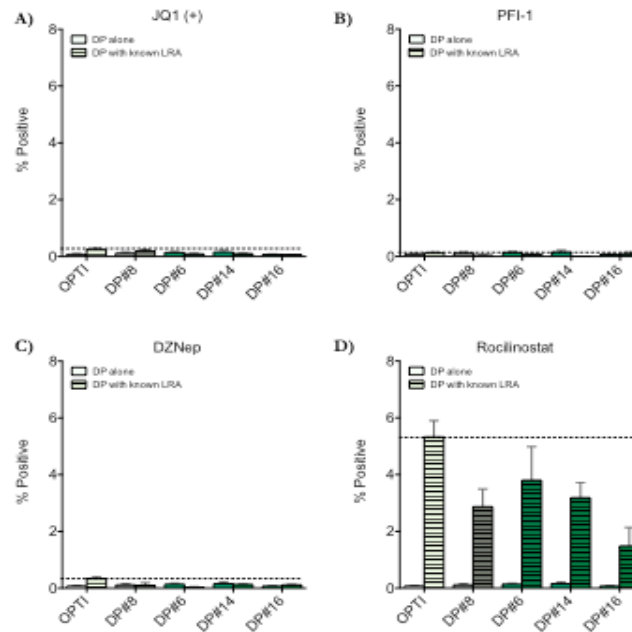


Figure 6.9: Induction of gene expression in J.Lat6.3FM cells using combinations of known and novel LRA. Treatment of J.Lat6.3FM dual reporter cell line with 4 of the known LRAs in combination with all 4 of the non-BDi novel DP compounds (at a single concentration each). LTR induction was measured by Green Fluorescent Protein expression at the 48hr time point. Induction is shown as percentage positive with the error bars representing standard deviation of n=3.

6.3.2.4 Bliss Independence in J.Lat6.3FM cells

As expected from the generally underwhelming results seen in Figure 6.9, combinations involving JQ1 (+) (A), PFI-1 (B) and DZNep (C) showed no synergy. Moreover, addition of DP compounds to Rocilinostat actually resulted in negative BIS, which may be due to true antagonism, although this has not been seen in either of the FlipIn models or the other J,Lat model tested, and may be due to enhanced drug toxicity from these combinations.

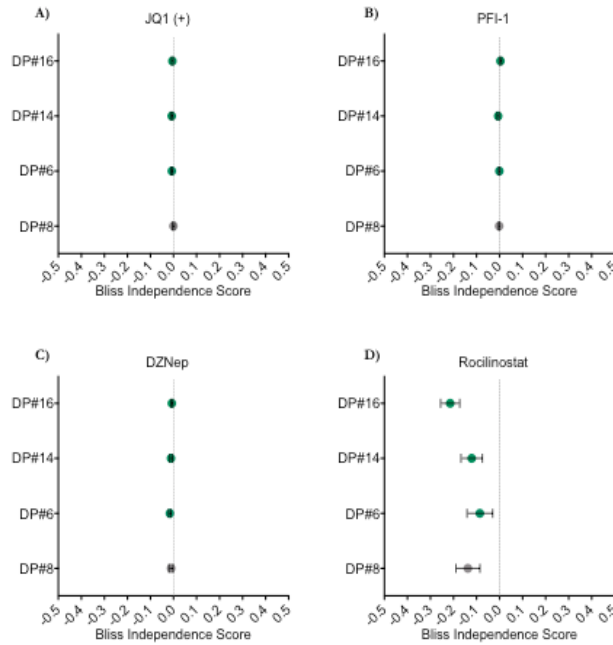


Figure 6.10: Bliss Independence scores seen in the J.Lat6.3FM cells using combinations of known and novel LRA Synergy measurements obtained following treatment of the J.Lat6.3FM dual reporter cell line measured using the Bliss Independence (BI) calculation. BI scores on the x-axis show synergy for positive values, independence for $x=0$ and antagonism for negative values. These calculations are performed from induction seen in Figure 6.9, with the error bars representing standard deviation of $n=3$.

6.3.3 Reactivation of leukapheresis derived primary CD4+ cells.

6.3.3.1 Viability of Leukapheresis cells 72hr post treatment.

Throughout this thesis, the focus has been on drug discovery using various cell line models of HIV-1 latency to identify and optimize interesting new chemical entities. While these cell lines have performed dutifully throughout this process, results in such artificial systems alone are not sufficient to build a strong case for potential drug leads. Primary cell experiments are therefore required and are the gold standard in terms of HIV-1 latency reversing agent discovery. For this reason, the capstone experiments of this thesis that previous chapters have built up to, utilize cells isolated through leukapheresis from HIV-1 positive patients undertaking successful combination antiretroviral therapy. These cells therefore provide the most authentic latent reservoir possible upon which to test the novel compounds that have progressed through the FlipIn and J.Lat cell line models. To compliment the MTS toxicity assays described in Chapters 4 and 5, live dead staining was performed at the harvest timepoint 72 hours after drug addition. Figure 6.11 shows the percentage of cells remaining alive, with intact cell membranes, within each population. Most notable was the reduction to 60% viability seen by treating with Romidepsin at 40nM and the reduction to 80% viability seen with Panobinostat at 30nM. These results are both in general agreement with those seen in the MTS assays performed in Chapter 4 using primary PBMCs. Interestingly, while treatment with 10nM PMA resulted in a near 300% increase in MTS readout (metabolism), the number of cells with intact cell membranes was shown here to actually decrease to 82%, suggesting that cells were activated to the point where some had died. DP#14 at 5 μ M showed a reduction to 90%, whereas Vorinostat (500nM), JQ1 (+) (1 μ M), DZNep (5 μ M), as well as DP#8 (5 μ M), DP#6 (5 μ M), and DP#16 (100nM) showed no decrease in viability. Combinations of JQ1 (+) and DZNep with DP#14 showed similar decreases to 86% viable, whereas combinations with DP#8 showed no decrease in viability.

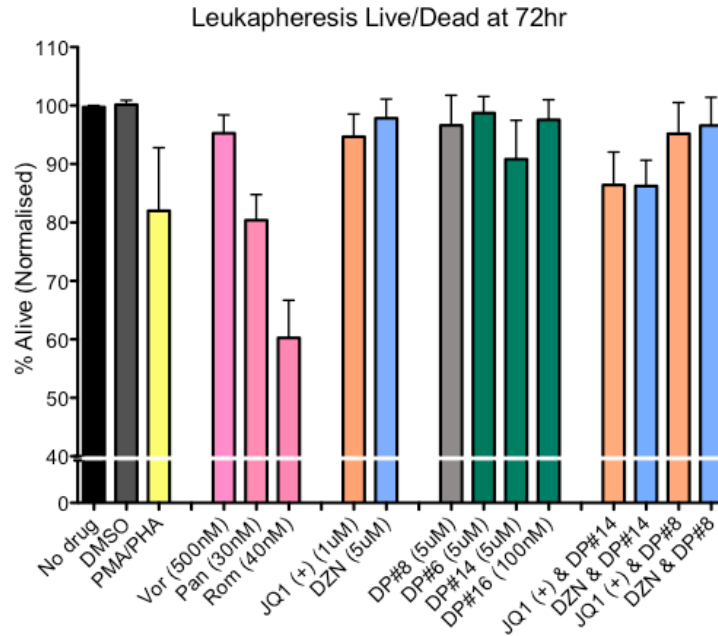


Figure 6.11: Viability of leukapheresis derived CD4+ T cells 72hrs post treatment using live/dead staining. Despite performing extensive toxicity studies on buffy coat-derived resting memory CD4+ T cells using the MTS assay in chapters 4 and 5, it was also prudent, considering the extremely valuable nature of the cells, to measure the proportion of live and dead cells 72hrs post treatment in the leukapheresis experiments. A small sample from each condition was set aside for live/dead staining, and analyzed by flow cytometry. The results were normalized to untreated cells with the error bars representing standard deviation of n=4 donors (the fifth donor could not be analyzed).

6.3.3.2 Single LRA reactivation of HIV-1 from leukapheresis samples.

After consulting the literature on LRAs that activate latent HIV-1 from primary cells, and from the data gained in the cell line models, a shortlist of well-known mechanistically diverse LRAs was assembled and used at their clinically or physiologically relevant concentrations. These drugs include: The transcription factor activator PMA, the HDAC inhibitors Vorinostat, Panobinostat and Romidepsin, the Bromodomain inhibitor JQ1 (+) and the histone methyltransferase DZNep (no clinical concentration). Alongside these in Figure 6.12 were the members of Series E, the Amidothiazoles (DP#6, #14 and #16) and Series F, the Amidopyridine (DP#8) our novel LRAs with currently unknown MOAs. The known LRAs all performed well, achieving statistically significant reactivation of HIV-1 RNA (unspliced), with the exception of DZNep. As expected, PMA achieved the highest level of reactivation, at 3.96-fold above the unstimulated baseline. The HDAC inhibitors Vorinostat, Panobinostat and Romidepsin all performed to a similar degree (although at different concentrations), achieving 2.50-fold, 2.56 and 2.95-fold respectively. Bromodomain inhibitor JQ1 (+) also performed relatively well, inducing a 2.22-fold change over baseline. DZNep failed to reactivate HIV-1 gene expression. Of the novel LRAs DP#8, DP#6, DP#14 produced induction of 1.74-fold, 1.84-fold and 1.76-fold over baseline, however only that of DP#6 was statistically significant. DP#16 also failed to induce viral gene expression, likely due to a dosing issue. Induction results in the J.Lats (Figure 5.8) and CD4+ primary toxicity data (Figure 5.11) made choosing a dose for DP#16 difficult. The p values shown were found using the Mann Whitney U test where n=5 donors.

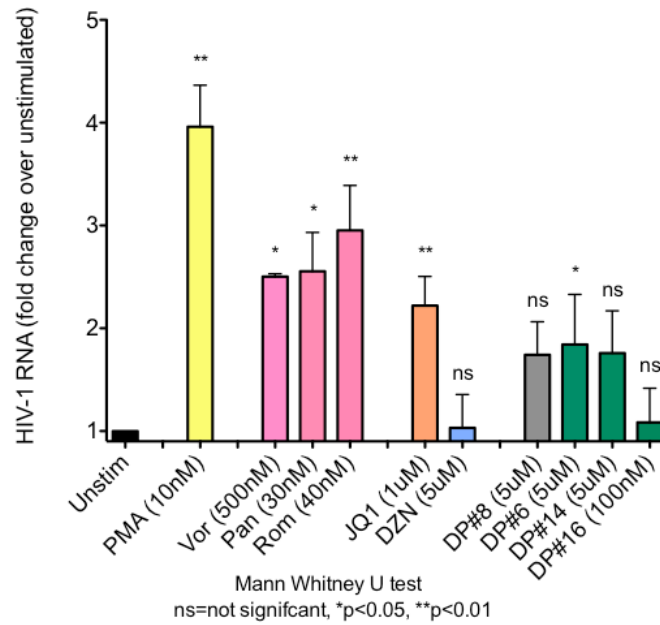


Figure 6.12: Induction of HIV-1 gene expression in leukapheresis samples using single LRAs. Resting memory CD4+ T cells isolated by leukapheresis from HIV+ donors on antiretroviral therapy were reactivated for 72hrs using single LRAs, and HIV-1 RNA detected through qPCR. Error bars represent standard deviation of n=5 donors. (*) indicates $p < 0.05$, (**) indicated $p < 0.01$ and ns indicated no statistical significance using the Mann Whitney U test when compared to the unstimulated control.

6.3.3.3 Synergistic reactivation of HIV-1 from leukapheresis samples.

Taking into account the very limited number of cells available for these leukapheresis studies, only 2 known LRAs (bromodomain inhibitor JQ1 (+) and histone methyltransferase inhibitor DZNep) could be paired with one representative of both of the novel LRA series (DP#8 and DP#14). These combinations were chosen based on their strong synergistic partnerships observed in the cell line models. Notable differences were evident between the cell line experiments and the leukapheresis experiments. While alone, DP#8 and DP#14 did not achieve statistical significance in their level of HIV reactivation from the unstimulated cells, but when combined with either JQ1 (+) or DZNep, statistical significance was achieved. For JQ1 (+) with DP#14, 3.33-fold induction was seen, whereas when JQ1 (+) was paired with DP#8 a 2.39-fold change was seen. Applying the Bliss independence calculation to these data, it was revealed that JQ1 (+) performed synergistically with DP#14, but not DP#8 in these experiments. Combination of DZNep with either DP#14 or DP#8 induced a 1.67-fold and 1.78-fold change in HIV-1 gene expression, however there was no synergistic effect. While these results are limited by only including 5 donors, they do show a trend towards synergy between JQ1 (+) and the Amidothiazole family. The p values shown were found using the Mann Whitney U test where n=5 donors.

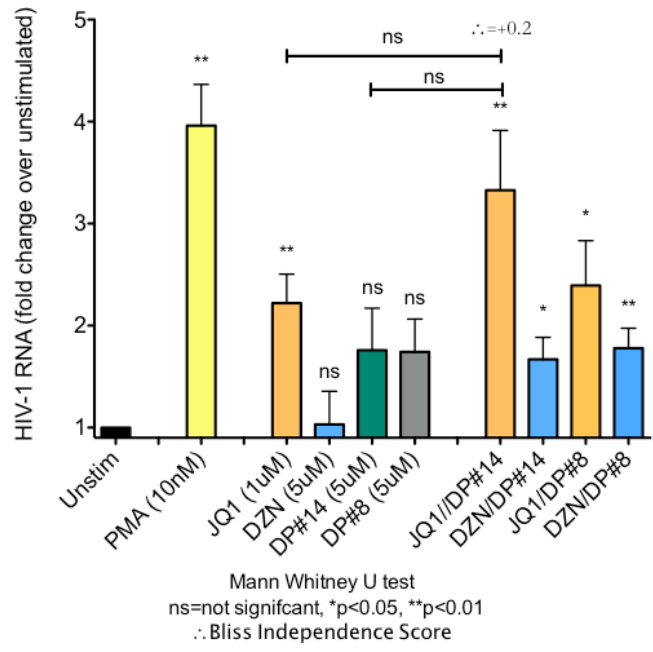


Figure 6.13: Synergistic induction of HIV-1 gene expression in leukapheresis samples. Resting memory CD4+ T cells isolated by leukapheresis from HIV+ donors on antiretroviral therapy were reactivated for 72hrs using single LRAs, and HIV-1 RNA detected through qPCR. Error bars represent standard deviation of n=5 donors. (*) indicates p<0.05, (**) indicated p<0.01 and ns indicated no statistical significance using the Mann Whitney U test when compared to the unstimulated control.

6.4 Discussion.

Following numerous studies in advanced HIV-1 latency models and in clinical trials, single latency reversing agent therapy has continually been shown to be insufficient at reducing the provirus pool of latently infected cells within patients on successful cART. Synergistic combinations, using mechanistically diverse latency reversing agents, offer an interesting area of study in the push towards a HIV-1 cure. HIV-1 latency is a highly complex problem, with the involvement of multiple molecular mechanisms, some of which are not yet fully understood. Appropriately, as more and more evidence comes to the fore, it is becoming clear that an equally multilayered solution will be necessary.

Recently, numerous studies have been published giving support to the synergistic LRA approach. These studies have included the use of Prostratin (PKC activator) with HDACis (Reuse, Calao et al. 2009), JQ1 (+) Bryostatin-1 and Ingenol-3-angelate PEP005 (Darcis, Kula et al. 2015, Jiang, Mendes et al. 2015) as well as Bryostatin-1 with HDACis (Laird, Bullen et al. 2015) to name a few. As time passes, we are sure to see less familiar drugs being used in synergistic combinations, which was the ultimate goal of this PhD project.

For calculating compound synergy, the field of HIV-1 latency research has adopted the Bliss Independence model, which serves this purpose well, providing appropriate controls are included in the experimental methodology. In this chapter, the fifteen known latency reversing agents from Chapter 4 were combined with the nine novel latency-reversing agents discovered in Chapter 5, again using the FlipIn and J.Lat models. Additionally, this project was lucky enough to be allocated leukapheresis samples from HIV positive patients on successful cART, a generous gift from collaborators in the Lewin laboratory (and the donors themselves).

In the FlipIn models, several trends emerged in terms of synergy. Importantly, the two LRAs being combined were not the only factors at play, the FlipIn models also express HIV-1 Tat protein at an artificial level, which biases the response in favor of drugs that interact with Tat (as intended from the onset). Members of Series E and F were shown to synergize well with the known bromodomain inhibitors. Conversely, the other five novel series (which were found to be bromodomain inhibitors themselves) did not synergise with the known bromodomain inhibitors, rather they showed additive relationships (where the BIS=0). These latter results seem highly intuitive, as the two drugs in each example will

share the same target (BRD4). Another interesting trend was the strong, and wide spread synergy that histone methyltransferase inhibitor DZNep had with all of the novel LRAs in the various cell line models. This synergy was also conserved for Series E and Series F with UNC-0638, although curiously not with the novel bromodomain inhibitor series. Another interesting trend that was conserved across both of the FlipIn models was the synergy seen in Series E and Series F with the HDAC6 inhibitor Rocilinostat. Rocilinostat may make Tat protein more active, by preventing removal of acetyl groups on Lysine 28, in support of enhancing the RNA pol II transcription complex for increased processivity through Tat posttranslational modification. Finally, none of the novel series of LRAs synergized with any of the conventional HDAC inhibitors.

To conclude the FlipIn synergy data, the novel series E and F synergized well with bromodomain inhibitors (which block BRD4, helping Tat to recruit P-TEFb), Rocilinostat (which keeps Tat in a highly processive acetylated form by blocking HDAC6) and DZNep (a histone methyltransferase inhibitor, involved in chromatin structure). It is possible that DZNep, which stops heterochromatin formation by blocking EZH2, also prevents the inhibitory methylation of Tat protein, possibly by EZH2 or other related methyltransferase enzymes. As the novel compounds of Series E and F synergize strongly with all of these classes, it may be that their unknown MOA is also involved in Tat processivity, as was sought from the onset of the project.

The bromodomain inhibitors JQ1 (+) and PFI-1, the methyltransferase inhibitor DZNep and the HDAC6 inhibitor Rocilinostat were advanced into the J.Lat models to assess potential for synergistic HIV activation with the novel LRA hits and analogues from Series E (DP#6, DP#14 and DP#16) as well as DP#8 of Series F. In the 10.6 clone, synergy was observed with the bromodomain inhibitors JQ1 (+) and PFI-1, as well as with the HDAC6 inhibitor Rocilinostat. Synergy was not seen, however with DZNep, which showed only an additive effect (BIS=0). Why combinations including DZNep proved to be non-synergistic is unclear, but may stem from a lack of basal levels of Tat protein in this model, relative to the FlipIn models where Tat is constitutively expressed. Several other J.Lat clones exist, as outlined by Jordan *et al.* (2003), so these combinations warrant testing in these clones in the near future. Interestingly, these combinations still failed to reactivate HIV-1 gene expression from the J.Lat6.3FM cells. As these combinations were all built around success in the Tat IRES-expression pathway and basal levels of Tat protein

itself, it seems apparent that the restrictions on the provirus within this clone are not Tat related. Data from Figure 4.4 showed that the HDAC inhibitors were able to reactivate this clone, so combinations involving at least one conventional HDACi should certainly be tested in the future. Interestingly, Rocilinostat, the HDAC6 inhibitor did achieve reactivation, however this was either antagonized by the presence of the novel LRAs or proved toxic, resulting in a BIS<0.

Finally, in the leukapheresis experiments PMA, Vorinostat, Panobinostat, Romidepsin and JQ1 (+) were all able to induce statistically significant bursts of HIV-1 unspliced RNA as single agents. Interestingly, DP#6 was also capable of inducing HIV-1 unspliced RNA expression, however the other members of Series E and F, as well as DZNep, were unable to induce statistically significant levels of HIV-1 RNA. JQ1 (+) was found to synergize with DP#14 in the leukapheresis experiments (BIS=+0.2) achieving a 3.33-fold increase in HIV-1 RNA expression over the unstimulated baseline ($p<0.01$). Alone JQ1 (+), DP#14 and PMA achieved 2.22-fold 1.76-fold 3.96-fold respectively. DZNep failed to synergize in the cells obtained through leukapheresis, as it had done in the J.Lats. While these leukapheresis experiments form the most important experiment included within this thesis, to the time of writing, only 5 donors assessed using 4 combinations and at one concentration. While these results are encouraging for the members of Series E, extensive work need to be further carried out to fully elucidate this novel class of latency reversing agents.

Chapter 7 General Discussion

7.1 Overall significance.

7.1.1 Overall significance.

Antiretroviral therapy has brought about a significant reduction in HIV-1 morbidity and mortality worldwide. For many HIV-1+ patients, HIV-1 is now a manageable chronic infection, and patients can expect a relatively high quality of life. Unfortunately, cART is incapable of curing these patients, due to the establishment of a reservoir of latently infected cells that can reseed infection if cART is interrupted, and cART is associated with secondary toxic effects that lower life expectancy. Additionally, providing necessary aid for an ever-growing global HIV-1 burden becomes increasingly costly with each year that passes. With no vaccine currently available, focused attention has turned to developing strategies for achieving a “functional cure” where HIV-1 could be controlled without the need for ongoing therapy.

Our understanding of the molecular mechanisms controlling HIV-1 latency has grown considerably. The availability of essential host transcription factors, HIV-1 Tat protein, and the chromatin landscape surrounding the integrated provirus are all now under investigation. Several FDA approved drugs which target these various molecular restrictions are currently undergoing clinical trials as potential HIV-1 LRAs. Re-appropriating drugs from the cancer therapeutic field has several drawbacks however, including toxicity and a lack of specificity for HIV-1 reactivation. Today, there is a lack of LRAs that specifically target HIV proviral gene expression, while avoiding unwanted global gene activation, resulting in many of the potential LRAs tested being deemed too toxic for clinical application for chronically manageable HIV infection.

7.2 Summary by chapter.

This ultimate goal of this thesis was to address the lack of HIV-1 specific LRAs, which potentially reactivate HIV-1 gene expression from latency, while avoiding non-specific activation.

Chapter 3:

In Chapter 3, HTCS platforms that can be used to identify highly specific HIV-1 LRAs were designed and generated. The FlipIn.FM and FlipIn.RV cell lines attempt to recapitulate HIV-1 latency by expressing a sub-activating low level of HIV-1 Tat protein through the *taI*RES pathway. The models also allow for high throughput screening of large compound libraries, without the need for PC3 biocontainment, by utilizing dual luciferase activity using a single substrate (ChromaGlo technology). Finally, the models allow for early exclusion of non-specific or toxic compounds which modulate the inbuilt non-specific reporter gene. The models also responded predictably to Tat plasmid and recombinant protein in a dose-dependent manner.

Chapter 4:

In Chapter 4, the FlipIn.FM and FlipIn.RV cell lines developed in Chapter 3 were further assessed for fidelity as HIV-1 latency models by assessing their response when treated with a panel of well-defined mechanistically diverse LRAs. The FlipIn.FM and FlipIn.RV cell lines were shown to perform in a highly consistent manner to each other and to the previously established J.Lat10.6 model of HIV-1 latency. FlipIn models ability to accurately map toxicity as seen in primary resting CD4⁺ T cells was questionable.

Chapter 5:

In Chapter 5, seven series of novel LRAs were discovered using the FlipIn.FM cell line to screen a library of ~114,000 compounds. These compounds were shown to specifically reactivate HIV-1 gene expression while avoiding off-target activation. Five of these seven series were found to target bromodomain containing proteins, and are therefore not of great interest from an intellectual property (IP) perspective. The remaining two series, however, have unknown mechanisms of action, and remain of great interest for the Purcell laboratory. The potency of series E was increased approximately 100-fold to EC₅₀=140nM (Gen3 DP#16)

Chapter 6:

In Chapter 6, the ability of the seven novel series of LRAs discovered in Chapter 5 was assessed for their ability to synergize with the known LRAs from Chapter 4. Of note was the synergy observed between series F and the three members of series E with known BDi LRAs. Synergy was seen across the FlipIn models, the J.Lat10.6 model and primary cells derived from HIV-1+ patients on cART. The ability to reactivate HIV-1 gene expression from primary (leukapheresis-derived) CD4+ T cells using the combination of JQ1 (+) and series E is a very encouraging result that may play a role in future HIV-1 cure regimes.

7.3 Discussion and future directions.

General LRA and HIV-1 cure future directions:

The transcription factor activators TNF α and PMA served as positive control compounds, rather than true LRAs, and are not suitable for use in HIV-1 cure regimes, due to the global cell activation that would occur. Bryostatins have shown promise in *ex vivo* experiments (Laird et al 2015), both as a single agent and in synergy with JQ1 (+) and various HDACis demonstrating that PKC activators may prove an important component in future LRA studies.

HDAC inhibitors, extensively studied in the HIV-1 cure field, with Romidepsin being shown to be capable of inducing viremia during cART (Winckelmann et al 2017). HDACis should, however, be used with caution due to their largely non-specific mechanism of action, which may lead to long term off-target gene activation. This may have detrimental effects for patients. To date, Vorinostat (Burnett et al 2010, Archin et al 2012), Panobinostat (Rasmussen et al 2013) and Romidepsin (Ying et al 2012) have all undergone various advanced trials. Due to their ability to reactivate a broad range of silenced provirus (evident in the J.Lat6.3 experiments above).

Methylation, of DNA and protein may also contribute to future HIV-1 cure regimes. It is the contention of this thesis however that preventing the inhibitory methylation of HIV-1 Tat protein should be prioritized if possible, to allow for a more specific regime. As with HDACis, indiscriminate modification of histone methylation may likewise result in undesired off target effects. An example of the benefits of targeting HIV-1 Tat protein

directly may be evident in the results seen with Rocilinostat, the HDAC6 inhibitor, which prevents the removal of activating K28^{Ac} modifications on Tat protein, resulting in effective HIV-1 reactivation in all 4 models tested here.

P-TEFb activators, in particular JQ1 (+), have proven to be a strong synergy partner with a range of different LRAs (Laird et al 2015). BDis also synergize with Tat protein itself, presenting a very attractive target for future therapies. Due to their activity in freeing cellular P-TEFb however, BDis like JQ1 (+) do show some off target effects (Banerjee et al 2012).

Finally, while this thesis is predominantly concerned with reactivation of HIV-1 gene expression and the “shock and kill” method, research into Tat inhibitors like Didehydro-Cortistatin A and the “block and lock” method are also of interest in the HIV-1 cure field (Kessing and Valente et al 2017; Mousseau and Valente et al 2015). In this approach, the provirus would be pushed into “deep latency” so that capacity for viral rebound, by stochastic activation of the host cell, is greatly reduced. While this is certainly an attractive scenario, it is not clear whether this will allow for long term remission, or whether adherence to cART and/or a Tat blocker would be mandated. In the opinion of the author, the strategy to eliminate, rather than suppress an infected cell remains more attractive.

Project specific future directions:

The FlipIn models of HIV-1 latency provide the HIV-1 cure field with a useful new tool in the detection of novel LRAs. A publication describing the generation of the cell line models is in preparation, as is a second and third publication describing the development of Series E. The WECC library of 114,000 compounds represents a relatively small compound library relative to the libraries of various large pharmaceutical companies, which house libraries containing millions of compounds. The FlipIn cell lines may therefore be used in the future in much larger drug screens allowing for collaboration with industry partners.

While this thesis did yield seven series of novel LRAs that activated HIV gene expression specifically, ie LTR induction but not CMV induction, the question remains as to whether these compounds act in a Tat-dependent or Tat-independent manner. To address this,

future studies involving the FlipIn model will include the generation of a third cell line, the FlipIn.OFF cell line which, like the FlipIn.FM line, contains the LTR-CBR reporter and the CMV-CBG reporter, but which lacks any *tat* gene. The FlipIn.OFF (Tat- cell line) would therefore act as a necessary control for distinguishing between Tat-dependent and Tat-independent LTR induction. Compounds found to be LTR-specific but Tat-independent may remain of interest, however our goal was to find compounds that synergized with the *tat*IRES pathway of Tat expression, and therefore would be LTR-specific and Tat-dependent.

The five novel LRAs discovered through HTCS which were subsequently shown to be BDis have little potential for further commercial development, as they lack the potency of BDis currently on the market and their MOA is not novel. The Purcell lab, with collaborators at the WEHI are in the process of preparing a manuscript describing the Quinazoline series (DP#7 of Series D). The Amidothiazole series (DP#6, DP#14 and DP#16 of series E) present a different scenario. Their novel, HIV-1 specific mechanism of action and synergy with known LRAs make this series of great interest to the Purcell lab. We are undergoing primary cell experiments using a larger number of donors and conditions to better understand Series E's potential as a synergistic LRA.

The protein target of Series E will also be investigated using CRISPR-Cas9 library screening technology. The FlipIn.FM cells will be transduced with a library of 100,000 unique sgRNA expressing lentivirus clones, and knockouts of the Series E target selected for using lethal doses of Series E members DP#14 and DP#19. The target will then be identified using NextGen sequencing technology and the most statistically significant knocked-out genes further assessed to determine the target of Series E.

7. Concluding remarks.

In conclusion, the failure of current LRA therapies to efficiently reactivate HIV-1 gene expression and significantly deplete the latent reservoir suggests that novel approaches are needed for a functional HIV-1 cure (Archin and Margolis 2012; Elliot and Lewin et al 2014; Rasmussen and Søgaard et al 2014; Søgaard and Tolstrup et al 2015). It is the contention of this thesis that unique pathways of viral gene expression may present exploitable targets in future shock and kill strategies. HIV-1 Tat protein, expressed through an IRES mechanism, may represent one such target. This thesis therefore makes an addition to the wider understanding of the role of HIV-1 Tat protein in HIV-1 latency and on LRA synergy. It is the authors hope that the works herein may contribute towards a future HIV-1 functional cure.

relative to that of the Tat72aa plasmid. *bGH* was included as a negative control construct. Error bars representing standard deviation (n=3).

IRES mediated expression of Tat from *tat* exon 2.

To explore the hypothesis outlined in Figure 3.1, and in fulfillment of the requirements for the Bachelor of Science Honors degree (Mechanisms controlling the translation of HIV-1 Tat protein, Jonathan Jacobson 2011), *tat* exon 2 was introduced into the *bGH* gene to model integration, transcriptional interference and alternative splicing to produce chimeric *cellular/tat* mRNAs. A range of constructs were generated to examine the various translation mechanisms that may be involved in Tat production. In brief:

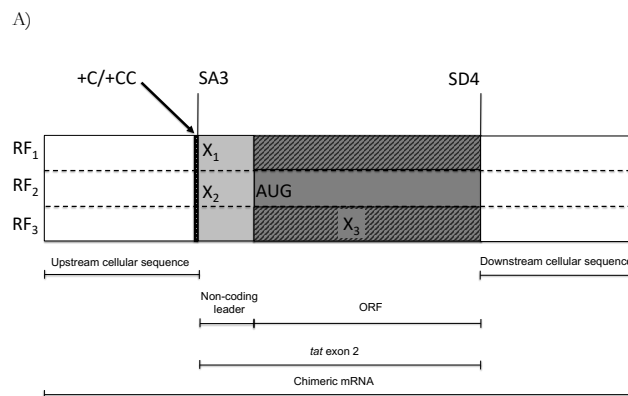
Proximity of *tat* exon 2 to *bGH* start codon.

To examine the effects placing *tat* exon 2 increasing distances from the *bGH* start codon, *tat* exon 2 replaced each of the 4 introns of *bGH*, making the initial 4 constructs: *tat1-*, *tat2-*, *tat3-* and *tat4-(72aa) bGH* (Figure A2.2). It was shown that *tat1(72aa) bGH* was capable of inducing LTR transactivation at 79% of the control construct (Figure A2.3), whereas the three other constructs only produced 15%, 16% and 14% respectively. The loss of Tat expression in the more downstream constructs likely due to two factors affecting protein translation.

- 1) Context dependent leaky scanning, where the ribosomal subunit bypasses the *bGH* start codon and initiates translation at the *tat* start codon, is more favorable the closer the *tat* exon is to the 5' end of the mRNA. When *tat* is further downstream, as for the *tat2-*, *tat3-* and *tat4-(72aa) bGH* constructs, leaky scanning is severely hindered.
- 2) Ribosome re-initiation, where the ribosome initiates translation at the *bGH* start codon, but terminates at a stop codon within the introduced *tat* gene (Figure A2.1). The ribosome would then re-initiate translation at the downstream *tat* start codon. Ribosome re-initiation has been shown to be favorable when the upstream ORF is shorter in sequence, so again the *tat2-*, *tat3-* and *tat4-(72aa) bGH* constructs, which have longer upstream open reading frames, are less likely to allow for re-initiation.

Ability to initiate translation internally, via an IRES element.

From the conclusions above, the intron 4 set of constructs: *tat4*-(72aa) *bGH*, *tat4*-(72aa)+C *bGH* and *tat4*-(72aa)+CC *bGH*, are unlikely to express Tat efficiently through conventional eukaryotic translation mechanisms (leaky scanning and re-initiation). It was possible however, that an IRES was contributing to the Tat expression seen. To examine this, +C and +CC nucleotide additions were introduced to move the *tat* exon into different reading frames. The *tat4*(72aa)+CC *bGH*, construct placed the *bGH* AUG codon in RF₃, where translation of the upstream ORF would terminate at X₃ downstream of the *tat* AUG codon. This does not allow for translation at the *tat* AUG, as ribosomes are incapable of moving backwards along a mRNA (in a 3'-5' direction). From this context, only IRES mediated internally initiating translation events are capable of expressing the Tat protein seen from this construct at 13% of the control (Figure A2.3).



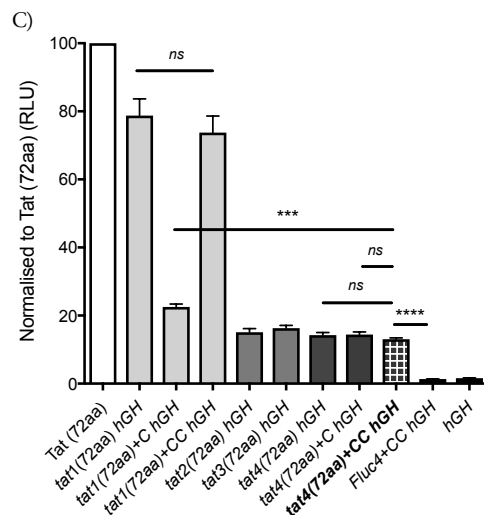
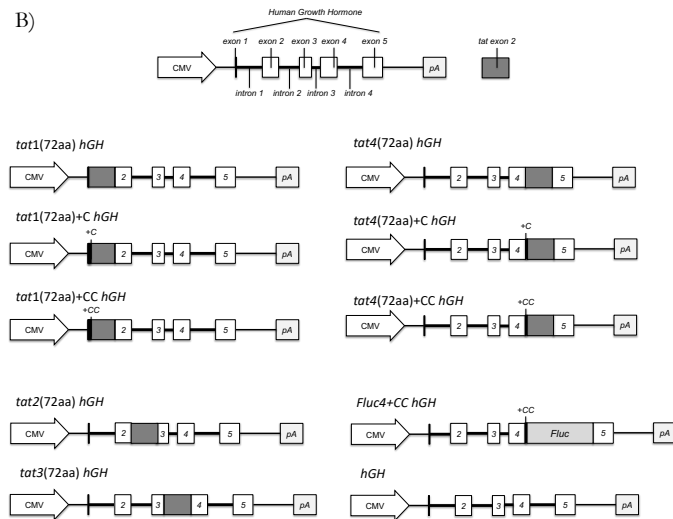


Figure A2. Chimeric *hGH/tat* constructs differentially express Tat protein. 1) The chimeric mRNA is made up of three reading frames (RF₁, RF₂ and RF₃), and shows the cellular sequence as white, and the *tat* exon 2 as gray. Splice acceptor 3 (SA3) and donor 4 (SD4) are also shown. The *tat* exon 2 contains a short 53 nucleotide non-coding leader sequence (light gray) upstream of the *tat* start codon (AUG). The non-coding leader sequence contains two stop codons (X₁ and X₂). The *tat* ORF (dark gray) contains a third stop codon (X₃) downstream of the *tat* AUG, but in a reading frame that does not encode for Tat (RF₁ and RF₃, which are shaded). The arrow designates where the +C and +CC nucleotide additions can be introduced to move the *tat* gene into a different reading frame. 2) The various chimeric *hGH/tat* mRNAs used. 3) Tat expression, normalized to a control construct. Error bars represent standard deviation (n=3).

Primary *in vitro* models:

Primary T cell models (Saleh et al. 2007; Wightman et al. 2011) have significant advantages over cell lines, as they typically involve authentic HIV-1 infection, and resting T cells, which make up a large portion of the latent reservoir in nature. Primary T cell models are typically constrained, however, by the number of infected cells available, require a PC3 level laboratory and are generally much more laborious. Many studies have been instrumental in the development of primary T cell models (Marrack 2004; MacLeod et al. 2010; Chun, Engel et al. 1998; Wang, Xu et al. 2005, Sahu, Lee et al. 2006; Marini *et al.* 2008; Bosque *et al.* 2009 and Tyagi *et al.* 2010). Collaborators in the Sharon Lewin/Paul Cameron laboratory overcame many previous problems with their CCL19 chemokine *in vitro* primary cell latency model where incubation of T cells in the presence of CCL19 allows for efficient infection and integration without inducing T cell activation. The CCL19 *in vitro* model represents a robust model of HIV-1 latency, generating a heterogeneous latent reservoir in the native host cell of HIV-1.

Primary *ex vivo* (Leukapheresis) samples:

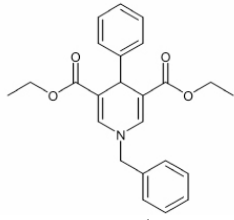
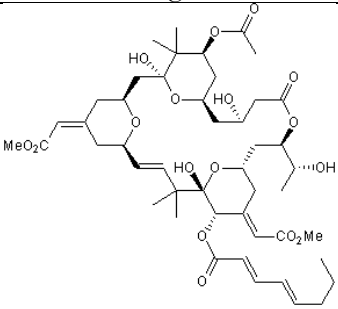
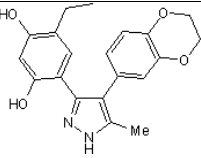
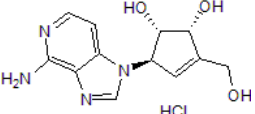
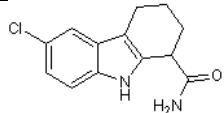
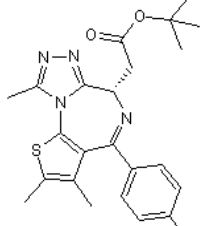
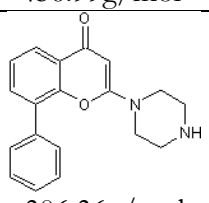
In more recent years, several research groups, including collaborators in the Lewin/Cameron laboratory, acquired large number of PBMCs from generous HIV+ patients on long-term successful cART who volunteered for leukapheresis. The latent infected T cells from these samples represent the absolute gold standard for *in vitro/ex vivo* HIV-1 latency experiments. Work presented in later (Chapter 6) has benefitted greatly from using these cells.

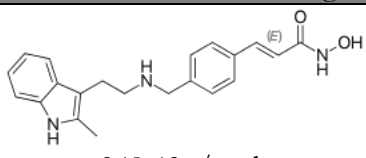
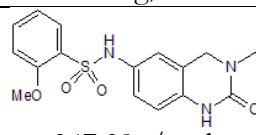
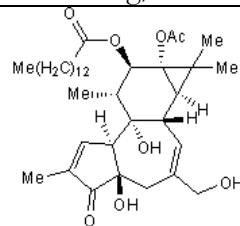
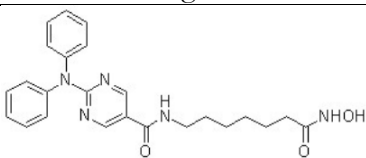
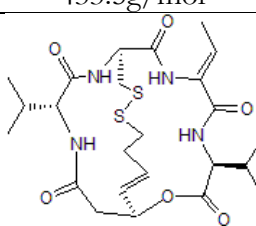
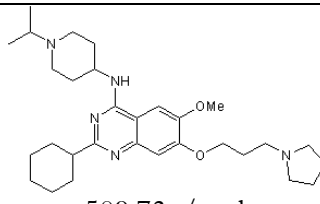
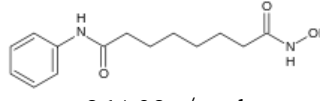
In vivo models (huMice)

In vivo models add significantly to the depth of assessment of lead compounds, as assessment of drug metabolism in the liver and the presence of immune pressures can be considered. In humanized mouse models NOD/SCID BLT and Rag2 $^{-/-}$ $\gamma c^{-/-}$ models permit stem cells to reconstitute the circulatory human immune system as well as engraftment of mucosal tissues allowing for HIV-1 infection (Denton 2009; Van Duyne, Pedati et al. 2009). While these models undoubtedly provide the best possible model for HIV-1 latency, they also take a long time to generate the animals, perform the infection, administer successful cART and then begin reactivation studies. Additionally, this long experimental period results in high costs, meaning that these experiments are best suited for advanced drug leads that have progressed through *in vitro/ex vivo* models.

Appendix 3: Latency Reversing Agents.

Table A.1: Known Latency Reversing Agents and their mechanisms of action.

Drug Name	Drug Class/Target	Structure & Molecular weight	[Highest]
BML-278	SIRT1 activator	 391.47g/mol	20µM
Bryostatin-1	PKC activator	 905.04g/mol	800nM
CCT-018159	Hsp90 inhibitor	 253.30g/mol	20µM
DZNep (3-Dezaneplanocin A)	HMT inhibitor / EZH2 HMT & SAH hydrolase inhibitor	 298.73g/mol	20µM
EX-527	SIRT1 inhibitor (selective)	 248.71g/mol	20µM
JQ1 (+)	BET bromodomain (BRD2, BRD3, BDR4) inhibitor	 456.99g/mol	20µM
LY-303511	BET bromodomain (BRD2, BRD3, BDR4) inhibitor	 306.36g/mol	20µM

Drug Name	Drug Class/Target	Structure & Molecular weight	[Highest]
Panobinostat (LBH-589)	HDAC (pan) inhibitor	 349.43g/mol	800nM
PFI-1	BET bromodomain (BRD2, BDR4) inhibitor	 347.39g/mol	20μM
PMA (Phorbol 12-myristate 13-acetate)	PKC activator	 616.83g/mol	125nM
Rocilinostat (ACY-1215)	HDAC6 inhibitor (selective)	 433.5g/mol	20μM
Romidepsin (FK 228)	HDAC1/2 inhibitor (selective)	 540.7g/mol	20nM
TNFα	Inflammatory cytokine. NF-κB and MAPK activator	NA	20ng/mL
UNC-0638	Selective G9a & GLP HMT	 509.73g/mol	20μM
Vorinostat (SAHA)	HDAC (pan) inhibitor	 264.32g/mol	20μM

SIRT1 ~ protein deacetylase

PKC ~ protein kinase C

Hsp90 ~ heat shock protein 90

Brd ~ bromodomain

(H)DAC ~ (histone) deacetylase

(H)MT ~ (histone) methyltransferase

BML-278 is a selective SIRT1 activator (Mai, Valente et al. 2009). For this study, SIRT1 was for its ability to modulate the posttranslational modification of Tat protein. By deacetylating key lysine residues on Tat, the protein is converted from the form required for the TAR independent late phase of transcription elongation to an inactive form following subsequent methylation events. SIRT1 activators would presumably augment this process and lock Tat in its inactive state.

Bryostatins-1 is a potent protein kinase C (PKC) modulator (Gschwend, Fair et al. 2000), with interest as a potential LRA through its ability to reactivate HIV-1 via activation of NF- κ B, NF-AT and AP1 pathways.

CCT-018159 is a novel selective inhibitor of human heat shock protein 90 (hsp90) (Sugiyama, Kageyama et al. 2015). Hsp90 plays a role in the NF- κ B release from I κ B and the nuclear translocation of p65/p50 as well as the Tat mediated recruitment of the P-TEFb complex to phosphorylate RNA pol II. Hsp90 may also play an important role in chromatin remodelling with the cellular SWI/SNF complex shortly after integration. Inhibition of Hsp90 therefore can potentially suppress viral gene expression from latency.

DZNep (3-deazaneplanocin A) is marketed as a broad spectrum HMTi (Girard, Bazille et al. 2014; Braun, Mathur et al. 2015) which has shown promise in reactivating viral gene expression from latency, presumably through inhibition of EZH2 protein H3K27me3 HMTase and S-adenosyl-L-homocysteine (SAH) hydrolase, although the compound may have numerous other targets within the cell.

EX-527 is a selective SIRT1 inhibitor specific for SIRT1 but not other sirtuin deacetylase family members or HDACs (Napper, Hixon et al. 2005). For this study SIRT1 was of interest due to the post translational modification it can directly make to Tat protein, by deacetylating key Lysine residues on Tat, converting it from a form required for Tat-transactivation to an inactive form following subsequent methylation events. SIRT1 inhibitors would presumably block this step, allowing the active form to persist.

JQ1 (+) is a broad-spectrum bromodomain inhibitor (BDi) shown to affect multiple epigenetic restrictions that contribute to HIV-1 latency (Filippakopoulos, Qi et al. 2010; Li, Guo et al. 2012). Such effects include freeing P-TEFb from the 7SK snRNP complex, preventing Bromodomain 4 protein (BRD4) from sequestering P-TEFb from Tat, induction of Sirt1 expression and also inhibition of BRD2 inhibitory complexes.

LY-303511 although originally obtained as a negative control compound for the PI3-kinase inhibitor LY-294002 (Dittmann, Werner et al. 2013) (not used in this study), was used in this study as it functions as a BRD2, BRD3 and BRD4 inhibitor.

Panobinostat (LBH-589) is a non-selective (pan) histone deacetylase inhibitor (HDACi) with FDA approval for use in patients with multiple myeloma (Atadja 2009). HDACi compounds have since received much interest in the HIV-1 latency field for their ability to reverse the epigenetic suppression of viral gene expression.

PFI-1 is a potent inhibitor of BRD2 and BRD4. PFI-1 has not received as much attention as JQ1 (+) in the HIV-1 latency field, but is believed to act in a very similar MOA, despite being from a totally unrelated drug family (Picaud, Da Costa et al. 2013).

PMA (Phorbol 12-myristate 13-acetate) is an extensively used and highly potent phorbol ester activator of PKC, activating HIV-1 gene expression through the NF- κ B pathway. For this study, PMA is commonly used along side TNF α as a positive control compound (Szallasi, Smith et al. 1994).

Rocilinostat (ACY-1215) is a selective and potent HDAC6 inhibitor, being >10-fold more selective for HDAC6 than HDAC1/2/3, and having minimal activity on the Sirtuin deacetylases (Raje, Hari et al. 2012). Its use in this study again involved posttranslational modification to Tat protein, inhibiting HDAC6 preventing the conversion of Tat to a transcriptionally active form.

Romidepsin (FK228) is a potent HDAC1 and HDAC2 inhibitor, but shows only weak inhibition of HDAC6. While being a HDAC inhibitor, Romidepsin belongs to a family of drugs unrelated Vorinostat and Panobinostat. Romidepsin has shown promise as an LRA (Furumai, Matsuyama et al. 2002; Sasakawa, Naoe et al. 2002).

TNF α is a pro inflammatory cytokine released early in the inflammation process, primarily used in the regulation of immune cells. For this study we have used TNF α for its ability to activate the NF- κ B and MAPK pathways as a positive control compound alongside PMA (Beg, Finco et al. 1993).

UNC-0638 is a selective G9a & GLP histone methyltransferase inhibitor (Chen, Skutt-Kakaria et al. 2012)

Vorinostat (suberanilohydroxamic acid or SAHA) is a well-characterized Class I and Class II HDACi, which has received great attention in the field of HIV-1 latency including in clinical trials (Marks 2007).

Table A.2: Known Latency Reversing Agent summary table.

Drug Name	Drug Class	Target mechanism
TNF α	NF- κ B activator	Transcription factor activators
PMA	PKC activator	
Bryostatins-1	PKC activator	
Vorinostat	HDAC (pan) inhibitor	Chromatin architecture modulators
Panobinostat	HDAC (pan) inhibitor	
Romidepsin	HDAC1/2 inhibitor	
DZNep	HMT inhibitor	Methylation inhibitors
UNC-0638	HMT inhibitor	
JQ1 (+)	BRD2/3/4 inhibitor	P-TEFb activators
PFI-1	BRD2/4 inhibitor	
LY-303511	BRD2/3/4 inhibitor	
CCT-018159	Hsp90 inhibitor	
BML-278	SIRT1 activator	Tat post translational modifications
EX-527	SIRT1 inhibitor	
Rocilinostat	HDAC6 inhibitor	

References

- Albanese, A., D. Arosio, M. Terreni, and A. Cereseto. 2008. HIV-1 pre-integration complexes selectively target decondensed chromatin in the nuclear periphery. *PLoS ONE* 3:e2413.
- Alexaki, A., Y. Liu, and B. Wigdahl. 2008. Cellular reservoirs of HIV-1 and their role in viral persistence. *Current HIV Research* 6:388-400.
- Anand, K., A. Schulte, K. Vogel-Bachmayr, K. Scheffzek, and M. Geyer. 2008. Structural insights into the Cyclin T1,-Tat,-TAR RNA transcription activation complex from EIAV. *Nature structural & molecular biology* 15:1287-1292.
- Andersen, J.L., J.L. DeHart, E.S. Zimmerman, O. Ardon, B. Kim, G. Jacquot, S. Benichou, and V. Planelles. 2006. HIV-1 Vpr-induced apoptosis is cell cycle dependent and requires Bax but not ANT. *PLoS Pathogens* 2:e127.
- Andersen, J.L., E. Le Rouzic, and V. Planelles. 2008. HIV-1 Vpr: mechanisms of G 2 arrest and apoptosis. *Experimental and Molecular Pathology* 85:2-10.
- Anderson, R.M., and G.F. Medley. 1988. Epidemiology of HIV infection and AIDS: incubation and infectious periods, survival and vertical transmission. *Aids* 2:S57-64.
- Atkins, K.M., L. Thomas, R.T. Youker, M.J. Harriff, F. Pissani, H. You, and G. Thomas. 2008. HIV-1 Nef Binds PACS-2 to Assemble a Multikinase Cascade That Triggers Major Histocompatibility Complex Class I (MHC-I) Down-regulation analysis using short interfering RNA and knock-out mice. *Journal of Biological Chemistry* 283:11772-11784.
- Archin, N., A. Liberty, et al. (2012). "Administration of vorinostat disrupts HIV-1 latency in patients on antiretroviral therapy." *Nature* 487(7408): 482.
- Archin, N. M., A. Espeseth, et al. (2009). "Expression of latent HIV induced by the potent HDAC inhibitor suberoylanilide hydroxamic acid." *AIDS Research and Human Retroviruses* 25(2): 207-212.
- Agosto, L. M., M. Gagne, et al. (2015). "Impact of Chromatin on HIV Replication." *Genes* 6(4): 957-976.
- Alexaki, A., Y. Liu, et al. (2008). "Cellular reservoirs of HIV-1 and their role in viral persistence." *Current HIV Research* 6(5): 388-400.
- Ammassari, A., R. Murri, et al. (2001). "Self-reported symptoms and medication side effects influence adherence to highly active antiretroviral therapy in persons with HIV infection." *JAIDS Journal of Acquired Immune Deficiency Syndromes* 28(5): 445-449.
- Atadja, P. (2009). "Development of the pan-DAC inhibitor panobinostat (LBH589): successes and challenges." *Cancer letters* 280(2): 233-241.

- Alexaki, A., Y. Liu, et al. (2008). "Cellular reservoirs of HIV-1 and their role in viral persistence." *Current HIV Research* 6(5): 388-400.
- Amorim, R., S. M. Costa, et al. (2014). "HIV-1 transcripts use IRES-initiation under conditions where Cap-dependent translation is restricted by poliovirus 2A protease." *PLoS ONE* 9(2): e88619.
- Anderson, J. L., A. T. Johnson, et al. (2007). "Both linear and discontinuous ribosome scanning are used for translation initiation from bicistronic human immunodeficiency virus type 1 env mRNAs." *Journal of Virology* 81(9): 4664-4676.
- Baeuerle, P.A., and D. Baltimore. 1988. I κ B: a specific inhibitor of the NF- κ B transcription factor. *Science* 242:540.
- Barre-Sinoussi, F., J. Chermann, F. Rey, M. Nugeyre, S. Chamaret, J. Gruest, C. Dautet, C. Axler-Blin, F. Vezinet-Brun, C. Rouzioux, W. Rozenbaum, and L. Montagnier. 1983. Isolation of a T-lymphotropic retrovirus from a patient at risk for acquired immune deficiency syndrome (AIDS). *Science* 220:868-871.
- Bayfield, M.A., R. Yang, and R.J. Maraia. 2010. Conserved and divergent features of the structure and function of La and La-related proteins (LARPs). *Biochimica et Biophysica Acta (BBA)-Gene Regulatory Mechanisms* 1799:365-378.
- Bebenek, K., J. Abbotts, J.D. Roberts, S.H. Wilson, and T.A. Kunkel. 1989. Specificity and mechanism of error-prone replication by human immunodeficiency virus-1 reverse transcriptase. *Journal of Biological Chemistry* 264:16948-16956.
- Beck, D.B., H. Oda, S.S. Shen, and D. Reinberg. 2012. PR-Set7 and H4K20me1: at the crossroads of genome integrity, cell cycle, chromosome condensation, and transcription. *Genes & Development* 26:325-337.
- Bell, N.M., and A.M. Lever. 2013. HIV Gag polyprotein: processing and early viral particle assembly. *Trends in Microbiology* 21:136-144.
- Berger, E.A., P.M. Murphy, and J.M. Farber. 1999. Chemokine receptors as HIV-1 coreceptors: roles in viral entry, tropism, and disease. *Annual Review of Immunology* 17:657-700.
- Berkhout, B., A. Gatignol, A.B. Rabson, and K.-T. Jeang. 1990. TAR-independent activation of the HIV-1 LTR: evidence that tat requires specific regions of the promoter. *Cell* 62:757-767.
- Berkhout, B., R.H. Silverman, and K.-T. Jeang. 1989. Tat trans-activates the human immunodeficiency virus through a nascent RNA target. *Cell* 59:273-282.
- Berkhout, B., and J.L. van Wamel. 2000. The leader of the HIV-1 RNA genome forms a compactly folded tertiary structure. *Rna* 6:282-295.
- Berkowitz, R.D., and S.P. Goff. 1994. Analysis of binding elements in the human immunodeficiency virus type 1 genomic RNA and nucleocapsid protein. *Virology* 202:233-246.

Binette, J., J. Mercier, D. Halawani, M. Latterich, and A. Cohen. 2007. Requirements for the selective degradation of CD4 receptor molecules by the human immunodeficiency virus type 1 Vpu protein in the endoplasmic reticulum. *Retrovirology* 4:75.

Bogerd, H.P., and B.R. Cullen. 2008. Single-stranded RNA facilitates nucleocapsid: APOBEC3G complex formation. *Rna* 14:1228-1236.

Boyer, J.C., K. Bebenek, and T.A. Kunkel. 1992. Unequal human immunodeficiency virus type 1 reverse transcriptase error rates with RNA and DNA templates. *Proceedings of the National Academy of Sciences* 89:6919-6923.

Bres, V., R. Kiernan, S.p. Emiliani, and M. Benkirane. 2002a. Tat acetyl-acceptor lysines are important for human immunodeficiency virus type-1 replication. *Journal of Biological Chemistry* 277:22215-22221.

Bres, V., H. Tagami, J.Ä. Loret, K. Jeang, Y. Nakatani, S. Emiliani, M. Benkirane, and R.E. Kiernan. 2002b. Differential acetylation of Tat coordinates its interaction with the co-Äactivators cyclin T1 and PCAF. *The EMBO Journal* 21:6811-6819.

Bres, V., S.M. Yoh, and K.A. Jones. 2008. The multi-tasking P-TEFb complex. *Current opinion in cell biology* 20:334-340.

Brenchley, J.M., T.W. Schacker, L.E. Ruff, D.A. Price, J.H. Taylor, G.J. Beilman, P.L. Nguyen, A. Khoruts, M. Larson, and A.T. Haase. 2004. CD4+ T cell depletion during all stages of HIV disease occurs predominantly in the gastrointestinal tract. *Journal of Experimental Medicine* 200:749-759.

Briggs, J.A., and H.-G. Krausslich. 2011. The molecular architecture of HIV. *Journal of Molecular Biology* 410:491-500.

Bukrinsky, M.I., N. Sharova, T.L. McDonald, T. Pushkarskaya, W.G. Tarpley, and M. Stevenson. 1993. Association of integrase, matrix, and reverse transcriptase antigens of human immunodeficiency virus type 1 with viral nucleic acids following acute infection. *Proceedings of the National Academy of Sciences* 90:6125-6129.

Bushman, F.D., and R. Craigie. 1991. Activities of human immunodeficiency virus (HIV) integration protein in vitro: specific cleavage and integration of HIV DNA. *Proceedings of the National Academy of Sciences* 88:1339-1343.

Banerjee, C., N. Archin, et al. (2012). "BET bromodomain inhibition as a novel strategy for reactivation of HIV-1." *Journal of Leukocyte Biology* 92(6): 1147-1154.

Bouchat, S., J.-S. p. Gatot, et al. (2012). "Histone methyltransferase inhibitors induce HIV-1 recovery in resting CD4+ T cells from HIV-1-infected HAART-treated patients." *Aids* 26(12): 1473-1482.

Burnett, J. C., K.-i. Lim, et al. (2010). "Combinatorial latency reactivation for HIV-1 subtypes and variants." *Journal of Virology* 84(12): 5958-5974.

Beg, A. A., T. S. Finco, et al. (1993). "Tumor necrosis factor and interleukin-1 lead to phosphorylation and loss of I kappa B alpha: a mechanism for NF-kappa B activation." *Molecular and Cellular Biology* 13(6): 3301-3310.

Braun, F. K., R. Mathur, et al. (2015). "Inhibition of methyltransferases accelerates degradation of cFLIP and sensitizes B-cell lymphoma cells to TRAIL-induced apoptosis." *PLoS ONE* 10(3): e0117994.

Bosque, A. and V. Planelles (2009). "Induction of HIV-1 latency and reactivation in primary memory CD4+ T cells." *Blood* 113(1): 58-65.

Buck, C. B., X. Shen, et al. (2001). "The human immunodeficiency virus type 1 gag gene encodes an internal ribosome entry site." *Journal of Virology* 75(1): 181-191.

Cai, R., B. Carpick, R.F. Chun, K.-T. Jeang, and B.R. Williams. 2000. HIV-I TAT inhibits PKR activity by both RNA-dependent and RNA-independent mechanisms. *Archives of biochemistry and biophysics* 373:361-367.

Carbone, A., E. Cesarman, M. Spina, A. Gloghini, and T.F. Schulz. 2009. HIV-associated lymphomas and gamma-herpesviruses. *Blood* 113:1213-1224.

Carrozza, M.J., B. Li, L. Florens, T. Suganuma, S.K. Swanson, K.K. Lee, W.-J. Shia, S. Anderson, J. Yates, and M.P. Washburn. 2005. Histone H3 methylation by Set2 directs deacetylation of coding regions by Rpd3S to suppress spurious intragenic transcription. *Cell* 123:581-592.

Chaudhuri, R., O.W. Lindwasser, W.J. Smith, J.H. Hurley, and J.S. Bonifacino. 2007. CD4 downregulation by HIV-1 Nef is dependent on clathrin and involves a direct interaction of Nef with the AP2 clathrin adaptor. *Journal of Virology*

Cheutin, T., A.J. McNairn, T. Jenuwein, D.M. Gilbert, P.B. Singh, and T. Misteli. 2003. Maintenance of stable heterochromatin domains by dynamic HP1 binding. *Science* 299:721-725.

Chiu, T.K., and D.R. Davies. 2004. Structure and function of HIV-1 integrase. *Current topics in medicinal chemistry* 4:965-977.

Chun, T.-W., R.T. Davey, M. Ostrowski, J.S. Justement, D. Engel, J.I. Mullins, and A.S. Fauci. 2000. Relationship between pre-existing viral reservoirs and the re-emergence of plasma viremia after discontinuation of highly active anti-retroviral therapy. *Nature medicine* 6:757-761.

Chun, T.W., D. Engel, M.M. Berrey, T. Shea, L. Corey, and A.S. Fauci. 1998. Early establishment of a pool of latently infected, resting CD4+ T cells during primary HIV-1 infection. *Proceedings of the National Academy of Sciences of the United States of America* 95:8869-8873.

Chun, T.W., L. Stuyver, S.B. Mizell, L.A. Ehler, J.A.M. Mican, M. Baseler, A.L. Lloyd, M.A. Nowak, and A.S. Fauci. 1997. Presence of an inducible HIV-1 latent reservoir

during highly active antiretroviral therapy. *Proceedings of the National Academy of Sciences of the United States of America* 94:13193-13197.

Cicala, C., E. Martinelli, J.P. McNally, D.J. Goode, R. Gopaul, J. Hiatt, K. Jelacic, S. Kottlilil, K. Macleod, and A. O'Shea. 2009. The integrin $\alpha 4\beta 7$ forms a complex with cell-surface CD4 and defines a T cell subset that is highly susceptible to infection by HIV-1. *Proceedings of the National Academy of Sciences* 106:20877-20882.

Ciuffi, A., M. Llano, E. Poeschla, C. Hoffmann, J. Leipzig, P. Shinn, J.R. Ecker, and F. Bushman. 2005. A role for LEDGF/p75 in targeting HIV DNA integration. *Nature medicine* 11:1287-1289.

Clapham, P.R., and Å. McKnight. 2001. HIV-1 receptors and cell tropism. *British Medical Bulletin* 58:43-59.

Coffin, J., A. Haase, J.A. Levy, L. Montagnier, S. Oroszlan, N. Teich, H. Temin, K. Toyoshima, H. Varmus, and P. Vogt. 1986. What to call the AIDS virus? *Nature* 321:10-10.

Core, L.J., J.J. Waterfall, and J.T. Lis. 2008. Nascent RNA sequencing reveals widespread pausing and divergent initiation at human promoters. *Science* 322:1845-1848.

Cullen, B.R. 1991. Human immunodeficiency virus as a prototypic complex retrovirus. *Journal of Virology* 65:1053.

Chang, Y.-F., J. S. Imam, et al. (2007). "The nonsense-mediated decay RNA surveillance pathway." *Annu. Rev. Biochem.* 76: 51-74.

Chun, T.-W., R. T. Davey, et al. (2000). "Relationship between pre-existing viral reservoirs and the re-emergence of plasma viremia after discontinuation of highly active anti-retroviral therapy." *Nature medicine* 6(7): 757-761.

Chun, T.-W., D. Engel, et al. (1998). "Induction of HIV-1 replication in latently infected CD4+ T cells using a combination of cytokines." *Journal of Experimental Medicine* 188(1): 83-91.

Chun, T.-W., R. T. Davey Jr, et al. (1999). "AIDS: re-emergence of HIV after stopping therapy." *Nature* 401(6756): 874.

Carrozza, M. J., B. Li, et al. (2005). "Histone H3 methylation by Set2 directs deacetylation of coding regions by Rpd3S to suppress spurious intragenic transcription." *Cell* 123(4): 581-592.

Dafonseca, S., N. Chomont, et al. (2010). "Purging the HIV-1 reservoir through the disruption of the PD-1 pathway." *Journal of the International AIDS Society* 13(3).

Dahl, V., L. Josefsson, et al. (2010). "HIV reservoirs, latency, and reactivation: prospects for eradication." *Antiviral Research* 85(1): 286-294.

Denton, P. W. and J. V. Garcia (2009). "Novel humanized murine models for HIV research." *Current HIV/AIDS Reports* 6(1): 13-19.

Davey, R. T., N. Bhat, et al. (1999). "HIV-1 and T cell dynamics after interruption of highly active antiretroviral therapy (HAART) in patients with a history of sustained viral suppression." *Proceedings of the National Academy of Sciences* 96(26): 15109-15114.

Dittmann, A., T. Werner, et al. (2013). "The commonly used PI3-kinase probe LY294002 is an inhibitor of BET bromodomains." *ACS Chemical Biology* 9(2): 495-502.

Chen, X., K. Skutt-Kakaria, et al. (2012). "G9a/GLP-dependent histone H3K9me2 patterning during human hematopoietic stem cell lineage commitment." *Genes & Development* 26(22): 2499-2511.

Chomont, N., M. El-Far, et al. (2009). "HIV reservoir size and persistence are driven by T cell survival and homeostatic proliferation." *Nature medicine* 15(8): 893-900.

Chun, T.-W., R. T. Davey, et al. (2000). "Relationship between pre-existing viral reservoirs and the re-emergence of plasma viremia after discontinuation of highly active anti-retroviral therapy." *Nature medicine* 6(7): 757-761.

Csermely, P. t., T. s. Schnaider, et al. (1998). "The 90-kDa molecular chaperone family: structure, function, and clinical applications. A comprehensive review." *Pharmacology & Therapeutics* 79(2): 129-168.

Dalgleish, A.G., P.C. Beverley, P.R. Clapham, D.H. Crawford, M.F. Greaves, and R.A. Weiss. 1984. The CD4 (T4) antigen is an essential component of the receptor for the AIDS retrovirus. *Nature* 312:763-767.

Dames, S.A., A. Schonichen, A. Schulte, M. Barboric, B.M. Peterlin, S. Grzesiek, and M. Geyer. 2007. Structure of the Cyclin T binding domain of Hexim1 and molecular basis for its recognition of P-TEFb. *Proceedings of the National Academy of Sciences* 104:14312-14317.

Darcis, G., B. Van Driessche, and C. Van Lint. 2017. HIV Latency: Should We Shock or Lock? *Trends in Immunology*

Darcis, G., A. Kula, et al. (2015). "An in-depth comparison of latency-reversing agent combinations in various in vitro and ex vivo HIV-1 latency models identified bryostatin-1+ JQ1 and ingenol-B+ JQ1 to potently reactivate viral gene expression." *PLoS Pathogens* 11(7): e1005063.

Darcis, G., A. Kula, et al. (2015). "An in-depth comparison of latency-reversing agent combinations in various in vitro and ex vivo HIV-1 latency models identified bryostatin-1+ JQ1 and ingenol-B+ JQ1 to potently reactivate viral gene expression." *PLoS Pathogens* 11(7): e1005063.

Das, A.T., B. Klaver, and B. Berkhout. 1998. The 5' and 3' TAR elements of human immunodeficiency virus exert effects at several points in the virus life cycle. *Journal of Virology* 72:9217-9223.

Dorr, P., M. Westby, S. Dobbs, P. Griffin, B. Irvine, M. Macartney, J. Mori, G. Rickett, C. Smith-Burchnell, and C. Napier. 2005. Maraviroc (UK-427,857), a potent, orally bioavailable, and selective small-molecule inhibitor of chemokine receptor CCR5 with broad-spectrum anti-human immunodeficiency virus type 1 activity. *Antimicrobial Agents and Chemotherapy* 49:4721-4732.

Epsztejn-Litman, S., N. Feldman, M. Abu-Remaileh, Y. Shufaro, A. Gerson, J. Ueda, R. Deplus, F.o. Fuks, Y. Shinkai, and H. Cedar. 2008. De novo DNA methylation promoted by G9a prevents reprogramming of embryonically silenced genes. *Nature structural & molecular biology* 15:1176-1183.

Feinberg, M.B., D. Baltimore, and A.D. Frankel. 1991. The role of Tat in the human immunodeficiency virus life cycle indicates a primary effect on transcriptional elongation. *Proceedings of the National Academy of Sciences* 88:4045-4049.

Felice, B., C. Cattoglio, D. Cittaro, A. Testa, A. Miccio, G. Ferrari, L. Luzi, A. Recchia, and F. Mavilio. 2009. Transcription factor binding sites are genetic determinants of retroviral integration in the human genome. *PLoS ONE* 4:e4571.

Ferrari, K.J., A. Scelfo, S. Jammula, A. Cuomo, I. Barozzi, A. Fischle, T. Bonaldi, and D. Pasini. 2014. Polycomb-dependent H3K27me1 and H3K27me2 regulate active transcription and enhancer fidelity. *Molecular cell* 53:49-62.

Finzi, D., M. Hermankova, T. Pierson, L.M. Carruth, C. Buck, R.E. Chaisson, T.C. Quinn, K. Chadwick, J. Margolick, R. Brookmeyer, J. Gallant, M. Markowitz, D.D. Ho, D.D. Richman, and R.F. Siliciano. 1997. Identification of a reservoir for HIV-1 in patients on highly active antiretroviral therapy. *Science* 278:1295-1300.

Fischle, W., Y. Wang, S.A. Jacobs, Y. Kim, C.D. Allis, and S. Khorasanizadeh. 2003. Molecular basis for the discrimination of repressive methyl-lysine marks in histone H3 by Polycomb and HP1 chromodomains. *Genes & Development* 17:1870-1881.

Flanagan, J.F., L.-Z. Mi, M. Chruszcz, M. Cymborowski, K.L. Clines, Y. Kim, W. Minor, F. Rastinejad, and S. Khorasanizadeh. 2005. Double chromodomains cooperate to recognize the methylated histone H3 tail. *Nature* 438:1181-1185.

Frankel, A.D. 1992. Activation of HIV transcription by Tat. *Current Opinion in Genetics & Development* 2:293-298.

Fritz, C.C., and M.R. Green. 1996. HIV Rev uses a conserved cellular protein export pathway for the nucleocytoplasmic transport of viral RNAs. *Current Biology* 6:848-854.

Fu, T.-J., J. Peng, G. Lee, D.H. Price, and O. Flores. 1999. Cyclin K functions as a CDK9 regulatory subunit and participates in RNA polymerase II transcription. *Journal of Biological Chemistry* 274:34527-34530.

Fujinaga, K., T.P. Cujec, J. Peng, J. Garriga, D.H. Price, X. and B.M. Peterlin. 1998. The ability of positive transcription elongation factor B to transactivate human immunodeficiency virus transcription depends on a functional kinase domain, cyclin T1, and Tat. *Journal of Virology* 72:7154-7159.

Furfine, E.t., and J. Reardon. 1991. Reverse transcriptase. RNase H from the human immunodeficiency virus. Relationship of the DNA polymerase and RNA hydrolysis activities. *Journal of Biological Chemistry* 266:406-412.

Filippakopoulos, P., J. Qi, et al. (2010). "Selective inhibition of BET bromodomains." *Nature* 468(7327): 1067.

Furumai, R., A. Matsuyama, et al. (2002). "FK228 (depsipeptide) as a natural prodrug that inhibits class I histone deacetylases." *Cancer Research* 62(17): 4916-4921.

Finzi, D., M. Hermankova, et al. (1997). "Identification of a reservoir for HIV-1 in patients on highly active antiretroviral therapy." *Science* 278(5341): 1295-1300.

Gorry, P. R., J. L. Howard, et al. (1999). "Diminished Production of Human Immunodeficiency Virus Type 1 in Astrocytes Results from Inefficient Translation of gag, env, and nef mRNAs despite Efficient Expression of Tat and Rev." *Journal of Virology* 73(1): 352-361.

Gray, L. R., H. On, et al. (2016). "Toxicity and in vitro activity of HIV-1 latency-reversing agents in primary CNS cells." *Journal of neurovirology* 22(4): 455-463.

Gulick, R. M., J. W. Mellors, et al. (1997). "Treatment with indinavir, zidovudine, and lamivudine in adults with human immunodeficiency virus infection and prior antiretroviral therapy." *New England Journal of Medicine* 337(11): 734-739.

Girard, N., C. I. Bazille, et al. (2014). "3-Deazaneplanocin A (DZNep), an inhibitor of the histone methyltransferase EZH2, induces apoptosis and reduces cell migration in chondrosarcoma cells." *PLoS ONE* 9(5): e98176.

Greger, I. H., F. Demarchi, et al. (1998). "Transcriptional interference perturbs the binding of Sp1 to the HIV-1 promoter." *Nucleic Acids Research* 26(5): 1294-1300.
Grewal, S. I. S. and D. Moazed (2003). "Heterochromatin and Epigenetic Control of Gene Expression." *Science* 301(5634): 798-802.

Gschwend, J. r. E., W. R. Fair, et al. (2000). "Bryostatins induce prolonged activation of extracellular regulated protein kinases in and apoptosis of LNCaP human prostate cancer cells overexpressing protein kinase C- α ." *Molecular Pharmacology* 57(6): 1224-1234.

Gallo, R.C., S.Z. Salahuddin, M. Popovic, G.M. Shearer, M. Kaplan, B.F. Haynes, T.J. Palker, R. Redfield, J. Oleske, and B. Safai. 1984. Frequent detection and isolation of cytopathic retroviruses (HTLV-III) from patients with AIDS and at risk for AIDS. *Science* 224:500-503.

Garriga, J., 2004. Cellular control of gene expression by T-type cyclin/CDK9 complexes. *Gene* 337:15-23.

Gatignol, A., and A. Buckler-White. 1991. Characterization of a human TAR RNA-binding protein that activates the HIV-1 LTR. *Science* 251:1597.

Gottlieb, M.S., R. Schroff, H.M. Schanker, J.D. Weisman, P.T. Fan, R.A. Wolf, and A. Saxon. 1981. Pneumocystis carinii pneumonia and mucosal candidiasis in previously healthy homosexual men. Evidence of a new acquired cellular immunodeficiency. *New England Journal of Medicine* 305:1425-1431.

Guadalupe, M., E. Reay, S. Sankaran, T. Prindiville, J. Flamm, A. McNeil, and S. Dandekar. 2003. Severe CD4+ T cell depletion in gut lymphoid tissue during primary human immunodeficiency virus type 1 infection and substantial delay in restoration following highly active antiretroviral therapy. *Journal of Virology* 77:11708-11717.

Gulick, R.M., J.W. Mellors, D. Havlir, J.J. Eron, C. Gonzalez, D. McMahon, D.D. Richman, F.T. Valentine, L. Jonas, and A. Meibohm. 1997. Treatment with indinavir, zidovudine, and lamivudine in adults with human immunodeficiency virus infection and prior antiretroviral therapy. *New England Journal of Medicine* 337:734-739.

Harrison, K. M., R. Song, et al. (2010). "Life expectancy after HIV diagnosis based on national HIV surveillance data from 25 states, United States." *JAIDS Journal of Acquired Immune Deficiency Syndromes* 53(1): 124-130.

Hodges, C., L. Bintu, et al. (2009). "Nucleosomal fluctuations govern the transcription dynamics of RNA polymerase II." *Science* 325(5940): 626-628.

Jones, P. A. and D. Takai (2001). "The role of DNA methylation in mammalian epigenetics." *Science* 293(5532): 1068-1070.

Han, Y., Y. B. Lin, et al. (2008). "Orientation-dependent regulation of integrated HIV-1 expression by host gene transcriptional readthrough." *Cell Host & Microbe* 4(2): 134-146.

Harrison, K. M., R. Song, et al. (2010). "Life expectancy after HIV diagnosis based on national HIV surveillance data from 25 states, United States." *JAIDS Journal of Acquired Immune Deficiency Syndromes* 53(1): 124-130.

Hodges, C., L. Bintu, et al. (2009). "Nucleosomal fluctuations govern the transcription dynamics of RNA polymerase II." *Science* 325(5940): 626-628.

Hammer, S.M., K.E. Squires, M.D. Hughes, J.M. Grimes, L.M. Demeter, J.S. Currier, J.J. Eron, J.E. Feinberg, H.H. Balfour, L.R. Deyton, J.A. Chodakewitz, M.A. Fischl, J.P. Phair, L. Pedneault, B.-Y. Nguyen, and J.C. Cook. 1997. A Controlled Trial of Two Nucleoside Analogues plus Indinavir in Persons with Human Immunodeficiency Virus Infection and CD4 Cell Counts of 200 per Cubic Millimeter or Less. *New England Journal of Medicine* 337:725-733.

Han, Y., K. Lassen, D. Monie, A.R. Sedaghat, S. Shimoji, X. Liu, T.C. Pierson, J.B. Margolick, R.F. Siliciano, and J.D. Siliciano. 2004. Resting CD4+ T cells from human immunodeficiency virus type 1 (HIV-1)-infected individuals carry integrated HIV-1 genomes within actively transcribed host genes. *Journal of Virology* 78:6122-6133.

Harrich, D., C. Ulich, L.n.F. Garcia-Martinez, and R.B. Gaynor. 1997. Tat is required for efficient HIV-1 reverse transcription. *The EMBO Journal* 16:1224-1235.

Hayakawa, T., and J.-i. Nakayama. 2010. Physiological roles of class I HDAC complex and histone demethylase. *BioMed Research International* 2011:

Heinzinger, N.K., M. Bukinsky, S.A. Haggerty, A.M. Ragland, V. Kewalramani, M.-A. Lee, H.E. Gendelman, L. Ratner, M. Stevenson, and M. Emerman. 1994. The Vpr protein of human immunodeficiency virus type 1 influences nuclear localization of viral nucleic acids in nondividing host cells. *Proceedings of the National Academy of Sciences* 91:7311-7315.

Henderson, B.R., and P. Percipalle. 1997. Interactions between HIV Rev and nuclear import and export factors: the Rev nuclear localisation signal mediates specific binding to human importin-Beta. *Journal of Molecular Biology* 274:693-707.

Ho, Y.-C., L. Shan, N.N. Hosmane, J. Wang, S.B. Laskey, D.I. Rosenbloom, J. Lai, J.N. Blankson, J.D. Siliciano, and R.F. Siliciano. 2013. Replication-competent noninduced proviruses in the latent reservoir increase barrier to HIV-1 cure. *Cell* 155:540-551.

Hodges, C., L. Bintu, L. Lubkowska, M. Kashlev, and C. Bustamante. 2009. Nucleosomal fluctuations govern the transcription dynamics of RNA polymerase II. *Science* 325:626-628.

Hong, L., G. Schroth, H. Matthews, P. Yau, and E. Bradbury. 1993. Studies of the DNA binding properties of histone H4 amino terminus. Thermal denaturation studies reveal that acetylation markedly reduces the binding constant of the H4" tail" to DNA. *Journal of Biological Chemistry* 268:305-314.

Howcraft, T.K., K. Strebler, M.A. Martin, and D.S. Singer. 1993. Repression of MHC class I gene promoter activity by two-exon Tat of HIV. *Science* 260:1320-1323.

Huo, L., D. Li, L. Sun, M. Liu, X. Shi, X. Sun, J. Li, B. Dong, X. Dong, and J. Zhou. 2011a. Tat acetylation regulates its actions on microtubule dynamics and apoptosis in T lymphocytes. *The Journal of pathology* 223:28-36.

Huo, L., D. Li, X. Sun, X. Shi, P. Karna, W. Yang, M. Liu, W. Qiao, R. Aneja, and J. Zhou. 2011b. Regulation of Tat acetylation and transactivation activity by the microtubule-associated deacetylase HDAC6. *Journal of Biological Chemistry* 286:9280-9286.

Imai, K., H. Togami, and T. Okamoto. 2010. Involvement of histone H3 lysine 9 (H3K9) methyltransferase G9a in the maintenance of HIV-1 latency and its reactivation by BIX01294. *Journal of Biological Chemistry* 285:16538-16545.

Itoh, M., J. Inoue, H. Toyoshima, T. Akizawa, M. Higashi, and M. Yoshida. 1989. HTLV-1 rex and HIV-1 rev act through similar mechanisms to relieve suppression of unspliced RNA expression. *Oncogene* 4:1275-1279.

Jablonski, J.A., A.L. Amelio, M. Giacca, and M. Caputi. 2009. The transcriptional transactivator Tat selectively regulates viral splicing. *Nucleic Acids Research* 38:1249-1260.

Jang, M.K., K. Mochizuki, M. Zhou, H.-S. Jeong, J.N. Brady, and K. Ozato. 2005. The bromodomain protein Brd4 is a positive regulatory component of P-TEFb and stimulates RNA polymerase II-dependent transcription. *Molecular cell* 19:523-534.

Janvier, K., H. Craig, S. Le Gall, R. Benarous, J. Guatelli, O. Schwartz, and S. Benichou. 2001. Nef-induced CD4 downregulation: a diacidic sequence in human immunodeficiency virus type 1 Nef does not function as a protein sorting motif through direct binding to beta-COP. *Journal of Virology* 75:3971-3976.

Jenuwein, T., and C.D. Allis. 2001. Translating the histone code. *Science* 293:1074-1080.

Jeronimo, C.I., D. Forget, A. Bouchard, Q. Li, G. Chua, C. Poitras, C. Bergeron, S. Bourassa, and J. Greenblatt. 2007. Systematic analysis of the protein interaction network for the human transcription machinery reveals the identity of the 7SK capping enzyme. *Molecular cell* 27:262-274.

Jiang, G., E. A. Mendes, et al. (2015). "Synergistic reactivation of latent HIV expression by ingenol-3-angelate, PEP005, targeted NF- κ B signaling in combination with JQ1 induced p-TEFb activation." *PLoS Pathogens* 11(7): e1005066.

Laird, G. M., C. K. Bullen, et al. (2015). "Ex vivo analysis identifies effective HIV-1 latency-reversing drug combinations." *The Journal of Clinical Investigation* 125(5): 1901.

Jonckheere, H., J. Anne, and E. De Clercq. 2000. The HIV-1 Reverse Transcription (RT) Process as Target for RT Inhibitors. *Medicinal research reviews* 20:129-154.

Jones, N., P. Rigby, and E. Ziff. 1988. Trans-acting protein factors and the regulation of eukaryotic transcription: lessons from studies on DNA tumor viruses. *Genes & Development* 2:267-281.

Jones, P.A., and D. Takai. 2001. The role of DNA methylation in mammalian epigenetics. *Science* 293:1068-1070.

Jordan, A., D. Bisgrove, et al. (2003). "HIV reproducibly establishes a latent infection after acute infection of T cells in vitro." *The EMBO Journal* 22(8): 1868-1877.

Kao, S.-Y., A. F. Calman, et al. (1987). "Anti-termination of transcription within the long terminal repeat of HIV-1 by tat gene product." *Nature* 330(6147): 489-493.

Karmodiya, K., A. R. Krebs, et al. (2012). "H3K9 and H3K14 acetylation co-occur at many gene regulatory elements, while H3K14ac marks a subset of inactive inducible promoters in mouse embryonic stem cells." *BMC Genomics* 13(1): 424.

Kiernan, R. E., C. Vanhulle, et al. (1999). "HIV-1 tat transcriptional activity is regulated by acetylation." *The EMBO Journal* 18(21): 6106-6118.

Kao, S.-Y., A. F. Calman, et al. (1987). "Anti-termination of transcription within the long terminal repeat of HIV-1 by tat gene product." *Nature* 330(6147): 489-493.

Karn, J. (2011). "The molecular biology of HIV latency: breaking and restoring the Tat-dependent transcriptional circuit." *Current opinion in HIV and AIDS* 6(1): 4.

Kao, S.-Y., A.F. Calman, P.A. Luciw, and B.M. Peterlin. 1987a. Anti-termination of transcription within the long terminal repeat of HIV-1 by tat gene product. *Nature* 330:489-493.

Karmodiya, K., A.R. Krebs, M. Oulad-Abdelghani, H. Kimura, and L. Tora. 2012. H3K9 and H3K14 acetylation co-occur at many gene regulatory elements, while H3K14ac marks a subset of inactive inducible promoters in mouse embryonic stem cells. *BMC Genomics* 13:424.

Kauder, S.E., A. Bosque, A. Lindqvist, V. Planelles, and E. Verdin. 2009. Epigenetic regulation of HIV-1 latency by cytosine methylation. *PLoS Pathogens* 5:e1000495.

Kiernan, R.E., C. Vanhulle, L. Schiltz, E. Adam, H. Xiao, F.d.r. Maudoux, C. Calomme, A.n. Burny, Y. Nakatani, and K.Å. Jeang. 1999. HIV-1 tat transcriptional activity is regulated by acetylation. *The EMBO Journal* 18:6106-6118.

Kohl, N.E., E.A. Emini, W.A. Schleif, L.J. Davis, J.C. Heimbach, R. Dixon, E.M. Scolnick, and I.S. Sigal. 1988. Active human immunodeficiency virus protease is required for viral infectivity. *Proceedings of the National Academy of Sciences* 85:4686-4690.

Kowenz-Leutz, E., and A. Leutz. 1999. AC/EBP beta isoform recruits the SWI/SNF complex to activate myeloid genes. *Molecular cell* 4:735-743.

Krueger, B.J., C.I. Jeronimo, B.B. Roy, A. Bouchard, C. Barrandon, S.A. Byers, C.E. Searcey, J.J. Cooper, O. Bensaude, and A. Cohen. 2008. LARP7 is a stable component of the 7SK snRNP while P-TEFb, HEXIM1 and hnRNP A1 are reversibly associated. *Nucleic Acids Research* 36:2219-2229.

Krueger, B.J., K. Varzavand, J.J. Cooper, and D.H. Price. 2010. The mechanism of release of P-TEFb and HEXIM1 from the 7SK snRNP by viral and cellular activators includes a conformational change in 7SK. *PLoS ONE* 5:e12335.

Kuzmichev, A., K. Nishioka, H. Erdjument-Bromage, P. Tempst, and D. Reinberg. 2002. Histone methyltransferase activity associated with a human multiprotein complex containing the Enhancer of Zeste protein. *Genes & Development* 16:2893-2905.

Laird, G.M., C.K. Bullen, D.I. Rosenbloom, A.R. Martin, A.L. Hill, C.M. Durand, J.D. Siliciano, and R.F. Siliciano. 2015. Ex vivo analysis identifies effective HIV-1 latency, reversing drug combinations. *The Journal of Clinical Investigation* 125:1901.

Lassen, K., Y. Han, Y. Zhou, J. Siliciano, and R.F. Siliciano. 2004. The multifactorial nature of HIV-1 latency. *Trends in Molecular Medicine* 10:525-531.

Lassen, K.G., K.X. Ramyar, J.R. Bailey, Y. Zhou, and R.F. Siliciano. 2006. Nuclear retention of multiply spliced HIV-1 RNA in resting CD4+ T cells. *PLoS Pathogens* 2:e68.

- Lawrence, D.M., L.C. Durham, L. Schwartz, P. Seth, D. Maric, and E.O. Major. 2004. Human immunodeficiency virus type 1 infection of human brain-derived progenitor cells. *Journal of Virology* 78:7319-7328.
- Le Gall, S., M.-C. Prevost, J.-M. Heard, and O. Schwartz. 1997. Human immunodeficiency virus type I Nef independently affects virion incorporation of major histocompatibility complex class I molecules and virus infectivity. *Virology* 229:295-301.
- Lehnertz, B., Y. Ueda, A.A. Derijck, U. Braunschweig, L. Perez-Burgos, S. Kubicek, T. Chen, E. Li, T. Jenuwein, and A.H. Peters. 2003. Suv39h-mediated histone H3 lysine 9 methylation directs DNA methylation to major satellite repeats at pericentric heterochromatin. *Current Biology* 13:1192-1200.
- Lener, D., V.r. Tanchou, B.P. Roques, S.F. Le Grice, and J.-L. Darlix. 1998. Involvement of HIV-I Nucleocapsid Protein in the Recruitment of Reverse Transcriptase into Nucleoprotein Complexes Formed in Vitro. *Journal of Biological Chemistry* 273:33781-33786.
- Leth, S., M.H. Schleimann, S.K. Nissen, J.F. Hojen, R. Olesen, M.E. Graversen, S. Jorgensen, A.S. Kjeer, P.W. Denton, and A. Mork. 2016. Combined effect of Vacc-4x, recombinant human granulocyte macrophage colony-stimulating factor vaccination, and romidepsin on the HIV-1 reservoir (REDUC): a single-arm, phase 1B/2A trial. *The Lancet HIV* 3:e463-e472.
- Li, B., M. Carey, and J.L. Workman. 2007. The role of chromatin during transcription. *Cell* 128:707-719.
- Li, Q., L. Duan, J.D. Estes, Z.-M. Ma, T. Rourke, Y. Wang, C. Reilly, J. Carlis, C.J. Miller, and A.T. Haase. 2005. Peak SIV replication in resting memory CD4⁺ T cells depletes gut lamina propria CD4⁺ T cells. *Nature* 434:1148-1152.
- Li, Y., G.D. Kao, B.A. Garcia, J. Shabanowitz, D.F. Hunt, J. Qin, C. Phelan, and M.A. Lazar. 2006. A novel histone deacetylase pathway regulates mitosis by modulating Aurora B kinase activity. *Genes & Development* 20:2566-2579.
- Lin, N., X. Li, K. Cui, I. Chepelev, F. Tie, B. Liu, G. Li, P. Harte, K. Zhao, and S. Huang. 2011. A barrier-only boundary element delimits the formation of facultative heterochromatin in *Drosophila melanogaster* and vertebrates. *Molecular and Cellular Biology* 31:2729-2741.
- Lister, R., M. Pelizzola, R.H. Dowen, R.D. Hawkins, G. Hon, J. Tonti-Filippini, J.R. Nery, L. Lee, Z. Ye, and Q.-M. Ngo. 2009. Human DNA methylomes at base resolution show widespread epigenomic differences. *Nature* 462:315-322.
- Little, S.J., A.R. McLean, C.A. Spina, D.D. Richman, and D.V. Havlir. 1999. Viral dynamics of acute HIV-1 infection. *Journal of Experimental Medicine* 190:841-850.
- Lusic, M., A. Marcello, A. Cereseto, and M. Giacca. 2003. Regulation of HIV-1 gene expression by histone acetylation and factor recruitment at the LTR promoter. *The EMBO Journal* 22:6550-6561.

Li, Z., J. Guo, et al. (2013). "The BET bromodomain inhibitor JQ1 activates HIV latency through antagonizing Brd4 inhibition of Tat-transactivation." *Nucleic Acids Research* 41(1): 277-287.

Li, Z., J. Guo, et al. (2012). "The BET bromodomain inhibitor JQ1 activates HIV latency through antagonizing Brd4 inhibition of Tat-transactivation." *Nucleic Acids Research* 41(1): 277-287.

Lafeuillade, A., C. c. Poggi, et al. (2001). "Pilot study of a combination of highly active antiretroviral therapy and cytokines to induce HIV-1 remission." *Journal of acquired immune deficiency syndromes* (1999) 26(1): 44-55.

Mai, A., S. Valente, et al. (2009). "Study of 1, 4-dihydropyridine structural scaffold: discovery of novel sirtuin activators and inhibitors." *Journal of Medicinal Chemistry* 52(17): 5496-5504.

Margolis, D. M., J. V. Garcia, et al. (2016). "Latency reversal and viral clearance to cure HIV-1." *Science* 353(6297): aaf6517.

Marks, P. (2007). "Discovery and development of SAHA as an anticancer agent." *Oncogene* 26(9): 1351.

MacLeod, M. K., J. W. Kappler, et al. (2010). "Memory CD4 T cells: generation, reactivation and re-assignment." *Immunology* 130(1): 10-15.

Marini, A., J. M. Harper, et al. (2008). "An in vitro system to model the establishment and reactivation of HIV-1 latency." *The Journal of Immunology* 181(11): 7713-7720.

Marrack, P. and J. Kappler (2004). "Control of T cell viability." *Annu. Rev. Immunol.* 22: 765-787.

Mbonye, U. and J. Karn (2014). "Transcriptional control of HIV latency: cellular signaling pathways, epigenetics, happenstance and the hope for a cure." *Virology* 454: 328-339.

Malim, M., and B. Cullen. 1991. HIV-1 structural gene expression requires the binding of multiple Rev monomers to the viral RRE: implications for HIV-1 latency. *Cell* 65:241 - 248.

Malim, M.H., J. Hauber, S.-Y. Le, J.V. Maizel, and B.R. Cullen. 1989. The HIV-1 rev trans-activator acts through a structured target sequence to activate nuclear export of unspliced viral mRNA. *Nature* 338:254-257.

Mancebo, H.S., G. Lee, J. Flygare, J. Tomassini, P. Luu, Y. Zhu, J. Peng, C. Blau, D. Hazuda, and D. Price. 1997. P-TEFb kinase is required for HIV Tat transcriptional activation in vivo and in vitro. *Genes & Development* 11:2633-2644.

Mangasarian, A., V. Piguet, J.-K. Wang, Y.-L. Chen, and D. Trono. 1999. Nef-induced CD4 and major histocompatibility complex class I (MHC-I) down-regulation are governed by distinct determinants: N-terminal alpha helix and proline repeat of Nef selectively regulate MHC-I trafficking. *Journal of Virology* 73:1964-1973.

Mangeat, B., P. Turelli, G. Caron, M. Friedli, L. Perrin, and D. Trono. 2003. Broad antiretroviral defence by human APOBEC3G through lethal editing of nascent reverse transcripts. *Nature* 424:99-103.

Mansky, L.M., S. Preveral, L. Selig, R. Benarous, and S. Benichou. 2000. The interaction of vpr with uracil DNA glycosylase modulates the human immunodeficiency virus type 1 In vivo mutation rate. *Journal of Virology* 74:7039-7047.

Marban, C.I., L. Redel, S. Suzanne, C. Van Lint, D. Lecestre, S. Chasserot-Golaz, M. Leid, D. Aunis, E. Schaeffer, and O. Rohr. 2005. COUP-TF interacting protein 2 represses the initial phase of HIV-1 gene transcription in human microglial cells. *Nucleic Acids Research* 33:2318-2331.

Margolis, D.M., J.V. Garcia, D.J. Hazuda, and B.F. Haynes. 2016. Latency reversal and viral clearance to cure HIV-1. *Science* 353:aaf6517.

Markert, A., M. Grimm, J. Martinez, J. Wiesner, A. Meyerhans, O. Meyuhas, A. Sickmann, and U. Fischer. 2008. The La-related protein LARP7 is a component of the 7SK ribonucleoprotein and affects transcription of cellular and viral polymerase II genes. *EMBO reports* 9:569-575.

Marzio, G., M. Tyagi, M.I. Gutierrez, and M. Giacca. 1998. HIV-1 tat transactivator recruits p300 and CREB-binding protein histone acetyltransferases to the viral promoter. *Proceedings of the National Academy of Sciences* 95:13519-13524.

Masur, H., M.A. Michelis, J.B. Greene, I. Onorato, R. Stouwe, R.S. Holzman, G. Wormser, L. Brettman, M. Lange, and H.W. Murray. 1981. An outbreak of community-acquired *Pneumocystis carinii* pneumonia: initial manifestation of cellular immune dysfunction. *The New England Journal of Medicine* 305:1431-1438.

McElrath, M.J., R.M. Steinman, and Z.A. Cohn. 1991. Latent HIV-1 infection in enriched populations of blood monocytes and T cells from seropositive patients. *Journal of Clinical Investigation* 87:27.

Mellors, J.W., C.R. Rinaldo Jr, P. Gupta, R.M. White, J.A. Todd, and L.A. Kingsley. 1996. Prognosis in HIV-1 infection predicted by the quantity of virus in plasma. *SCIENCE-NEW YORK THEN WASHINGTON*- 1167-1169.

Meusser, B., and T. Sommer. 2004. Vpu-mediated degradation of CD4 reconstituted in yeast reveals mechanistic differences to cellular ER-associated protein degradation. *Molecular cell* 14:247-258.

Mikovits, J.A., N.C. Lohrey, R. Schulof, J. Courtless, and F. Ruscetti. 1992. Activation of infectious virus from latent human immunodeficiency virus infection of monocytes in vivo. *Journal of Clinical Investigation* 90:1486.

Mingyan, Y., L. Xinyong, and E. De Clercq. 2009. NF- κ B: the inducible factors of HIV-1 transcription and their inhibitors. *Mini reviews in medicinal chemistry* 9:60-69.

Mink, S., B. Haenig, and K.-H. Klempnauer. 1997. Interaction and functional collaboration of p300 and C/EBP β . *Molecular and Cellular Biology* 17:6609-6617.

Mondal, D., J. Alam, and O. Prakash. 1994. NF- κ B site-mediated negative regulation of the HIV-1 promoter by CCAAT/enhancer binding proteins in brain-derived cells. *Journal of Molecular Neuroscience* 5:241-258.

Morris, A. 2008. Is there anything new in *Pneumocystis jirovecii* pneumonia? Changes in *P. jirovecii* pneumonia over the course of the AIDS epidemic. In *The University of Chicago Press*.

Murakami, T., and E.O. Freed. 2000. The long cytoplasmic tail of gp41 is required in a cell type-dependent manner for HIV-1 envelope glycoprotein incorporation into virions. *Proceedings of the National Academy of Sciences* 97:343-348.

Nathan, D., and D.M. Crothers. 2002. Bending and flexibility of methylated and unmethylated EcoRI DNA. *Journal of Molecular Biology* 316:7-17.

Neil, S.J., S.W. Eastman, N. Jouvenet, and P.D. Bieniasz. 2006. HIV-1 Vpu promotes release and prevents endocytosis of nascent retrovirus particles from the plasma membrane. *PLoS Pathogens* 2:e39.

Neil, S.J., T. Zang, and P.D. Bieniasz. 2008. Tetherin inhibits retrovirus release and is antagonized by HIV-1 Vpu. *Nature* 451:425-430.

Neuwald, A.F., and D. Landsman. 1997. GCN5-related histone N-acetyltransferases belong to a diverse superfamily that includes the yeast SPT10 protein. *Trends in biochemical sciences* 22:154-155.

Nguyen, V.T., T.s. Kiss, A.A. Michels, and O. Bensaude. 2001. 7SK small nuclear RNA binds to and inhibits the activity of CDK9/cyclin T complexes. *Nature* 414:322-325.

Napper, A. D., J. Hixon, et al. (2005). "Discovery of indoles as potent and selective inhibitors of the deacetylase SIRT1." *Journal of Medicinal Chemistry* 48(25): 8045-8054.

O'Keeffe, B., Y. Fong, D. Chen, S. Zhou, and Q. Zhou. 2000. Requirement for a kinase-specific chaperone pathway in the production of a Cdk9/cyclin T1 heterodimer responsible for P-TEFb-mediated tat stimulation of HIV-1 transcription. *Journal of Biological Chemistry* 275:279-287.

Ott, M., M. Geyer, and Q. Zhou. 2011. The control of HIV transcription: keeping RNA polymerase II on track. *Cell Host & Microbe* 10:426-435.

Ott, M., M. Schnalzer, J. Garnica, W. Fischle, S. Emiliani, H.-R. Rackwitz, and E. Verdin. 1999. Acetylation of the HIV-1 Tat protein by p300 is important for its transcriptional activity. *Current Biology* 9:1489-1493.

Otteken, A., P.L. Earl, and B. Moss. 1996. Folding, assembly, and intracellular trafficking of the human immunodeficiency virus type 1 envelope glycoprotein analyzed with monoclonal antibodies recognizing maturational intermediates. *Journal of Virology* 70:3407-3415.

Pagano, J.M., H. Kwak, C.T. Waters, R.O. Sprouse, B.S. White, A. Ozer, K. Szeto, D. Shalloway, H.G. Craighead, and J.T. Lis. 2014. Defining NELF-E RNA binding in HIV-1 and promoter-proximal pause regions. *PLoS genetics* 10:e1004090.

Pagans, S., S.E. Kauder, K. Kaehlcke, N. Sakane, S. Schroeder, W. Dormeyer, R.C. Trievel, E. Verdin, M. Schnolzer, and M. Ott. 2010. The Cellular lysine methyltransferase Set7/9-KMT7 binds HIV-1 TAR RNA, monomethylates the viral transactivator Tat, and enhances HIV transcription. *Cell Host & Microbe* 7:234-244.

Palmer, S., F. Maldarelli, A. Wiegand, B. Bernstein, G.J. Hanna, S.C. Brun, D.J. Kempf, J.W. Mellors, J.M. Coffin, and M.S. King. 2008. Low-level viremia persists for at least 7 years in patients on suppressive antiretroviral therapy. *Proceedings of the National Academy of Sciences of the United States of America* 105:3879-3884.

Perelson, A.S., A.U. Neumann, M. Markowitz, J.M. Leonard, and D.D. Ho. 1996. HIV-1 dynamics in vivo: virion clearance rate, infected cell life-span, and viral generation time. *Science* 271:1582-1586.

Piller, S., G. Ewart, A. Premkumar, G. Cox, and P. Gage. 1996. Vpr protein of human immunodeficiency virus type 1 forms cation-selective channels in planar lipid bilayers. *Proceedings of the National Academy of Sciences* 93:111-115.

Popov, S., M. Rexach, G. Zybarth, N. Reiling, M. Lee, L. Ratner, C.M. Lane, M.S. Moore, G.n. Blobel, and M. Bukrinsky. 1998. Viral protein R regulates nuclear import of the HIV-1 pre-integration complex. *The EMBO Journal* 17:909-917.

Price, D.H. 2000. P-TEFb, a cyclin-dependent kinase controlling elongation by RNA polymerase II. *Molecular and Cellular Biology* 20:2629-2634.

Purcell, D., and M. Martin. 1993. Alternative splicing of human immunodeficiency virus type 1 mRNA modulates viral protein expression, replication, and infectivity. *J Virol* 67:6365 - 6378.

Plank, T.-D. M., J. T. Whitehurst, et al. (2013). "Cell type specificity and structural determinants of IRES activity from the 5' leaders of different HIV-1 transcripts." *Nucleic Acids Research* 41(13): 6698-6714.

Perez, M. s., A. G. de Vinuesa, et al. (2010). "Bryostatins synergize with histone deacetylase inhibitors to reactivate HIV-1 from latency." *Current HIV Research* 8(6): 418-429.

Purcell, D. and M. Martin (1993). "Alternative splicing of human immunodeficiency virus type 1 mRNA modulates viral protein expression, replication, and infectivity." *J Virol* 67(11): 6365 - 6378.

Pagans, S., S. E. Kauder, et al. (2010). "The Cellular lysine methyltransferase Set7/9-KMT7 binds HIV-1 TAR RNA, monomethylates the viral transactivator Tat, and enhances HIV transcription." *Cell Host & Microbe* 7(3): 234-244.

Picaud, S., D. Da Costa, et al. (2013). "PFI-1, a highly selective protein interaction inhibitor, targeting BET Bromodomains." *Cancer Research* 73(11): 3336-3346.

Qian, S., X. Zhong, L. Yu, B. Ding, P. de Haan, and K. Boris-Lawrie. 2009. HIV-1 Tat RNA silencing suppressor activity is conserved across kingdoms and counteracts translational repression of HIV-1. *Proceedings of the National Academy of Sciences* 106:605-610.

Rasmussen, T., M. Tolstrup, A. Winckelmann, L. Østergaard, and O. Schmelz Sogaard. 2013. Eliminating the latent HIV reservoir by reactivation strategies: advancing to clinical trials. *Human vaccines & immunotherapeutics* 9:790-799.

Reuse, S., M. Calao, et al. (2009). "Synergistic activation of HIV-1 expression by deacetylase inhibitors and prostratin: implications for treatment of latent infection." *PLoS ONE* 4(6): e6093.

Richman, R., L.G. Chicoine, M. Collini, R.G. Cook, and C.D. Allis. 1988. Micronuclei and the cytoplasm of growing *Tetrahymena* contain a histone acetylase activity which is highly specific for free histone H4. *The Journal of cell biology* 106:1017-1026.

Roeth, J.F., and K.L. Collins. 2006. Human immunodeficiency virus type 1 Nef: adapting to intracellular trafficking pathways. *Microbiology and Molecular Biology Reviews* 70:548-563.

Roeth, J.F., M. Williams, M.R. Kasper, T.M. Filzen, and K.L. Collins. 2004. HIV-1 Nef disrupts MHC-I trafficking by recruiting AP-1 to the MHC-I cytoplasmic tail. *J Cell Biol* 167:903-913.

Roy, S., U. Delling, C.-H. Chen, C. Rosen, and N. Sonenberg. 1990. A bulge structure in HIV-1 TAR RNA is required for Tat binding and Tat-mediated trans-activation. *Genes & Development* 4:1365-1373.

Raje, N., P. N. Hari, et al. (2012). Rocilinostat (ACY-1215), a selective HDAC6 inhibitor, alone and in combination with bortezomib in multiple myeloma: preliminary results from the first-in-humans phase I/II study, *Am Soc Hematology*.

Rasmussen, T. A., O. S. Sogaard, et al. (2013). "Comparison of HDAC inhibitors in clinical development: effect on HIV production in latently infected cells and T cell activation." *Human vaccines & immunotherapeutics* 9(5): 993-1001.

Reuse, S., M. Calao, et al. (2009). "Synergistic activation of HIV-1 expression by deacetylase inhibitors and prostratin: implications for treatment of latent infection." *PLoS ONE* 4(6): e6093.

Rasmussen, T. A. and S. R. Lewin (2016). "Shocking HIV out of hiding: where are we with clinical trials of latency reversing agents?" *Current Opinion in HIV and AIDS*.

Sahu, G. K., K. Lee, et al. (2006). "A novel in vitro system to generate and study latently HIV-infected long-lived normal CD4+ T-lymphocytes." *Virology* 355(2): 127-137.

Saleh, S., A. Solomon, et al. (2007). "CCR7 ligands CCL19 and CCL21 increase permissiveness of resting memory CD4+ T cells to HIV-1 infection: a novel model of HIV-1 latency." *Blood* 110(13): 4161-4164.

Saleh, S., F. Wightman, et al. (2011). "Expression and reactivation of HIV in a chemokine induced model of HIV latency in primary resting CD4+ T cells." *Retrovirology* 8(1): 80.

Schröder, A. R. W., P. Shinn, et al. (2002). "HIV-1 integration in the human genome favors active genes and local hotspots." *Cell* 110(4): 521-529.

Singh, A. and L. S. Weinberger (2009). "Stochastic gene expression as a molecular switch for viral latency." *Current Opinion in Microbiology* 12(4): 460-466.

Saleh, S., F. Wightman, et al. (2011). "Expression and reactivation of HIV in a chemokine induced model of HIV latency in primary resting CD4+ T cells." *Retrovirology* 8(1): 80.

Stellbrink, H.-J. r., J. van Lunzen, et al. (2002). "Effects of interleukin-2 plus highly active antiretroviral therapy on HIV-1 replication and proviral DNA (COSMIC trial)." *Aids* 16(11): 1479-1487.

Sasakawa, Y., Y. Naoe, et al. (2002). "Effects of FK228, a novel histone deacetylase inhibitor, on human lymphoma U-937 cells in vitro and in vivo." *Biochemical Pharmacology* 64(7): 1079-1090.

Sgarbanti, M. and A. Battistini (2013). "Therapeutics for HIV-1 reactivation from latency." *Current opinion in virology* 3(4): 394-401.

Sugiyama, A., K. Kageyama, et al. (2015). "Inhibition of heat shock protein 90 decreases ACTH production and cell proliferation in AtT-20 cells." *Pituitary* 18(4): 542-553.

Szallasi, Z., C. B. Smith, et al. (1994). "Differential regulation of protein kinase C isozymes by bryostatin 1 and phorbol 12-myristate 13-acetate in NIH 3T3 fibroblasts." *Journal of Biological Chemistry* 269(3): 2118-2124.

Sakane, N., H.-S. Kwon, S. Pagans, K. Kaehlcke, Y. Mizusawa, M. Kamada, K.G. Lassen, J. Chan, W.C. Greene, and M. Schnoelzer. 2011. Activation of HIV transcription by the viral Tat protein requires a demethylation step mediated by lysine-specific demethylase 1 (LSD1/KDM1). *PLoS Pathogens* 7:e1002184.

Schotta, G., M. Lachner, K. Sarma, A. Ebert, R. Sengupta, G. Reuter, D. Reinberg, and T. Jenuwein. 2004. A silencing pathway to induce H3-K9 and H4-K20 trimethylation at constitutive heterochromatin. *Genes & Development* 18:1251-1262.

Schröder, A.R.W., P. Shinn, H. Chen, C. Berry, J.R. Ecker, and F. Bushman. 2002. HIV-1 integration in the human genome favors active genes and local hotspots. *Cell* 110:521-529.

Schulte, A., N. Czudnochowski, M. Barboric, A. Schonichen, D. Blazek, B.M. Peterlin, and M. Geyer. 2005. Identification of a cyclin T-binding domain in Hexim1 and biochemical analysis of its binding competition with HIV-1 Tat. *Journal of Biological Chemistry* 280:24968-24977.

Schwartz, O., V. Marechal, S. Le Gall, F. Lemonnier, and J. Heard. 1996b. Endocytosis of major histocompatibility complex class I molecules is induced by the HIV-1 Nef protein. *Nat Med* 2:338 - 342.

Sehgal, P.B., J.E. Darnell, and I. Tamm. 1976. The inhibition of DRB (5, 6-dichloro-1-beta-d-ribofuranosylbenzimidazole) of hnRNA and mRNA production in HeLa cells. *Cell* 9:473-480.

Shan, L., K. Deng, N.S. Shroff, C.M. Durand, S.A. Rabi, H.-C. Yang, H. Zhang, J.B. Margolick, J.N. Blankson, and R.F. Siliciano. 2012. Stimulation of HIV-1-specific cytolytic T lymphocytes facilitates elimination of latent viral reservoir after virus reactivation. *Immunity* 36:491-501.

Sheehy, A.M., N.C. Gaddis, J.D. Choi, and M.H. Malim. 2002. Isolation of a human gene that inhibits HIV-1 infection and is suppressed by the viral Vif protein. *Nature* 418:646-650.

Siliciano, J.D., J. Kajdas, D. Finzi, T.C. Quinn, K. Chadwick, J.B. Margolick, C. Kovacs, S.J. Gange, and R.F. Siliciano. 2003. Long-term follow-up studies confirm the stability of the latent reservoir for HIV-1 in resting CD4+ T cells. *Nat Med* 9:727-728.

Sobhian, B., N. Laguette, A. Yatim, M. Nakamura, Y. Levy, R. Kiernan, and M. Benkirane. 2010. HIV-1 Tat assembles a multifunctional transcription elongation complex and stably associates with the 7SK snRNP. *Molecular cell* 38:439-451.

Stark, L.A., and R.T. Hay. 1998. Human immunodeficiency virus type 1 (HIV-1) viral protein R (Vpr) interacts with Lys-tRNA synthetase: implications for priming of HIV-1 reverse transcription. *Journal of Virology* 72:3037-3044.

Steininger, C., E. Puchhammer, and T. Popow-Kraupp. 2006. Cytomegalovirus disease in the era of highly active antiretroviral therapy (HAART). *Journal of Clinical Virology* 37:1-9.

Stephenson, K.E., and D.H. Barouch. 2016. Broadly neutralizing antibodies for HIV eradication. *Current HIV/AIDS Reports* 13:31-37.

Stewart, S.A., B. Poon, J.Y. Song, and I.S. Chen. 2000. Human immunodeficiency virus type 1 vpr induces apoptosis through caspase activation. *Journal of Virology* 74:3105-3111.

Temin, H.M., and D. Baltimore. 1972. RNA-directed DNA synthesis and RNA tumor viruses. *Advances in virus research* 17:129-186.

Tong-Starksen, S.E., A. Baur, X.-b. Lu, E. Peck, and B.M. Peterlin. 1993. Second exon of Tat of HIV-2 is required for optimal trans-activation of HIV-1 and HIV-2 LTRs. *Virology* 195:826-830.

Torchia, J., C. Glass, and M.G. Rosenfeld. 1998. Co-activators and co-repressors in the integration of transcriptional responses. *Current opinion in cell biology* 10:373-383.

Tyagi, M., and J. Karn. 2007. CBF, Δ 1 promotes transcriptional silencing during the establishment of HIV-1 latency. *The EMBO Journal* 26:4985-4995.

Tripathy, M. K., W. Abbas, et al. (2011). "Epigenetic regulation of HIV-1 transcription." *Epigenomics* 3(4): 487-502.

Van Lint, C., S. Bouchat, et al. (2013). "HIV-1 transcription and latency: an update." *Retrovirology* 10(1): 67.

Tyagi, M., R. J. Pearson, et al. (2010). "Establishment of HIV latency in primary CD4+ cells is due to epigenetic transcriptional silencing and P-TEFb restriction." *Journal of Virology* 84(13): 6425-6437.

Ulich, C., A. Dunne, E. Parry, C.W. Hooker, R.B. Gaynor, and D. Harrich. 1999. Functional domains of Tat required for efficient human immunodeficiency virus type 1 reverse transcription. *Journal of Virology* 73:2499-2508.

Van Lint, C., S. Bouchat, and A. Marcello. 2013. HIV-1 transcription and latency: an update. *Retrovirology* 10:67.

Vaquero, A., R. Sternglanz, and D. Reinberg. 2007. NAD⁺-dependent deacetylation of H4 lysine 16 by class III HDACs. *Oncogene* 26:5505-5520.

Vire, E., C. Brenner, R. Deplus, L.Ø. Blanchon, M. Fraga, C.I. Didelot, L. Morey, A. Van Eynde, D. Bernard, and J.-M. Vanderwinden. 2006. The Polycomb group protein EZH2 directly controls DNA methylation. *Nature* 439:871-874.

Wei, D. G., V. Chiang, et al. (2014). "Histone deacetylase inhibitor romidepsin induces HIV expression in CD4 T cells from patients on suppressive antiretroviral therapy at concentrations achieved by clinical dosing." *PLoS Pathogens* 10(4): e1004071.

Van Duyne, R., C. Pedati, et al. (2009). "The utilization of humanized mouse models for the study of human retroviral infections." *Retrovirology* 6(1): 76.

Van Lint, C., S. Bouchat, et al. (2013). "HIV-1 transcription and latency: an update." *Retrovirology* 10(1): 67.

Verhoef, K., M. Tijms, et al. (1997). "Optimal Tat-mediated activation of the HIV-1 LTR promoter requires a full-length TAR RNA hairpin." *Nucleic Acids Research* 25(3): 496-502.

Wang, F.-X., Y. Xu, et al. (2005). "IL-7 is a potent and proviral strain,Àspecific inducer of latent HIV-1 cellular reservoirs of infected individuals on virally suppressive HAART." *Journal of Clinical Investigation* 115(1): 128.

Wang, F.-X., Y. Xu, et al. (2005). "IL-7 is a potent and proviral strain, a specific inducer of latent HIV-1 cellular reservoirs of infected individuals on virally suppressive HAART." *Journal of Clinical Investigation* 115(1): 128.

Wei, X., J. M. Decker, et al. (2002). "Emergence of resistant human immunodeficiency virus type 1 in patients receiving fusion inhibitor (T-20) monotherapy." *Antimicrobial Agents and Chemotherapy* 46(6): 1896-1905.

Wilusz, C. J., W. Wang, et al. (2001). "Curbing the nonsense: the activation and regulation of mRNA surveillance." *Genes & Development* 15(21): 2781-2785.

Weinberger, L. S., J. C. Burnett, et al. (2005). "Stochastic Gene Expression in a Lentiviral Positive-Feedback Loop: HIV-1 Tat Fluctuations Drive Phenotypic Diversity." *Cell* 122(2): 169-182.

Williams, S. A., L. F. Chen, et al. (2006). "NF-κB p50 promotes HIV latency through HDAC recruitment and repression of transcriptional initiation." *EMBO Journal* 25(1): 139-149.

Williams, S. A. and W. C. Greene (2007). "Regulation of HIV-1 latency by T cell activation." *Cytokine* 39(1): 63-74.

Williams, S.A., L.Ä. Chen, H. Kwon, E. Verdin, and W.C. Greene. 2006. NFκB p50 promotes HIV latency through HDAC recruitment and repression of transcriptional initiation. *The EMBO Journal* 25:139-149.

Wu, S., W. Wang, X. Kong, L.M. Congdon, K. Yokomori, M.W. Kirschner, and J.C. Rice. 2010. Dynamic regulation of the PR-Set7 histone methyltransferase is required for normal cell cycle progression. *Genes & Development* 24:2531-2542.

Xing, S., C. K. Bullen, et al. (2011). "Disulfiram reactivates latent HIV-1 in a Bcl-2-transduced primary CD4+ T cell model without inducing global T cell activation." *Journal of Virology* 85(12): 6060-6064.

Yamada, T., Y. Yamaguchi, N. Inukai, S. Okamoto, T. Mura, and H. Handa. 2006. P-TEFb-mediated phosphorylation of hSpt5 C-terminal repeats is critical for processive transcription elongation. *Molecular cell* 21:227-237.

Yamaguchi, Y., T. Takagi, T. Wada, K. Yano, A. Furuya, S. Sugimoto, J. Hasegawa, and H. Handa. 1999. NELF, a multisubunit complex containing RD, cooperates with DSIF to repress RNA polymerase II elongation. *Cell* 97:41-51.

Yang, Z., J.H. Yik, R. Chen, N. He, M.K. Jang, K. Ozato, and Q. Zhou. 2005. Recruitment of P-TEFb for stimulation of transcriptional elongation by the bromodomain protein Brd4. *Molecular cell* 19:535-545.

Yang, Z., Q. Zhu, K. Luo, and Q. Zhou. 2001. The 7SK small nuclear RNA inhibits the CDK9/cyclin T1 kinase to control transcription. *Nature* 414:317-322.

Yates, A., J. Stark, N. Klein, R. Antia, and R. Callard. 2007. Understanding the slow depletion of memory CD4+ T cells in HIV infection. *PLoS Medicine* 4:e177.

Ying, H., Y. Zhang, et al. (2012). "Selective histone deacetylase inhibitor M344 intervenes in HIV-1 latency through increasing histone acetylation and activation of NF-kappaB." *PLoS ONE* 7(11): e48832.

Yamada, T., Y. Yamaguchi, et al. (2006). "P-TEFb-mediated phosphorylation of hSpt5 C-terminal repeats is critical for processive transcription elongation." *Molecular cell* 21(2): 227-237.

Yang, Z., J. H. N. Yik, et al. (2005). "Recruitment of P-TEFb for Stimulation of Transcriptional Elongation by the Bromodomain Protein Brd4." *Molecular Cell* 19(4): 535-545.

Yang, Z., Q. Zhu, et al. (2001). "The 7SK small nuclear RNA inhibits the CDK9/cyclin T1 kinase to control transcription." *Nature* 414(6861): 317-322.

Zhu, Y., T. Pe'ery, et al. (1997). "Transcription elongation factor P-TEFb is required for HIV-1 tat transactivation in vitro." *Genes & Development* 11(20): 2622-2632.

ZHANG, Z., S.-M. KANG, and C.D. MORROW. 1998. Genetic evidence of the interaction between tRNALys, 3 and U5 facilitating efficient initiation of reverse transcription by human immunodeficiency virus type 1. *AIDS Research and Human Retroviruses* 14:979-988.

Zhou, M., L. Deng, V. Lacoste, H.U. Park, A. Pumfery, F. Kashanchi, J.N. Brady, and A. Kumar. 2004. Coordination of transcription factor phosphorylation and histone methylation by the P-TEFb kinase during human immunodeficiency virus type 1 transcription. *Journal of Virology* 78:13522-13533.

Zhou, Q., D. Chen, E. Pierstorff, and K. Luo. 1998. Transcription elongation factor P-TEFb mediates Tat activation of HIV-1 transcription at multiple stages. *The EMBO Journal* 17:3681-3691.

Zhu, P., J. Liu, J. Bess, E. Chertova, J.D. Lifson, H. Ofek, K.A. Taylor, and K.H. Roux. 2006. Distribution and three-dimensional structure of AIDS virus envelope spikes. *Nature* 441:847-852.

Zhu, Y., J. Peng, Y. Ramanathan, N. Marshall, T. Marshall, B. Amendt, M.B. Mathews, and D.H. Price. 1997. Transcription elongation factor P-TEFb is required for HIV-1 tat transactivation in vitro. *Genes & Development* 11:2622-2632.

Table for reporting responses to reviewers' comments

**italicised points were not changed by the author, with reasons provided*

Examiners comment	Change made to thesis (if any)
Examiner 1: Chapter 1 -Definitions -Explanation of progeny release -Minor spelling/grammar	-Definitions of sterilizing/functional cure expanded -release of progeny explanation expanded -Spelling and grammar corrected as suggested
Examiner 1: Chapter 2 -None	-None
Examiner 1: Chapter 3 -More detail regarding Tat IRES -Shorten Discussion -Minor spelling/grammar	-In depth discussion on Tat IRES added in Appendix 1 -Discussion significantly shortened -Spelling and grammar corrected as suggested
Examiner 1: Chapter 4 -Shorten Introduction -Minor spelling/grammar	-Introduction significantly shortened -Spelling and grammar corrected as suggested
Examiner 1: Chapter 5 -Shorten Introduction -Minor spelling/grammar	-Introduction significantly shortened -Spelling and grammar corrected as suggested
Examiner 1: Chapter 6 -Minor spelling/grammar	-Spelling and grammar corrected as suggested
Examiner 1: Chapter 7 -None	-None

Examiners comment	Change made to thesis (if any)
Examiner 2: Chapter 1 -PRMT6 reference -Figures not labelled A, B, C... -Minor spelling/grammar	-More detail on PRMT6 included with reference -Figures now labelled appropriately -Spelling and grammar corrected as suggested
Examiner 2: Chapter 2 -None	-None
Examiner 2: Chapter 3 -Shorten Introduction -n=3 use -definition of “authentic” -describe molecular events -Minor spelling/grammar -References added	-Introduction significantly shortened -n=3 defined in materials and methods -wording softened to better accommodate reviewer -molecular events involved in HIV-1 latency described here -Spelling and grammar corrected as suggested -References added as suggested
Examiner 2: Chapter 4 -Shorten Introduction -Issue with MTS assay <i>*Remove “known” from LRA</i> <i>*homogeneous definition</i> -MTS y-axis -Discussion revision -Didehydro-Cortistatin A -Minor spelling/grammar -References added	-Introduction re-written and Tables moved to Appendix 3 -limitations of MTS assay added to materials and methods <i>*known allows for distinction from novel LRAs, so will remain</i> <i>*definition of homogeneous is provided in chapter 3</i> -explanation of normalised Dead-Cell only y-axis scale given in materials and methods -Discussion heavily revised and shortened - Details of “Block and Lock” using Didehydro-Cortistatin A Given with appropriate references -Spelling and grammar corrected as suggested -References added as suggested
Examiner 2: Chapter 5 <i>*Screening data in introduction</i> <i>*”hits” terminology</i> <i>*bromodomain alpha screen</i> <i>*hour abbreviation</i> -Minor spelling/grammar -References added	<i>*HTCS was performed by the WEHI, not generated by the author and therefore introduction not results</i> <i>*”hits” is the term used by the WEHI to describe compounds at this level of the workflow. The term is appropriate.</i> <i>*Experiment carried out by the WEHI and accredited accordingly. No methodological information has been given to the author, so examiners request cannot be satisfied</i> <i>*The examiner abbreviates hour h, but this thesis abbreviates hour hr, as stated accordingly in the abbreviations section</i> -Spelling and grammar corrected as suggested -References added as suggested
Examiner 2: Chapter 6 -PEP005 -Minor spelling/grammar -References added	-PEP500 corrected to PEP005 -Spelling and grammar corrected as suggested -References added as suggested
Examiner 2: Chapter 7 -Discussion revision -Tat mutant recommendation -Didehydro-Cortistatin A	-Discussion heavily revised and lengthened to address reviewers comments -Tat mutant (FlipInOFF) discussion added to satisfy reviewer

-References added	- Discussion of “Block and Lock” using Didehydro-Cortistatin A given with appropriate references -References added as suggested
-------------------	---

Dear Jonathan,

We are pleased to inform you that your examination result is now available.

Examination outcome

The examiners of your thesis have requested that certain revisions be made to your thesis to the satisfaction of the Chair of Examiners.

Thesis corrections

You are required to make changes to your thesis as per examiners' comments, which are set out in the attached reports. The revisions are to be incorporated into the text of the thesis. You should consult your supervisor and Chair of Examiners, **Professor Andrew Brooks**, on how to respond to the examiner(s) comments.

Submitting final thesis

Once you have completed all required revisions, you are requested to provide an index summarising the changes (for your convenience we have attached a template for you to use) with your revised thesis to the Chair of Examiners via email.

Once the Chair of Examiners has given their approval, you are then required to upload a digital copy of the final thesis, preferably in PDF format, to the University's institutional repository: minerva-access.unimelb.edu.au prior to **16 January 2019**. Detailed information is available at: gradresearch.unimelb.edu.au/examination/my-thesis-in-the-library.

If your thesis is placed on Full Embargo your Chair of Examiners will only be able to view the thesis metadata. We would suggest that you provide your Chair of Examiners with the exact file that is uploaded to Minerva Access (via secure means, e.g. CloudSTOR) so that they can certify the final thesis.

Meeting degree requirements

You will be considered eligible to pass once the final thesis is endorsed by the Chair of Examiners and an approved citation prepared by your supervisor has been received by the Examinations Office. Once these requirements are met you will receive your completion letter along with graduation information.

Extension to submit final thesis

If you require further time to submit your final thesis, you can request an extension by sending an email, with either supervisor or Chair of Examiners approval, to gr-exams@unimelb.edu.au. As outlined in the [Graduate Research Training Policy \(MPF1321\)](#), the final thesis must be submitted within three months of the initial due date. For further extensions, you are required to complete an *Application for an Extension to Submit Final Thesis* available at: gradresearch.unimelb.edu.au/examination/submitting-my-thesis#extension-forms.

With kind regards,

Russell Wilkinson
on behalf of the Graduate Research team
University Services
The University of Melbourne
Victoria 3010 Australia



Minerva Access is the Institutional Repository of The University of Melbourne

Author/s:

Jacobson, Jonathan

Title:

Development of novel HIV-1 latency reversing agents

Date:

2018

Persistent Link:

<http://hdl.handle.net/11343/220633>

File Description:

Jonathan Jacobson PhD Thesis- Development of Novel HIV-1 Latency Reversing Agents

Terms and Conditions:

Terms and Conditions: Copyright in works deposited in Minerva Access is retained by the copyright owner. The work may not be altered without permission from the copyright owner. Readers may only download, print and save electronic copies of whole works for their own personal non-commercial use. Any use that exceeds these limits requires permission from the copyright owner. Attribution is essential when quoting or paraphrasing from these works.